



Universitäts-Sternwarte
München

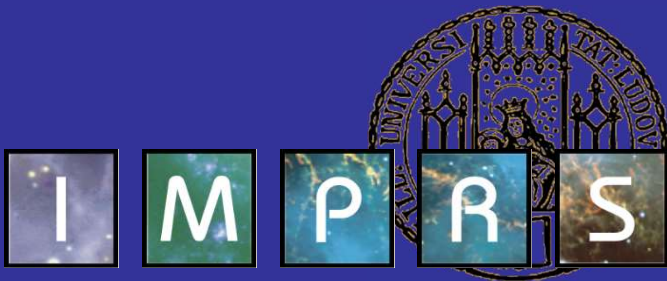
Radiative Transfer, Stellar Atmospheres and Winds

Five lectures (four hours each) within the
IMPRS advanced course

Joachim Puls

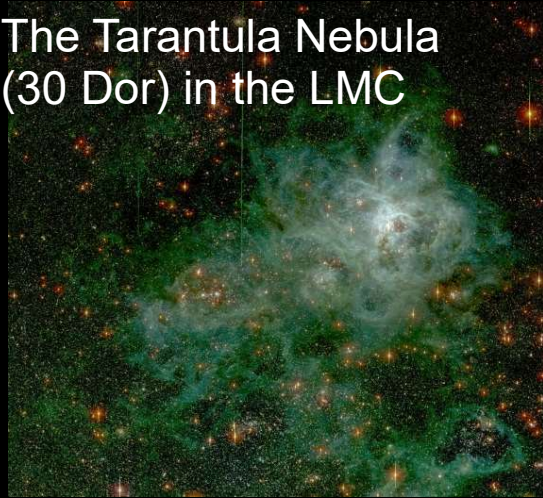
University Observatory Munich

NLTE Group



Radiative transfer, stellar atmospheres and winds

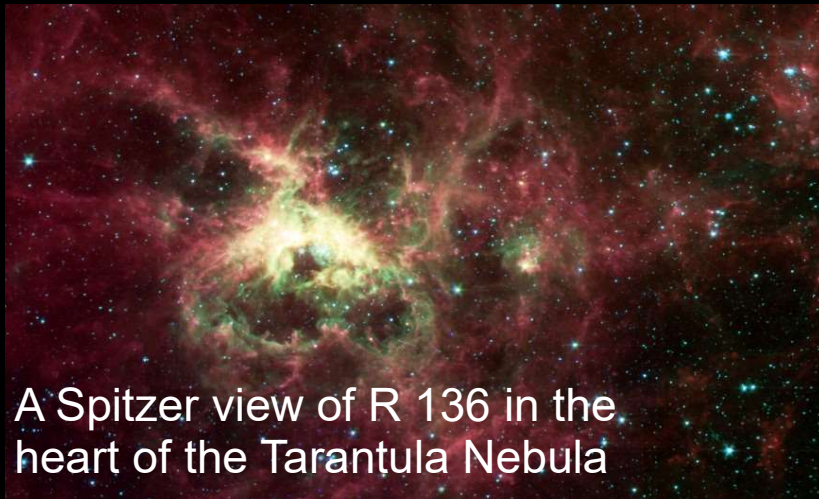
The Tarantula Nebula
(30 Dor) in the LMC



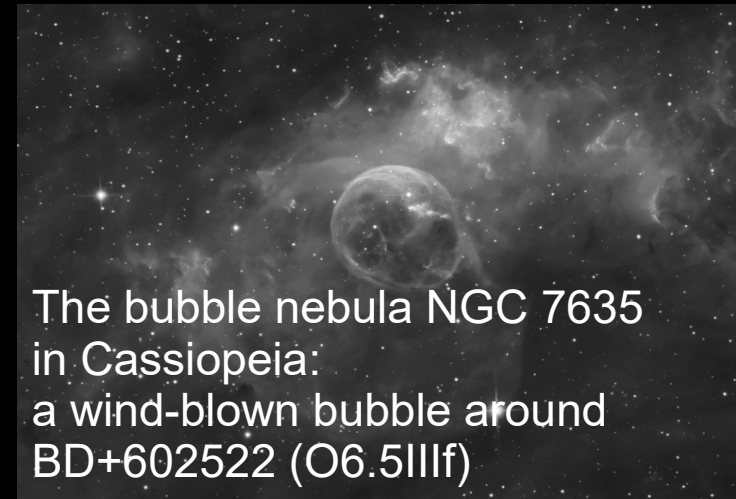
The wind-blown bubble
N44F in the LMC



A Spitzer view of R 136 in the
heart of the Tarantula Nebula



The bubble nebula NGC 7635
in Cassiopeia:
a wind-blown bubble around
BD+602522 (O6.5IIIIf)





Content



1. *Prelude*: What are stars good for? A brief tour through present hot topics (not complete, personally biased)
2. *Quantitative spectroscopy*: the astrophysical tool to measure stellar and interstellar properties
3. *The radiation field*: specific and mean intensity, radiative flux and pressure, Planck function
4. *Coupling with matter*: opacity, emissivity and the equation of radiative transfer (incl. angular moments)
5. *Radiative transfer*: simple solutions, spectral lines and limb darkening
6. *Stellar atmospheres*: basic assumptions, hydrostatic, radiative and local thermodynamic equilibrium, temperature stratification and convection
7. *Microscopic theory*
 1. *Line transitions*: Einstein-coefficients, line-broadening and curve of growth, continuous processes and scattering
 2. *Ionization and excitation in LTE*: Saha- and Boltzmann-equation
 3. *Non-LTE*: motivation and introduction

Intermezzo: Stellar Atmospheres in practice -- A tour de modeling and analysis of stellar atmospheres throughout the HRD

A first application: The D4000 break in early-type galaxies

8. *Stellar winds* - overview, pressure and radiation driven winds
9. *Quantitative spectroscopy*: stellar/atmospheric parameters and how to determine them, for the exemplary case of hot stars



- ▶ Carroll, B.W., Ostlie, D.A., “An Introduction to Modern Astrophysics”, 2nd edition, Pearson International Edition, San Francisco, 2007, Chap. 3,5,8,9
- ▶ Mihalas, D., “Stellar atmospheres”, 2nd edition, Freeman & Co., San Francisco, 1978
- ▶ Hubeny, I., & Mihalas, D., “Theory of Stellar Atmospheres”, Princeton Univ. Press, 2014
- ▶ Unsöld, A., “Physik der Sternatmosphären”, 2nd edition, Springer Verlag, Heidelberg, 1968
- ▶ Shu, F.H., “The physics of astrophysics, Volume I: radiation”, University science books, Mill Valley, 1991
- ▶ Rybicki, G.B., Lightman, A., “Radiative Processes in Astrophysics”, New York, Wiley, 1979
- ▶ Osterbrock, D.E., “Astrophysics of Gaseous Nebulae and Active Galactic Nuclei”, University science books, Mill Valley, 1989
- ▶ Mihalas, D., Weibel Mihalas, B., “Foundations of Radiation Hydrodynamics”, Oxford University Press, New York, 1984
- ▶ Cercignani, C., “The Boltzmann Equation and Its Applications”, Appl. Math. Sciences 67, Springer, 1987
- ▶ Kudritzki, R.-P., Hummer, D.G., “Quantitative spectroscopy of hot stars”, Annual Review of Astronomy and Astrophysics, Vol. 28, p. 303, 1990
- ▶ Sobolev, V.V., “Moving envelopes of stars”, Cambridge: Harvard University Press, 1960
- ▶ Kudritzki, R.-P., Puls, J., “Winds from hot stars”, Annual Review of Astronomy and Astrophysics, Vol. 38, p. 613, 2000
- ▶ Puls, J., Vink, J.S., Najarro, F., “Mass loss from hot massive stars”, Astronomy & Astrophysics Review Vol. 16, ISSUE 3, p. 209, Springer, 2008
- ▶ Puls, J., “Radiative Transfer in the (Expanding) Atmospheres of Early-Type Stars, and Related Problems”, in: “Radiative Transfer in Stellar and Planetary Atmospheres”, Canary Islands Winter School of Astrophysics, Vol. XXIX, Cambridge University Press, 2019, in press



- ▶ cosmology, galaxies, dark energy, dark matter, ...

What are stars good for?

- ▶ ... and who cares for radiative transfer and stellar atmospheres?
- ▶ Remember
 - ▶ galaxies consist of stars (and gas, dust)
 - ▶ most of the (visible) light originates from stars
 - ▶ astronomical experiments are (mostly) observations of light:
have to understand how it is created and transported

The cosmic circuit of matter

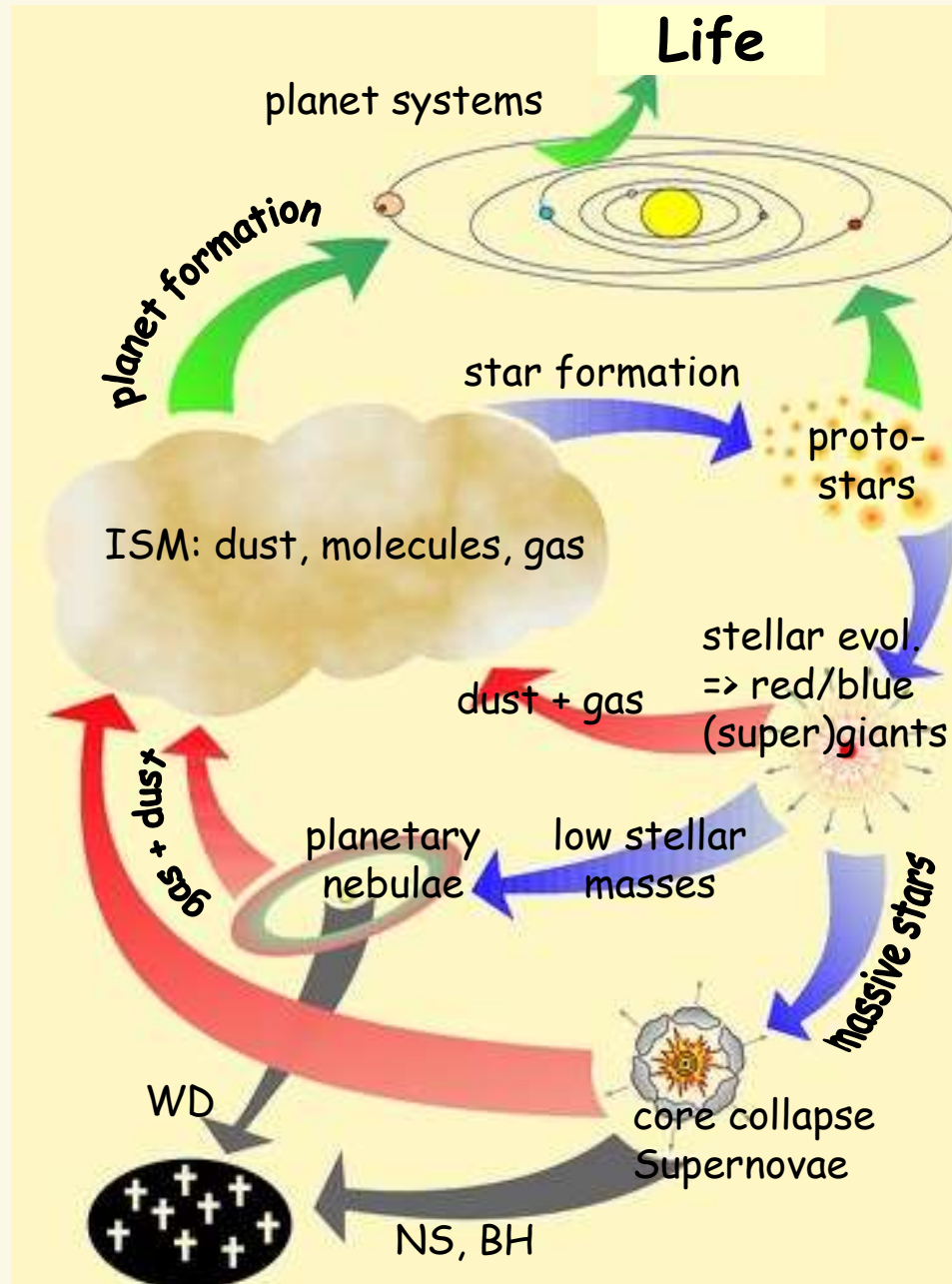


What are stars good for?

- ▶ Us!
- ▶ (whether this is really good, is another question...)

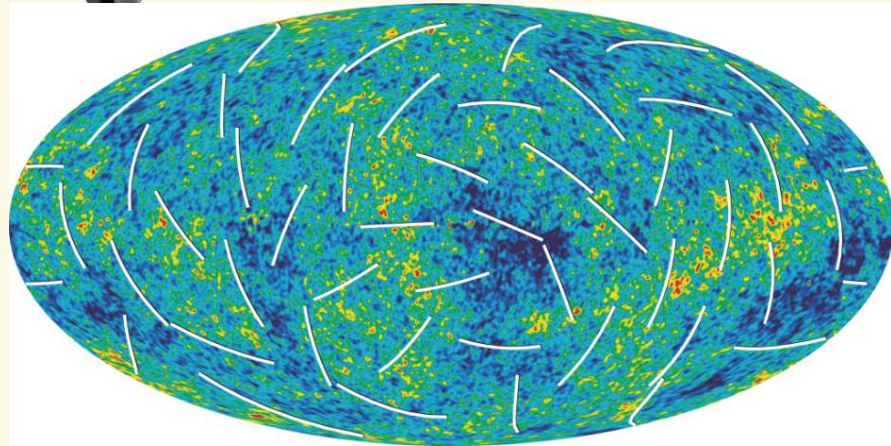
Joni Mitchell - Woodstock (1970!)

“... We are stardust
Billion year old carbon...”



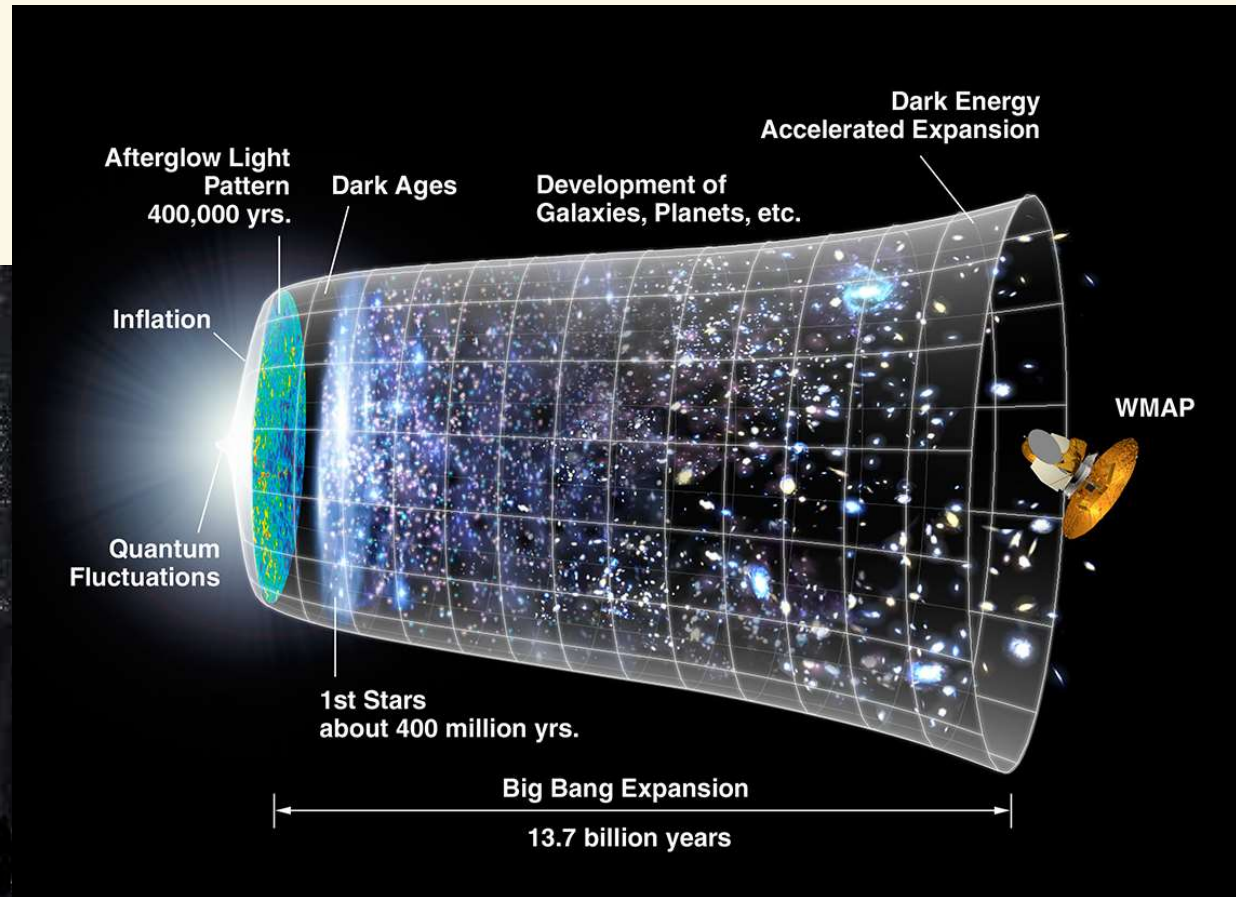
adapted from <http://astro.physik.tu-berlin.de/~sonja/Materiekreislauf/index.html>

First stars and reionization



WMAP = Wilkinson Microwave Anisotropy Probe
color coding: ΔT range $\pm 200 \mu\text{K}$, $\Delta T/T \sim \text{few } 10^{-5}$
 \Rightarrow “anisotropy” of last scattering surface (before recomb.)
white bars: polarization vector
 \Rightarrow CMB photons scattered at electrons (reionized gas)
[NOTE: newer data from PLANCK]

credit: NASA/WMAP Science Team





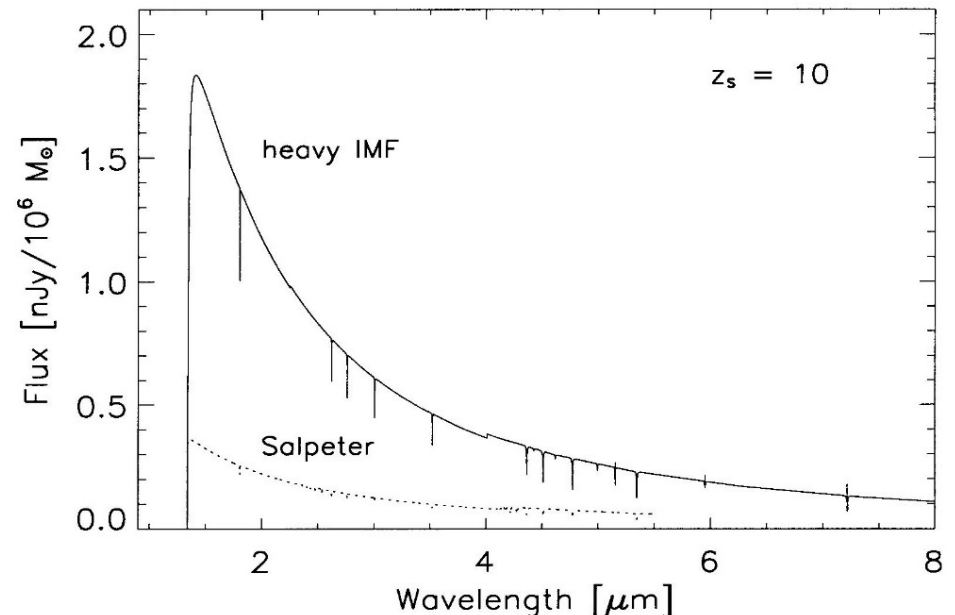
The first stars ...



- cosmic reionization:
 - $z = 7.7 \pm 0.8$ (from PLANCK, assuming instantaneous reionization, state 2018)
 - $z \approx 11$ (begin) to 7 (from WMAP)
- quasars **alone** not capable to reionize Universe at that high redshift, since rapid decline in space density for $z > 3$ (Madau et al. 1999, ApJ 514, Fan et al. 2006, ARA&A 44)

Bromm et al. (2001, ApJ 552)

- (almost) metal free: Pop III
- very massive stars (VMS) with $1000 M_{\odot} > M > 100 M_{\odot}$, L prop. to M , $T_{\text{eff}} \sim 100$ kK
- large H/He ionizing fluxes: 10^{48} (10^{47}) H (He) ionizing photons per second *and solar mass*
- **assume** that primordial IMF is *heavy*, i.e., **favours** formation of VMS
- **then** VMS capable to reionize universe alone



But: theoretical models indicate more typical masses around $40 M_{\odot}$ (fragmentation!, Hosokawa et al. 2011), though (much) more massive stars might have formed as well

Present status: Massive stars important for reionization, but not exclusive

see also: Abel et al. 2000, ApJ 540; Bromm et al. 2002, ApJ 564; Cen 2003, ApJ 591; Furnaletto & Loeb 2005, ApJ 634; Wise & Abel 2008, ApJ 684; Johnson et al. 2008, Proc IAU Symp 250 (review); Maio et al. 2009, A&A 503; Maio et al. 2010, MNRAS 407; Weber et al. 2013, A&A 555

... and many more publications

... might be observable in the NIR

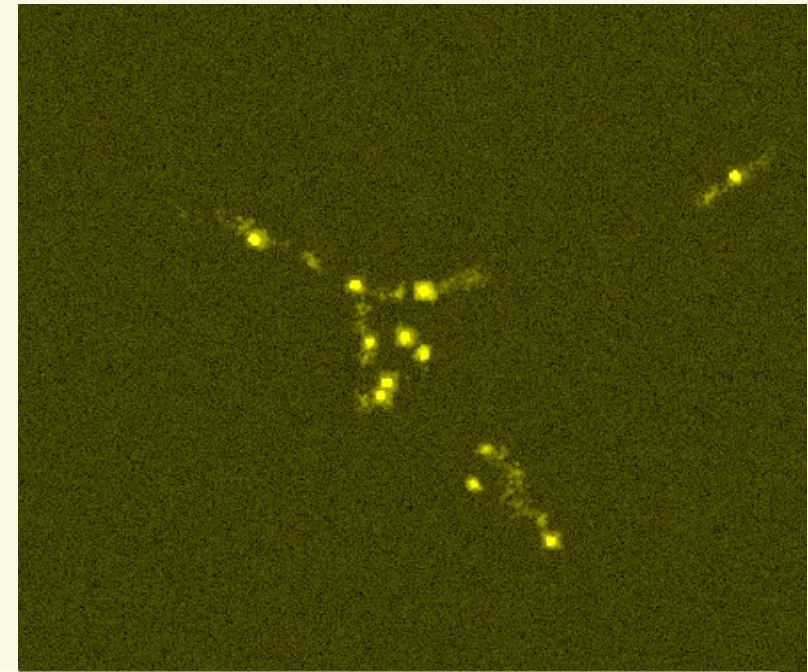
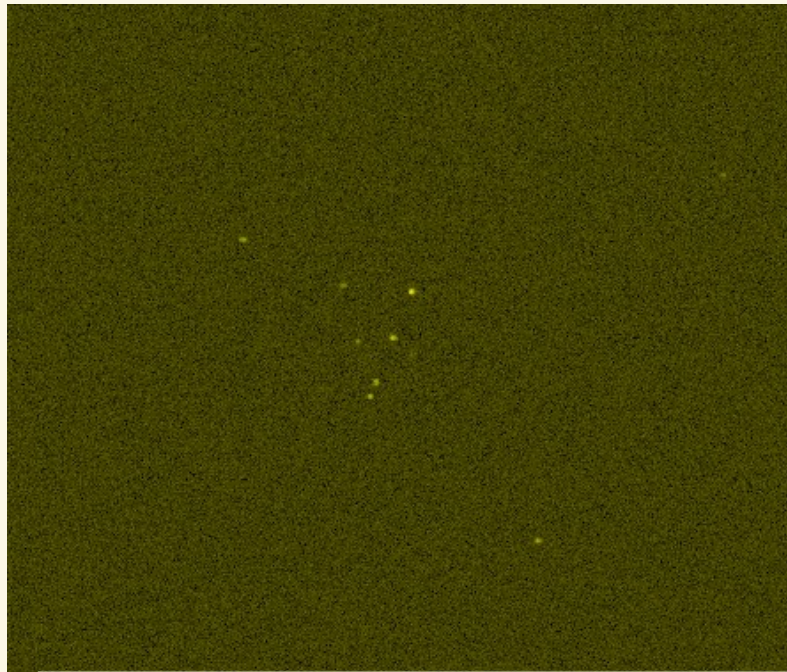


with a $\geq 30\text{m}$ telescope, e.g. via H α $\lambda 1640 \text{ \AA}$ (strong ISM recomb. line)

Standard IMF

1 Mpc (comoving)

Heavy IMF, zero metallicity



GSMT Science Working Group Report, 2003, Kudritzki et al.

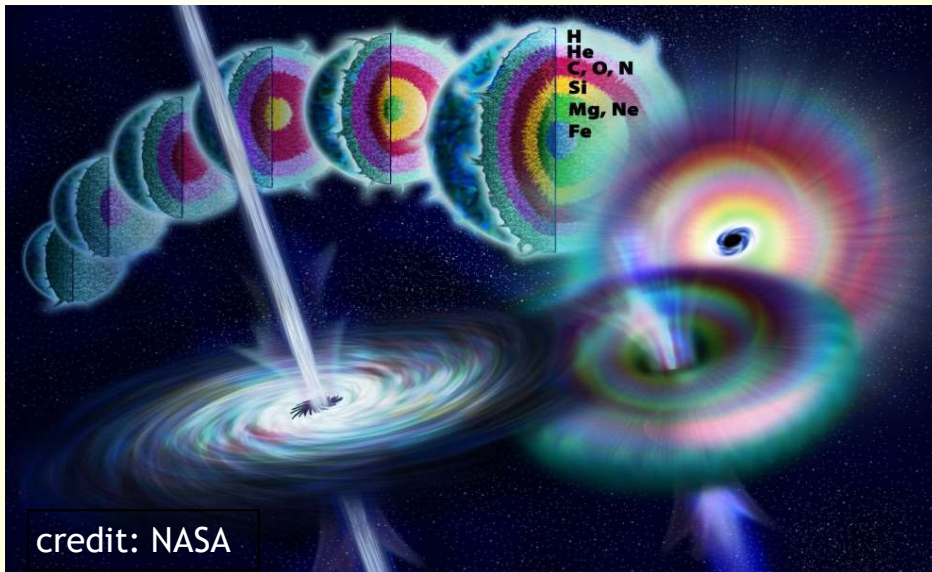
http://www.aura-nio.noao.edu/gsm_t_swg/SWG_Report/SWG_Report_7.2.03.pdf

(Hydro-simulations by
Davé, Katz, & Weinberg)

As observed through 30-meter telescope
R=3000, 10^5 seconds (favourable conditions, see
also Barton et al., 2004, ApJ 604, L1)

Long Gamma Ray Bursts

- long: $>2s$
- Collapsar: death of a massive star

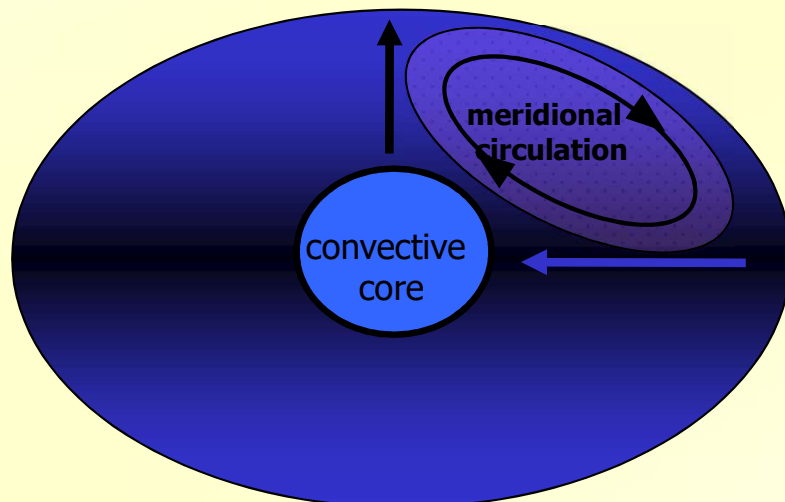


Collapsar Scenario for Long GRB (Woosley 1993)

- massive core (enough to produce a BH)
- removal of hydrogen envelope
- rapidly rotating core (enough to produce an accretion disk)

requires chemically homogeneous evolution of rapidly rotating massive star

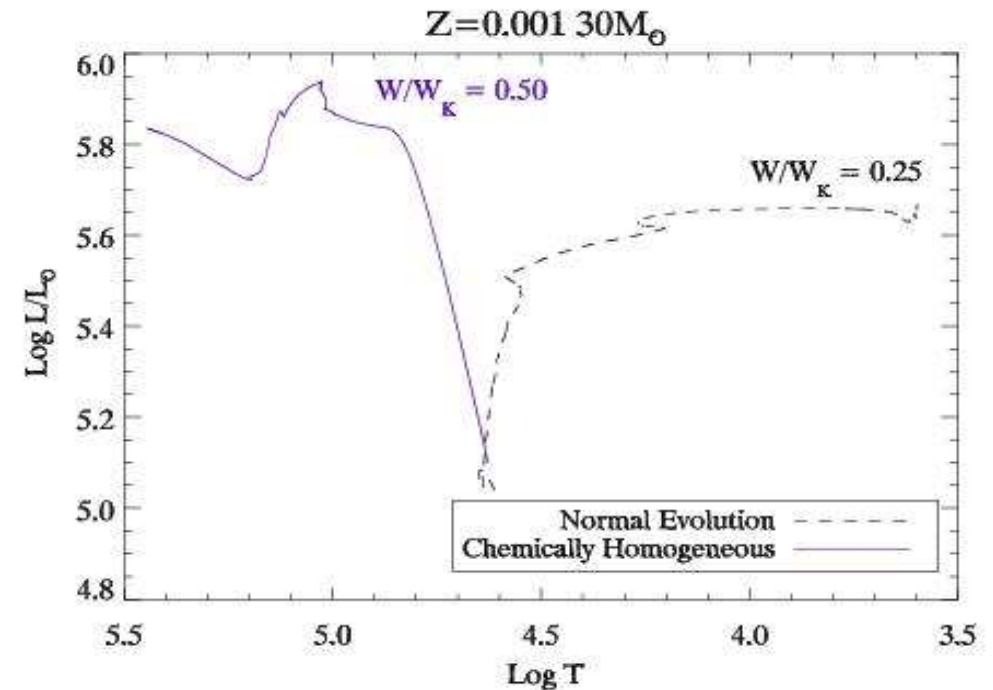
- pole hotter than equator (von Zeipel)
- rotational mixing due to meridional circulation (Eddington-Sweet)



Chemically Homogeneous Evolution ...

- ...if rotational mixing during main sequence *faster than* built-up of chemical gradients due to nuclear fusion (*Maeder 1987*)
- bluewards evolution directly towards Wolf-Rayet phase (no RSG phase). Due to meridional circulation, envelope and core are mixed -> no hydrogen envelope
- since no RSG phase, higher angular momentum in the core (*Yoon & Langer 2005*)

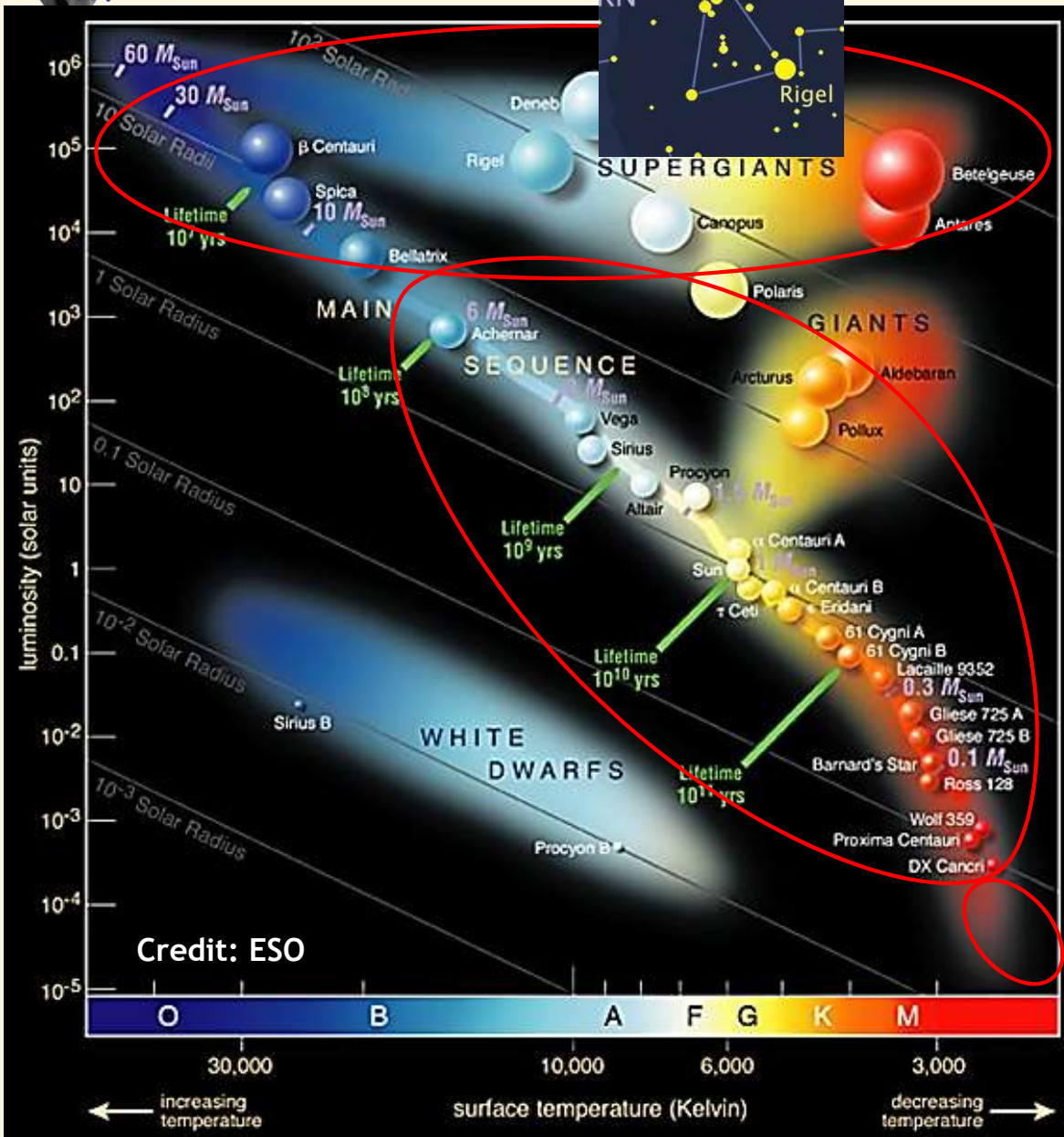
W/W_k : rotational frequency in units of critical one



massive stars as progenitors of high redshift GRBs:

- ✓ early work: Bromm & Loeb 2002, Ciardi & Loeb 2001, Kulkarni et al. 2000, Djorgovski et al. 2001, Lamb & Reichart 2000
- ✓ At low metallicity stars are expected to be rotating faster because of weaker stellar winds
- ✓ weaker winds also possible for stars with significant magnetic fields (Petit et al. 2017, Keszthelyi et al. 2019). Roughly 10% of O-stars possess significant B-fields in their outer layers.

Massive vs intermediate-/low-mass stars



- ▶ massive stars ($M_{\text{ZAMS}} > 8 M_{\text{sun}}$)
 - ▶ short life-times (few to 20 million years)
 - ▶ end products: core-collapse SNe (sometimes as slow GRBs) → neutron stars, black holes (or even complete disruption in case of pair-instability SNe)
 - ▶ Grav. waves from BH mergers!
- ▶ intermediate-/low-mass stars ($0.1 \dots 0.8 M_{\text{sun}} < M_{\text{ZAMS}} < 8 M_{\text{sun}}$)
 - ▶ long life-times (0.1 to 100 billion years)
 - ▶ end products: White dwarfs, SNIa
- ▶ brown dwarfs ($13 M_{\text{Jupiter}} < M < 0.08 M_{\text{sun}}$)
 - ▶ ‘failed stars’, core temperature not sufficient to ignite H-fusion
 - ▶ instead, Deuterium and, for higher masses, Lithium fusion

ZAMS: Zero Age Main Sequence

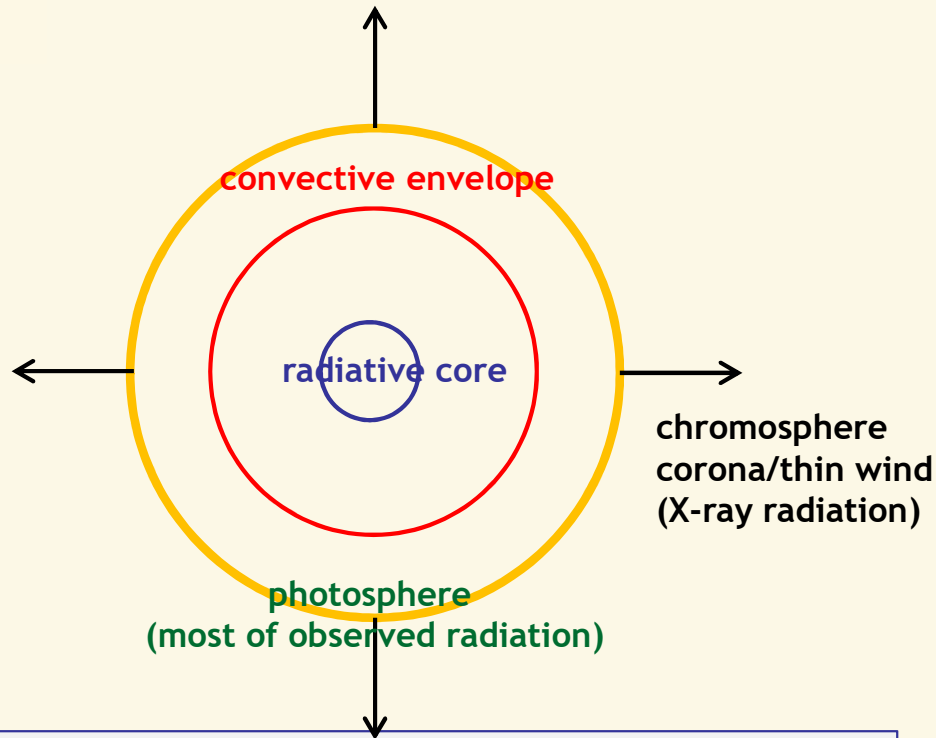
MS: Main sequence, core hydrogen burning

low-mass vs. massive star during the MS



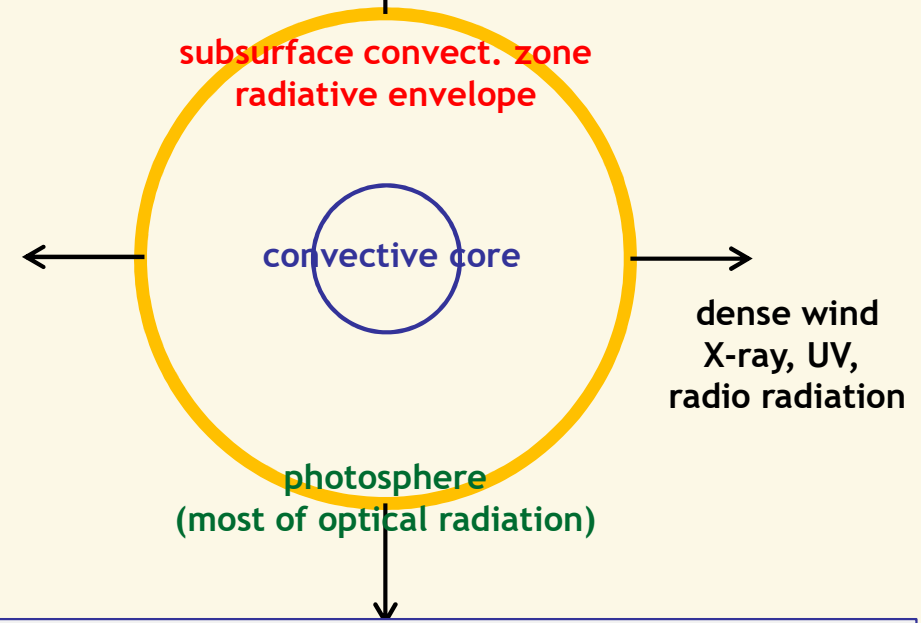
USM

low-mass star (e.g., the sun)



- radiative core
- convective envelope
- geometrically thin photosphere
 - level populations collisionally dominated
→ Local thermodynamic equilibrium (LTE):
Saha-Boltzmann population
- chromosphere (temp. begins to increase outwards)
- hot corona/thin wind (very low mass-loss rate)

massive star
factor 10...20 larger than sun
factor 10^4 ... 10^6 more luminous than sun



- convective core
- radiative envelope with subsurface convection zone
- geometrically thin photosphere + dense wind
 - level populations radiatively dominated
→ non-LTE level population
(all transition-probabilities need to be
calculated explicitly)

NOTE: evolved objects (red giants and supergiants) and brown dwarfs are fully convective

Examples for current research:

Observations ...



USM

- ▶ ... in all frequency bands
- ▶ both earthbound and via satellites
- ▶ Gamma-rays (Integral), X-rays (Chandra, XMM-Newton), (E)UV (IUE, HST), optical (VLT), IR (VLT, →JWST, →ELT), (sub-) mm (ALMA), radio (VLA, VLBI, →SKMA) ...
- ▶ photometry, spectroscopy, polarimetry, interferometry, gravitational waves (aLIGO!)
- ▶ current telescopes allow for high S/N and high spatial resolution
- ▶ because of their high luminosity, massive stars can be spectroscopically observed not only in the Milky Way, but also in many Local Group (and beyond) galaxies ('record-holder': blue supergiants in NGC 4258 at a distance of ≈ 7.8 Mpc, Kudritzki+ 2013)

Abbreviations:

IUE – International Ultraviolet Explorer

HST – Hubble Space Telescope

VLT – Very Large Telescope (Cerro Paranal, Chile)

JWST – James Webb Space Telescope

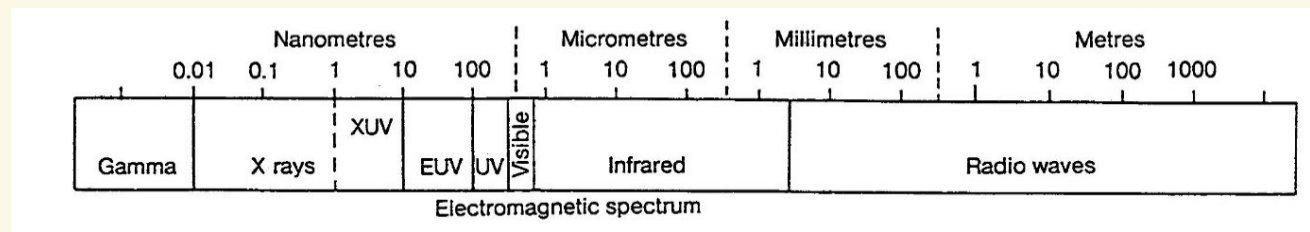
ELT – Extremely Large Telescope (Cerro Armazones, Chile, 20 km away from VLT))

ALMA – Atacama Large Millimeter/Submillimeter Array (Chajnantor-Plateau, Chile, 5000 m altitude)

VLA – Very Large Array (Socorro, New Mexico, USA)

VLBI – Very Large Baseline Interferometer

SKMA – Square Kilometer Array (South Africa and Australia)

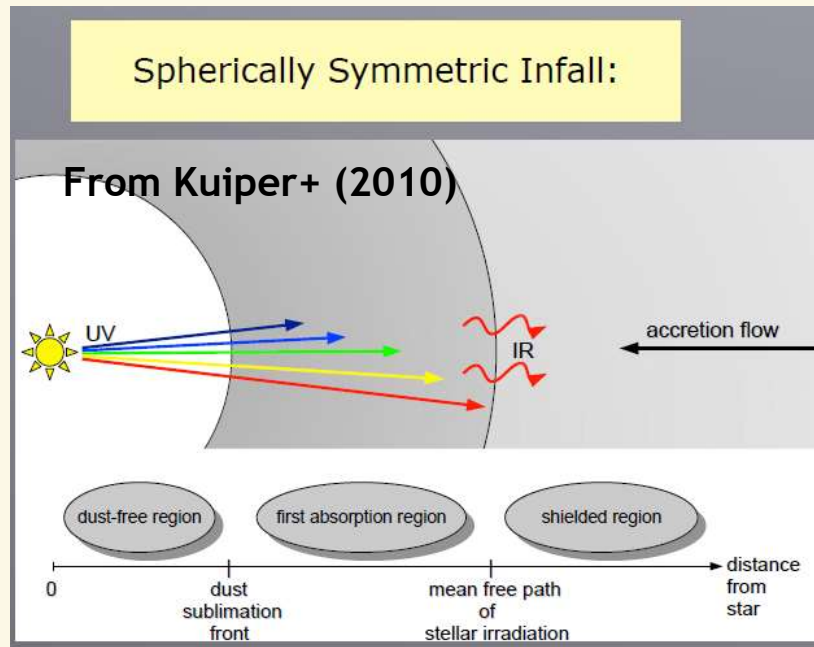


Examples for current research:

Star formation



- ▶ **Star formation** – formation of massive stars
 - ▶ until 2010, it was **not** possible to ‘make’ stars with $M > 40 M_{\text{sun}}$

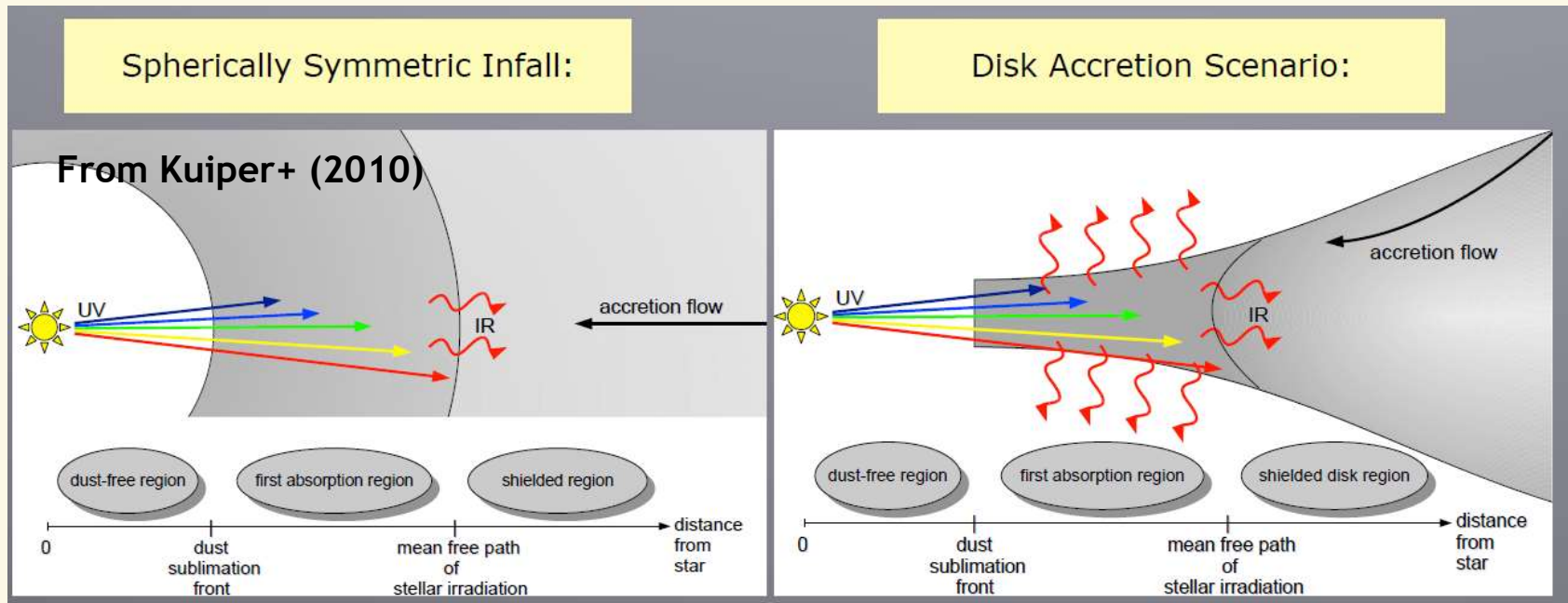


- ▶ **Radiation pressure barrier** for spherical infall:
when core becomes massive, high luminosity heats ‘first absorption region’, radiation pressure due to re-processed IR radiation stops and reverts accretion flow.

Examples for current research: Star formation



- ▶ **Star formation** – formation of massive stars
 - ▶ until 2010, it was **not** possible to ‘make’ stars with $M > 40 M_{\text{sun}}$



- ▶ **Radiation pressure barrier** for spherical infall: when core becomes massive, high luminosity heats ‘first absorption region’, radiation pressure due to re-processed IR radiation stops and reverts accretion flow.
- ▶ If accretion **via disk**, re-processes radiation-field becomes **highly anisotropic**, the radial component of the radiative acceleration becomes diminished, and further accretion becomes possible. **Stars with $M > 40 M_{\text{sun}}$ (... $140 M_{\text{sun}}$) can be formed.** (see work by R. Kuiper and collaborators)

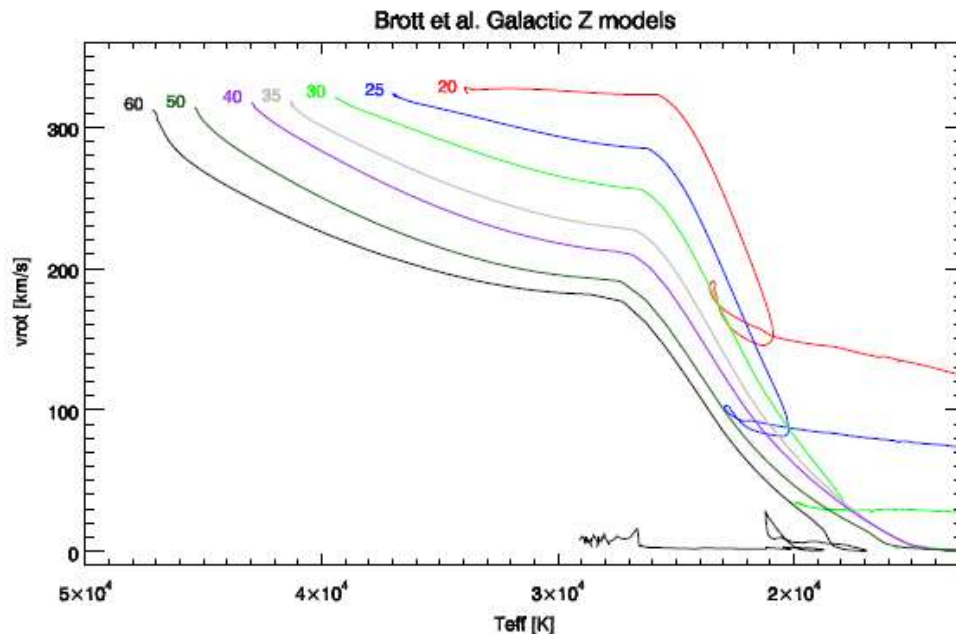
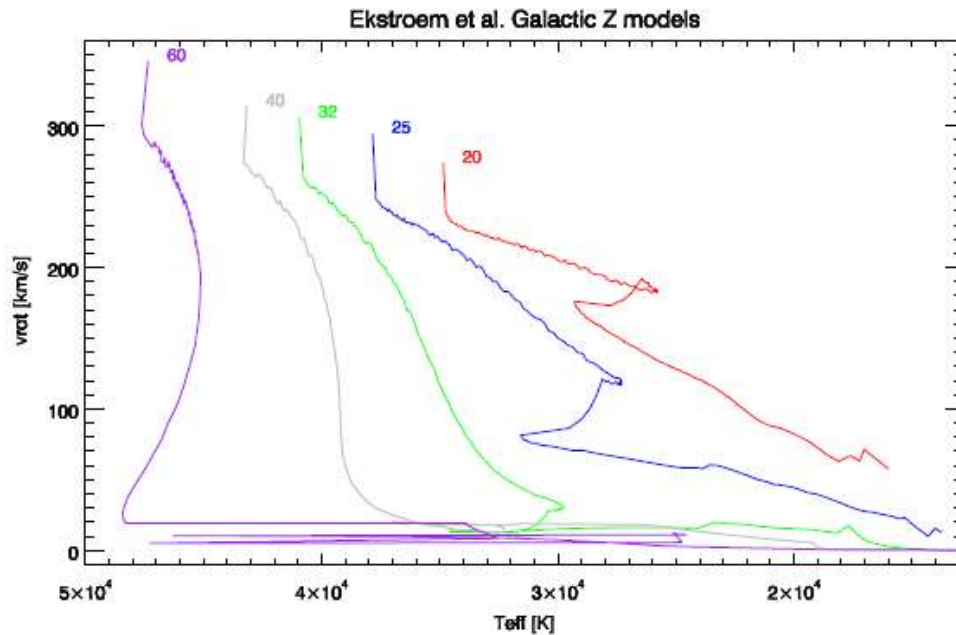
Examples for current research: Stellar structure and evolution



USM

- ▶ **Stellar structure and evolution**
 - ▶ implementation/improved description of various processes, e.g.,
 - ▶ impact of mass-loss and rotation (mixing!) in massive stars
 - ▶ generation and impact of B-fields
 - ▶ convection, mixing processes, core-overshoot etc. still described by simplified approximations in 1-D (e.g., diffusive processes), needs to be studied in 3-D (work in progress)

Examples for current research: Stellar structure and evolution



- ▶ v_{rot} vs. T_{eff} , for rotating Galactic massive-star models from Ekström+(2012, ‘GENEC’) and Brott+ (2011, ‘STERN’), with $v_{rot}(initial) \approx 300\text{km/s}$
- ▶ The main difference on the MS is due to the lack (Ekström) and presence (Brott) of *assumed* internal magnetic fields and the treatment of angular momentum transport.
- ▶ **NOTE: Even at main sequence, stellar evolution of massive stars unclear in many details!!!!**
- ▶ Do not believe in statements such as ‘stellar evolution is understood’

Examples for current research:

Stellar structure and evolution

- binarity fraction of Galactic stars
M-stars: 25%, solar-type: 45%, A-stars: 55% (Duchene & Kraus 2013, review)
O-stars in Galactic clusters:
 - 70% of all stars will interact with a companion during their lifetime (Sana+ 2012)
- THUS: needs to be included in evolutionary calculations
 - even more approximations regarding tidal effects, mass-transfer, merging ... (e.g., 'binary_c' by Izzard+ 2004/06/09)
- predictions on pulsations
 - frequency spectrum of excited oscillations
 - period-luminosity relations as a function of metallicity

Asteroseismology: Revealing the **internal** structure



non-radial pulsations: examples for different models

following slides adapted from C. Aerts (Leuven)

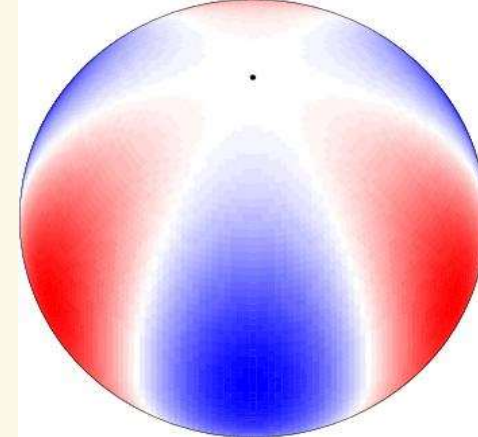
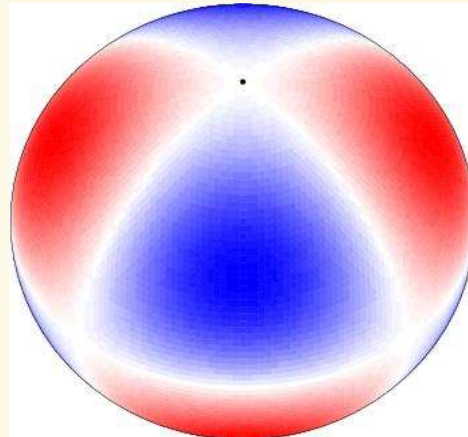
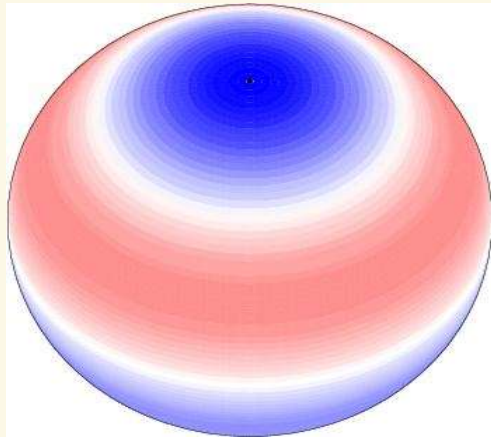
Blue: Moving towards Observer

Red: Moving away from Observer

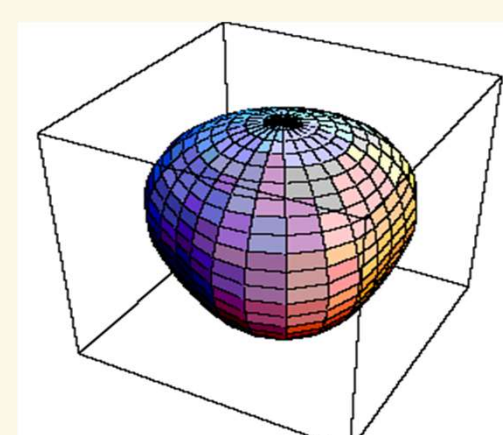
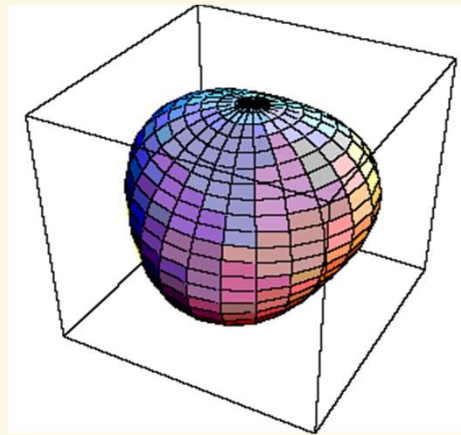
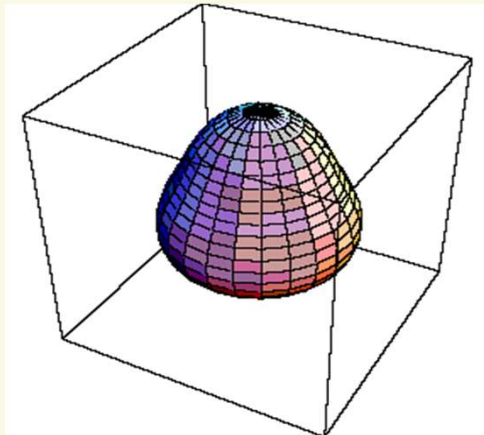
$(l,m) = (3,2)$
tesseral

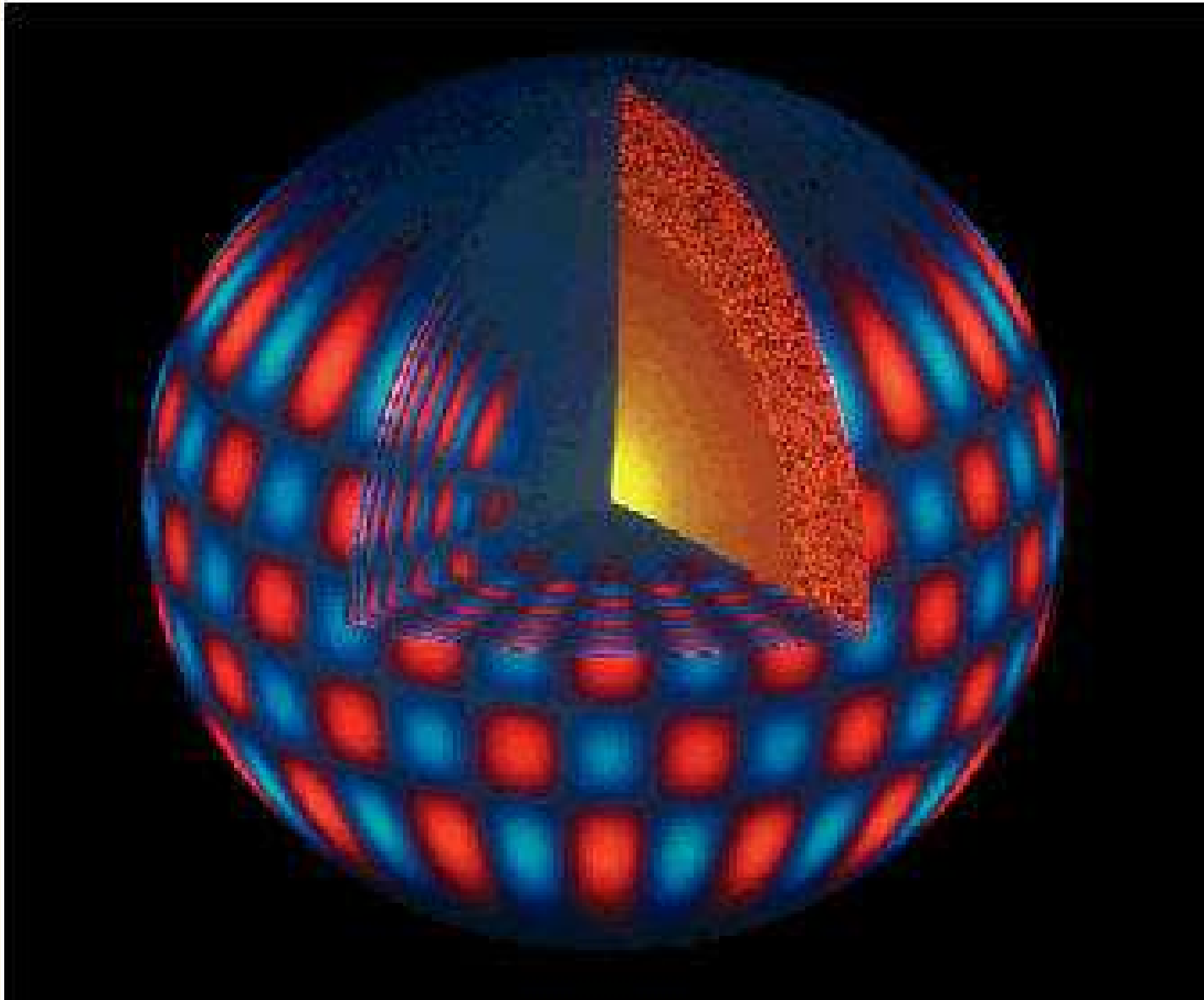
$(l,m) = (3,0)$
axisymmetric

$(l,m) = (3,3)$
sectoral



l : nonradial degree, m : azimuthal order





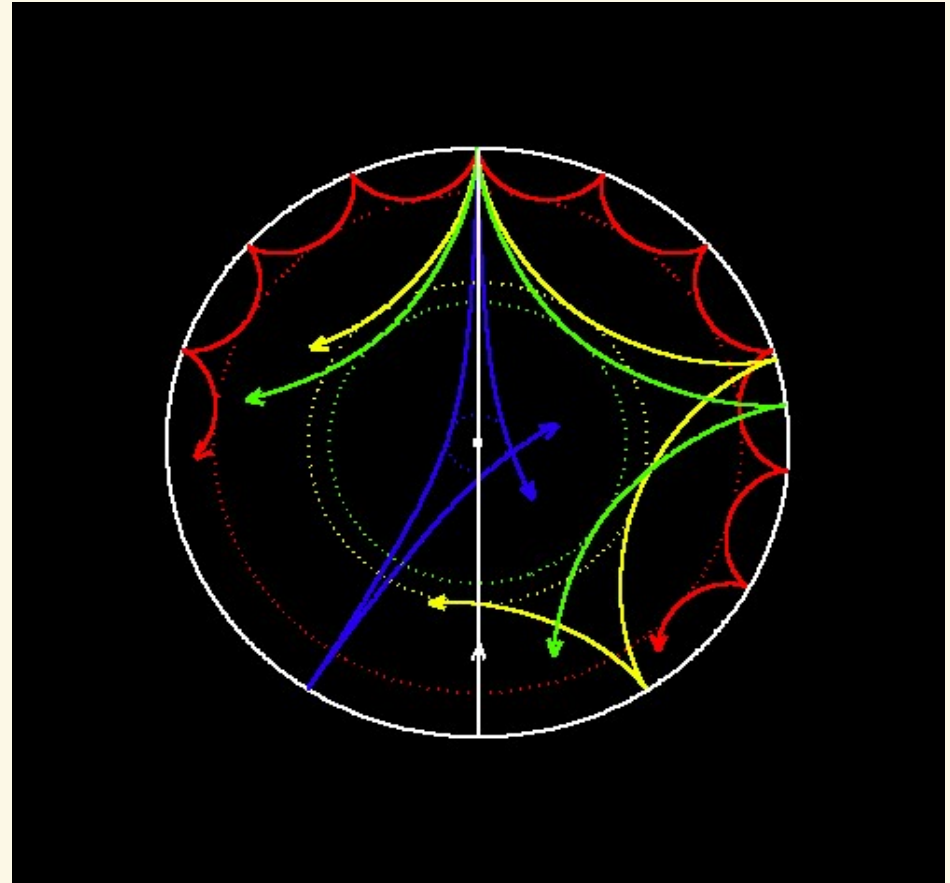
The oscillation pattern at the surface propagates in a continuous way towards the stellar centre.

Study of the surface patterns hence allows to characterize the oscillation throughout the star.

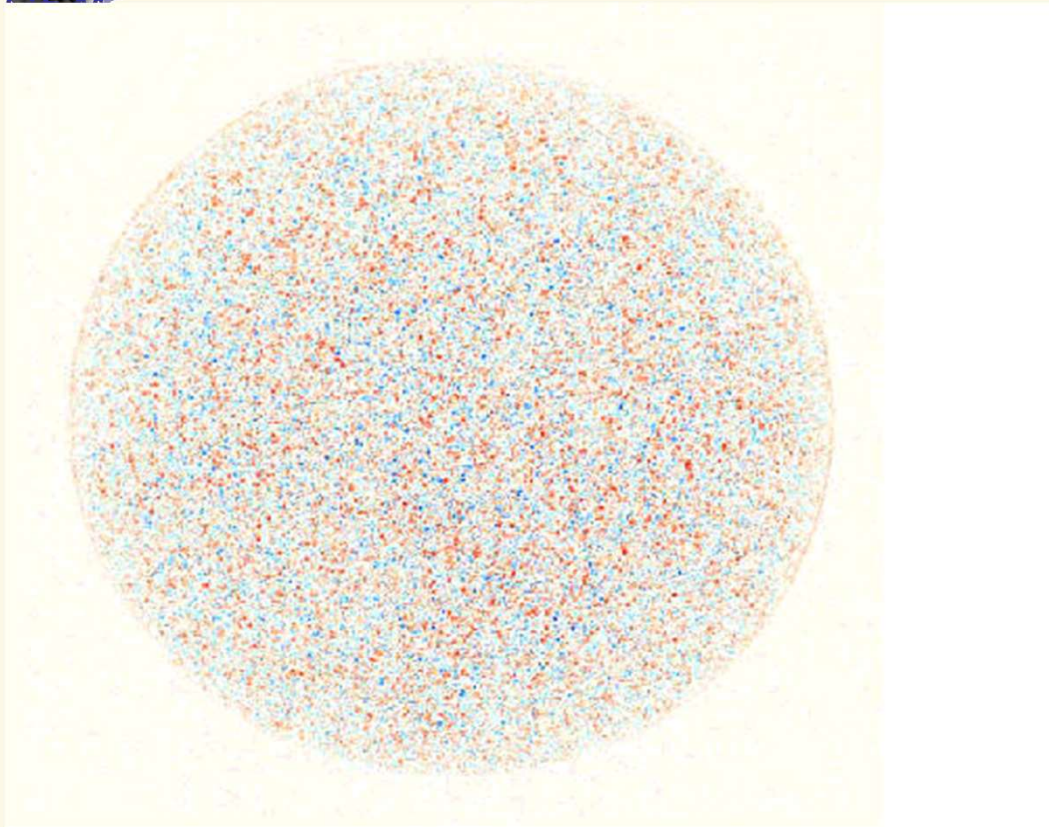


The oscillations are standing sound waves that are reflected within a cavity

Different oscillations penetrate to different depths and hence probe different layers



Doppler map of the Sun

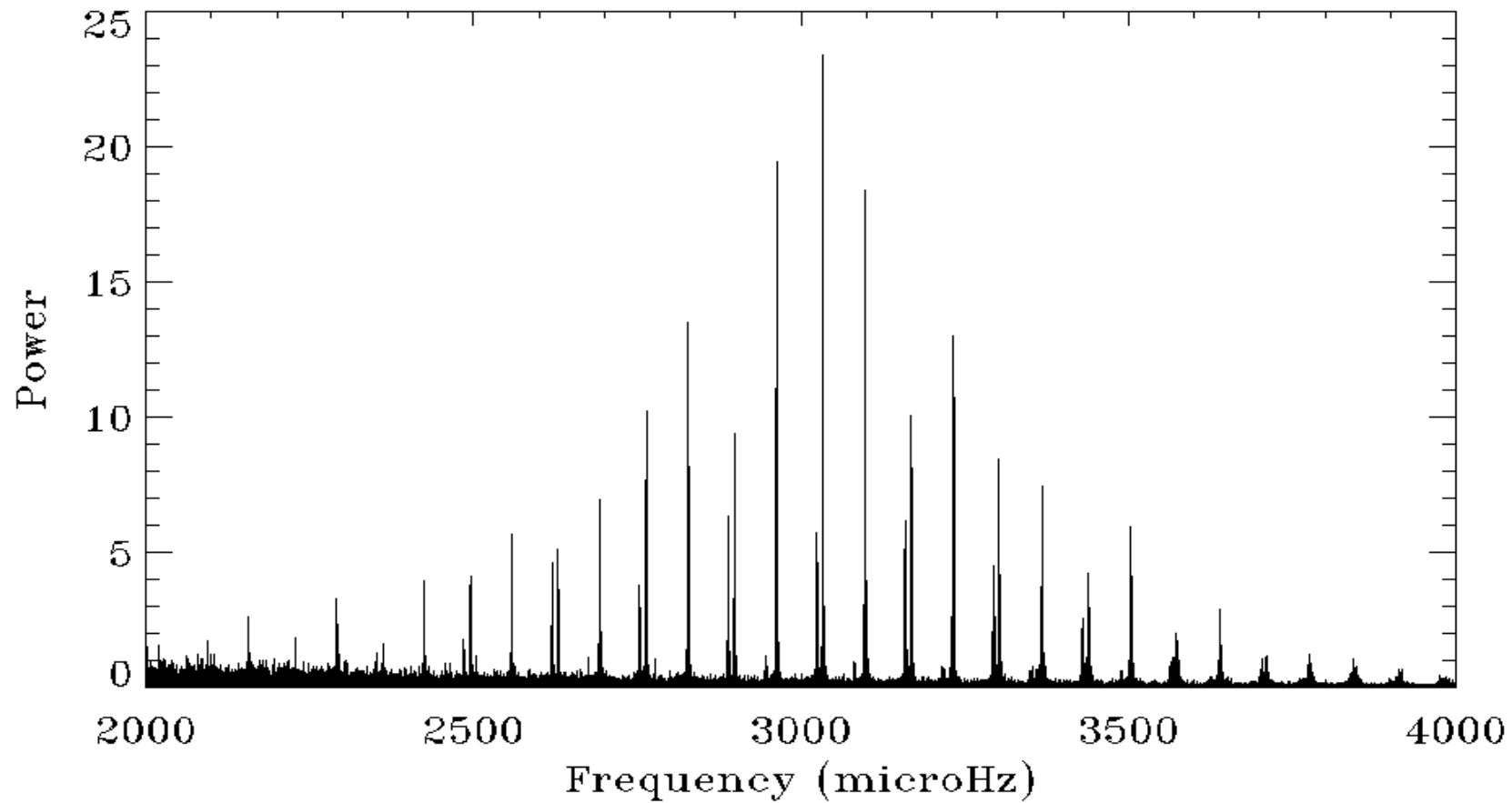


The Sun oscillates in thousands of non-radial modes with periods of ~ 5 minutes

The Dopplermap shows velocities on the order of some cm/s

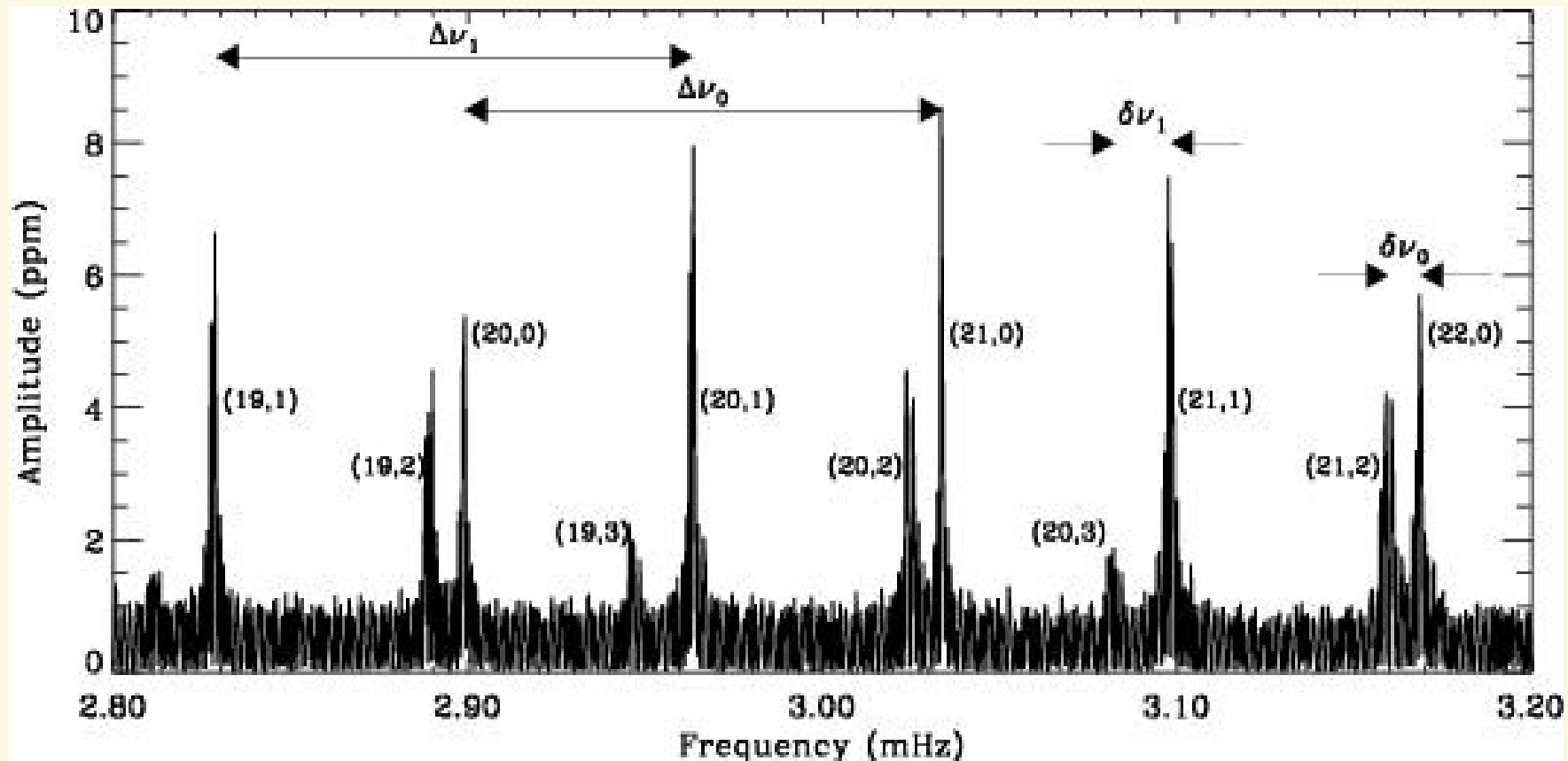


Solar frequency spectrum from ESA/NASA satellite SoHO: systematics !



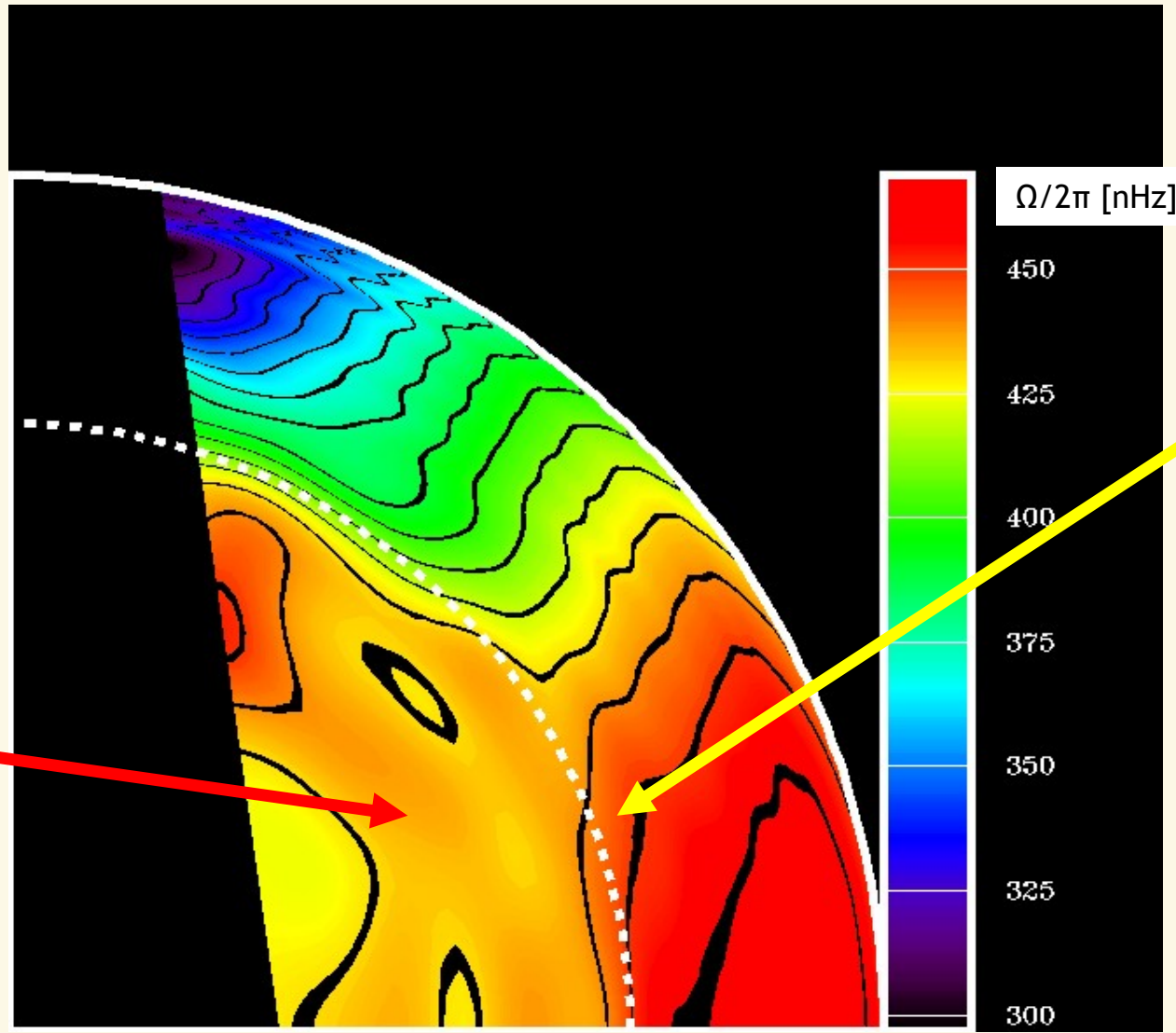


Frequency separations in the Sun



Result: internal sound speed and internal rotation could be determined very accurately by means of helioseismic data from SoHO

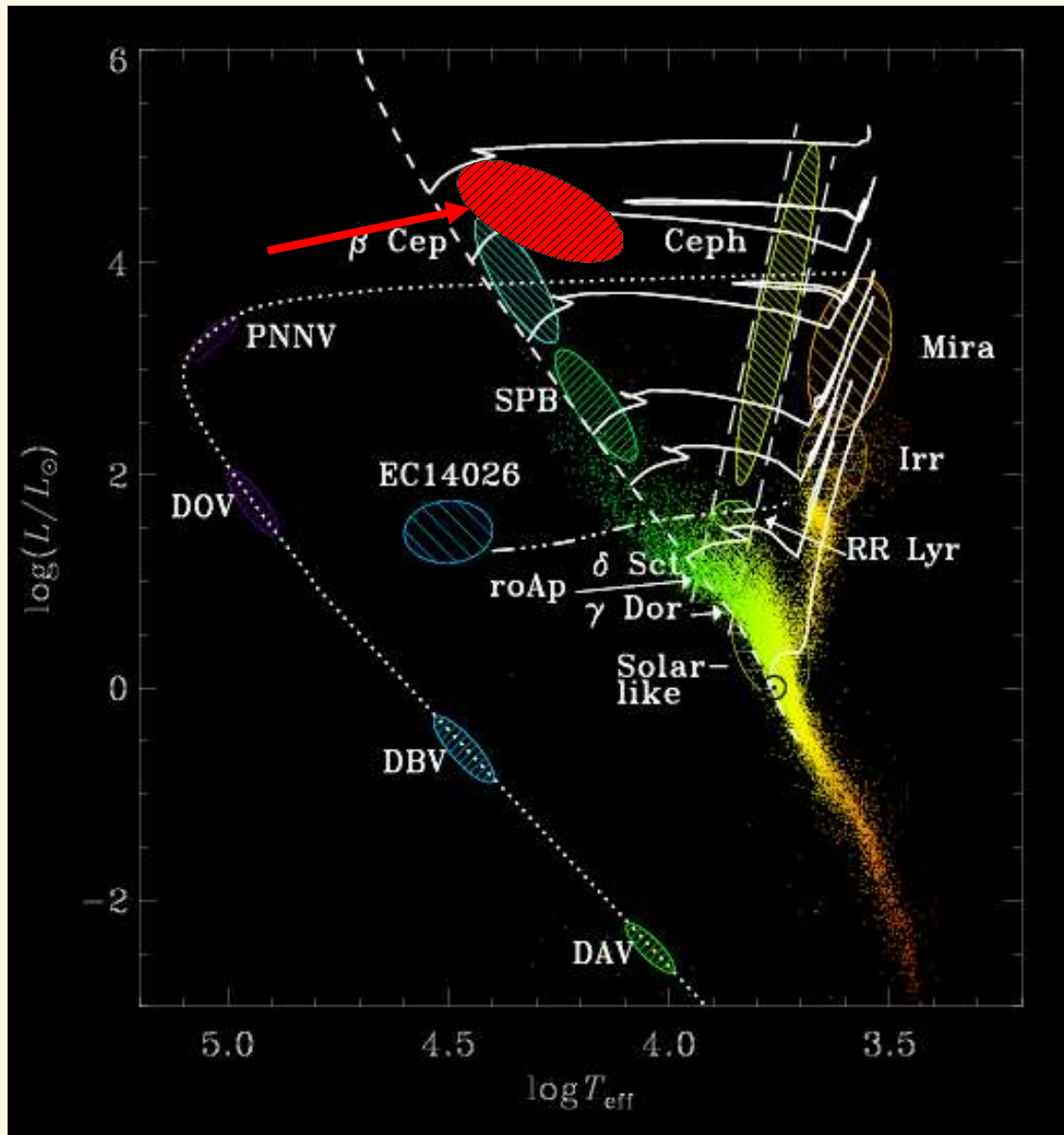
Internal rotation of the Sun



Solar interior has rigid rotation

Beginning of outer convection zone

... towards massive star seismology



(radial) order: number of nodes between center and surface

- β Cep:
low order p- and g-modes
- SPB
slowly pulsating B-stars
high order g-modes
- Hipparcos:
29 periodically variable
B-supergiants
(Waelkens et al. 1998)
- no instability region
predicted at that time
- nowadays: additional
region for high order
g-mode instability
- ➔ asteroseismology of
evolved massive stars
becomes possible

p-modes: pressure
g-modes: gravity
as restoring force

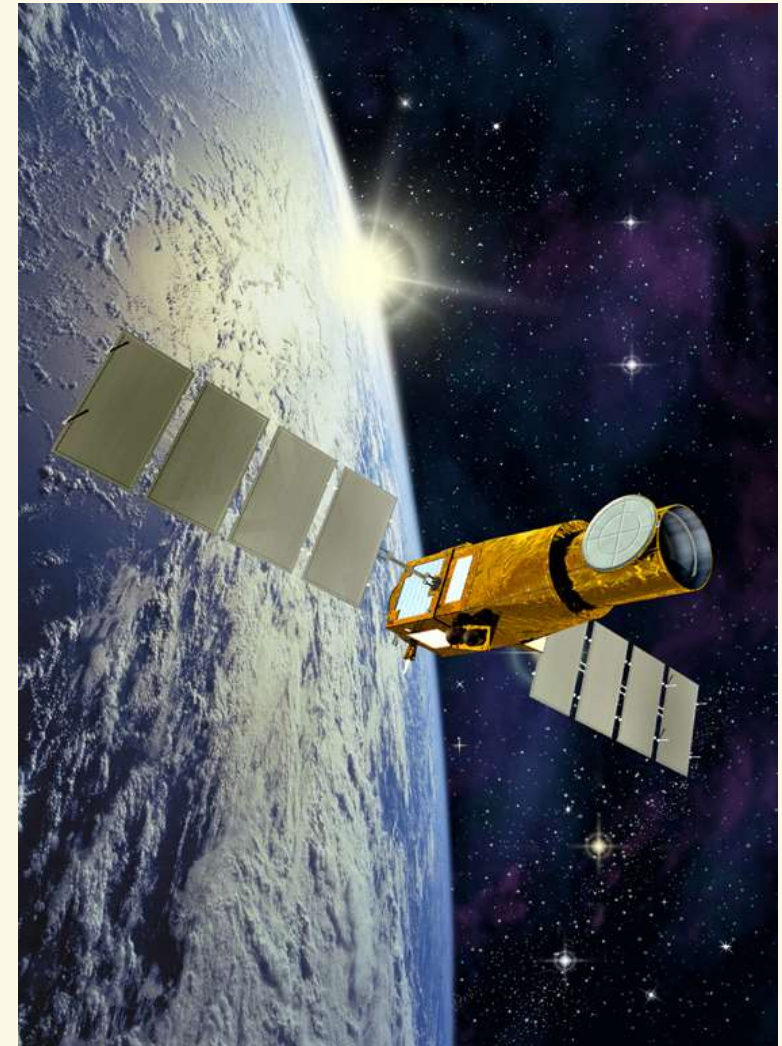
USM

COROT: **C**onvection **R**Otation and planetary **T**ransits
French-European mission (27 cm mirror)
launched December 2006

Kepler: NASA mission (1.2m mirror),
launched March 2009

MOST: Canadian mission
(65 x 65 x 30 cm, 70 kg)
launched in June 2003

BRITE-Constellation:
Canadian-Austrian-Polish mission
(six 20³ cm nano-satellites, 7kg)
first one launched 2013
asteroseismology of bright (= massive) stars



Examples for current research:

End phases of evolution



USM

▶ End phases

- ▶ evolutionary tracks towards ‘the end’
- ▶ models for SNe and Gamma-ray bursters
- ▶ models for neutron stars and white dwarfs
- ▶ accretion onto black holes
- ▶ X-ray binaries (‘normal’ star + white dwarf/neutron star/black hole)
- ▶ synthetic spectra of SN-remnants in various phases
- ▶ observations (now including gravitational waves) and comparison with theory
 - ▶ first detection of aLIGO was the merger of two black holes with masses around $30 M_{\text{sun}}$ (Abbott et al. 2016)
 - ▶ Corresponding theoretical scenario published **just before announcement of detection** (Marchant+ 2016), predicting one BH merger for 1000 cc-SNe, and a high detection rate with aLIGO

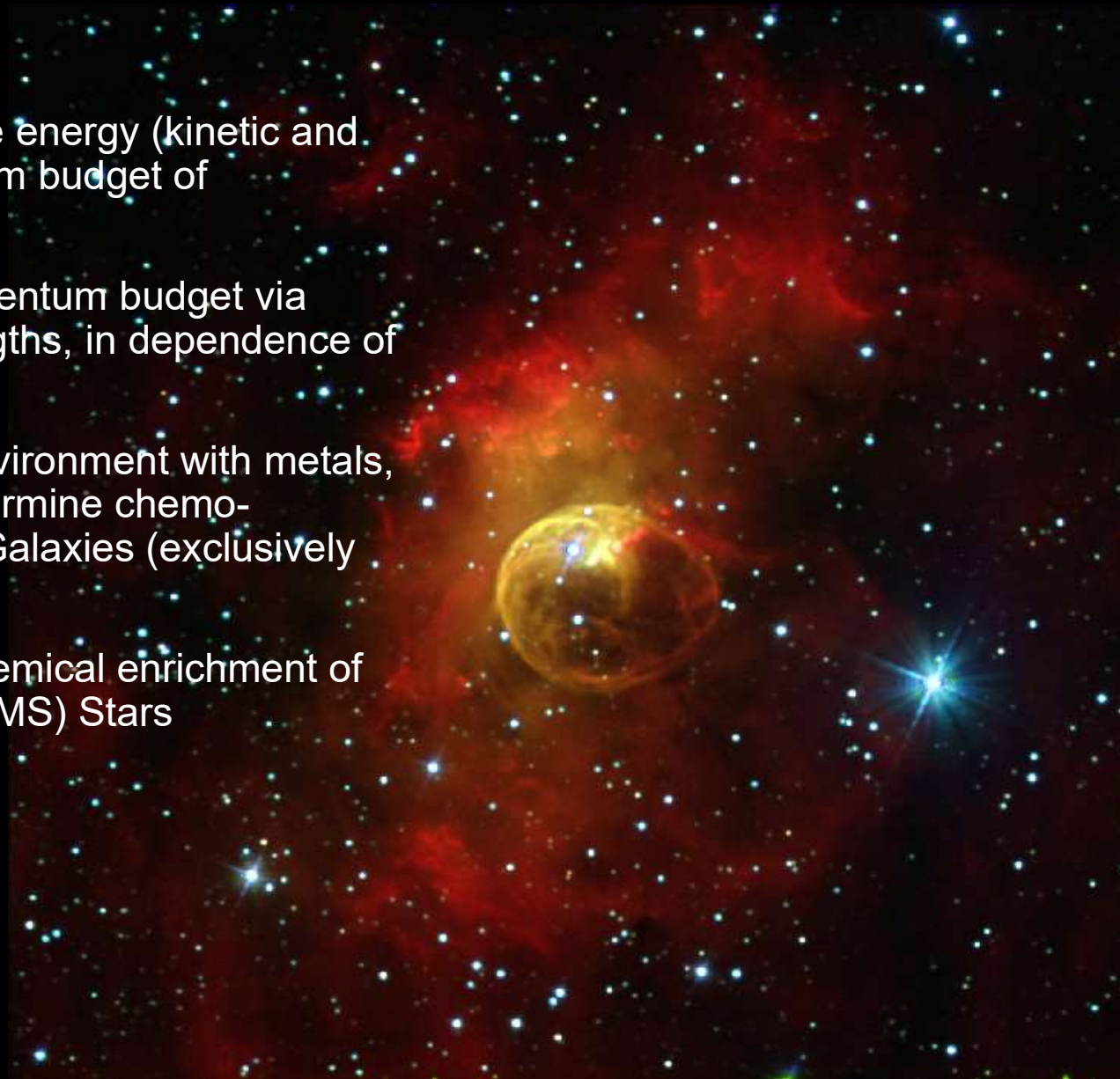
Examples for current research: Impact on environment

- cosmic re-ionization and chemical enrichment
- chemical yields (due to SNe and winds)
- ionizing fluxes (for HII regions)
- Planetary nebulae (excited by hot central stars)
- impact of winds on ISM (energy/momentum transfer, triggering of star formation)
- stars and their (exo)planets

Feedback

- massive stars determine energy (kinetic and radiation) and momentum budget of surrounding ISM
- kinetic energy and momentum budget via winds (of different strengths, in dependence of evolutionary status)
- massive stars enrich environment with metals, via winds and SNe, determine chemo-dynamical evolution of Galaxies (exclusively before onset of SNe Ia)
 - in particular: first chemical enrichment of Universe by First (VMS) Stars

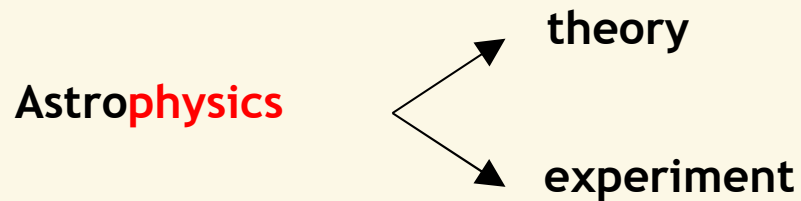
→“FEEDBACK”



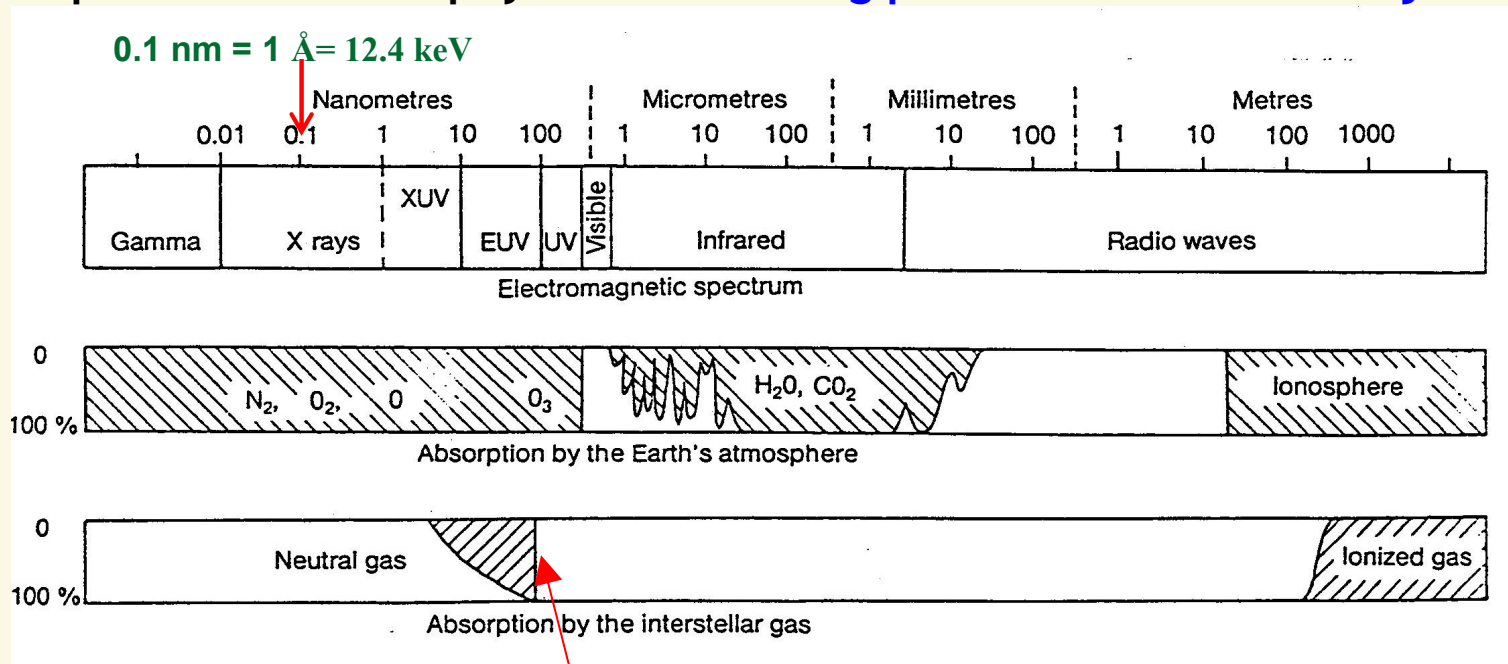
Bubble Nebula
(NGC 7635)
in Cassiopeia

wind-blown
bubble around
BD+602522
(O6.5III_f)

Chap. 2 – Quantitative spectroscopy



Experiment in astrophysics = **Collecting photons from cosmic objects**



hydrogen Lyman edge

$$1 \text{ \AA} = 10^{-8} \text{ cm} = 10^{-4} \text{ \mu m (micron)}; \quad 1 \text{ nm} = 10 \text{ \AA}$$

Collecting: earthbound and via satellites!

Note: Most of these photons originate from the atmospheres of **stellar**(-like) objects.

Even galaxies consist of stars!



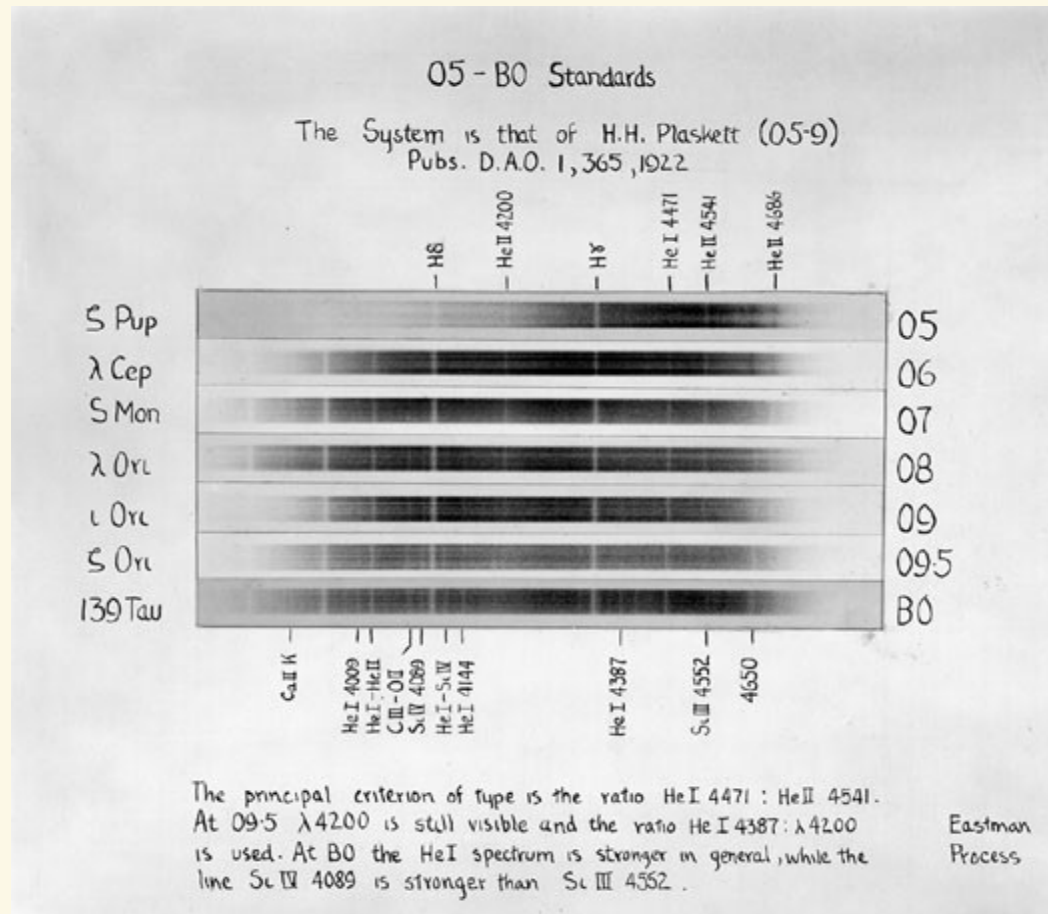
Astrophys. monographs, Univ. Chicago Press (1943)



AN ATLAS OF STELLAR SPECTRA

WITH AN OUTLINE OF SPECTRAL CLASSIFICATION

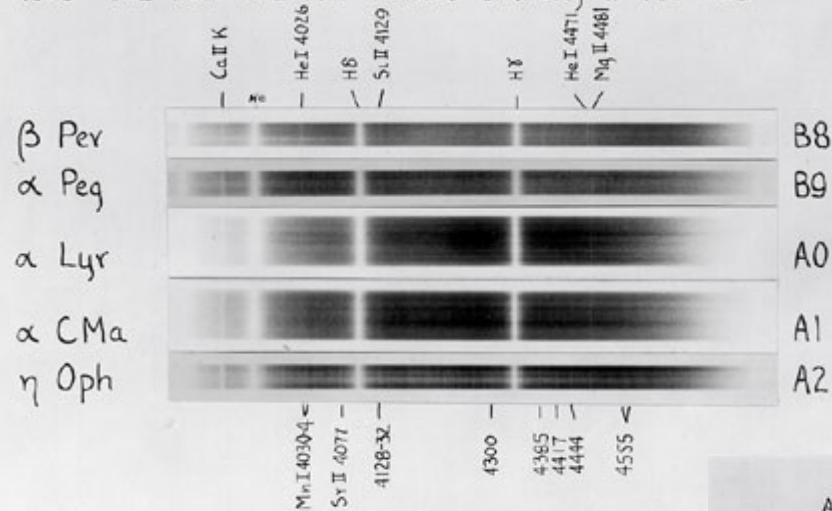
Morgan, Keenan, Kellman





Main Sequence B8-A2

He I 4026, which is equal in intensity to K in the B8 dwarf β Per, becomes fainter at B9 and disappears at A0. In the B9 star α Peg He I 4026 = Si II 4129. He I 4471 behaves similarly to He I 4026.



The singly ionized metallic lines are progressively stronger and η Oph than in α Lyr. The spectral type is determined by ratios: B8, B9: He I 4026: Ca II K, He I 4026: Si II 4129, He I 4471: Mg II 4481: 4385, Si II 4129: Mn I 4030-4.

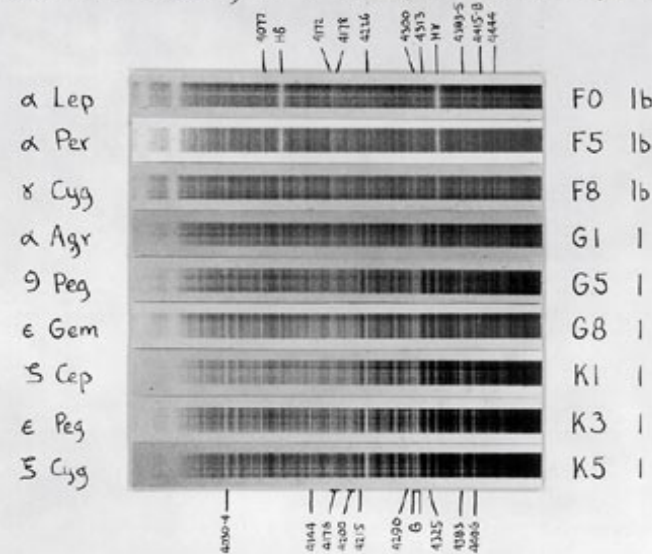
Empirical system

=>

Physical system

Supergiants FO-K5

Accurate spectral types of supergiants cannot be determined by direct comparison with normal giants and dwarfs. It is advisable to compare supergiants with a standard sequence of stars of similar luminosity. Useful criteria are: Intensity of H lines (FO-G5), change in appearance



of G-band (FO-K5), growth of λ 4226 relative to H ϵ (F5-K5), growth of the blend at λ 4406 (G5-K5), and the relative intensity of the two blends near λ 4200 and λ 4176 (K1-K5). The last-named blend degenerates into a line at K5. (Cramer H ϵ -Speed Spectra)

Digitized spectra

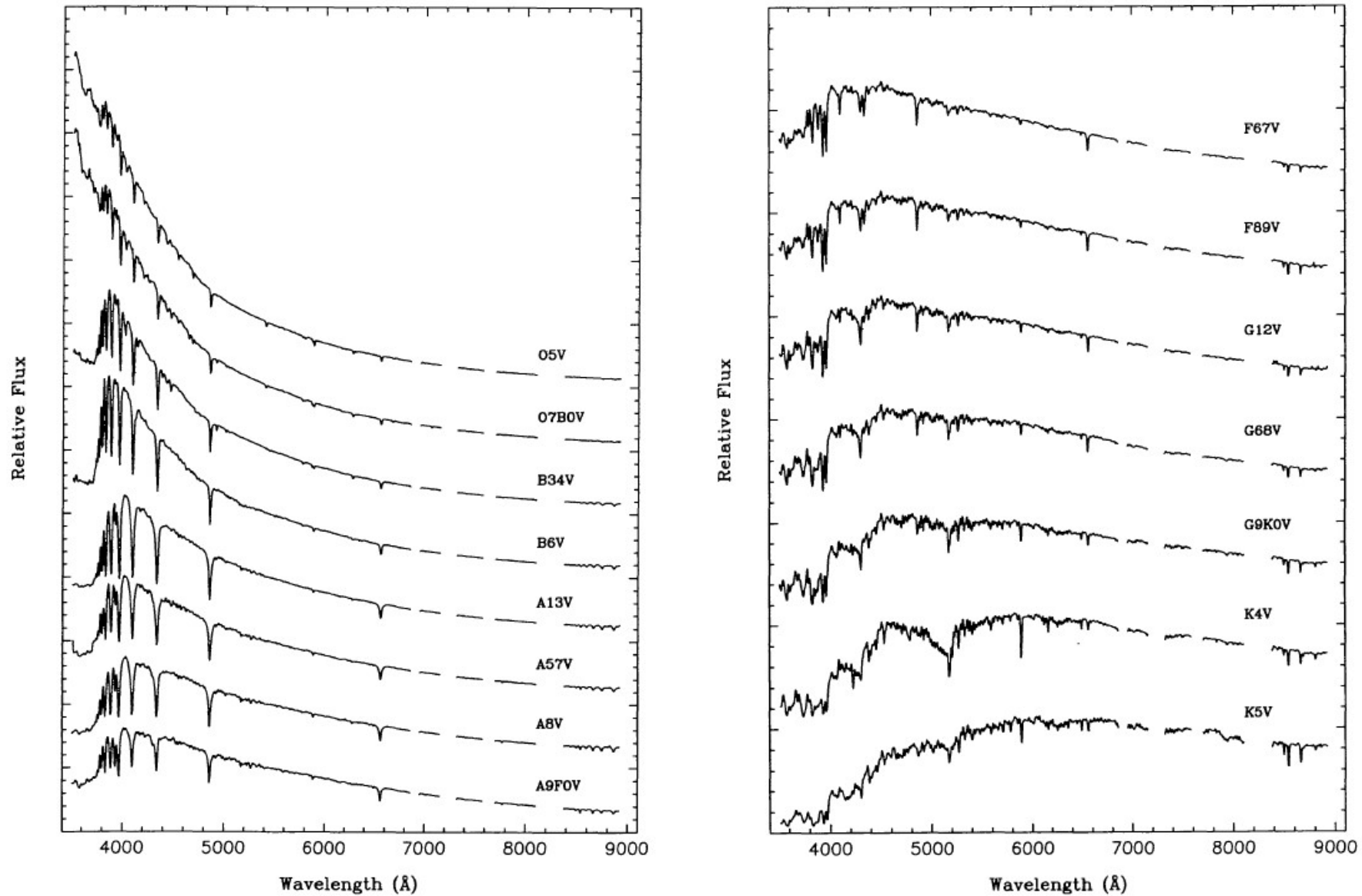


FIG. 1.—Dwarf-type library stars. Near-IR gaps are excised telluric absorption bands. All spectra have been normalized to 100 at 5450 Å. Major tick marks on “Relative Flux” axis are separated by 100 relative units. The M dwarf library stars are displayed with the M giants in Fig. 3.
from Silva & Cornell, 1992

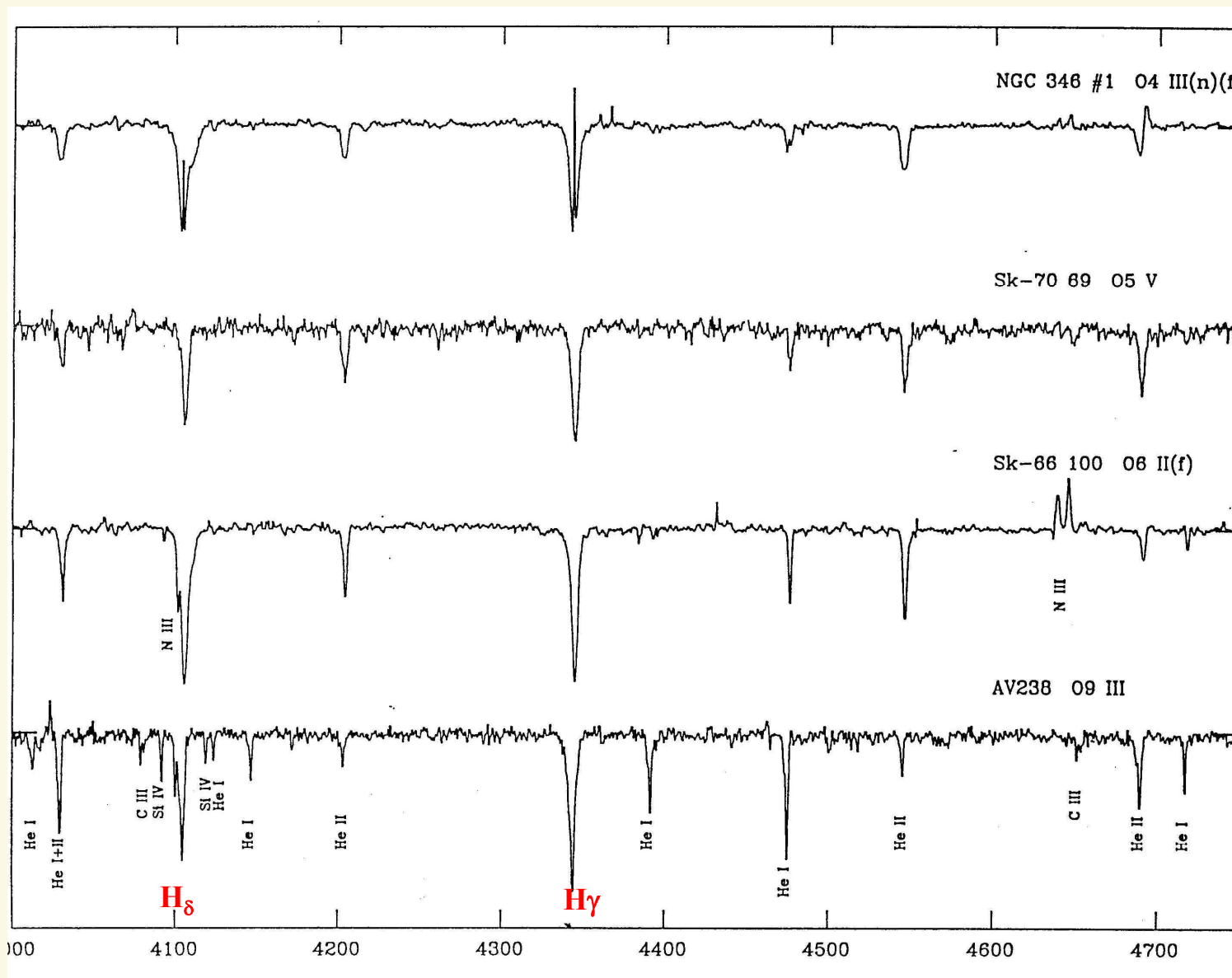
Spectral lines formed in (quasi-)hydrostatic atmospheres



ESO 3.6m
CASPEC

$\Delta\lambda \approx 0.5\text{\AA}$
S/N 30...70

(Walborn
et al., 1995)



SMC

LMC

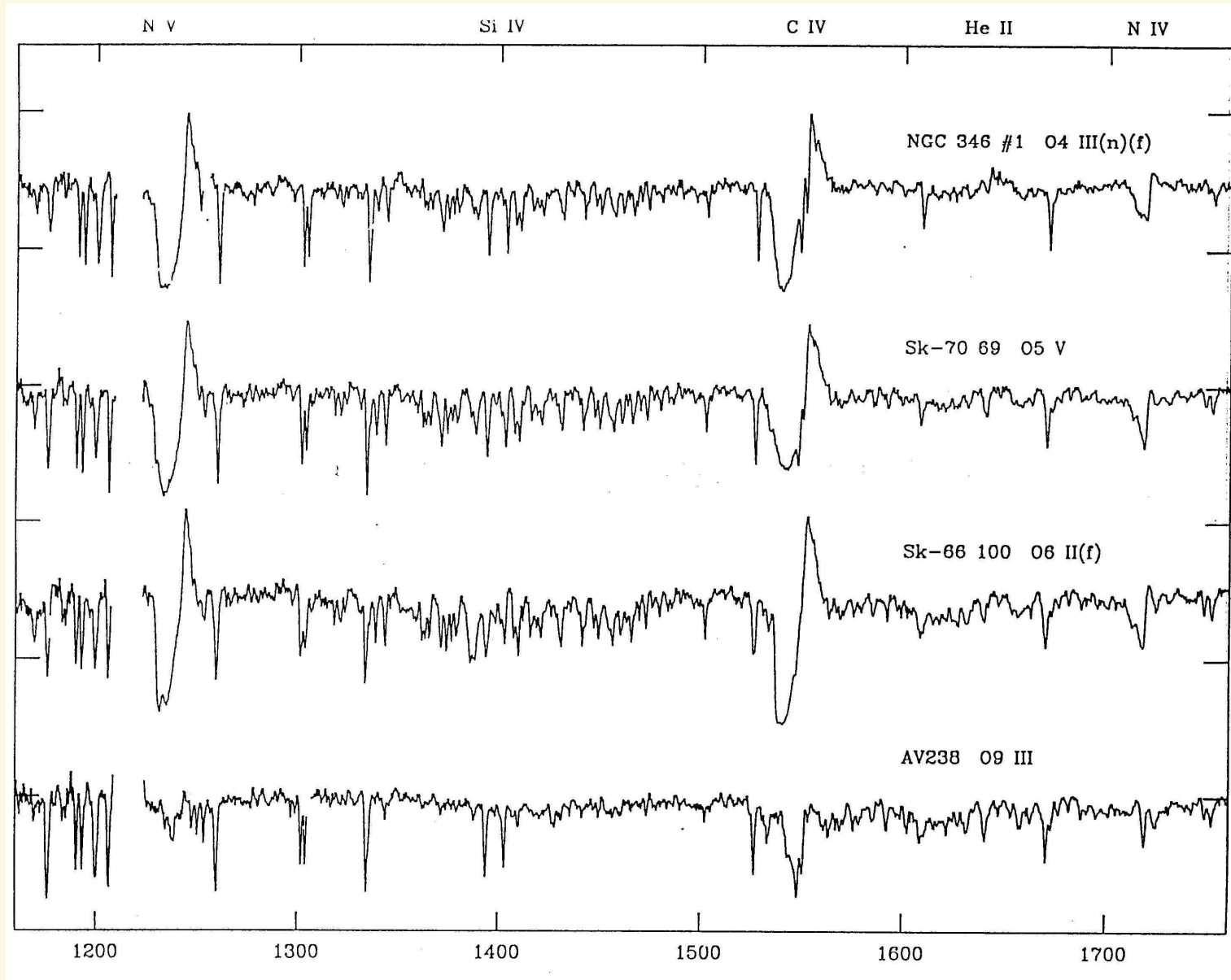
LMC

SMC

P-Cygni lines formed in hydrodynamic atmospheres



HST-FOS



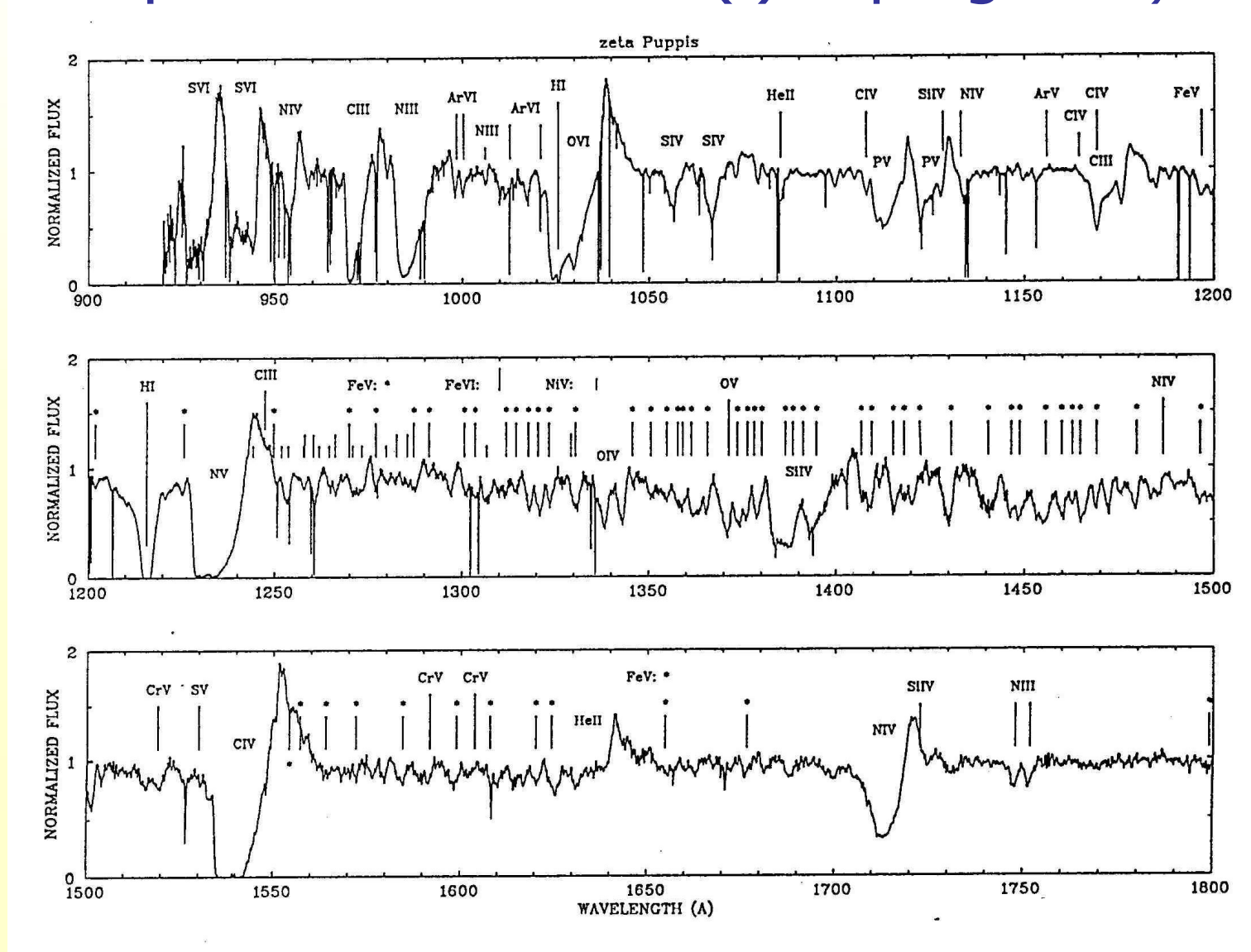
SMC

LMC

LMC

SMC

UV spectrum of the O4I(f) supergiant ζ Pup



montage of **Copernicus** ($\lambda < 1500 \text{ \AA}$, high res. mode, $\Delta\lambda \approx 0.05 \text{ \AA}$, Morton & Underhill 1977) and **IUE** ($\Delta\lambda \approx 0.1 \text{ \AA}$) observations

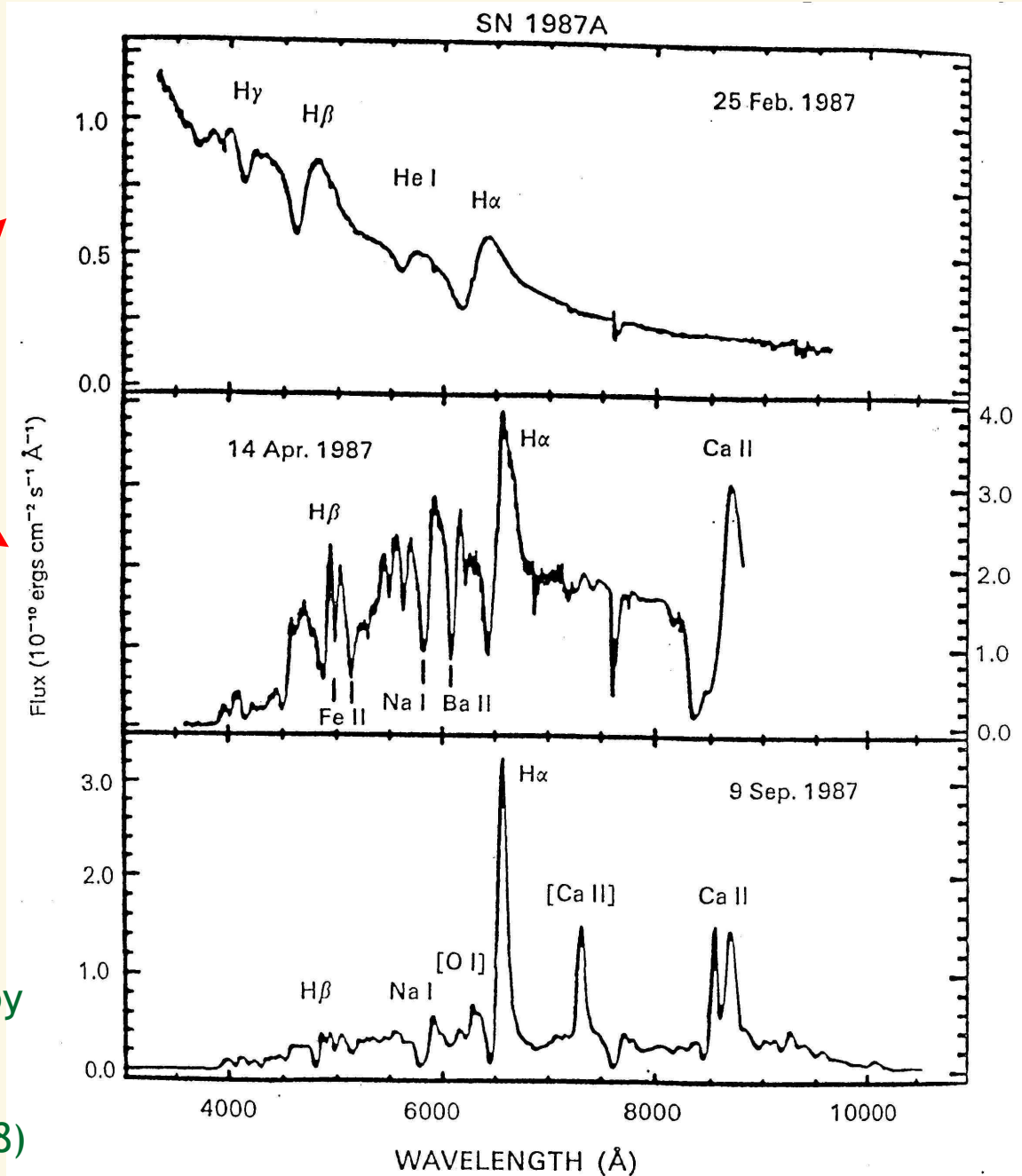
Supernova Type II in different phases



photospheric phase

transition to nebular phase

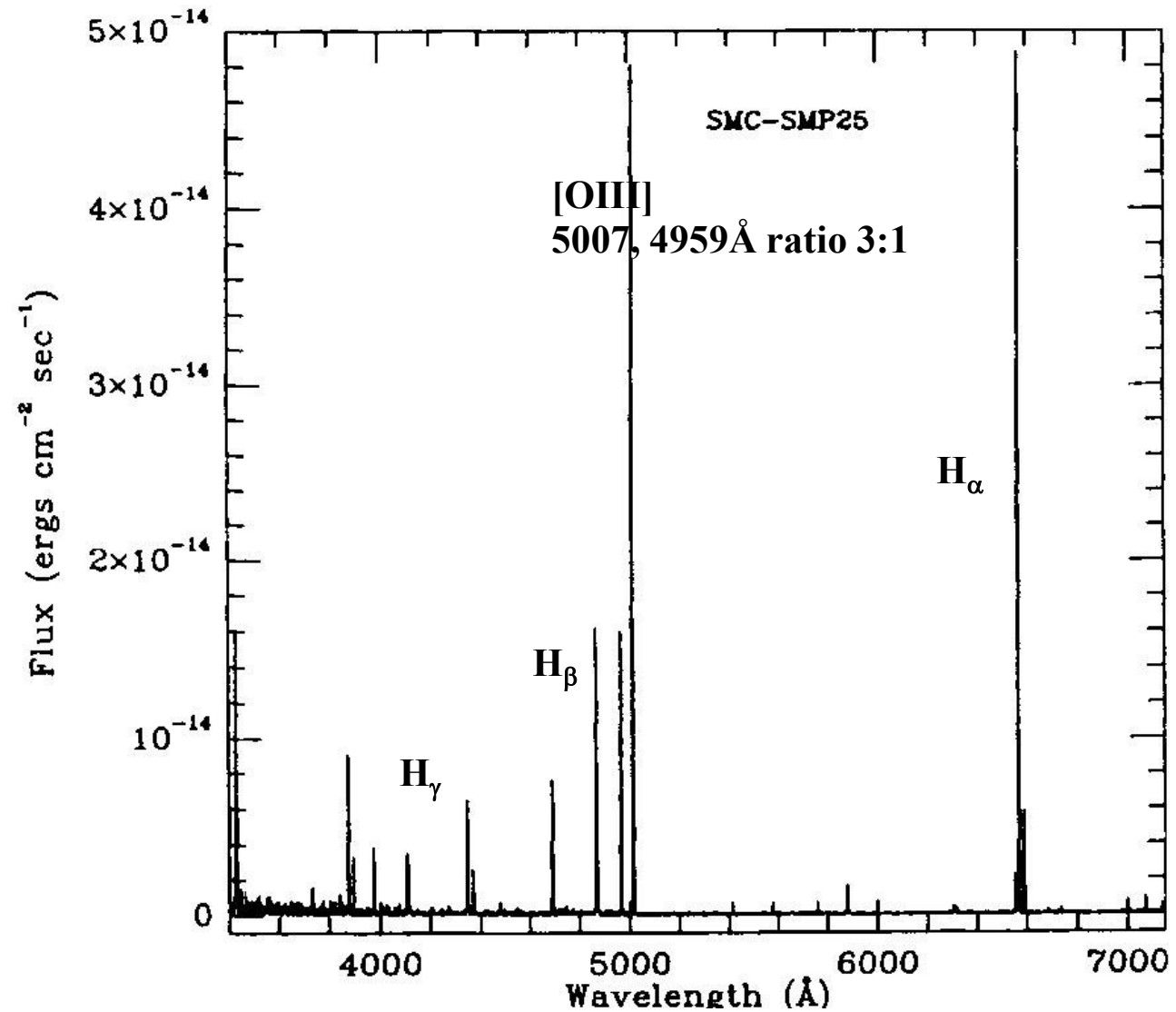
figure prepared by
Mark M. Phillips,
reproduced from
McCray & Li (1988)



Spectrum of Planetary Nebula



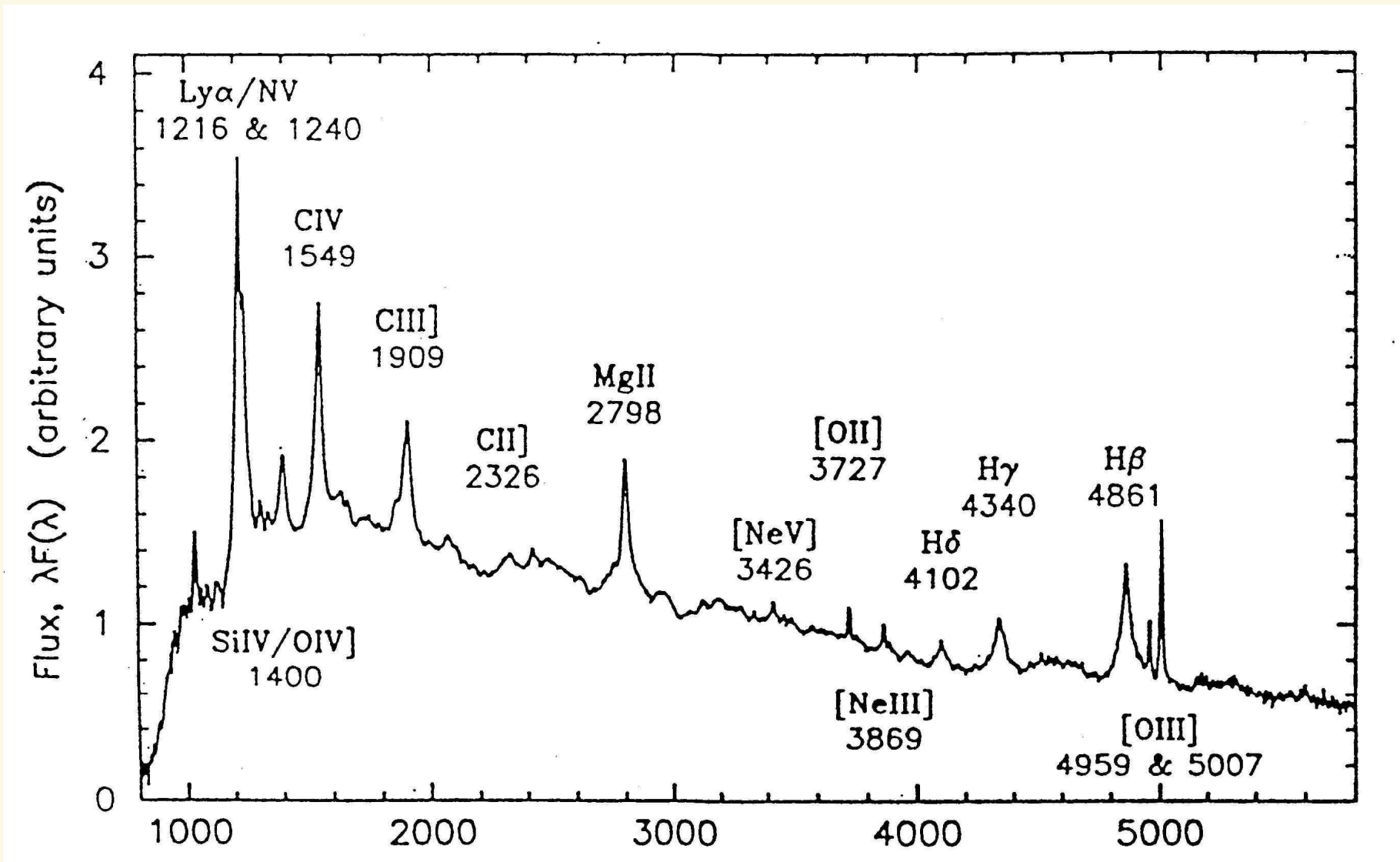
pure emission
line spectrum
with forbidden
lines of O III



From Meatheringham & Dopita, 1991, ApJS 75

FIG. 1a

Quasar spectrum in rest frame of quasar

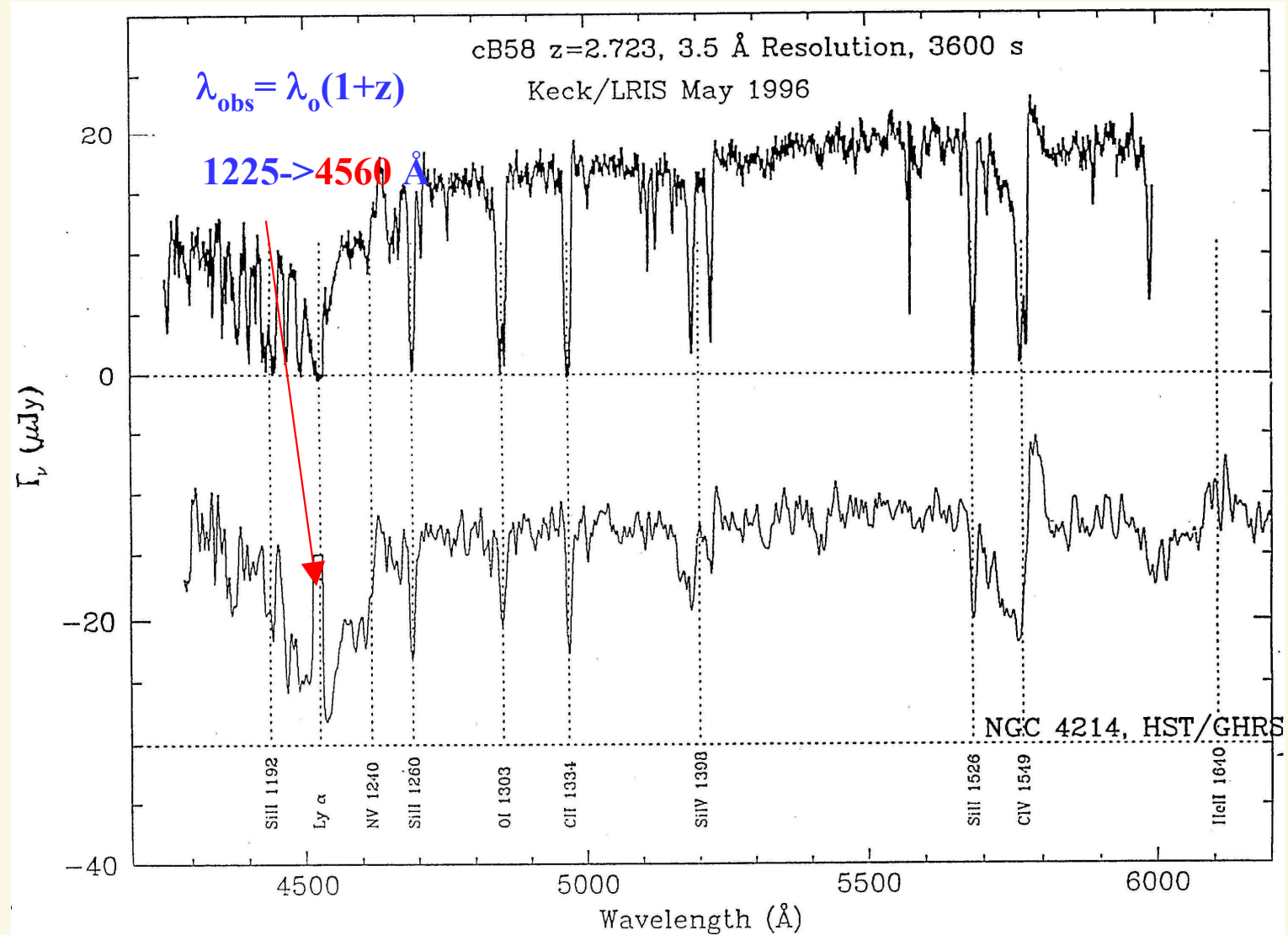


“UV”-spectra of starburst galaxies



galaxy at $z = 2.72$

local
starburst galaxy,
wavelengths shifted



From Steidel et al. (1997)

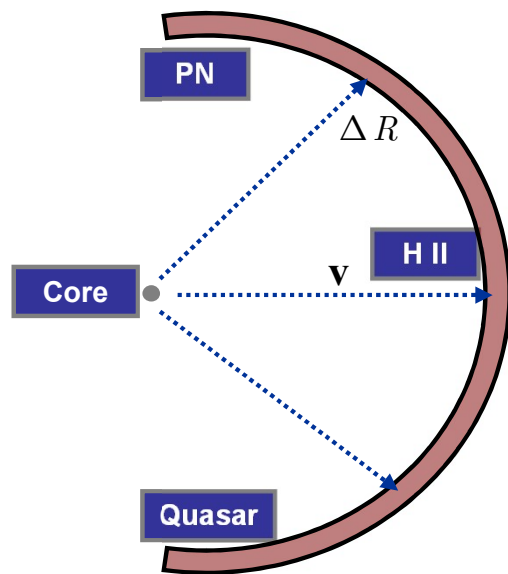
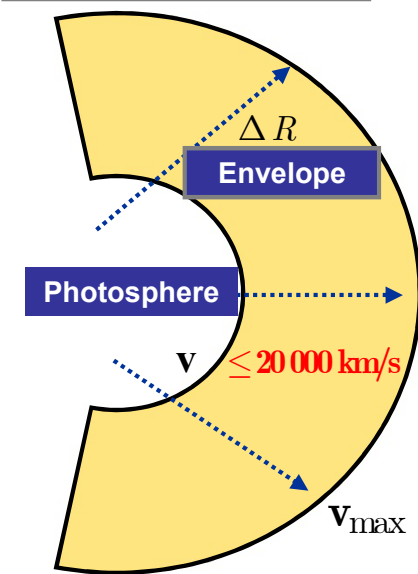
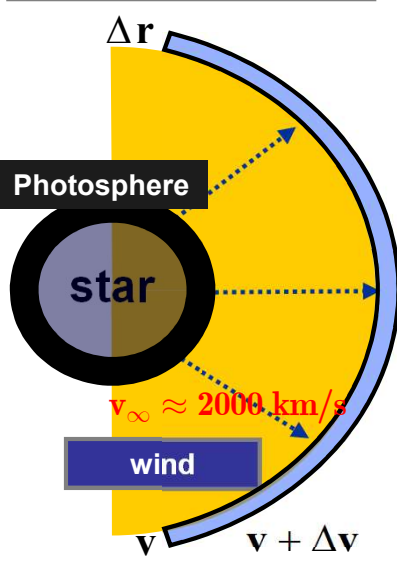
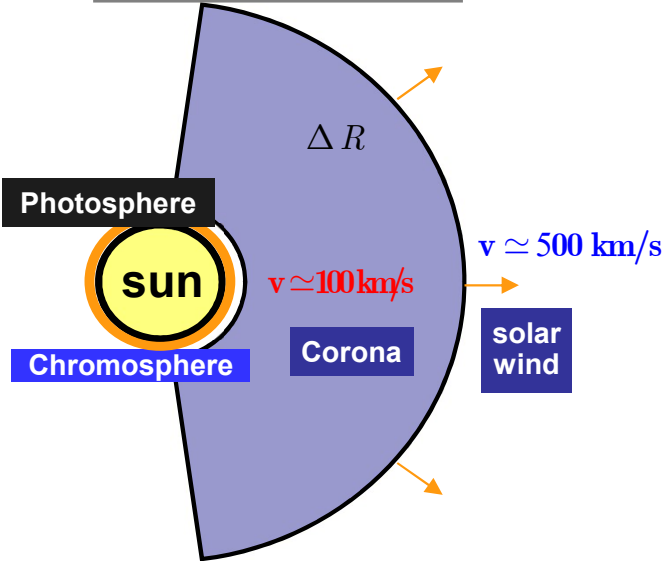
Atmospheres and nebulae - an overview

Sun

hot, massive star

Supernova Ia

Gaseous Nebula



Core:
 $M_{\odot} = 2 \cdot 10^{33} \text{ g}$
 $R_{\odot} = 7 \cdot 10^{10} \text{ cm}$
 $L_{\odot} = 4 \cdot 10^{33} \text{ erg s}^{-1}$

Photosphere:
 $\Delta R \sim 200 \text{ km}$
 $T \sim 6000 \text{ K}$
 $n \sim 10^{15} \text{ cm}^{-3}$

Chromosphere:
 $\Delta R \sim 1000 \text{ km}$
 $T \sim 20000 \text{ K}$
 $n \sim 10^{12} \text{ cm}^{-3}$

Corona:
 $\Delta R \sim R_{\odot}$
 $T \sim 10^6 \text{ K}$
 $n \sim 2 \cdot 10^6 \text{ cm}^{-3}$

Core:
 $M \sim 50 M_{\odot}$
 $R \sim 20 R_{\odot}$
 $L \sim 10^5 \rightarrow 10^6 L_{\odot}$

Photosphere:
 $\Delta R / R \sim \Delta R_{\odot} / R_{\odot}$
 $T \sim 20000 \rightarrow 50000 \text{ K}$
 $n \sim 10^{14} \rightarrow 10^{12} \text{ cm}^{-3}$

Wind:
 $\Delta R \sim 100 R_*$
 $T \sim 0.9 \dots 0.3 \cdot T_{\text{eff}}$
 $n \sim 10^{12} \dots 10^8 \text{ cm}^{-3}$

Core:
 $M \sim 1.44 M_{\odot}$
 exploded
 $L_{\text{max}} \sim 10^{11} L_{\odot}$

Envelope:
 $\Delta R \sim 10^5 R_{\odot}$
 $T \sim 12000 \text{ K}$
 $n \sim 10^6 \text{ cm}^{-3}$

Core:
 $M_{\text{PN}} \sim 1 M_{\odot}$
 $M_{\text{H II}} \sim 50 \rightarrow 10^5 M_{\odot}$
 $M_{\text{Q}} \sim 10^9 \rightarrow 10^{11} M_{\odot}$
 $L_{\text{PN}} \sim 10^4 L_{\odot}$
 $L_{\text{H II}} \sim 10^6 L_{\odot}$
 $L_{\text{Q}} \sim 10^{12} L_{\odot}$

Envelope:
 $\Delta R \sim 0.1 \text{ pc (PN)}$
 $\Delta R \sim 10 \text{ pc (H II)}$
 $\Delta R \sim 10^3 \text{ pc (Quasar)}$

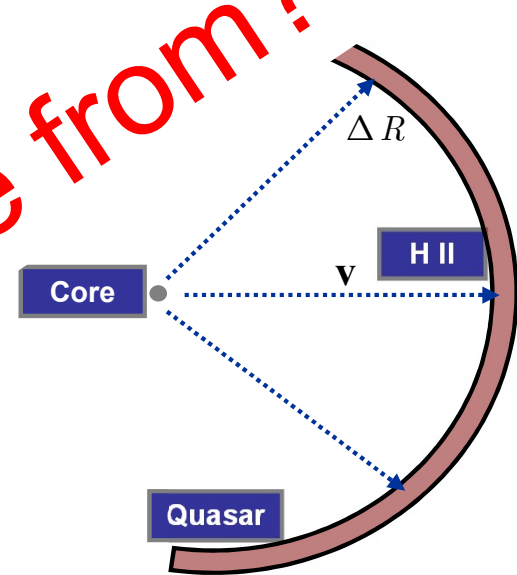
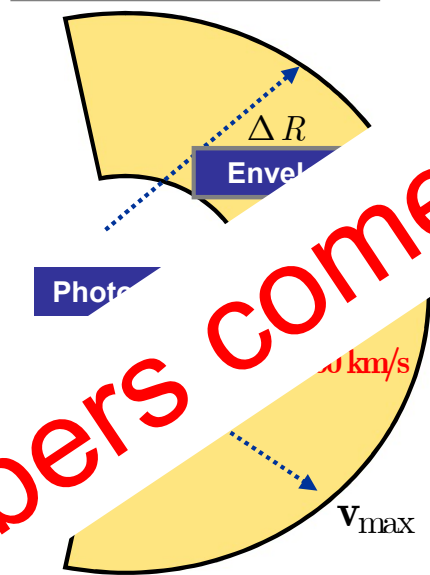
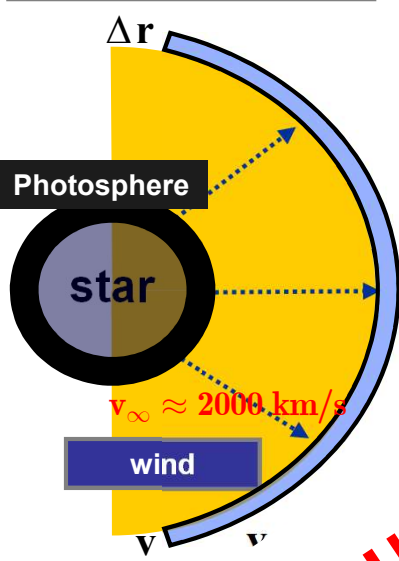
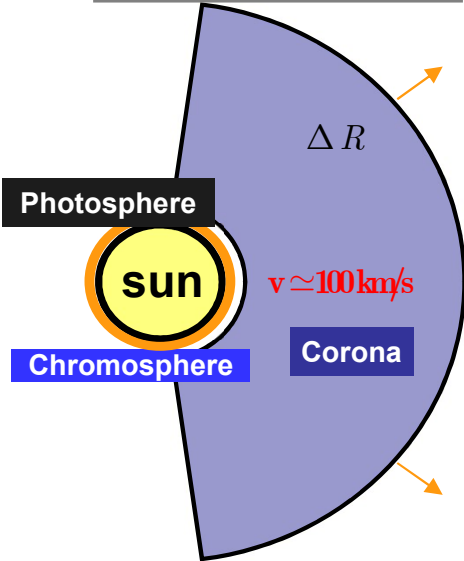
Stellar atmospheres - an overview

Sun

hot, massive star

Supernova Ia

Quasar



Core:
 $M_{\odot} = 2 \cdot 10^{33} \text{ g}$
 $R_{\odot} = 7 \cdot 10^{10} \text{ cm}$
 $L_{\odot} = 4 \cdot 10^{33} \text{ erg s}^{-1}$

Photosphere:
 $\Delta R \sim 200 \text{ km}$
 $T \sim 6000 \text{ K}$
 $n \sim 10^{15} \text{ cm}^{-3}$

Chromosphere:
 $\Delta R \sim R_{\odot}$
 $T \sim 10^6 \text{ K}$
 $n \sim 2 \cdot 10^6 \text{ cm}^{-3}$

Core:
 $M \sim 10^5 \rightarrow 10^6 L_{\odot}$

Photosphere:
 $\Delta R / R \sim \Delta R_{\odot} / R_{\odot}$
 $T \sim 20000 \rightarrow 50000 \text{ K}$
 $n \sim 10^{14} \rightarrow 10^{12} \text{ cm}^{-3}$

Wind:
 $\Delta R \sim 100 R_*$
 $T \sim 0.9 \dots 0.3 \cdot T_{\text{eff}}$
 $n \sim 10^{12} \dots 10^8 \text{ cm}^{-3}$

Core:
 $M \sim 1.44 M_{\odot}$
 exploded
 $L_{\text{max}} \sim 10^{11} L_{\odot}$

Envelope:
 $\Delta R \sim 10^5 R_{\odot}$
 $T \sim 12000 \text{ K}$
 $n \sim 10^6 \text{ cm}^{-3}$

Core:
 $M_{\text{PN}} \sim 1 M_{\odot}$
 $M_{\text{H II}} \sim 50 \rightarrow 10^5 M_{\odot}$
 $M_{\text{Q}} \sim 10^9 \rightarrow 10^{11} M_{\odot}$
 $L_{\text{PN}} \sim 10^4 L_{\odot}$
 $L_{\text{H II}} \sim 10^6 L_{\odot}$
 $L_{\text{Q}} \sim 10^{12} L_{\odot}$

Envelope:
 $\Delta R \sim 0.1 \text{ pc (PN)}$
 $\Delta R \sim 10 \text{ pc (H II)}$
 $\Delta R \sim 10^3 \text{ pc (Quasar)}$

Where do these numbers come from?

...gives insight into and understanding of our cosmos

Quantitative spectroscopy = quantitative diagnostics of spectra

- ▶ provides
 - ▶ **stellar properties**, mass, radius, luminosity, energy production, chemical composition, properties of outflows
 - ▶ **properties of (inter) stellar plasmas**, temperature, density, excitation, chemical comp., magnetic fields
- ▶ INPUT for stellar, galactic and cosmologic **evolution** and for stellar and galactic **structure**
- ▶ requires
 - ▶ **plasma physics**, plasma is "normal" state of atmospheres and interstellar matter (plasma diagnostics, line broadening, influence of magnetic fields,...)
 - ▶ **atomic physics/quantum mechanics**, interaction light/matter (micro quantities)
 - ▶ **radiative transfer**, interaction light/matter (macroscopic description)
 - ▶ **thermodynamics**, thermodynamic equilibria: TE, LTE (local), NLTE (non-local)
 - ▶ **hydrodynamics**, atmospheric structure, velocity fields, shockwaves,...

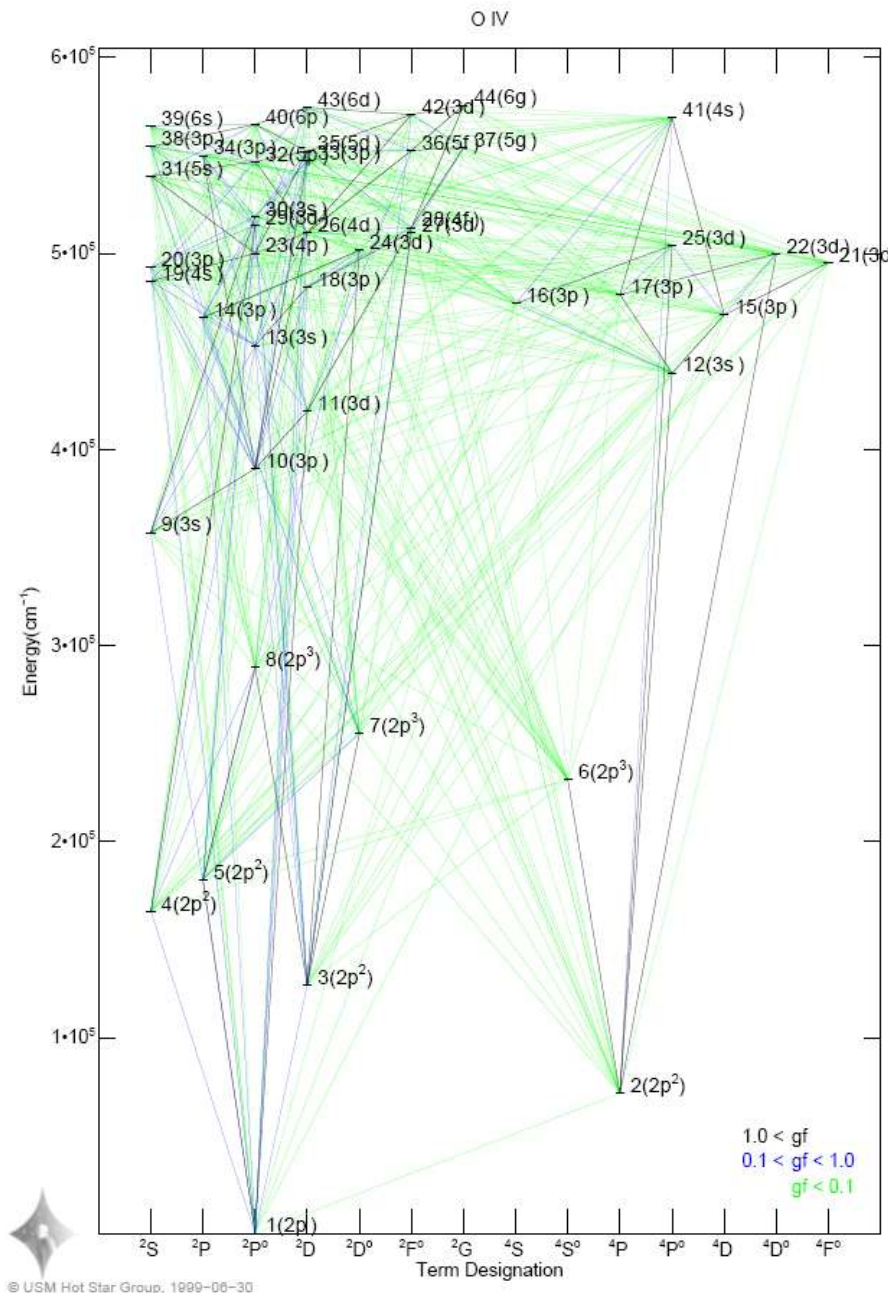


one example ...



atomic levels and allowed transitions ("Grotrian-diagram") in **OIV**

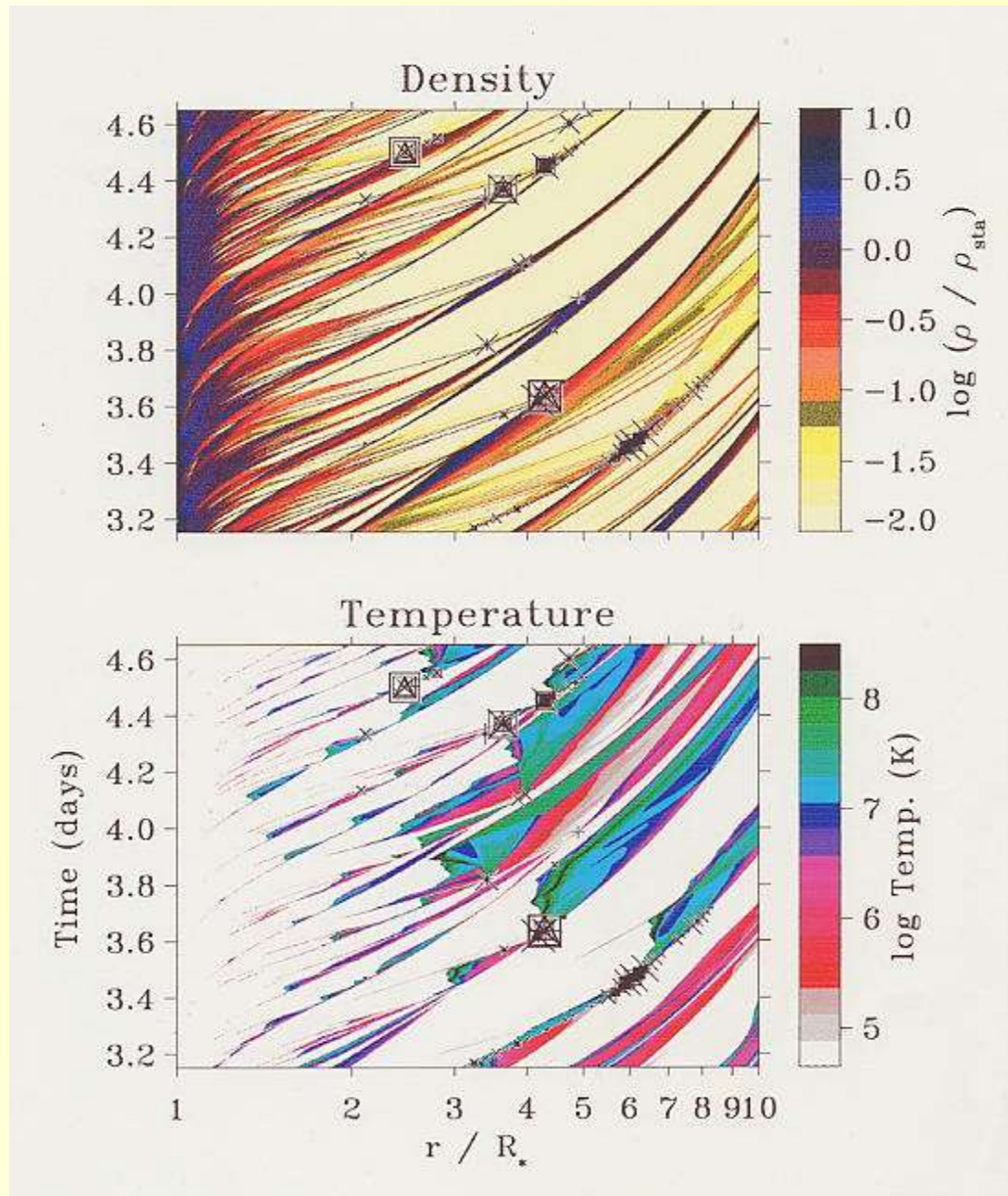
gf oscillator strength, measures "strength" of transition (cf. Chap 7)



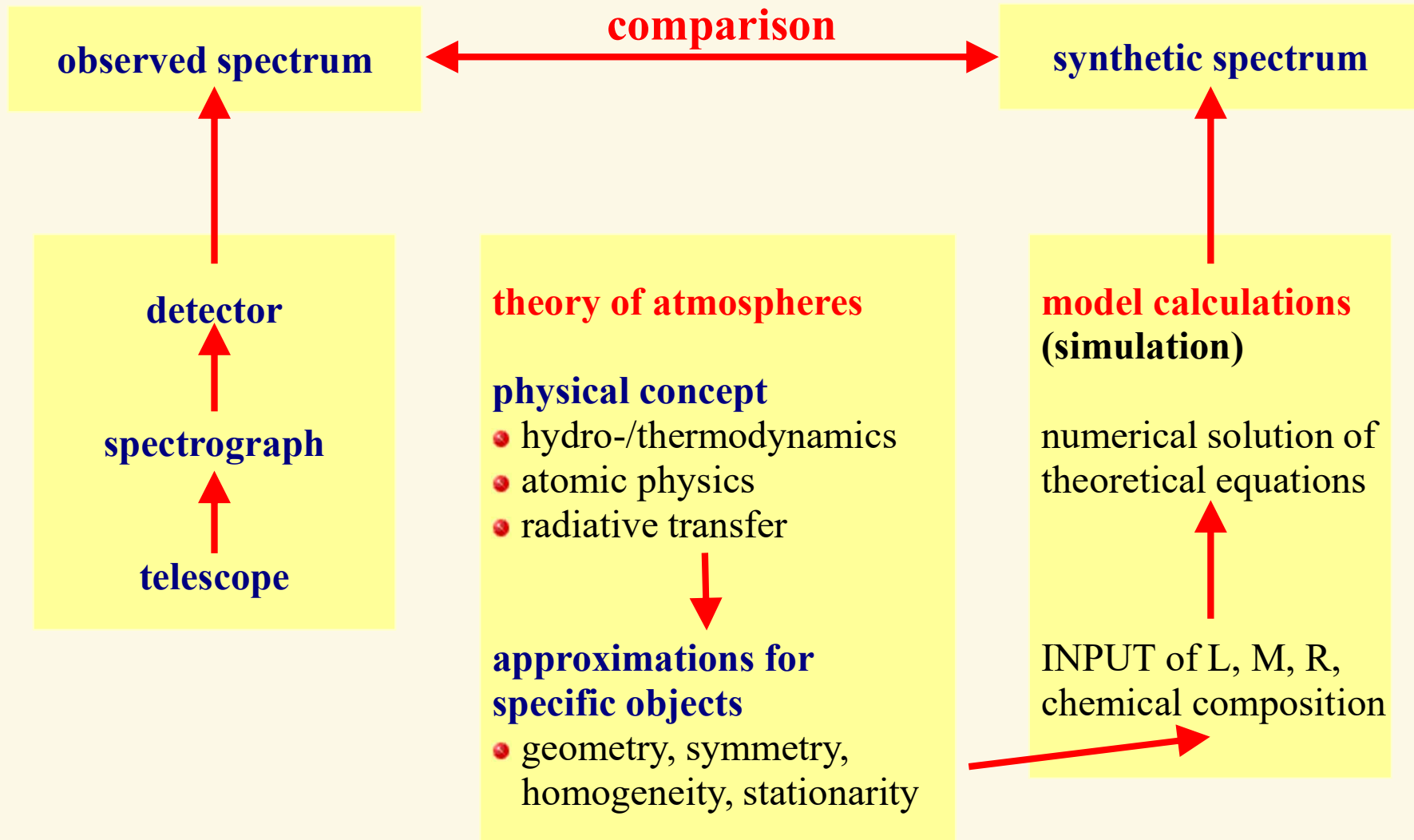
sites of X-ray emission in hot stars:

shell collisions

hydrodynamical simulations of instable hot star winds, from A. Feldmeier, by permission

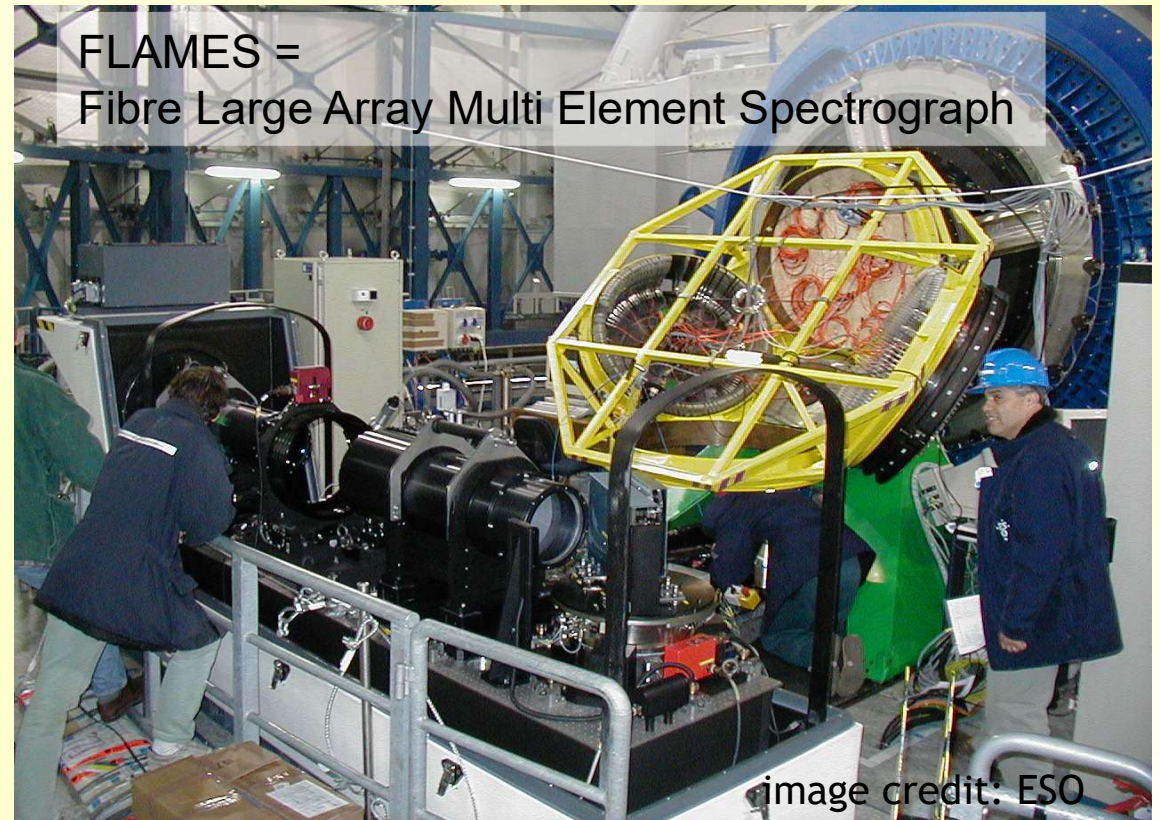
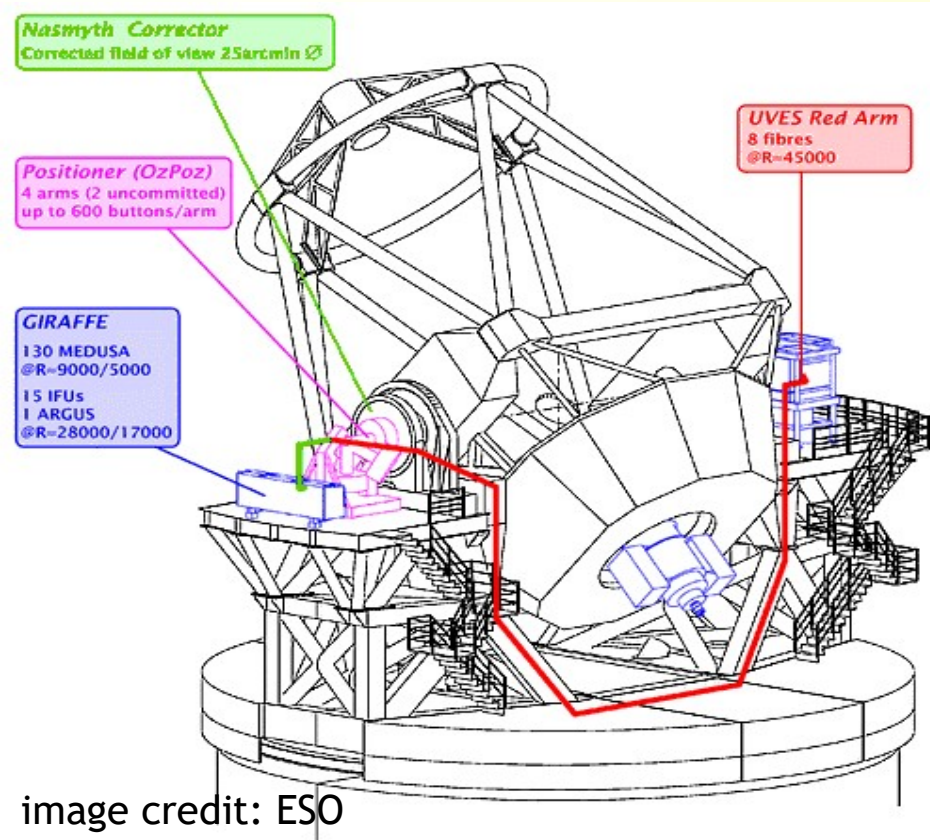


Concept of spectral analysis



The VLT-FLAMES survey of massive stars ('FLAMES I')

The VLT-FLAMES Tarantula survey ('FLAMES II')



- **FLAMES I:** high resolution spectroscopy of massive stars in 3 Galactic, 2 LMC and 2 SMC clusters (young and old)
 - total of 86 O- and 615 B-stars
- **FLAMES II:** high resolution spectroscopy of more than 1000 massive stars in Tarantula Nebula (incl. 300 O-type stars)

Major objectives

- rotation and abundances (test rotational mixing)
- stellar mass-loss as a function of metallicity
- binarity/multiplicity (fraction, impact)
- detailed investigation of the closest 'proto-starburst'

summary of FLAMES I results: Evans et al. (2008),
summary of FLAMES II results: Evans et al. (2019, in prep.)

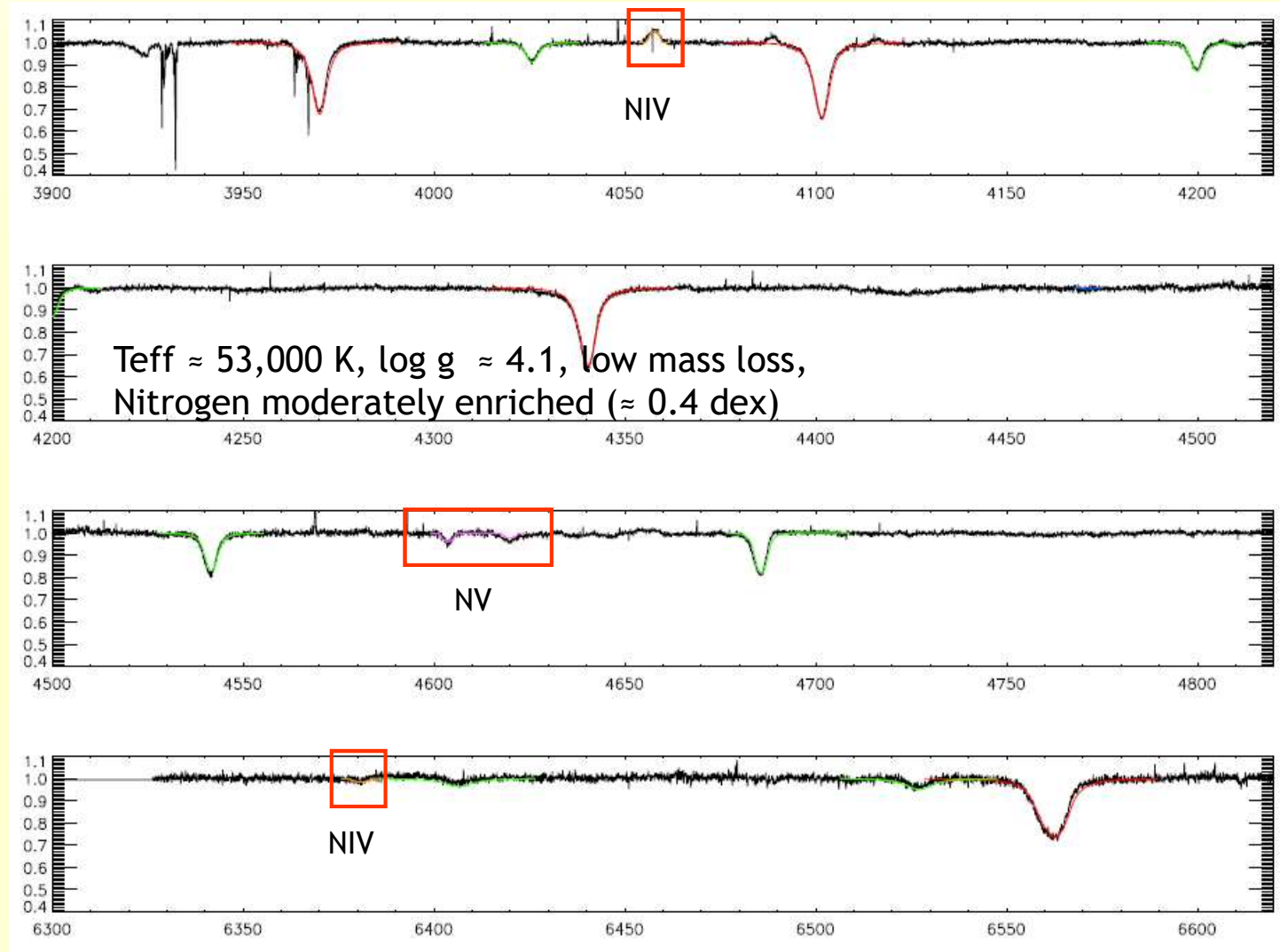
Optical spectrum of a very hot O-star

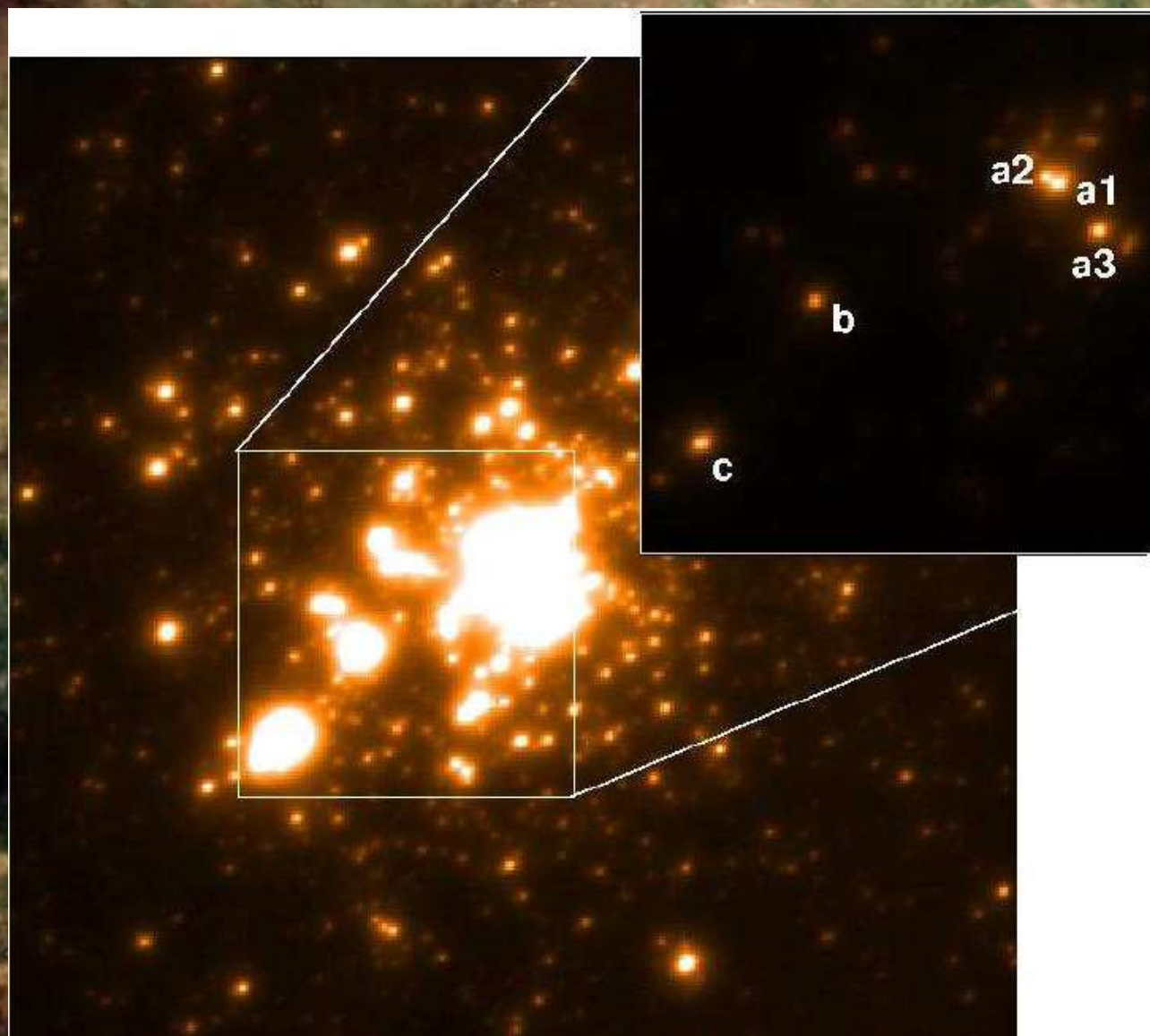
Theory vs. observations

BI237 O2V (f*) (LMC) – vsini = 140 km/s

- Synthetic spectra from Rivero-Gonzalez et al. (2012)

red: H I
 blue: He I
 green: He II
 orange: N IV
 magenta: N V

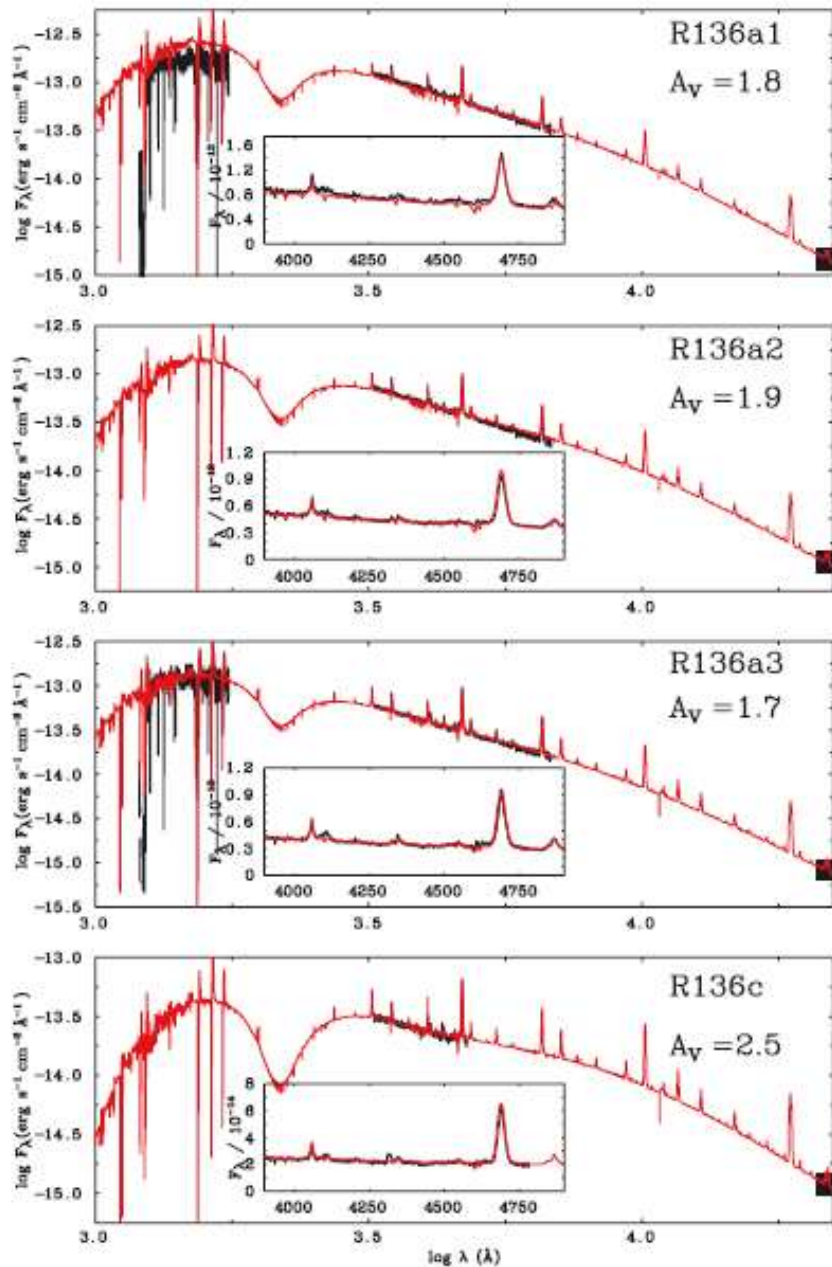




- Tarantula Nebula (30 Dor) in the LMC
- Largest starburst region in Local Group
- Target of VLT-FLAMES Tarantula survey ('FLAMES II', PI: Chris Evans)
- Cluster R136 contains some of the *most massive, hottest, and brightest* stars known
- Crowther et al. (2010): 4 stars with initial masses from 165-320 (!!!) M_{\odot}
- problems with IR-photometry (background-correction), lead to overestimated luminosities \rightarrow initial masses become reduced: 140 - 195 M_{\odot} (Rubio-Diez et al., IAUS 329, 2016, and in prep. for A&A)

Spectral energy distribution of the most massive stars in our “neighbourhood” - theory vs. observations

from Crowther et al. 2010
lower masses from Rubio-Diez et al 2016



initial mass (Msun)	current mass (Msun)
320	265
→	<194
240	195
→	<140
165	135
→	141
220	175
typical uncertainty ± 40 Msun	

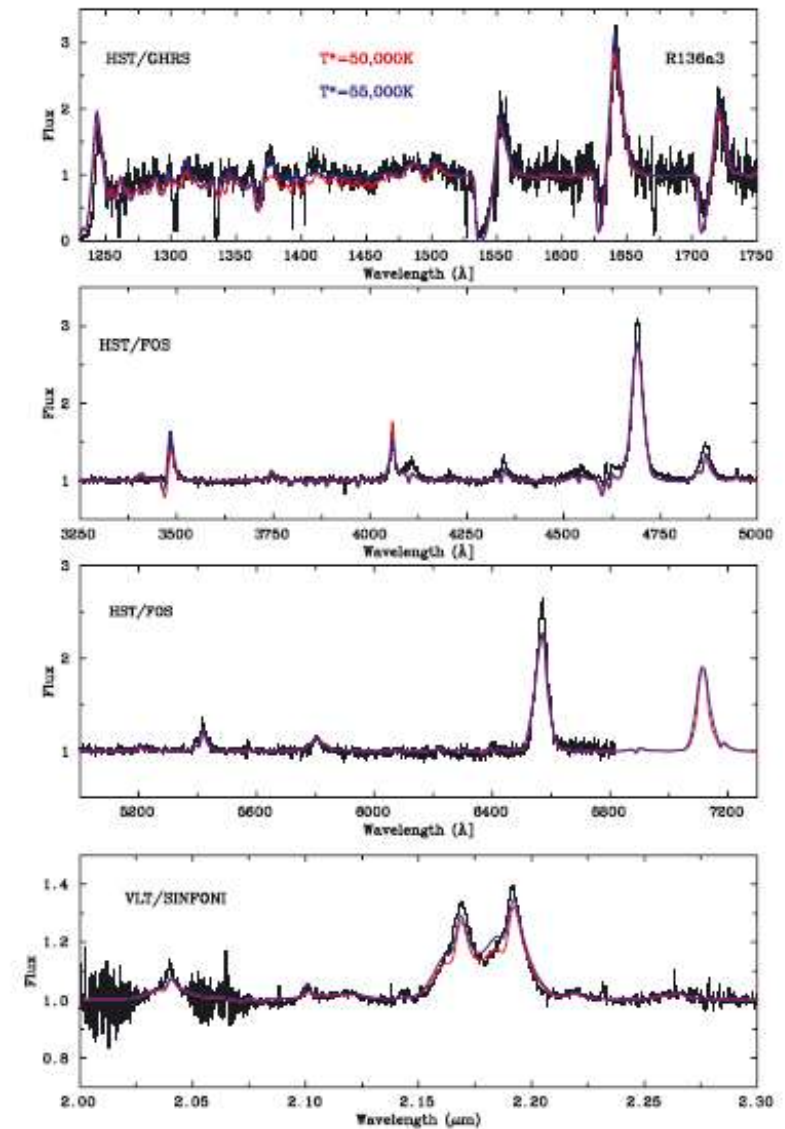


Figure 5. Rectified, ultraviolet (*HST*/GHRS), visual (*HST*/FOS) and near-IR (VLT/SINFONI) spectroscopy of the WN 5h star R136a3 together with synthetic UV, optical and near-IR spectra, for $T_* = 50\,000\text{ K}$ (red) and $T_* = 55\,000\text{ K}$ (blue). Instrumental broadening is accounted for, plus an additional rotational broadening of 200 km s^{-1} .

Figure 4. Spectral energy distributions of R136 WN 5h stars from *HST*/FOS together using K_s photometry from VLT/SINFONI calibrated with VLT/MAD imaging. Reddened theoretical spectral energy distributions are shown as red lines.

Chap. 3 – The radiation field



Number of particles in $(\mathbf{r}, \mathbf{r} + d\mathbf{r})$ with momenta $(\mathbf{p}, \mathbf{p} + d\mathbf{p})$ at time t

$$\delta N(\mathbf{r}, \mathbf{p}, t) = f(\mathbf{r}, \mathbf{p}, t) d^3\mathbf{r} d^3\mathbf{p}$$

distribution function f

i) $f(\mathbf{r}, \mathbf{p}, t)$ is Lorentz-invariant

ii) $\delta N_0 = f(\mathbf{r}_0, \mathbf{p}_0, t_0) d^3\mathbf{r}_0 d^3\mathbf{p}_0$

evolution

$$\delta N = f(\mathbf{r}_0 + d\mathbf{r}, \mathbf{p}_0 + d\mathbf{p}, t_0 + dt) d^3\mathbf{r} d^3\mathbf{p}$$

$$(\dot{\mathbf{p}} = \mathbf{F}) = f(\mathbf{r}_0 + \mathbf{v}dt, \mathbf{p}_0 + \mathbf{F}dt, t_0 + dt) d^3\mathbf{r} d^3\mathbf{p}$$

Theoretical mechanics: If no collisions, conservation of phase space volume:

$$d^3\mathbf{r}_0 d^3\mathbf{p}_0 = d^3\mathbf{r} d^3\mathbf{p}$$

and

$$\delta N_0 = \delta N \text{ (particles do not "vanish", again no collisions supposed)}$$

$$\Rightarrow f(\mathbf{r}, \mathbf{p}, t) = \text{const, if no collisions}$$

For a detailed derivation and discussion, see, e.g., Cercignani, C., "The Boltzmann Equation and Its Applications", Appl. Math. Sciences 67, Springer, 1987

$$\Rightarrow \frac{\partial f}{\partial t} + \sum \frac{\partial f}{\partial r_i} \frac{\partial r_i}{\partial t} + \sum \frac{\partial f}{\partial p_i} \frac{\partial p_i}{\partial t} =$$

$$= \underbrace{\frac{\partial f}{\partial t} + (\mathbf{v} \cdot \nabla) f + (\mathbf{F} \cdot \nabla_p) f}_{\text{D/Dt } f, \text{ Lagrangian derivative}} = \begin{cases} 0 & \text{Vlasov} \\ \left(\frac{\delta f}{\delta t}\right)_{\text{coll}} & \text{Boltzmann if collisions} \end{cases}$$

D/Dt f, Lagrangian derivative
total derivative of f measured in fluid frame, at times $t, t+\Delta t$ and positions $\mathbf{r}, \mathbf{r} + \mathbf{v} \Delta t$

• implications for photon gas

$$\mathbf{p} = \frac{h\nu}{c} \mathbf{n}$$

$$d^3\mathbf{p} = p^2 dp d\Omega \quad \leftarrow \text{solid angle with respect to } \mathbf{n}$$

absolute value

$$= \left(\frac{h\nu}{c}\right)^2 \frac{h}{c} d\nu d\Omega = \frac{h^3}{c^3} \nu^2 d\nu d\Omega$$

$$\Rightarrow f(\mathbf{r}, \mathbf{p}, t) d^3\mathbf{r} d^3\mathbf{p} = \frac{h^3}{c^3} \nu^2 f(\mathbf{r}, \mathbf{n}, \nu, t) d^3\mathbf{r} d\nu d\Omega = \Psi(\mathbf{r}, \mathbf{n}, \nu, t) d^3\mathbf{r} d\nu d\Omega$$



$$d^3\mathbf{p} = J(\mathbf{p}, \mathbf{p}') d^3\mathbf{p}', \quad \mathbf{p}' = (p, \theta, \phi)$$

cartesian Jacobi-det. spherical

$$p_x = p \sin \theta \cos \phi$$

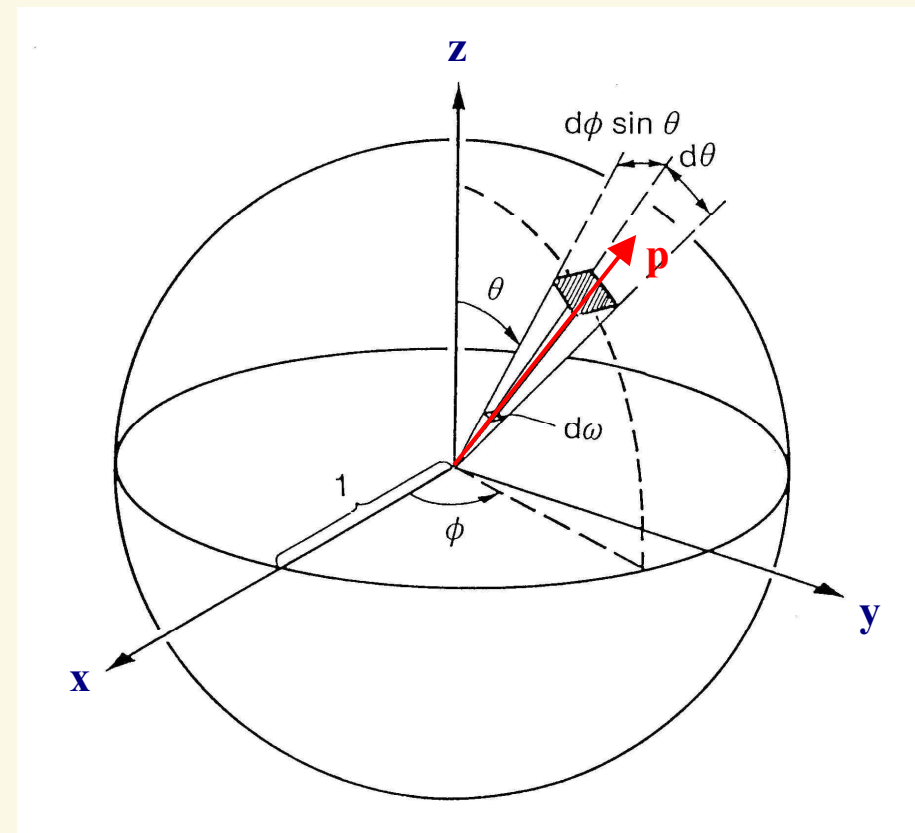
$$p_y = p \sin \theta \sin \phi$$

$$p_z = p \cos \theta$$

$$J = \det \begin{pmatrix} \frac{\partial p_x}{\partial p} & \frac{\partial p_x}{\partial \theta} & \frac{\partial p_x}{\partial \phi} \\ \frac{\partial p_y}{\partial p} & \frac{\partial p_y}{\partial \theta} & \frac{\partial p_y}{\partial \phi} \\ \frac{\partial p_z}{\partial p} & \frac{\partial p_z}{\partial \theta} & \frac{\partial p_z}{\partial \phi} \end{pmatrix} = \det \begin{pmatrix} \sin \theta \cos \phi & p \cos \theta \cos \phi & -p \sin \theta \sin \phi \\ \sin \theta \sin \phi & p \cos \theta \sin \phi & p \sin \theta \cos \phi \\ \cos \theta & -p \sin \theta & 0 \end{pmatrix}$$

$$= (\text{exercise}) \quad p^2 \sin \theta$$

$$\Rightarrow d^3\mathbf{p} = dp_x dp_y dp_z = p^2 dp \underbrace{\sin \theta d\theta d\phi}_{d\Omega}$$

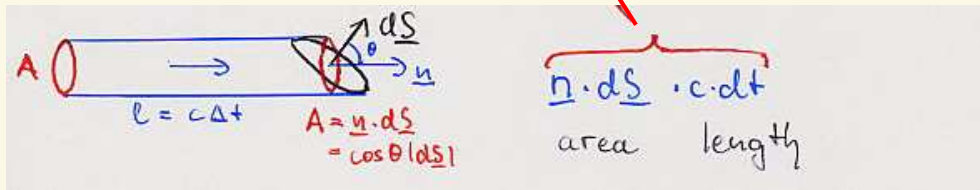


The specific intensity



Number of photons with ν , $\nu+d\nu$ which propagate through surface element dS into direction \mathbf{n} and solid angle $d\Omega$, at time t and with velocity c :

$$\delta N = \frac{h^3 \nu^2}{c^3} f(\mathbf{r}, \mathbf{n}, \nu, t) d^3\mathbf{r} d\nu d\Omega$$



$$= \frac{h^3 \nu^2}{c^3} f(\mathbf{r}, \mathbf{n}, \nu, t) \underbrace{\cos \theta}_{\langle \mathbf{n}, d\mathbf{S} \rangle} c dt dS d\nu d\Omega$$

- corresponding energy transport

$$\delta E = h\nu \delta N = \underbrace{\frac{h^4 \nu^3}{c^2} f(\mathbf{r}, \mathbf{n}, \nu, t) \cos \theta}_{I(\mathbf{r}, \mathbf{n}, \nu, t)} dS d\nu dt d\Omega$$

specific intensity
[erg cm⁻² Hz⁻¹ s⁻¹sr⁻¹]

summarized

$$I = ch\nu \Psi = \frac{h^4 \nu^3}{c^2} f \quad \text{function of } \mathbf{r}, \mathbf{n}, \nu, t$$

specific intensity is radiation energy, which is transported into direction \mathbf{n} through surface dS , per frequency, time and solid angle.

basic quantity in theory of radiative transfer

invariance of specific intensity

since $\frac{Df}{Dt} = 0$ without collisions (Vlasov equation) and without GR (i.e., $\mathbf{F} \equiv \mathbf{0}$), we have

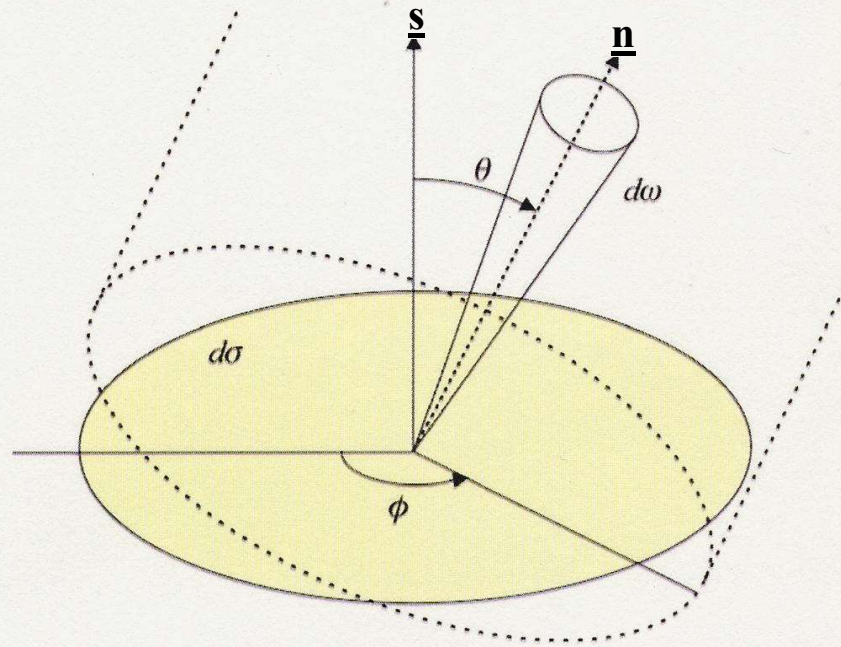
$$I \sim f$$

$\Rightarrow I = \text{const}$ in fluid frame, as long as no interaction with matter!

If stationary process, i.e. $\partial/\partial t = 0$, then $\underline{\mathbf{n}} \nabla I = d/ds I = 0$, where ds is path element, i.e.

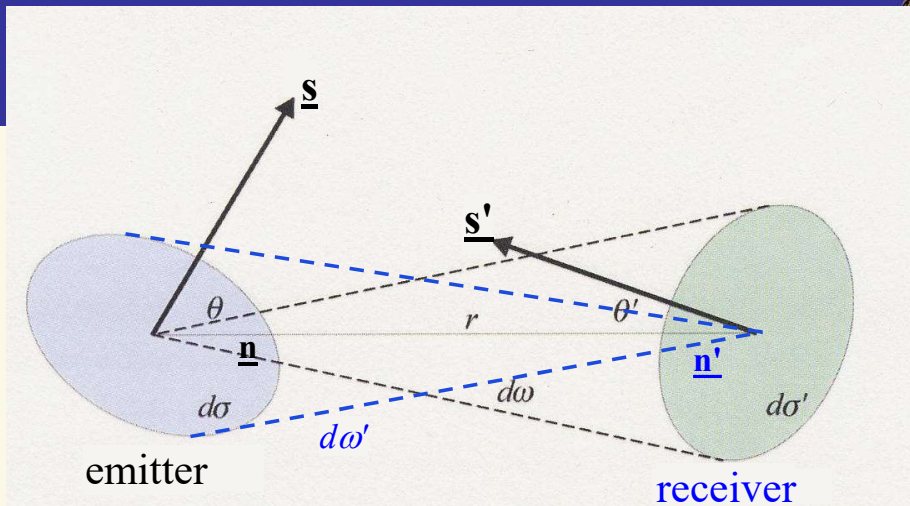
$I = \text{const}$ also spatially!

(this is the major reason for working with specific intensities)



specific intensity is radiation energy with frequencies $(\nu, \nu + d\nu)$, which is transported through *projected* area element $d\sigma \cos\theta$ into direction \underline{n} , per time interval dt and solid angle $d\omega$.

$$\delta E = I(\vec{r}, \vec{n}, \nu, t) \cos\theta d\sigma d\nu dt d\omega$$



Invariance of specific intensity

Consider pencil of light rays which passes through both area elements $\delta\sigma$ (emitter) and $\delta\sigma'$ (receiver).

If no energy sinks and sources in between, the amount of energy which passes through both areas is given by

$$\delta E = I_\nu \cos\theta d\sigma dt d\omega =$$

$$\delta E' = I'_\nu \cos\theta' d\sigma' dt d\omega', \text{ and, cf. figure,}$$

$$d\omega = \frac{\text{projected area}}{\text{distance}^2} = \frac{\cos\theta' d\sigma'}{r^2}$$

$$d\omega' = \frac{\cos\theta d\sigma}{r^2}$$

$$\Rightarrow I_\nu = I'_\nu, \text{ independent of distance}$$

... but energy/unit area dilutes with r^{-2} !

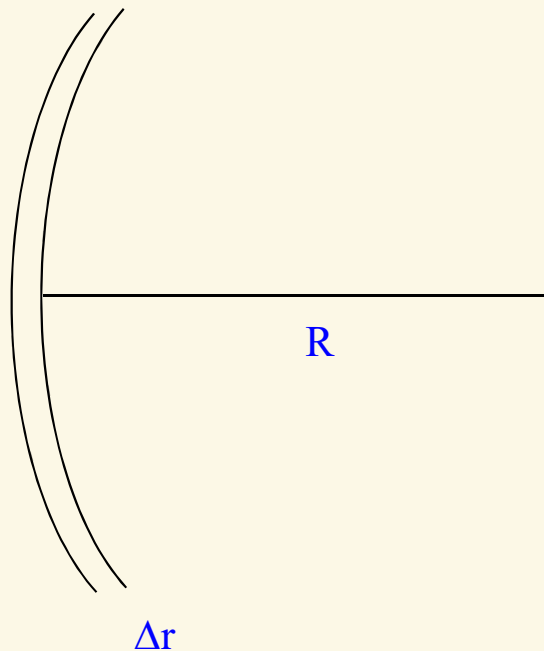
Plane-parallel and spherical symmetries



stars = gaseous spheres => spherical symmetry

BUT rapidly rotating stars (e.g., Be-stars, $v_{\text{rot}} \approx 300 \dots 400$ km/s) rotationally flattened, only axis-symmetry can be used

AND atmospheres usually very thin, i.e. $\Delta r / R \ll 1$



example: the sun

$$R_{\text{sun}} \approx 700,000 \text{ km}$$
$$\Delta r (\text{photo}) \approx 300 \text{ km}$$

$$\Rightarrow \Delta r / R \approx 4 \cdot 10^{-4}$$

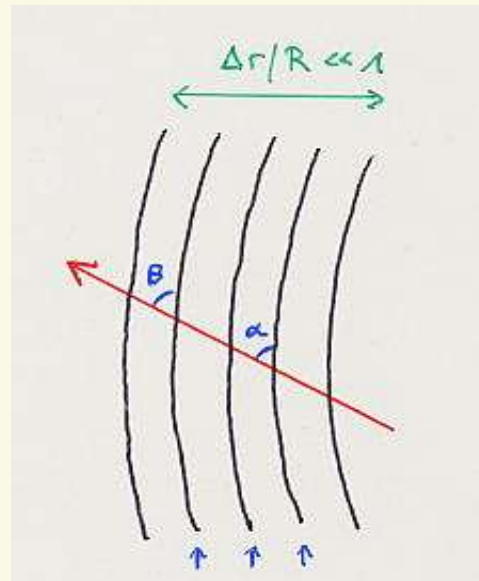
BUT corona

$$\Delta r / R (\text{corona}) \approx 3$$



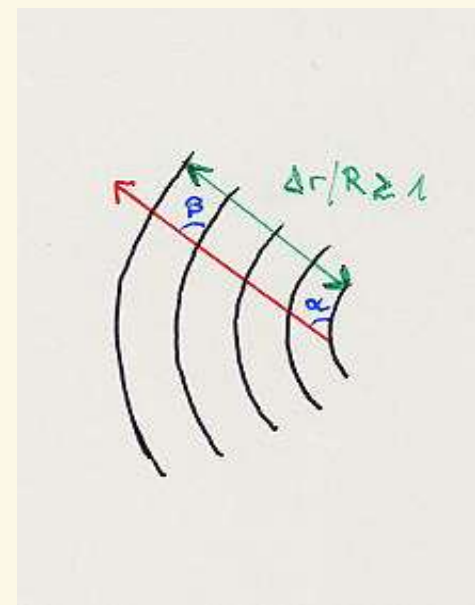
as long as $\Delta r / R \ll 1 \Rightarrow$ plane-parallel symmetry

light ray through atmosphere



lines of constant temperature and density (isocontours)

curvature of atmosphere insignificant for photons' path : $\alpha = \beta$



significant curvature : $\alpha \neq \beta$, spherical symmetry

examples

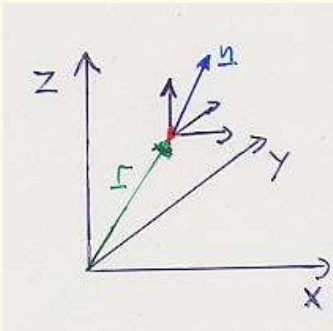
solar photosphere / cromosphere
atmospheres of
main sequence stars
white dwarfs
giants (partly)

solar corona
atmospheres of
supergiants
expanding envelopes (stellar winds)
of OBA stars, M-giants and supergiants

Co-ordinate systems/symmetries



Cartesian



$$\mathbf{r} = x\mathbf{e}_x + y\mathbf{e}_y + z\mathbf{e}_z$$

$\mathbf{e}_x, \mathbf{e}_y, \mathbf{e}_z$ right-handed, orthonormal $\mathbf{e}_\Theta, \mathbf{e}_\Phi, \mathbf{e}_r$

specific intensity:

$$I(x, y, z, \mathbf{n}, \nu, t)$$

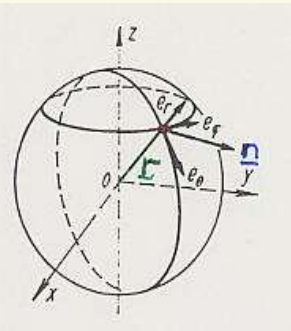
important symmetries

plane-parallel

physical quantities depend only on z , e.g.

$$I(\mathbf{r}, \mathbf{n}, \nu, t) \rightarrow I(z, \mathbf{n}, \nu, t)$$

spherical



$$\mathbf{r} = \Theta\mathbf{e}_\Theta + \Phi\mathbf{e}_\Phi + r\mathbf{e}_r$$

$$I(\Theta, \Phi, r, \mathbf{n}, \nu, t)$$

spherically symmetric

.... depend only on r , e.g.

$$I(\mathbf{r}, \mathbf{n}, \nu, t) \rightarrow I(r, \mathbf{n}, \nu, t)$$

intensity has direction \mathbf{n} into $d\Omega$

\mathbf{n} requires additional angles θ, ϕ with respect to

$\mathbf{e}_x, \mathbf{e}_y, \mathbf{e}_z$

$\mathbf{e}_\Theta, \mathbf{e}_\Phi, \mathbf{e}_r$

and

$$\theta = \angle(\mathbf{e}_z, \mathbf{n})$$

$$\theta = \angle(\mathbf{e}_r, \mathbf{n})$$

$$I_\nu(x, y, z, \theta, \phi, t)$$

$$I_\nu(\Theta, \Phi, r, \theta, \phi, t)$$

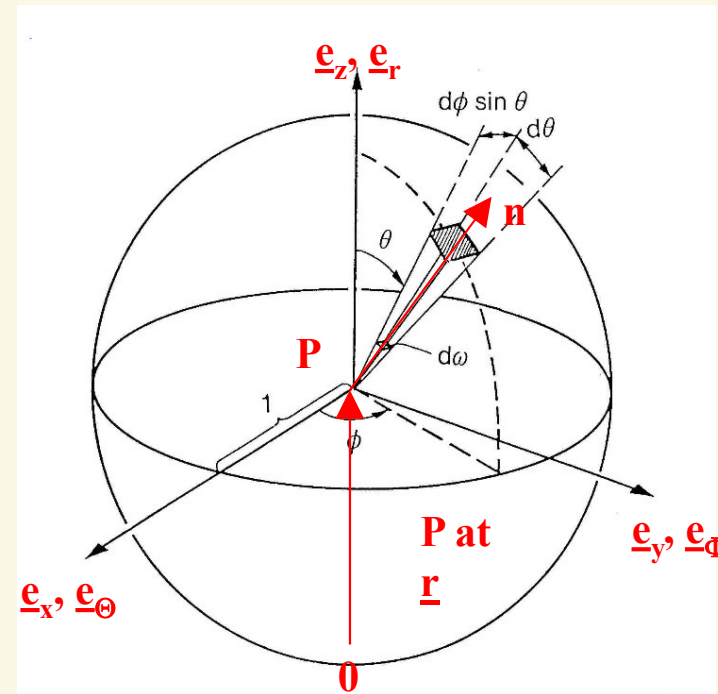
p-p symmetry

spherical symmetry

independent of azimuthal direction, ϕ

$$\rightarrow I_\nu(z, \theta, t)$$

$$\rightarrow I_\nu(r, \theta, t)$$



Moments of the specific intensity

1. Mean intensity

$$\bar{J}(\underline{r}, \nu, t) = \frac{1}{4\pi} \oint I(\underline{r}, \underline{n}, \nu, t) d\Omega$$

specific intensity, averaged over solid angle

def. of solid angle

solid angle = ratio of area of sphere to radius²

$$\text{total solid angle} = \frac{4\pi r^2}{r^2} = 4\pi$$

$$d\Omega \text{ with } r=1 = dA$$

$$\text{area} = d\theta \times \sin\theta d\phi$$

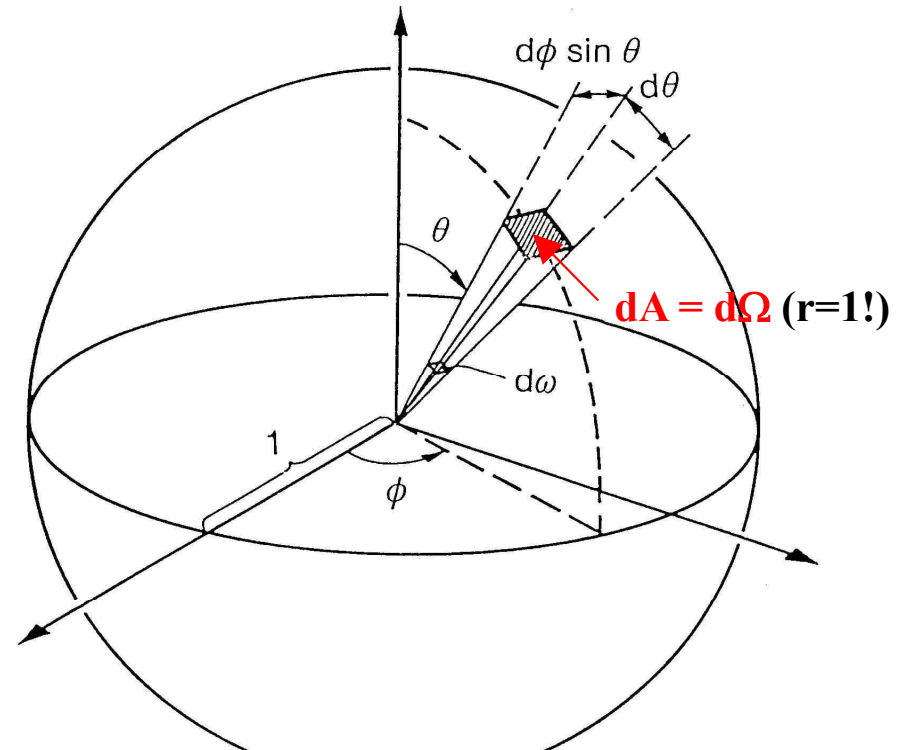
$$\text{def: } \mu = \cos\theta$$

$$d\mu = -\sin\theta d\theta \Rightarrow d\Omega = -d\mu d\phi$$

THUS

$$\bar{J}(\underline{r}, \nu, t) = \frac{1}{4\pi} \int_0^{2\pi} d\phi \int_{-1}^{+1} I(\underline{r}, \underline{n}, \nu, t) \underbrace{\sin\theta d\theta}_{-d\mu}$$

usually $f(\theta, \phi)$



In plane-parallel or spherical symmetry:

$$\bar{J}_\nu(\underline{r}, t) = \frac{1}{4\pi} \int_0^{2\pi} d\phi \int_{-1}^{+1} I_\nu(\underline{r}, \mu, t) d\mu =$$

$$= \frac{1}{2} \int_{-1}^{+1} I_\nu(\mu) d\mu \quad \text{"0+4" moment}$$

The Planck function



... on the other hand

energy density (i.e., per Volume d^3r) per $d\nu$ (i.e., spectral) = $h\nu \oint (\text{distr. function}) d\Omega$

$$u_\nu(r, t) = h\nu \oint \Psi_\nu(r, \mu, t) d\Omega$$

$$\stackrel{\text{def.}}{=} \frac{1}{c} \oint I_\nu(r, \mu, t) d\Omega = \frac{4\pi}{c} J_\nu(r, t)$$

$$\dim[u_\nu] = \text{erg cm}^{-3} \text{Hz}^{-1}$$

$$\dim[J_\nu] = \text{erg cm}^{-2} \text{Hz}^{-1} \text{s}^{-1}$$

- from thermodynamics, we know spectral energy density of a cavity or black body radiator (in thermodynamic equilibrium, "TE", with isotropic radiation, independent of material)

$$u_\nu(\tau) = \frac{8\pi h\nu^3}{c^3} \frac{1}{e^{h\nu/kT} - 1}$$

$$\Rightarrow J_\nu = \frac{c}{4\pi} u_\nu \quad \text{and} \quad J_\nu = \frac{1}{2} \int_{-1}^{+1} I_\nu d\mu = I_\nu \quad \text{isotropic}$$

specific intensity of a cavity/black body radiator at temperature T

$$I_\nu^* \stackrel{\leftarrow \text{TE}}{=} B_\nu(T) = \frac{2h\nu^3}{c^2} \frac{1}{e^{h\nu/kT} - 1} \quad \text{"Planck-Function"}$$

properties of Planck function

- $B_\nu(T_1) > B_\nu(T_2) \quad \forall \nu$, if $T_1 > T_2$
i.e., Planck functions do not cross each other!

- maximum is shifted towards higher wavelengths with decreasing temperature
 $\frac{\nu_{\text{max}}}{T} = \text{const}$, Wien's displacement law

- Wien regime $\frac{h\nu}{kT} \gg 1 \Rightarrow B_\nu \approx \frac{2h\nu^3}{c^2} e^{-h\nu/kT}$

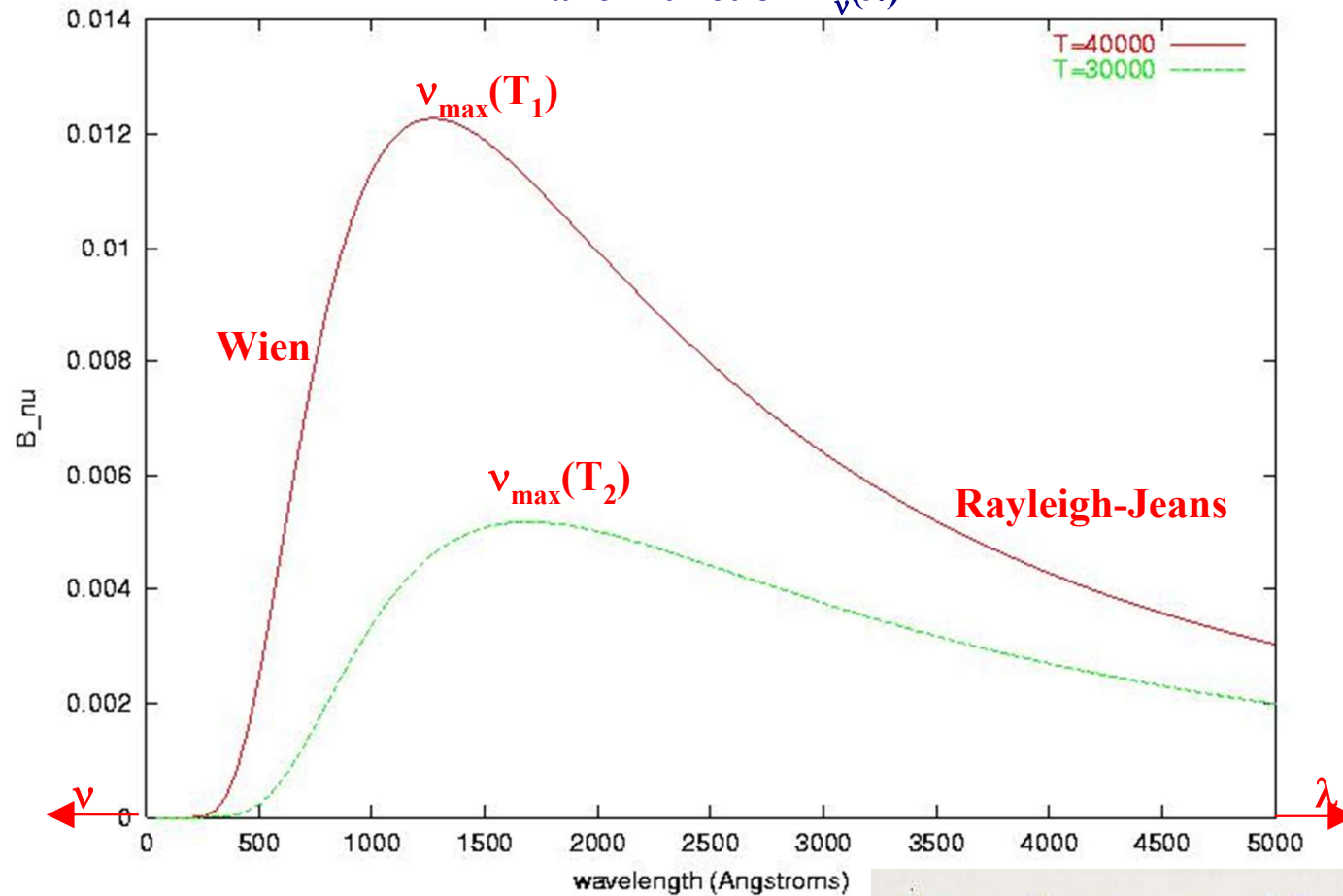
- Rayleigh Jeans regime $\frac{h\nu}{kT} \ll 1 \Rightarrow B_\nu \approx \frac{2h\nu^3}{c^2} \frac{kT}{h\nu} = \frac{2\nu^2}{c^2} kT$

NOTE: in a number of cases one finds $B_\lambda \neq B_\nu$ since $B_\lambda d\lambda = B_\nu d\nu$

$$\Rightarrow B_\lambda = B_\nu \left| \frac{d\nu}{d\lambda} \right| = B_\nu \frac{c}{\lambda^2} = \frac{2hc^2}{\lambda^5} \frac{1}{e^{hc/kT\lambda} - 1}$$

$$\Rightarrow \text{Max}(B_\lambda) \neq \text{Max}(B_\nu)!$$

Planck function $B_\nu(\lambda)$



$$\text{Max } B_\nu : \nu_{\text{max}} / T = \text{const}^1 \Rightarrow \lambda_{\text{max}}^1 = \frac{5.0995 \cdot 10^7}{T(K)} \text{ \AA}$$

$$\text{Max } B_\lambda : \lambda_{\text{max}} \cdot T = \text{const}^2 \Rightarrow \lambda_{\text{max}}^2 = \frac{2.898 \cdot 10^3}{T(K)} \text{ \AA}$$

• Stefan - Boltzmann law

$$\int_0^\infty B_\nu(T) d\nu = \int_0^\infty B_\lambda(T) d\lambda = \frac{\sigma}{\pi} T^4 \quad \text{with}$$

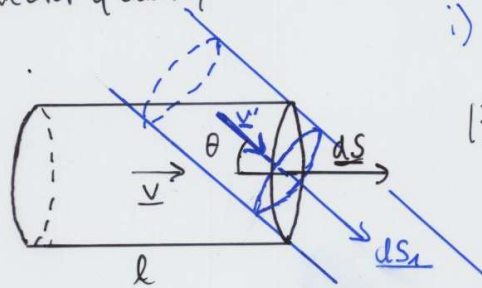
$$\sigma = 5.67 \cdot 10^{-5} \frac{\text{erg}}{\text{cm}^2 \text{s K}^4}, \quad \sigma / \pi = \frac{2 K_B^4}{c^2 h^3} \frac{\pi^4}{15}$$

1st moment: radiative flux

a) general definition

flux: rate of flow of a quantity across a given surface

flux-density: flux/unit area, also called flux vector quantity



i) mass flux $\underline{v} \perp \underline{dS}$

$$|\underline{F}| = \frac{m}{\Delta t |dS|} = \frac{m}{Vol} \frac{l}{\Delta t} = g |v|$$

mass flux = mass density · velocity

ii) \underline{v}' arbitrarily oriented with respect to \underline{dS}

$$|\underline{F}| = \frac{m}{\Delta t |dS|} = \frac{m}{\Delta t |dS_{\perp}|} \frac{|dS_{\perp}|}{|dS|} = \frac{m}{Vol} |v'| \frac{|dS| \cos \theta}{|dS|}$$

\uparrow $Vol = |v'| \Delta t |dS_{\perp}|$

$$= g |v'| \cos \theta$$

⇒ mass flux through $\underline{dS} = \underline{F} \cdot \underline{dS} = g \cdot \underbrace{v' \cdot \underline{dS}}_{|v'| |dS| \cos \theta}$
 is reduced by factor $\cos \theta$,
 since less material is transported across smaller **effective area** \perp flow (in same Δt)

iii) mass-loss rate for spherically sym. outflow

$$\dot{M} = \underbrace{(g v)}_{\text{mass flux}} \cdot \underbrace{4 \pi r^2}_{\text{surface area}} \quad \text{transported mass/unit time across surface with radius } r$$

$\cos \theta = 1!$

b) application to radiation field

- photon flux through surface \underline{dS} into direction \underline{n} and solid angle $d\Omega$ ("radiation pencil")

$$\frac{dN}{dt dv} = \underbrace{\left(\Psi(\underline{r}, \underline{n}, \nu, t) d\Omega \right)}_{\text{number DENSITY}} \cdot \underbrace{c \cdot \underline{n}}_{\text{velocity}} \cdot \underline{dS}$$

- net rate of total photon flow across \underline{dS} (i.e., contribution of all pencils)

$$\frac{N}{dt dv} = \left(c \oint \Psi(\underline{r}, \underline{n}, \nu, t) \underline{n} d\Omega \right) \cdot \underline{dS}$$

- net rate of radiant energy flow across \underline{dS}

$$\frac{E}{dt dv} = \left(c h \nu \oint \Psi(\underline{r}, \underline{n}, \nu, t) \underline{n} d\Omega \right) \underline{dS} =$$

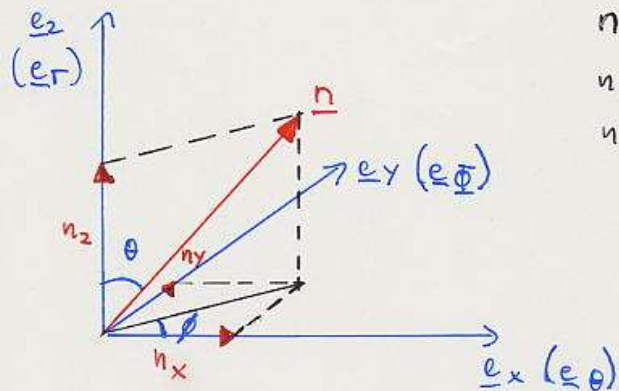
def. $\left(\oint \underline{I}(\underline{r}, \underline{n}, \nu, t) \underline{n} d\Omega \right) \underline{dS}$

$$= \underline{F}_{\nu}(\underline{r}, t) \cdot \underline{dS}$$

$\underline{F}_{\nu}(\underline{r}, t) = \oint \underline{I}_{\nu}(\underline{r}, \underline{n}, t) \underline{n} d\Omega$

radiative flux

$$\dim[\underline{F}_{\nu}] = \frac{\text{erg}}{\text{cm}^2 \text{s Hz}} = \dim[\underline{j}_{\nu}]$$



$$n_z = \cos \theta = \mu$$

$$n_x = \sin \theta \cos \phi$$

$$n_y = \sin \theta \sin \phi$$

Note: Cartesian (spherical co-ordinate system)

$$\begin{pmatrix} r \\ \theta \\ \phi \end{pmatrix} \cong (\text{locally}) \begin{pmatrix} e_x \\ e_y \\ e_z \end{pmatrix}, \quad \theta, \phi \text{ defined similarly}$$

$$\Rightarrow \underline{F} = \begin{pmatrix} F_{x,\theta} \\ F_{y,\phi} \\ F_{z,r} \end{pmatrix} = \begin{pmatrix} \int I_{nx} d\Omega \\ \int I_{ny} d\Omega \\ \int I_{nz} d\Omega \end{pmatrix} = \int_0^1 \int_0^{2\pi} \int_{-1}^1 d\phi \sin \theta \, d\mu I(\mu) \mu^2$$

p.p. / spherical symmetric

$I(r, \mu, \nu, t) \Rightarrow I(z, \mu, \nu, t)$ independent of ϕ ,
 $x(\theta), y(\phi)$ comp. cancel each other
 (math: $\cos \phi, \sin \phi$ integrals = 0)

$$\Rightarrow \underline{F} = (0, 0, 2\pi \int_{-1}^1 I(z, \mu, \nu, t) \mu d\mu)$$

- in analogy to mean intensity $J_\nu = \frac{1}{2} \int_{-1}^1 I(\mu) d\mu$
 we define the **Eddington flux**

$$H_\nu(z, t) = \frac{1}{2} \int_{-1}^1 I_\nu(z, \mu, t) \mu d\mu = \frac{1}{4\pi} \underline{F}_\nu(z, t)$$

"first moment"

- "flux" from a cavity radiator

small opening

$$\underline{F}_\nu = 2\pi \int_{-1}^1 I(\mu) \mu d\mu = 2\pi \int_0^1 I(\mu) \mu d\mu - 2\pi \int_0^1 I(-\mu) \mu d\mu$$

$$= F^+ - F^-$$

only photons escaping from radiator

$$I(\mu), \mu = 0 \dots 1 = B_\nu(T) \quad \text{isotropic radiation}$$

$$I(-\mu) = 0$$

$$\Rightarrow \underline{F} = \int_0^\infty \pi B_\nu(T) d\nu = \pi \cdot \frac{\sigma_B}{\pi} T^4 = \sigma_B T^4$$

REMEMBER Black Body

frequ. integrated	specific and mean intensity	$\frac{\sigma_B}{\pi} T^4$
"	energy density	$\frac{4\sigma_B}{c} T^4$
"	flux	$\sigma_B T^4$



Effective temperature



- total radiative energy loss is flux (outwards directed) times surface area of star =

$$\text{luminosity } L = \mathcal{F} + 4\pi R^2$$

$$\text{dim}[L] = \text{erg/s (units of power)}, \quad L_{\text{sun}} = 3.83 \cdot 10^{33} \text{ erg/s}$$

- definition: “effective temperature” is temperature of a star with luminosity L at radius R_* , if it were a black body (semi-open cavity?)
- T_{eff} corresponds roughly to stellar surface temperature (more precise \rightarrow later)

$$L =: \sigma_B T_{\text{eff}}^4 4\pi R^2 \quad \text{or} \quad T_{\text{eff}} = (L / \sigma_B 4\pi R^2)^{1/4}$$

Examples

USM i) spherical or plane-parallel symmetry, isotropic radiation

$$I_\nu(\mu) = I_0 \quad (\text{e.g., } B_\nu(T))$$

$$\Rightarrow J_\nu = \frac{1}{2} \int_{-1}^1 I_0 d\mu = I_0$$

$$H_\nu = \frac{1}{2} \int_{-1}^1 I_0 \mu d\mu = 0 \quad [\text{vanishing flux also in radial direction, since same number of photons}$$

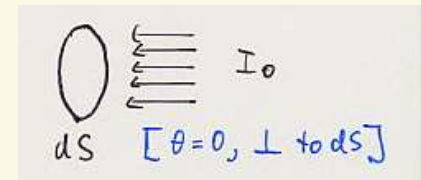
from above and below surface \perp radial direction]

$$\text{THUS: } I_\nu = I_0 \Rightarrow J_\nu = I_0, H_\nu = 0$$

ADVANCED READING: ii) extremely anisotropic radiation

$I_\nu(\mu, \phi) = I_0 \delta(\mu - \mu_0) \delta(\phi - \phi_0)$, with Dirac δ -function [planar wave]

$$\Rightarrow J_\nu = \frac{1}{4\pi} \int_0^{2\pi} d\phi \int_{-1}^1 I_0 \delta(\mu - \mu_0) \delta(\phi - \phi_0) d\mu = \frac{I_0}{4\pi}$$



$$\mathbf{H}_\nu = \frac{\mathbf{F}_\nu}{4\pi} = \begin{pmatrix} \frac{1}{4\pi} \int_0^{2\pi} \cos \phi d\phi \int_{-1}^1 I_0 \delta(\mu - \mu_0) \delta(\phi - \phi_0) (1 - \mu^2)^{1/2} d\mu \\ \frac{1}{4\pi} \int_0^{2\pi} \sin \phi d\phi \int_{-1}^1 I_0 \delta(\mu - \mu_0) \delta(\phi - \phi_0) (1 - \mu^2)^{1/2} d\mu \\ \frac{1}{4\pi} \int_0^{2\pi} d\phi \int_{-1}^1 I_0 \delta(\mu - \mu_0) \delta(\phi - \phi_0) \mu d\mu \end{pmatrix} = \frac{1}{4\pi} \begin{pmatrix} I_0 \cos \phi_0 (1 - \mu_0^2)^{1/2} \\ I_0 \sin \phi_0 (1 - \mu_0^2)^{1/2} \\ I_0 \mu_0 \end{pmatrix} \xrightarrow{\mu_0 \rightarrow 1} \begin{pmatrix} 0 \\ 0 \\ I_0 / 4\pi \end{pmatrix}$$

$$\text{Generally: } |\mathbf{H}_\nu| = \frac{I_0}{4\pi} \sqrt{\cos^2 \phi_0 (1 - \mu_0^2) + \sin^2 \phi_0 (1 - \mu_0^2) + \mu_0^2} = \frac{I_0}{4\pi}$$

THUS: uni-directional radiation $\Rightarrow J_\nu = |\mathbf{H}_\nu|$ (independent of co-ordinate system)



iii) $F_v^+ = 2\pi \int_0^1 I(\mu) \mu d\mu$ is stellar radiation energy,
 emitted into ALL directions (per dS, dv, dt)
 $= \frac{d^2}{R_x^2} f_v$, if f_v is the energy received
 on earth (per dS, dv, dt), d is the distance
 and $d \gg R_x$ [no extinction!]

proof if no extinction, totally emitted stellar
 energy remains conserved

$$L = \text{const} = F_v^+(R_x) \cdot 4\pi R_x^2 \stackrel{!}{=} \int_v^{\text{obs}}(d) 4\pi d^2$$

$$\Rightarrow \int_v^{\text{obs}}(d) = F_v^+(R_x) \frac{R_x^2}{d^2} \quad \text{q.e.d.}$$

("quadratic dilution")

iv) solar constant

total solar flux, measured on earth

$$\int_0^\infty f_\nu d\nu = f = 1.36 \cdot 10^6 \frac{\text{erg}}{\text{cm}^2 \text{s}} = 1360 \text{ Watt/m}^2 \approx 1 \text{ vacuum cleaner/m}^2$$

$$\text{distance earth sun} \approx 1.5 \cdot 10^{13} \text{ cm}$$

$$R_\odot = 6.96 \cdot 10^{10} \text{ cm}$$

$$\Rightarrow F_\odot^+(R_\odot) = 6.3 \cdot 10^{10} \frac{\text{erg}}{\text{cm}^2 \text{s}} = 6.3 \times 10^7 \text{ Watt/m}^2 \approx 0.05 \text{ nuclear power plant/m}^2$$

with def. of T_{eff}

$$\sigma_\odot T_{\text{eff}}^4 = F^+ \rightarrow T_{\text{eff}} = 5777 \text{ K}$$

$$\rightarrow B_\nu^{\text{max}} \text{ at } \lambda = 8826 \text{ \AA}$$

$$B_\lambda^{\text{max}} \text{ at } \lambda = 5020 \text{ \AA}$$

v) exercise

How many L_\odot is emitted by a typical O-supergiant with $T_{\text{eff}} = 40,000 \text{ K}$ and $R_x = 20 R_\odot$?
 Where is its spectral maximum?

2nd moment: radiation pressure (stress) tensor



US

P_{ij} is net flux of momentum, in the j -th direction, through a unit area oriented perpendicular to the i -th direction (per unit time and frequency)

- this is just the general definition of "pressure" in any fluid

$$P_{ij}(\underline{r}, \nu, t) = \oint \underbrace{\Psi(\underline{r}, \nu, \nu, t)}_{\substack{\text{transported quantity} \\ = \text{distrib. function} \cdot \text{momentum}}} \left(\frac{h\nu}{c} n_j \right) \underbrace{(c \cdot n_i)}_{\text{velocity}} d\Omega$$

$$\stackrel{\text{def}}{=} \frac{1}{c} \oint I(\underline{r}, \nu, \nu, t) n_i n_j d\Omega$$

- $P_{ij} = P_{ji}$ generally
- NOW** p-p/sph. symmetry
from def. of $n_i, i=1,3$ $P_{ij}=0$ for $i \neq j$

$$P = \begin{pmatrix} P_R & 0 & 0 \\ 0 & P_R & 0 \\ 0 & 0 & P_R \end{pmatrix} = \frac{1}{2} \begin{pmatrix} 3P_R - u & 0 & 0 \\ 0 & 3P_R - u & 0 \\ 0 & 0 & 0 \end{pmatrix}$$

with respect to

$$(\underline{e}_x, \underline{e}_y, \underline{e}_z) \text{ or } (\underline{e}_\theta, \underline{e}_\phi, \underline{e}_r)$$

$$P_R = \frac{4\pi}{c} K \quad \text{radiation pressure scalar}$$

$$u = \frac{4\pi}{c} J \quad \text{radiation energy density}$$

$$K_\nu = \frac{1}{2} \int_{-1}^{+1} I_\nu(\underline{r}, \mu, t) \mu^2 d\mu \quad \text{"2nd moment"}$$

Note In p-p/spherical symmetry the radiation pressure tensor is described by only two scalar quantities!

isotropic radiation (\rightarrow stellar interior) cavity radiation

$$I_\nu(r, \mu, t) \rightarrow I_\nu(r, t)$$

$$\left. \begin{aligned} K &= \frac{I}{2} \int_{-1}^{+1} \mu^2 d\mu \\ J &= \frac{I}{2} \int_{-1}^{+1} d\mu \end{aligned} \right\} K = \frac{1}{3} J \quad \text{or} \quad P_R = \frac{1}{3} u$$

$$\Rightarrow P_\nu = \begin{pmatrix} P_R & 0 & 0 \\ 0 & P_R & 0 \\ 0 & 0 & P_R \end{pmatrix} \quad \text{ONE quantity sufficient}$$



divergence of radiation pressure tensor

gas pressure \rightarrow pressure force $\sim -\nabla p$

here: radiative force = volume forces exerted by radiation field

$$(\underline{\nabla} \cdot \underline{P})_i = \sum_j \frac{\partial}{\partial x_j} P_{ij} \quad \text{ith component of divergence (Cartesian)}$$

- p-p symmetry $p_R, u = f(z)$

only $\frac{\partial}{\partial z} \neq 0 \Rightarrow$

$$(\underline{\nabla} \cdot \underline{P})_z = \frac{\partial p_R(z, t)}{\partial z}$$

- spherical symmetry

only $(\underline{\nabla} \cdot \underline{P})_r$ has non-vanishing component

$$(\underline{\nabla} \cdot \underline{P})_r = \frac{\partial p_R}{\partial r} + \frac{1}{r} (3p_R - u)$$

so far, this is the only expression which is different in p-p and spherical symmetry!

Divergence of radiation pressure tensor

For **symmetric** tensors T^{ij} ($i, j = \Theta, \Phi, r$) one can prove the following relations
(e.g., [Mihalas & Weibel Mihalas, "Foundations of Radiation Hydrodynamics", Appendix](#))

$$(\nabla \cdot T)_r = \frac{1}{r^2} \frac{\partial(r^2 T^{rr})}{\partial r} + f(T^{r\Theta}) + f(T^{r\Phi}) - \frac{1}{r} (T^{\Theta\Theta} + T^{\Phi\Phi})$$

$$(\nabla \cdot T)_\Theta = \frac{1}{r} \left\{ f(T^{r\Theta}) + \frac{1}{r \sin \theta} \frac{\partial(\sin \theta T^{\Theta\Theta})}{\partial \theta} + f(T^{\Theta\Phi}) + \frac{1}{r} (T^{r\Theta} - \cot \theta T^{\Phi\Phi}) \right\}$$

$$(\nabla \cdot T)_\Phi = \frac{1}{r \sin \theta} \left\{ f(T^{r\Phi}) + f(T^{\Theta\Phi}) + \frac{1}{r \sin \theta} \frac{\partial T^{\Phi\Phi}}{\partial \phi} + f(\cot \theta T^{\Theta\Phi}) \right\}$$

where f are (different) functions of the tensor-elements which are not relevant here.

Since in spherical symmetry the radiation pressure tensor P is diagonal (i.e., symmetric), and since p_R and u are functions of r alone, we have

$$(\nabla \cdot P)_r = \frac{1}{r^2} \left(2rP^{rr} + r^2 \frac{\partial P^{rr}}{\partial r} \right) - \frac{1}{r} (P^{\Theta\Theta} + P^{\Phi\Phi}) = \frac{\partial P^{rr}}{\partial r} + \frac{1}{r} (2P^{rr} - P^{\Theta\Theta} - P^{\Phi\Phi})$$

(which in the **isotropic** case would yield $(\nabla \cdot P)_r = \frac{\partial P^{rr}}{\partial r} = \frac{\partial p_R}{\partial r}$)

$$(\nabla \cdot P)_\Theta = \frac{1}{r^2 \sin \theta} \left(\cos \theta P^{\Theta\Theta} + \sin \theta \frac{\partial T^{\Theta\Theta}}{\partial \theta} \right) - \frac{1}{r^2} \cot \theta P^{\Phi\Phi} \rightarrow 0 \text{ (in spherical symmetry)}$$

$$(\nabla \cdot P)_\Phi \rightarrow 0 \text{ (in spherical symmetry).}$$

Finally, we obtain

$$(\nabla \cdot P) \rightarrow (\nabla \cdot P)_r = \mathbf{e}_r \cdot \left\{ \frac{\partial p_R}{\partial r} + \frac{1}{r} \left(2p_R - 2 \left(p_R - \frac{1}{2} (3p_R - u) \right) \right) \right\} =$$

$$= \mathbf{e}_r \cdot \left(\frac{\partial p_R}{\partial r} + \frac{1}{r} (3p_R - u) \right), \text{ q.e.d.}$$

Summarizing comparison: from p-p to spherical symmetry



USM

specific intensity and moments similarly defined if $z \rightarrow r$

$I(z, \mu) \rightarrow I(r, \mu)$ with $\mu = \cos \theta$ and $\theta = \angle(\mathbf{e}_r, \mathbf{n})$ [in the following, ν - and t -dependence suppressed]

from symmetry about azimuthal direction:

$$n^{\text{th}} \text{ moment} = \frac{1}{2} \int_{-1}^{+1} I(r, \mu) \mu^n d\mu, \quad \text{as in p-p case when } z \rightarrow r; \quad n=0,1,2 \rightarrow J(r), H(r), K(r)$$

$$\text{flux(-density)} \mathcal{F} = \begin{pmatrix} 0 \\ 0 \\ 4\pi H \end{pmatrix} : \text{only } z\text{- or } r\text{-component different from zero, prop. to Eddington-flux}$$

radiation stress tensor \mathbf{P} : only diagonal elements different from zero

only difference refers to divergence of radiation stress tensor, $\nabla \cdot \mathbf{P}$

in pp-symmetry, only z -component different from zero, and

$$(\nabla \cdot \mathbf{P})_z = \frac{\partial p_R}{\partial z} \quad \text{with } p_R \text{ (radiation pressure scalar)} = \frac{4\pi}{c} K(z)$$

in spherical symmetry, only r -component different from zero, and

$$(\nabla \cdot \mathbf{P})_r = \frac{\partial p_R}{\partial r} + \frac{3p_R - u}{r} \quad \text{with } u \text{ (radiation energy density)} = \frac{4\pi}{c} J(r)$$

Chap. 4 – Coupling with matter

The equation of radiative transfer

- had Boltzmann eq. for particle distrib. function f

$$\left(\frac{\partial}{\partial t} + \underline{v} \cdot \underline{\nabla} + \underline{F} \cdot \underline{\nabla}_p \right) f = \left(\frac{\delta f}{\delta t} \right)_{\text{coll}}$$

for photons $v = c \cdot \underline{n}$, $\underline{F} \equiv 0$ without GR

$$\Rightarrow \left(\frac{\partial}{\partial t} + c \underline{n} \cdot \underline{\nabla} \right) \Psi_\nu = \left(\frac{\delta \Psi_\nu}{\delta t} \right)_{\text{coll}} \leftarrow \begin{array}{l} \text{photon creation/destr.} \\ \text{along path in phase} \\ \text{space} \end{array}$$

with

$$\Psi_\nu(\underline{r}, \underline{n}, t) d\underline{r} d\underline{v} d\underline{\Omega} = f(\underline{r}, \underline{p}, t) d\underline{r} d\underline{p}$$

and

$$\left(\frac{\partial}{\partial t} + c \underline{n} \cdot \underline{\nabla} \right) \frac{I_\nu}{c h \nu} = \frac{1}{c h \nu} \left(\frac{\delta I_\nu}{\delta t} \right)_{\text{coll}}$$

$$\Rightarrow \left(\frac{1}{c} \frac{\partial}{\partial t} + \underline{n} \cdot \underline{\nabla} \right) I_\nu = \left(\frac{\delta I_\nu}{\delta s} \right)_{\text{coll}} = \frac{\delta I_\nu^{\text{em}} - \delta I_\nu^{\text{abs}}}{ds}$$

with

$$I_\nu = c h \nu \Psi_\nu, \quad ds = c \cdot \delta t$$

gain/loss by
interaction with
matter

Equation of radiative transfer for
specific intensity

Emissivity and opacity

- a) vacuum

\rightarrow no "collisions" \rightarrow Vlasov equation

$$\Rightarrow \left[\frac{1}{c} \frac{\partial}{\partial t} + \underline{n} \cdot \underline{\nabla} \right] I = 0$$

stationary

$$\left(\underline{n} \cdot \underline{\nabla} \right) I = \frac{d}{ds} I = 0 \Rightarrow I = \text{const} \quad (\text{cf. Chap 3})$$

↑
directional
derivative

- b) energy gain by emission

add energy to ray (matter in dV radiates)
by emission / photon creation

$$\begin{aligned} \delta E_\nu^+ &= \delta E_\nu^{\text{em}} \stackrel{\text{def}}{=} \eta_\nu(\underline{r}, \underline{n}, t) dV d\Omega d\nu dt \\ &\quad - \eta_\nu(\underline{r}, \underline{n}, t) \underbrace{\underline{n} \cdot d\underline{s}}_{\substack{\cos \theta ds \\ dV}} \cdot ds d\Omega d\nu dt \end{aligned}$$

compare with def. of specific energy

$$\delta E_\nu = I_\nu(\underline{r}, \underline{n}, t) \cos \theta ds d\Omega d\nu dt$$

$$\Rightarrow \delta I_\nu^{\text{em}} = \eta_\nu ds \quad \text{macroscopic emission coefficient}$$

$$\dim[\eta_\nu] = \text{erg cm}^{-3} \text{sr}^{-1} \text{Hz}^{-1} \text{s}^{-1}$$

USA

c) energy loss by **absorption**
 remove energy from ray (matter in dl absorbs)
 by **absorption** / photon destruction

NOTE i) energy gain/emission property of interacting matter
 ii) **BUT**: energy loss must depend on properties of **matter and radiation**, since
 no radiation field \Rightarrow no loss
 no matter \Rightarrow no loss

THUS following definition

$$\delta E_{\nu}^{-} = \delta E_{\nu}^{abs} = (\chi_{\nu} I_{\nu}) (\tau, \eta, t) \cos \theta dS ds d\Omega d\nu dt$$

$$\delta I_{\nu}^{abs} = \chi_{\nu} I_{\nu} ds$$

χ_{ν} absorption coefficient or opacity
 $\dim[\chi_{\nu}] = \text{cm}^{-1}$

d) optical depth

define $d\tau_{\nu} = \chi_{\nu} ds \rightarrow \tau_{\nu}(s) = \int_0^s \chi_{\nu}(s) ds$

$$\delta I_{\nu}^{abs} = I_{\nu} d\tau_{\nu} \quad \begin{matrix} \text{the higher } \tau, \\ \text{the more is absorbed} \end{matrix}$$

$\dim[\tau_{\nu}]$ dimensionless

interpretation later

e) emission and absorption in parallel

$$\left(\frac{\delta I_{\nu}}{ds} \right)_{\text{tot}} = \frac{\delta I_{\nu}^{em} - \delta I_{\nu}^{abs}}{ds} = \eta_{\nu} - \chi_{\nu} I_{\nu}$$

\Rightarrow finally

$$\left(\frac{1}{c} \frac{\partial}{\partial t} + \underline{n} \cdot \underline{\nabla} \right) I_{\nu} = \eta_{\nu} - \chi_{\nu} I_{\nu}$$

η_{ν}, χ_{ν} depend on microphysics of interacting matter

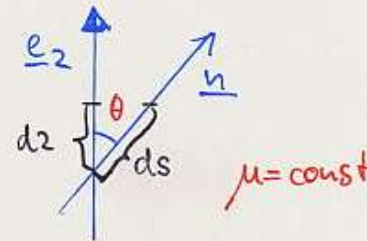
NOTE • in static media η_{ν}, χ_{ν} (mostly) isotropic
 • in moving media: Dopplereffect
 matter "sees" light at frequencies different than the observer \Rightarrow dependency on angle

The equation of transfer for specific geometries

a) plane-parallel symmetry

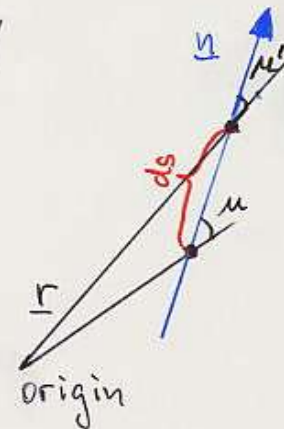
$$dz = \mu ds$$

$$\rightarrow (\underline{n} \cdot \underline{\nabla}) = \frac{d}{ds} = \mu \frac{d}{dz}$$



$$\left(\frac{1}{c} \frac{\partial}{\partial t} + \mu \frac{\partial}{\partial z} \right) I_\nu(z, \mu, t) = \eta_\nu - \chi_\nu I_\nu$$

b) spherical symmetry
along ds , $\mu \neq \text{const}$



without proof

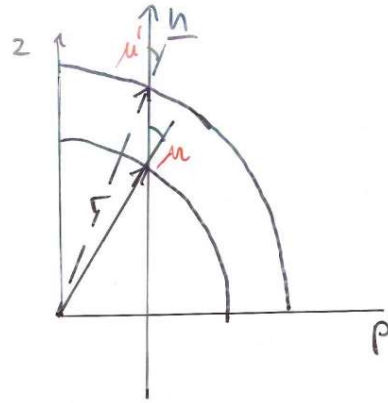
$$(\underline{n} \cdot \underline{\nabla}) = \frac{d}{ds} = \mu \frac{\partial}{\partial r} + \frac{1-\mu^2}{r} \frac{\partial}{\partial \mu}$$

$$\left(\frac{1}{c} \frac{\partial}{\partial t} + \mu \frac{\partial}{\partial r} + \frac{1-\mu^2}{r} \frac{\partial}{\partial \mu} \right) I_\nu(r, \mu, t) = \eta_\nu - \chi_\nu I_\nu$$

c) in general

$$\left[\frac{\partial}{\partial t}, \frac{\partial}{\partial r}, \frac{\partial}{\partial \theta}, \frac{\partial}{\partial \Phi}, \frac{\partial}{\partial \mu}, \frac{\partial}{\partial \phi} \right] I_\nu(\theta, \Phi, r, \mu, \phi, t)$$

The equation of transfer (cont'd)



so-called p-z geometry

$$\frac{d}{ds} = \frac{d}{dz} \Big|_p$$

mit $r^2 = z^2 + \rho^2$
 $\mu = \frac{z}{r}$

$$\Rightarrow \frac{d}{ds} = \frac{d}{dz} \Big|_p = \frac{\partial r}{\partial z} \Big|_p \frac{\partial}{\partial r} + \frac{\partial \mu}{\partial z} \Big|_p \frac{\partial}{\partial \mu}$$

$$r^2 = z^2 + \rho^2 \quad \rightarrow \quad \frac{\partial r}{\partial z} \Big|_p = \frac{z}{r} = \mu$$

$$\mu = \frac{z}{(z^2 + \rho^2)^{1/2}} \quad \rightarrow \quad \frac{\partial \mu}{\partial z} \Big|_p = \frac{1}{r} - \frac{z^2}{r^3} = \frac{1}{r}(1 - \mu^2)$$

$$\Rightarrow \underline{n \cdot \underline{D}} = \frac{d}{ds} = \mu \frac{\partial}{\partial r} + \frac{1 - \mu^2}{r} \frac{\partial}{\partial \mu}$$

$$\left\| \left(\frac{1}{c} \frac{\partial}{\partial t} + \mu \frac{\partial}{\partial r} + \frac{1 - \mu^2}{r} \frac{\partial}{\partial \mu} \right) I_v(r, \mu, t) = \eta_v - \chi_v I_v \right\|$$

General (without proof)

for θ, ϕ, r

$$\left(\frac{1}{c} \frac{\partial}{\partial t} + \mu \frac{\partial}{\partial r} + \frac{\gamma}{r} \frac{\partial}{\partial \theta} + \frac{\sigma}{r \sin \theta} \frac{\partial}{\partial \phi} + \frac{1 - \mu^2}{r} \frac{\partial}{\partial \mu} - \frac{\sigma \cot \theta}{r} \frac{\partial}{\partial \phi} \right) I_v(\theta, \phi, r, \mu, \phi, \nu, t) = \eta_v - \chi_v I_v$$

mit $\gamma = \cos \phi \sin \theta$
 $\sigma = \sin \phi \sin \theta$

Source function

transfer equation

$$\left(\frac{1}{c} \frac{\partial}{\partial t} + \underline{n} \cdot \underline{\nabla} \right) I_\nu = \eta_\nu - \chi_\nu I_\nu \quad \left| \frac{1}{\chi_\nu} \right.$$

now: stationary, $d\tau_\nu = \chi_\nu ds$, $\frac{\partial}{\partial s} = \underline{n} \cdot \underline{\nabla}$

$$\Rightarrow \frac{d}{\chi_\nu ds} I_\nu = \frac{d}{d\tau_\nu} I_\nu = \frac{\eta_\nu}{\chi_\nu} - I_\nu \stackrel{\text{def}}{=} S_\nu - I_\nu$$

compact form of transfer equation

$$\frac{dI_\nu}{d\tau_\nu} = S_\nu - I_\nu \quad \text{with source function } S_\nu$$

- valid in any geometry, if stationary + $\frac{d}{d\tau_\nu} = \frac{\underline{n} \cdot \underline{\nabla}}{\chi_\nu}$

physical interpretation

- later we will show that mean free path of photons corresponds to $\tau_\nu = 1$

$$\Rightarrow 1 \approx \chi_\nu \Delta s, \quad \Delta s = \frac{1}{\chi_\nu}$$

$$\Rightarrow S_\nu = \frac{\eta_\nu}{\chi_\nu} = \eta_\nu \Delta s$$

source function corresponds to emitted intensity $S I_\nu^{\text{em}}$ over mean free path

Kirchhoff-Planck law

- assume thermodynamic equilibrium (TE)

→ radiation field homogeneous stationary

$$\Rightarrow \left(\frac{1}{c} \frac{\partial}{\partial t} + \underline{n} \cdot \underline{\nabla} \right) = 0$$

intensity Planck-function

$$\Rightarrow 0 = I_\nu - S_\nu = B_\nu - S_\nu$$

TE: $S_\nu^* = \frac{\eta_\nu^*}{\chi_\nu^*} = B_\nu(T)$ ← Kirchhoff-Planck law
or other way round

TE: $\eta_\nu^* = \chi_\nu^* B_\nu(T)$ [only one quantity to be specified]

True absorption and scattering



USM

"true" absorption processes:

radiation energy \Rightarrow thermal pool
if not TE, temperature $T(r)$ is changed
examples: photo-ionization
bound-bound absorption with subsequent collisional de-excitation

scattering:

no interaction with thermal pool
absorbed photon energy is directly reemitted (as photon)
no influence on $T(r)$
But direction $\underline{n} \rightarrow \underline{n}'$ is changed (change in frequency mostly small)

examples: Thomson scattering at free electrons
Rayleigh scattering at atoms and molecules
resonance line scattering

ESSENTIAL POINT

true processes:

localized interaction with thermal pool,
drive physical conditions into local equilibrium
often (e.g., in LTE - [page 127](#)): $\eta_\nu(\text{true}) = \kappa_\nu B_\nu(T)$

scattering processes:

(almost) no influence on local thermodynamic properties of plasma
propagate information of radiation field (sometimes over large distances)
 η_ν (Thomson) = $\sigma_{\text{TH}} J_\nu$ (-> next page)

Thomson scattering

- limiting case for long wavelengths of Klein-Nishina scattering
- almost freq. independent
- major source of scattering opacity in hot stars (as long as enough free electrons and hydrogen ionized)
- dipole characteristics not important, isotropic approximation sufficient

$$\sigma_{\nu}(\underline{r}, \mu) \rightarrow \sigma(\underline{r}) = n_e(\underline{r}) \sigma_e,$$

$$\sigma_e = \frac{8\pi e^4}{3m_e^2 c^4} = 6.65 \cdot 10^{-25} \text{ cm}^2$$

$$\eta^{\text{TH}} = \sigma_e n_e(\underline{r}) \cdot \int_{\nu}(\underline{r}) \quad (\text{without proof})$$

"coherent scattering", $\nu_{\text{abs}} = \nu_{\text{em}}$

Total continuum opacity / source function

$$\chi_{\nu} = \kappa_{\nu}^{\dagger} + \sigma_{\nu} \quad (\dagger = \text{true})$$

$$\eta_{\nu} = \kappa_{\nu}^{\dagger} B_{\nu}(\tau) + \sigma_{\nu} J_{\nu}$$

$$\rightarrow S_{\nu}^{\text{cont}} = \frac{\kappa_{\nu}^{\dagger} B_{\nu} + \sigma_{\nu} J_{\nu}}{\kappa_{\nu}^{\dagger} + \sigma_{\nu}} \xrightarrow{\text{Th. scatt}} (1 - g_{\nu}^{\text{TH}}) B_{\nu} + g_{\nu}^{\text{TH}} J_{\nu}$$

$$g_{\nu}^{\text{TH}} = \frac{\sigma_e n_e}{\kappa_{\nu}^{\dagger} + \sigma_e n_e}$$

Moments of the transfer equation

transfer equation (\equiv Boltzmann equation with $\mathbb{F} \equiv 0$)

$$\left(\frac{1}{c} \frac{\partial}{\partial t} + \underline{n} \cdot \underline{\nabla}\right) I_\nu = \eta_\nu - \chi_\nu I_\nu$$

0th moment: $\oint d\Omega$

note: \underline{n} commutes with $\frac{\partial}{\partial t}$, $\underline{\nabla}$, since (t, r, μ) independent variables here)

- integrate transfer equation over $d\Omega$

$$\frac{4\pi}{c} \frac{\partial}{\partial t} J_\nu + \underline{\nabla} \cdot \underline{\mathcal{F}}_\nu = \oint (\eta_\nu - \chi_\nu I_\nu) d\Omega$$

- if χ_ν, η_ν isotropic, $\rightarrow = 4\pi(\eta_\nu - \chi_\nu J_\nu)$
i.e., no velocity fields

- Now frequency integration

$$\frac{4\pi}{c} \frac{\partial}{\partial t} J(\underline{r}, t) + \underline{\nabla} \cdot \underline{\mathcal{F}}(\underline{r}, t) = \int_0^\infty d\nu \left\{ \underset{\substack{\uparrow \\ \text{total rad. energy}}}{\eta_\nu} - \underset{\substack{\uparrow \\ \text{added and removed}}}{\chi_\nu} J_\nu \right\} d\Omega$$

- If energy transported by radiation alone (i.e., no convection) and no energy is created (which is true for stellar atmospheres)

\Rightarrow

$$\int_0^\infty d\nu \oint (\eta_\nu - \chi_\nu I_\nu) d\Omega = 0 \quad \text{"radiative equilibrium"}$$

static \rightarrow atm.

$$\int_0^\infty d\nu (\eta_\nu - \chi_\nu J_\nu) = \int_0^\infty d\nu \chi_\nu (S_\nu - J_\nu) = 0$$

- if radiation field time independent

$$\underline{\nabla} \cdot \underline{\mathcal{F}} = 0 \quad \text{"flux conservation"}$$

pp \swarrow \searrow spherical

$$\frac{L}{4\pi r^2} = \mathcal{F}(r) = \text{const} \quad r^2 \mathcal{F}(r) = \text{const} = \frac{L}{4\pi}$$

- radiative equilibrium and flux conservation equivalent formulations, are used to calculate $T(r)$

0th moment: frequency-dependent, stationary and static

$$\underline{\nabla} \cdot \underline{\mathcal{F}}_\nu = 4\pi(\eta_\nu - \chi_\nu J_\nu)$$

static: $v=0$ (or $v \ll v_{\text{sound}}$)

stationary: time-independent, $\partial/\partial t=0$



1st moment: $\oint \underline{n} d\Omega/c$

$$\oint \frac{d\Omega}{c} \left(\underline{n} \frac{1}{c} \frac{\partial}{\partial t} + \underline{n} \cdot \underline{\nabla} \right) I_\nu = \frac{1}{c} \oint (\eta_\nu - \chi_\nu I_\nu) \underline{n} d\Omega$$

→

$$\frac{1}{c^2} \frac{\partial}{\partial t} \underline{F}_\nu + \underline{\nabla} \cdot \underline{P}_\nu = \frac{1}{c} \oint (\eta_\nu - \chi_\nu I_\nu) \underline{n} d\Omega$$

Tensor, cf. Chap. 3

frequency integrated analogous

- can be shown

$$\frac{1}{c} \int_0^\infty dv \oint \chi_\nu I_\nu \underline{n} d\Omega \quad \text{is force/volume, by radiation on matter (momentum transfer photons} \rightarrow \text{matter via absorption)}$$

$$= \underline{g}_{\text{rad}}(\underline{r}) \quad \text{"radiation force"}$$

$$\frac{\text{force}}{\text{volume}} \cdot \frac{1}{\rho} = \frac{\text{force}}{\text{mass}} = \text{grad "radiative acceleration"}$$

and

$$\int dv \oint \eta_\nu \underline{n} d\Omega = 0 \quad \text{because of fore/aft symmetry of emission process (even in } \nu\text{-fields)}$$

- in total

$$\frac{1}{c^2} \frac{\partial}{\partial t} \underline{F}(\underline{r}, t) + \underline{\nabla} \cdot \underline{P}(\underline{r}, t) = -\frac{1}{c} \int dv \oint \chi_\nu I_\nu \underline{n} d\Omega = -\rho \underline{g}_{\text{rad}}(\underline{r})$$

- stationary

$$\underline{\nabla} \cdot \underline{P}(\underline{r}) = -\rho(\underline{r}) \underline{g}_{\text{rad}}(\underline{r}) = -\frac{1}{c} \int_0^\infty dv \oint d\Omega (\chi_\nu I_\nu) \underline{n}$$

- static

$$\rightarrow -\frac{1}{c} \int_0^\infty dv \chi_\nu \underline{F}_\nu(\underline{r})$$

1-D
→

$$\underline{g}_{\text{rad}}(\underline{r}) = \frac{4\pi}{c \rho(\underline{r})} \int_0^\infty dv \chi_\nu(\underline{r}) H_\nu(\underline{r})$$

1st moment: frequency-dependent, stationary and static

$$\underline{\nabla} \cdot \underline{P}_\nu = -\frac{1}{c} \chi_\nu \underline{F}_\nu$$

The change in radiative pressure drives the flux!

static: $v=0$ (or $v \ll v_{\text{sound}}$)

stationary: time-independent, $\partial/\partial t=0$



Summary: moments of the RTE ...



... expressed also in terms of J_ν , H_ν , K_ν

general case, 0th moment

$$\frac{4\pi}{c} \frac{\partial}{\partial t} J_\nu + \nabla \cdot \mathcal{F}_\nu = \oint (\eta_\nu - \chi_\nu I_\nu) d\Omega$$

plane-parallel, stationary ($\partial/\partial t = 0$) and static ($v \approx 0$)

$$\frac{dH_\nu}{dz} = \eta_\nu - \chi_\nu J_\nu$$

spherically symmetric, stationary and (quasi-)static

[no/negligible Dopplershifts \Rightarrow no winds or continuum problems (except for edges)]

Otherwise, opacities become angle-dependent (Doppler-shifts), and cannot be put in front of the integrals]

$$\frac{1}{r^2} \frac{\partial(r^2 H_\nu)}{\partial r} = \eta_\nu - \chi_\nu J_\nu$$

when frequency integrated, = 0, if ONLY radiation energy transported: **radiative equilibrium**
 \rightarrow (for stationary conditions) **flux conservation**

general case, 1st moment

$$\frac{1}{c^2} \frac{\partial}{\partial t} \mathcal{F} + \nabla \cdot \mathbf{P}_\nu = \frac{1}{c} \oint (\eta_\nu - \chi_\nu I_\nu) \mathbf{n} d\Omega$$

$$\frac{dK_\nu}{dz} = -\chi_\nu H_\nu$$

$$\frac{\partial K_\nu}{\partial r} + \frac{3K_\nu - J_\nu}{r} = -\chi_\nu H_\nu$$

when frequency integrated, = $-\mathbf{f}_{\text{rad}}$

Chap. 5 - Radiative transfer: simple solutions

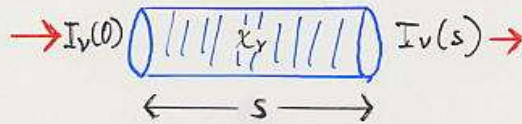


USM

Pure absorption and optical depth

- from here on, stationary description (→ stellar atmospheres)
- radiative transfer without emission

$$\frac{dI_\nu}{ds} = -\chi_\nu I_\nu$$



$$\frac{dI_\nu}{I_\nu} = -\chi_\nu(s) ds$$

$$\ln I_\nu(s) - \ln I_\nu(0) = - \int_0^s \chi_\nu(s') ds'$$

$$I_\nu(s) = I_\nu(0) e^{-\int_0^s \chi_\nu(s') ds'} = I_\nu(0) e^{-\tau_\nu(s)}$$

or

$$I_\nu(\tau_\nu) = I_\nu(0) e^{-\tau_\nu}$$

optical depth,
central quantity

(more precisely: optical
thickness)

- since $I_\nu \sim e^{-\tau_\nu}$, we look only until $\tau_\nu = 1$ (freq. dep.!).

- Question: What is the average distance over which photons travel?

$$\text{Answer: } \langle \tau_\nu \rangle = \int_0^\infty \tau_\nu p(\tau_\nu) d\tau_\nu$$

↑
expectation
value

↑
probability density function

$p(\tau_\nu) d\tau_\nu$ gives probability, that photon is absorbed in interval $\tau_\nu, \tau_\nu + d\tau_\nu$

- is probability, that photon is NOT absorbed between $0, \tau_\nu$ and then absorbed between $\tau_\nu, \tau_\nu + d\tau_\nu$

- a) prob., that photon is absorbed

$$P(0, \tau_\nu) = \frac{\Delta I(\tau_\nu)}{I_0} = \frac{I_0 - I(\tau_\nu)}{I_0} = 1 - \frac{I(\tau_\nu)}{I_0}$$

- b) prob., that photon is not absorbed

$$1 - P(0, \tau_\nu) = \frac{I(\tau_\nu)}{I_0} = e^{-\tau_\nu}$$

- c) prob., that photon is absorbed in $\tau_\nu, \tau_\nu + d\tau_\nu$

$$P(\tau_\nu, \tau_\nu + d\tau_\nu) = \left| \frac{dI(\tau_\nu)}{I(\tau_\nu)} \right| = d\tau_\nu$$

- d) total probability is $e^{-\tau_\nu} d\tau_\nu$

THUS

$$\langle \tau_\nu \rangle = \int_0^\infty \tau_\nu e^{-\tau_\nu} d\tau_\nu = 1$$

mean free path \bar{s} corresponds to $\langle \tau_\nu \rangle = 1$

$$\Delta \tau_\nu = \chi_\nu \Delta s \rightarrow \frac{\Delta s}{\bar{s}} = \frac{1}{\chi_\nu}, \text{ q.e.d.}$$

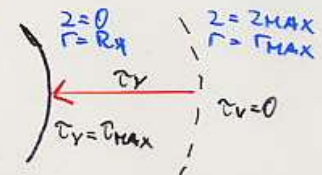
USUAL convention

- Since we "measure" from outside to inside, $\tau_\nu = 0$ is defined at outer "edge" of atmosphere

$$\Rightarrow ds = -dz \text{ (or } -dr)$$

$$\Rightarrow d\tau_\nu = -\chi_\nu \left(\frac{dz}{dr} \right)$$

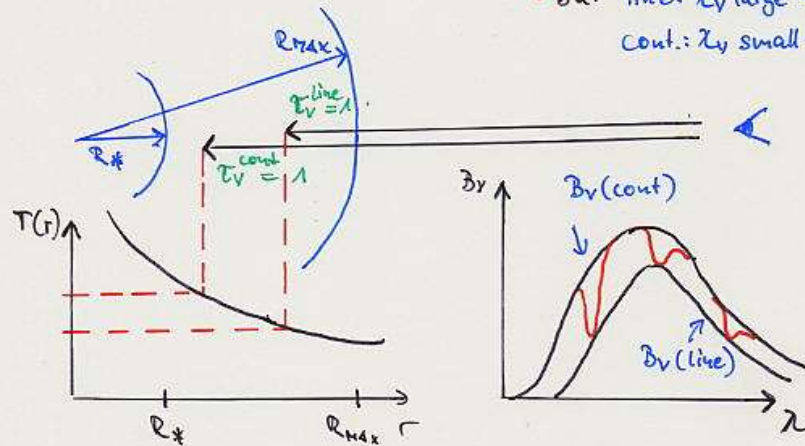
>0! <0!





Formation of spectral lines: the principle

- look always down to $\tau_v \neq 1$
- BAT line: χ_v large $\rightarrow \bar{s}$ small
cont.: χ_v small $\rightarrow \bar{s}$ large



$$T(\tau_{cont}) > T(\tau_{line})!$$

"Formal solution"

solve eq. of RT with **known** source function

- pp geometry

$$\mu \frac{dI_v}{dz} = \eta_v - \chi_v I_v$$

$$\rightarrow \mu \frac{dI_v}{d\tau_v} = I_v - S_v \quad (\tau_v = 0 \text{ outside!})$$

- solution with integrating factor $e^{-\tau_v/\mu}$
multiply equation, integrate between τ_1 and τ_2
 τ_2 (inside) $>$ τ_1 (outside)

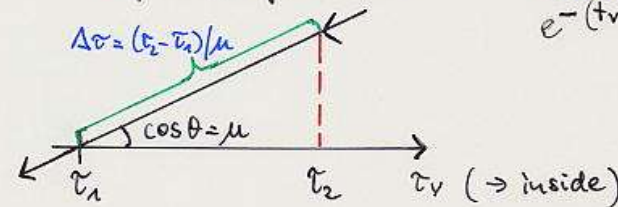
\Rightarrow

$$I_v(\tau_1, \mu) = I_v(\tau_2, \mu) e^{-\frac{(\tau_2 - \tau_1)}{\mu}} + \int_{\tau_1}^{\tau_2} S_v(\tau_v) e^{-\frac{(\tau_v - \tau_1)}{\mu}} \frac{d\tau_v}{\mu}$$

$> 0 \checkmark$ $> 0 \checkmark$

intensity "emitted" at τ_2 ,
loss (abs) by factor $e^{-\Delta\tau}$
 $\hat{=}$ pure absorption case

gain by emission
with subsequent
absorption
 $e^{-\frac{(\tau_v - \tau_1)}{\mu}}$



Boundary conditions

- a) incident intensity from inside

$$\mu > 0 \text{ at } \tau_2 = \tau_{max}$$

- either $I_v(\tau_2 = \tau_{max}, \mu) = I_v^+(\mu)$ (e.g., from diffusion approx)

- or "semi-infinite" atmosphere
 $\tau_2 = \tau_{max} \rightarrow \infty$ with $\lim_{\tau_v \rightarrow \infty} I_v(\tau_v, \mu) e^{-\tau_v/\mu} = 0$

($I_v(\tau_v, \mu)$ increases slower than exp.)

$$\Rightarrow I_v(\tau_v, \mu) = \int_{\tau_v}^{\infty} S_v(t) e^{-\frac{(t - \tau_v)}{\mu}} \frac{dt}{\mu} \quad \mu > 0$$



b) incident intensity from outside
 $\mu < 0$ at $\tau_v = 0$

- usually $I_v(0, \mu) = 0$ no irradiation from outside (however, binaries!)

$$\Rightarrow I_v(\tau_v, \mu) = \int_{\tau_v}^0 S_v(t) e^{-(t-\tau_v)/\mu} \frac{dt}{\mu} \quad \mu < 0$$
$$= \int_0^{\tau_v} S_v(t) e^{-(\tau_v-t)/(-\mu)} \frac{dt}{(-\mu)} \quad (-\mu) > 0$$

c) emergent intensity = observed intensity
(if no extinction)

$$\tau_v = 0, \quad \mu > 0$$

$$I_v^{em}(\mu) = \int_0^{\infty} S_v(t) e^{-t/\mu} \frac{dt}{\mu}$$

emergent intensity is Laplace-transformed of source function!

NOW: suppose that S_v is linear in τ_v , i.e.,

$$S_v(\tau_v) = S_{v0} + S_{v1} \cdot \tau_v \quad (\text{Taylor expansion around } \tau_v = 0)$$

$$\Rightarrow I_v^{em}(\mu) = \int_0^{\infty} (S_{v0} + S_{v1} \cdot t) e^{-t/\mu} \frac{dt}{\mu} = \dots$$
$$= S_{v0} + S_{v1} \cdot \mu = S_v(\tau_v = \mu)$$

Eddington-Barbier-relation



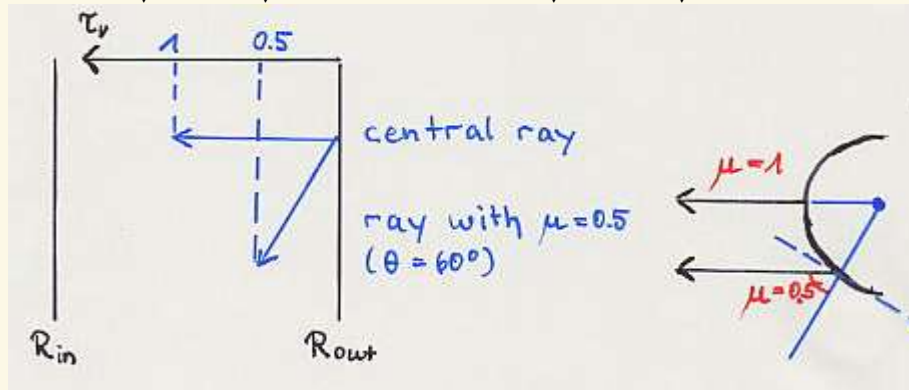
$$I_{\nu}^{\text{em}}(\mu) \approx S_{\nu}(\tau_{\nu} = \mu)$$

We “see” source function at location $\tau_{\nu} = \mu$ (remember: τ_{ν} radial quantity)
(corresponds to optical depth along path $\tau_{\nu} / \mu = 1$!)

Generalization of principle that we can see only until $\Delta\tau_{\nu} = 1$

i) spectral lines (as before)

for fixed μ , $\tau_{\nu} / \mu = 1$ is reached further out in lines (compared to continuum)
 $\Rightarrow S_{\nu}^{\text{line}}(\tau_{\nu}^{\text{line}} / \mu = 1) < S_{\nu}^{\text{cont}}(\tau_{\nu}^{\text{cont}} / \mu = 1) \Rightarrow$ “dip” is created



ii) limb darkening

for $\mu = 1$ (central ray), we reach maximum in depth (geometrical)
temperature / source function rises with τ
 \Rightarrow central ray: largest source function, limb darkening

iii) “observable” information only from layers with $\tau_{\nu} \leq 1$

deepest atmospheric layers can be analyzed only **indirectly**



Solar limb-darkening

Empirical temperature stratification

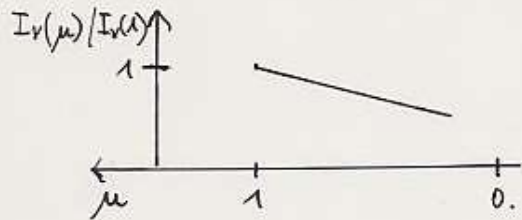


Application: solar limb-darkening

Had $I_\nu^{em}(\mu) = S_{\nu 0} + \mu S_{\nu 1}$

→ LTE $S_\nu \approx B_\nu$, $I_\nu^{em} = B_\nu(0) + \mu \left. \frac{dB_\nu}{d\tau_\nu} \right|_0$

→ $\frac{I_\nu(\mu)}{I_\nu(1)} = \frac{B_\nu(0) + \mu \frac{dB_\nu}{d\tau_\nu}}{B_\nu(0) + \frac{dB_\nu}{d\tau_\nu}}$



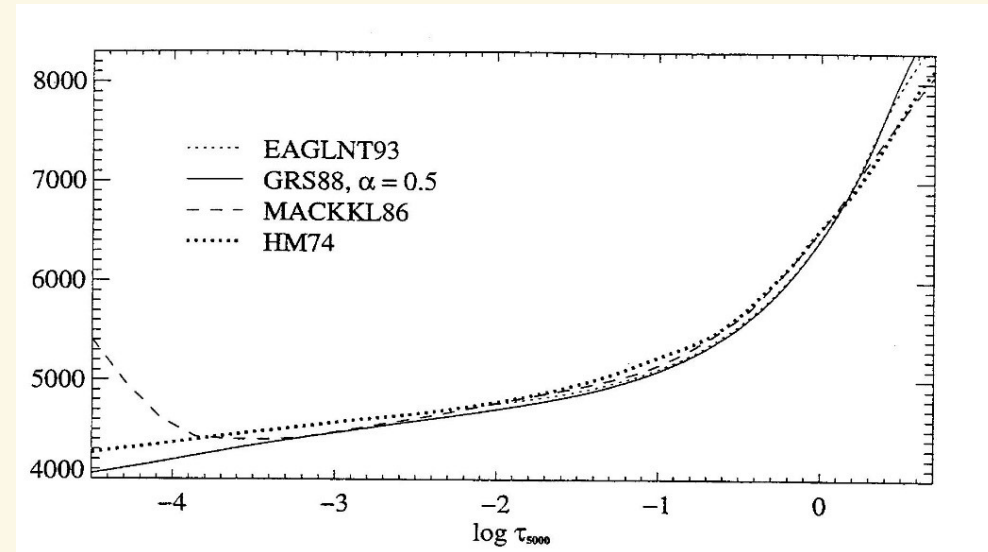
measurement $\Rightarrow B_\nu(0), \left. \frac{dB_\nu}{d\tau_\nu} \right|_0$

(one absolute measurement required, e.g., $B_\nu(0)$)

$\Rightarrow B_\nu(\tau) = B_\nu(0) + \left. \frac{dB_\nu}{d\tau_\nu} \right|_0 \cdot \tau =: \frac{2h\nu^3}{c^2} \frac{1}{e^{h\nu/kT(\tau)} - 1}$

$\Rightarrow T(\tau)$, empirical temperature stratification of solar photosphere

empirical temperature structure of solar photosphere by Holweger & Müller (1974)



Lambda operator

The Lambda operator

had mean intensity

$$J_\nu = \frac{1}{2} \int_{-1}^{+1} I_\nu(\mu) d\mu = \frac{1}{2} \int_0^1 [I_\nu^+(\mu) + I_\nu^-(-\mu)] d\mu \xrightarrow{\text{semi-infinite atm.}}$$

$$\frac{1}{2} \left\{ \int_0^1 d\mu \left[\int_{\tau_\nu}^{\infty} S_\nu(t) e^{-(t-\tau_\nu)/\mu} \frac{dt}{\mu} \right] + \int_0^{\tau_\nu} S_\nu(t) e^{-(\tau_\nu-t)/\mu} \frac{dt}{\mu} \right\}$$

outwards
inwards
(I(-μ))

$$= \left(x = \frac{1}{\mu}, \frac{dx}{x} = -\frac{d\mu}{\mu} \right)$$

$$\frac{1}{2} \int_{\tau_\nu}^{\infty} dt S_\nu(t) \int_1^{\infty} e^{-(t-\tau_\nu)x} \frac{dx}{x} + \frac{1}{2} \int_0^{\tau_\nu} dt S_\nu(t) \int_1^{\infty} e^{-(\tau_\nu-t)x} \frac{dx}{x}$$

$$\left(\int_1^{\infty} e^{-t \cdot x} \frac{dx}{x} = \int_t^{\infty} \frac{e^{-x}}{x} dx = E_1(t) \right)$$

1st Exponential integral

$$J_\nu(\tau_\nu) = \frac{1}{2} \int_0^{\infty} S_\nu(t) E_1(|t-\tau_\nu|) dt \quad \text{Karl Schwarzschild}$$

$$\text{with } \Lambda_\tau[f] = \frac{1}{2} \int_0^{\infty} f(t) E_1(|t-\tau|) dt \quad \text{"Lambda operator"}$$

$$J_\nu(\tau_\nu) = \Lambda_{\tau_\nu}(S_\nu) \quad \text{or} \quad J = \Lambda(S)$$

Diffusion approximation

The diffusion approximation

- for large optical depths $S_V \rightarrow B_V$
- **Question** What is response of radiation field?
- **expansion**

$$S_V(\tau_V) = \sum_{n=0}^{\infty} \frac{d^n B_V}{d\tau_V^n} \Big|_{\tau_V} (\tau_V - \tau_V)^n / n!$$

- put into formal solution

$$\Rightarrow I_V^+(\tau_V, \mu) = \sum_{n=0}^{\infty} \mu^n \frac{d^n B_V}{d\tau_V^n} = B_V(\tau_V) + \mu \frac{dB_V}{d\tau_V} + \mu^2 \frac{d^2 B_V}{d\tau_V^2} + \dots$$

I_V^- analogous, difference $0 (e^{-\tau_V/\mu})$

$$\Rightarrow J_V(\tau_V) = \sum_{n=0}^{\infty} (2n+1)^{-1} \frac{d^{2n} B_V}{d\tau_V^{2n}} = B_V(\tau_V) + \frac{1}{3} \frac{d^2 B_V}{d\tau_V^2} + \dots \text{ even}$$

$$H_V(\tau_V) = \sum_{n=0}^{\infty} (2n+3)^{-1} \frac{d^{2n+1} B_V}{d\tau_V^{2n+1}} = \frac{1}{3} \frac{dB_V}{d\tau_V} + \dots \text{ odd}$$

$$K_V(\tau_V) = \sum_{n=0}^{\infty} (2n+3)^{-1} \frac{d^{2n} B_V}{d\tau_V^{2n}} = \frac{1}{3} B_V + \frac{1}{5} \frac{d^2 B_V}{d\tau_V^2} + \dots \text{ even}$$

\Rightarrow diffusion approx. for radiation field

$\tau_V \gg 1$, use only first order

$$I_V = B_V(\tau_V) + \mu \frac{dB_V}{d\tau_V} \quad \text{required to obtain } H_V \neq 0$$

$$J_V = B_V(\tau_V)$$

$$H_V = \frac{1}{3} \frac{dB_V}{d\tau_V} = -\frac{1}{3} \frac{1}{\chi_V} \frac{\partial B_V}{\partial \tau} \frac{d\tau}{dz} \quad \left. \begin{array}{l} \text{ } \\ \text{ } \end{array} \right\} f_V = \frac{K_V}{J_V} = \frac{1}{3} (\tau_V \gg 1)$$

$$K_V = \frac{1}{3} B_V(\tau_V)$$

'Eddington factor'

$$\bullet H_V = -\frac{1}{3} \frac{1}{\chi_V} \frac{\partial B_V}{\partial \tau} \frac{d\tau}{dz}$$

$\underbrace{\hspace{1.5cm}}_{>0}$

\Rightarrow in order to transport flux $H_V > 0$, $\frac{d\tau}{dz} < 0$,
i.e., temperature must decrease!

From approximate solution of moments equations accounting for true plus scattering continuum opacity (**Milne-Eddington model** → advanced reading), it turns out that the difference between mean intensity and Planck-function (as a function of optical depth) can be written as

$$J_\nu - B_\nu \approx f(\varepsilon_\nu) \exp\left[-(3\varepsilon_\nu)^{1/2} \tau_\nu\right],$$

with *thermalization parameter*

$$\varepsilon_\nu = \frac{\kappa_\nu^t}{\kappa_\nu^t + \sigma_\nu}$$

given by the ratio of true and total opacity.

Thus, only for large arguments of the exponent we achieve $J_\nu \rightarrow B_\nu$, namely if

$$\tau_\nu \geq \frac{1}{\sqrt{\varepsilon_\nu}}$$

with $\frac{1}{\sqrt{\varepsilon_\nu}}$ the so-called **thermalization depth** [$\sqrt{3}$ in denominator neglected]

a) for $\sigma_\nu \ll \kappa_\nu^t$ (negligible scattering) $\rightarrow J_\nu(\tau_\nu \geq 4...5) \rightarrow B_\nu$

b) SN remnants: scattering dominated, very large thermalization depth

The Milne-Eddington model

The Milne-Eddington model for continua with scattering

- allows understanding of emergent (continuum) fluxes from stellar atmospheres
- can be extended to include lines
- required for curve of growth method (→ Chap. 7)

assume source function (→ page 78)

$$S_\nu = (1-g_\nu)B_\nu + g_\nu J_\nu \quad \text{with} \quad g_\nu = \frac{\sigma_{\nu e}}{K_\nu + \sigma_{\nu e}}$$

$$=: \epsilon_\nu B_\nu + (1-\epsilon_\nu) J_\nu, \quad \epsilon_\nu = 1-g_\nu$$

and

$$B_\nu = a_\nu + b_\nu \cdot \tau_\nu \quad + \quad \text{plane-parallel symmetry}$$

- 0th moment

$$\frac{\partial H_\nu}{\partial \tau_\nu} = J_\nu - S_\nu, \quad d\tau_\nu = -(K_\nu + \kappa_{\nu e}) dz$$

$$= J_\nu - (\epsilon_\nu B_\nu + (1-\epsilon_\nu) J_\nu) = \epsilon_\nu (J_\nu - B_\nu)$$

- 1st moment

$$\frac{\partial K_\nu}{\partial \tau_\nu} = H_\nu$$

in diffusion approximation, we had

$$K_\nu = \frac{1}{3} J_\nu \quad (\tau_\nu \rightarrow \infty)$$

- Eddington's approximation (1929, 'The formation of absorption lines')
use $K_\nu/J_\nu = \frac{1}{3}$ everywhere ... not so wrong

$$\Rightarrow \frac{\partial K_\nu}{\partial \tau_\nu} = H_\nu \Rightarrow \frac{1}{3} \left(\frac{\partial J_\nu}{\partial \tau_\nu} \right) = H_\nu$$

⇒ (with 0th moment)

$$\frac{1}{3} \frac{\partial^2 J_\nu}{\partial \tau_\nu^2} = \epsilon_\nu (J_\nu - B_\nu) = \frac{1}{3} \frac{\partial^2 (J_\nu - B_\nu)}{\partial \tau_\nu^2}$$

since B_ν linear in τ_ν !

assume $\epsilon_\nu = \text{const}$ (otherwise similar solution)

$$J_\nu - B_\nu = \text{const}' \cdot \exp\left(-(\sqrt{3}\epsilon_\nu)^{\frac{1}{2}} \tau_\nu\right) \quad \left[\begin{array}{l} \text{with lower b.c.} \\ J_\nu \rightarrow B_\nu \text{ for } \tau \rightarrow \infty \end{array} \right]$$

- Eddington's approximation implies also

a) $J_\nu(0) = \sqrt{3} H_\nu(0)$ (without proof)

b) $\frac{\partial K_\nu}{\partial \tau_\nu} = H_\nu \Rightarrow \frac{1}{3} \frac{\partial J_\nu}{\partial \tau_\nu} \Big|_0 = H_\nu(0)$

Thus $\frac{1}{\sqrt{3}} \frac{\partial J_\nu}{\partial \tau_\nu} \Big|_0 = J_\nu(0)$

⇒ insert in above equation

$$\text{const}' = \frac{b_\nu \sqrt{3} - a_\nu}{(1 + \epsilon_\nu^{\frac{1}{2}})}$$

$$\Rightarrow J_\nu = a_\nu + b_\nu \tau_\nu + \frac{b_\nu \sqrt{3} - a_\nu}{1 + \epsilon_\nu^{\frac{1}{2}}} e^{-(\sqrt{3}\epsilon_\nu)^{\frac{1}{2}} \tau_\nu}$$

$$J_\nu = a_\nu + b_\nu \tau_\nu + \frac{b_\nu \sqrt{13} - a_\nu}{1 + \epsilon_\nu^{\frac{1}{2}}} e^{-(3\epsilon_\nu)^{\frac{1}{2}} \tau_\nu}$$

$$J_\nu(0) = a_\nu + \frac{b_\nu \sqrt{13} - a_\nu}{1 + \epsilon_\nu^{\frac{1}{2}}}$$

$$H_\nu(0) = \frac{1}{\sqrt{13}} J_\nu(0)$$

- assume isothermal atmosphere, $b_\nu = 0$
(possible, if gradient not too strong)

$$\Rightarrow J_\nu(0) = \frac{\epsilon_\nu^{\frac{1}{2}}}{1 + \epsilon_\nu^{\frac{1}{2}}} a_\nu \begin{cases} \nearrow B_\nu/2 \text{ (for } \epsilon_\nu = 1, \text{ i.e. } \sigma = 0) \\ \searrow \epsilon_\nu^{\frac{1}{2}} B_\nu \ll B_\nu \text{ (for } \epsilon_\nu \ll 1) \end{cases}$$

$$\rightarrow J_\nu(0) < B_\nu(0) !!!$$

• Thermalization

only for large arguments of the exponent,
we have $J_\nu \approx B_\nu$

$$\Rightarrow \tau_\nu \geq \frac{1}{\epsilon_\nu^{\frac{1}{2}}} \quad \text{thermalisation depth}$$

a) $\sigma \ll \kappa^+ \Rightarrow J_\nu(\tau_\nu \geq 1) \rightarrow B_\nu$

b) SW remnants: scattering dominated,
very large thermalization depth

• pure scattering (test case)

$$\frac{\partial H_\nu}{\partial \tau_\nu} = J_\nu - S_\nu = 0 \quad \text{for } \epsilon_\nu = 0 \quad \text{Flux conservation}$$

$$+ H_\nu = \frac{1}{3} \frac{\partial B_\nu}{\partial \tau_\nu} \quad \text{from diffusion limit}$$

in Milne Eddington model

$$H_\nu(0) = \frac{1}{\sqrt{13}} \left(a_\nu + \frac{b_\nu \sqrt{13} - a_\nu}{1 + \epsilon_\nu^{\frac{1}{2}}} \right) \xrightarrow{\epsilon_\nu \rightarrow 0} \frac{b_\nu}{3} \approx \frac{1}{3} \frac{\partial B_\nu}{\partial \tau_\nu}$$

consistent result

- Question: why $J_\nu(0) \ll B_\nu(0)$?

- remember: $J_\nu(0)$ determined by $S_\nu(\tau_\nu = 1)$
- $J_\nu(1)$ might fall significantly below $B_\nu(1)$, since many photons can escape from photosphere (into interstellar medium)
- minimum value is given by incident flux, if no thermal emission

- interesting possibility

if ϵ_ν small, $H_\nu(0)$ can become larger than $H_\nu(0)$ ($\epsilon_\nu = 1$), if

$$a_\nu + \frac{b_\nu \sqrt{13} - a_\nu}{2} < \frac{b_\nu}{\sqrt{13}}, \quad \text{i.e. } \frac{b_\nu}{a_\nu} > \sqrt{13}$$

$$\underbrace{J_\nu(0, \epsilon_\nu = 1)} < \underbrace{J_\nu(0, \epsilon_\nu \ll 1)}$$

i.e. for large temperature gradients

(information is transported from hotter regions to outer boundary by scattering dominated stratifications)

- further consequences later

Basic assumptions

1. Geometry

plane-parallel or spherically symmetric (\rightarrow Chap. 3)

2. Homogeneity

atmospheres assumed to be homogenous (both vertical and horizontal)

BUT: **sun** with spots, granulation, non-radial pulsations ...

white dwarfs with depth dependent abundances (diffusion)

stellar winds of hot stars (partly) with clumping ($\langle \rho^2 \rangle \neq \langle \rho \rangle^2$)

HOPE: "mean" = homogenous model describes non-resolvable phenomena in a reasonable way

[attention for (magnetic) Ap-stars: *very* strong inhomogeneities!]

3. Stationarity

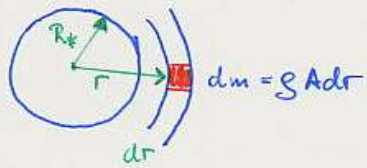
vast majority of spectra time-independent $\Rightarrow \partial/\partial t = 0$

BUT: explosive phenomena (supernovae)

pulsations

close binaries with mass transfer ...

Density stratification



mass element dm
in (spherically sym.) atmosphere

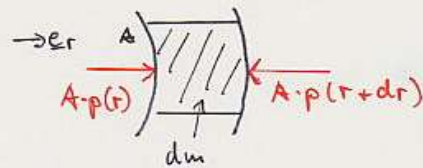
assume (at first) no velocity-fields, i.e. **hydrostatic stratification**

$\sum_i df_i = 0$, if f_i are forces acting on dm

• $df_{\text{grav}} = -G \frac{M_r dm}{r^2} = -g(r) dm$ with grav. accel.

$$g(r) = \frac{G M_r}{r^2} \text{ and } M_r \text{ mass within } r$$

• df_p pressure forces



gas pressure causes forces on surfaces $\perp \underline{e}_r$. Forces on surfaces $\parallel \underline{e}_r$ compensate each other in spherical (or p-p) symmetry

$$df_p = A \cdot p(r) - A p(r+dr) = -A \frac{dp}{dr} dr$$

• df_{rad} (radiation force) = $\text{grad}(r) dm$

$$\sum dk_i = -g(r) dm + \text{grad}(r) dm = A \frac{dp}{dr} dr = 0$$

$$dm = A \cdot g(r) dr$$

$$\Rightarrow \boxed{\frac{1}{g} \frac{dp}{dr} = -g(r) + \text{grad}(r)} \quad \text{or} \quad \text{Hydrostatic equilibrium}$$

$$\frac{dp}{dr} = -g(r) [g(r) - \text{grad}(r)]$$

Approximation $\parallel g(r) = \frac{G M_r}{r^2} \rightarrow \frac{G M_*}{r^2} \parallel$

since mass within atmsph: $M(r) - M(R_*) \ll M(R_*)$

example: The sun

$$\Delta M_{\text{phot}} = \bar{\rho} \frac{4\pi}{3} ((R+\Delta r)^3 - R^3) \approx \bar{\rho} 4\pi R^2 \Delta r$$

$R \approx 7 \cdot 10^{10} \text{ cm}$, $\Delta r \approx 3 \cdot 10^7 \text{ cm}$ (later), $\bar{\rho} \approx n_H \bar{m}$,
with $\bar{m} = 10^{-25} \text{ cm}^{-3}$ and $m_H \approx 1.7 \cdot 10^{-24} \text{ g}$

$$\Rightarrow \Delta M_{\text{phot}} \approx 3 \cdot 10^{21} \text{ g} \ll M_{\odot} \approx 2 \cdot 10^{33} \text{ g}$$

(same argument holds also if atmosphere is extended)

in plane-parallel geometry, we have additionally

$$\Delta r \ll R_*, \text{ thus } \parallel g(r) = g_* = \frac{G M_*}{R_*^2} \parallel$$

examples main seq. stars
supergiants
white dwarfs
Sun
earthly

$\log g [\text{cgs}] \approx 4$ (0 \rightarrow A)	3.5... 0.8 8!
Sun	4.44
earthly	3.0

• if stellar wind present, hydrodynamic description

$$\dot{M} = 4\pi r^2 g(r) v(r) \quad \text{equation of continuity}$$

$$\Rightarrow v(r) = \frac{\dot{M}}{4\pi} \frac{1}{r^2 g(r)} \neq 0 \text{ (everywhere)}$$

Question When are velocity fields important, i.e. induce significant deviations from hydrostatic equilibrium?



Hydrodynamic description: inclusion of velocity fields

Equation of continuity:

$$\frac{\partial \rho}{\partial t} + \nabla \cdot (\rho \mathbf{v}) = 0$$

Equation of momentum

("Euler equation")

$$\frac{\partial \rho \mathbf{v}}{\partial t} + \underbrace{\nabla \cdot (\rho \mathbf{v} \otimes \mathbf{v})}_{\mathbf{v}[\nabla \cdot (\rho \mathbf{v})] + [\rho \mathbf{v} \cdot \nabla] \mathbf{v}} = -\nabla p + \rho \mathbf{g}^{\text{ext}}$$

\Rightarrow
 stationarity, i.e., $\frac{\partial}{\partial t} = 0$
 and spherical symmetry,
 i.e., $\nabla \cdot \mathbf{u} \rightarrow \frac{1}{r^2} \frac{\partial}{\partial r} (r^2 u_r)$

$$r^2 \rho v = \text{const} = \frac{\dot{M}}{4\pi} \quad (\text{I})$$

with $\nabla \cdot (\rho \mathbf{v}) = 0$

$$\underbrace{\rho \mathbf{v} \frac{\partial \mathbf{v}}{\partial r}}_{\text{"advection term", (from inertia)}} = -\frac{\partial p}{\partial r} + \rho \mathbf{g}_r^{\text{ext}} \quad (\text{II})$$

I: Conservation of mass-flux

II: "Equation of motion"

with gravity and radiative acceleration

$$\Rightarrow \rho(r) v(r) \frac{\partial v}{\partial r} = -\frac{\partial p}{\partial r} + \rho(r) \left(-\frac{GM_*}{r^2} + g_{\text{Rad}}(r) \right)$$

or, to be compared with hydrostatic equilibrium

$$\frac{\partial p}{\partial r} = \rho(r) \left(-\frac{GM_*}{r^2} + g_{\text{Rad}}(r) \right) - \rho(r) v(r) \frac{\partial v}{\partial r}$$

hydrostatic equilibrium $\left\{ \begin{array}{l} \frac{\partial p}{\partial z} = \rho(z) \left(-\frac{GM_*}{R_*^2} + g_{\text{Rad}}(z) \right) \\ \text{in p-p symmetry:} \end{array} \right.$

Exercise:
 Show, by using the cont. eq.,
 that the Euler eq. can
 be alternatively written as

$$\frac{\partial \mathbf{v}}{\partial t} + (\mathbf{v} \cdot \nabla) \mathbf{v} = -\frac{\nabla p}{\rho} + \mathbf{g}^{\text{ext}}$$

When is (quasi-)hydrostatic approach justified?



By using $p = \frac{k_B T}{\mu m_H} \rho = v_{\text{sound}}^2 \rho$ (equation of state, with μ mean molecular weight, and v_{sound} the **isothermal sound speed**),

and $\dot{M} = 4\pi r^2 \rho v = \text{const}$ (for the hydrodynamic case)

the equations of motion and of hydrostatic equilibrium can be rewritten:

$$\left(v_{\text{sound}}^2 - v^2(r) \right) \frac{\partial \rho}{\partial r} = -\rho(r) \left(g_{\text{grav}}(r) - g_{\text{Rad}}(r) + \frac{dv_{\text{sound}}^2}{dr} - \frac{2v^2(r)}{r} \right) \quad \text{[hydrodynamic]}$$

$$v_{\text{sound}}^2 \frac{\partial \rho}{\partial z} = -\rho(z) \left(g_{\text{grav}}(R_*) - g_{\text{Rad}}(z) + \frac{dv_{\text{sound}}^2}{dz} \right) \quad \text{[hydrostatic, p-p]}$$

Conclusion:

- ❑ for $v \ll v_{\text{sound}}$, hydrodynamic density stratification becomes (“quasi”-) hydrostatic
- ❑ this is reached in deeper photospheric layers, well below the sonic point, defined by $v(r_s) = v_{\text{sound}}$
example: $v_{\text{sound}}(\text{sun}) \approx 6 \text{ km/s}$, $v_{\text{sound}}(\text{O-star}) \approx 20 \text{ km/s}$

Thus: p-p atmospheres using hydrostatic equilibrium give reasonable results **even in the presence of winds as long as investigated features** (continua, lines) **are formed below the sonic point.**

Barometric formula



The barometric formula

had hydrostatic equation ($v(r) \ll v_s$)

$$v_s^2 \frac{dg}{dr} = -g \left(g\text{-grad} + \frac{dv_s^2}{dr} \right) \text{ and } v_s^2 = \frac{k_B T}{\mu m_H}$$

→ for given $T(r)$, $g(r)$: $g(r)$ by num. integration

Now analytic approximation

Neglect photospheric extension → $g(r) = g_* = \text{const}$ ✓
 radiative acceleration → main seq. etc
 $\frac{dv_s^2}{dr}$, shall be small against other terms
 → neglect of $\frac{dT}{dr}$

$$\Rightarrow v_s^2 \frac{dg}{dr} = -g g_*$$

$$\frac{dg}{g} = -g_*/v_s^2$$

barometric formula

$$g(r) = g(r_0) e^{-\frac{(r-r_0)g_*}{v_s^2}} = g(r_0) e^{-\frac{r-r_0}{H}}$$

$$(g(z) = g(0) e^{-z/H})$$

with pressure scale height $H = \frac{k_B T}{\mu m_H g_*} = \frac{v_s^2}{g_*}$

- extension no longer negligible, if H significant fraction of R_*

$$H/R_* = \frac{k_B T R_*}{\mu m_H G M} = \frac{v_s^2}{g R_*} = \frac{2 v_s^2}{v_{\text{esc}}^2}$$

with v_{esc} photospheric esc. velocity

$$= \left(\frac{2GM}{R_*} \right)^{-1/2} = (2g R_*)^{-1/2} \quad \left[\text{from } \frac{m}{2} v^2 = \frac{GmM}{R_*} \right]$$

example sun $v_s \approx \left(\frac{1.38 \cdot 10^{-16} \cdot 5700}{1.2 \cdot 10^{-24}} \right)^{1/2} \approx 6.8 \text{ km/s}$

$$v_{\text{esc}} \approx (2 \cdot 10^{34} \cdot 7 \cdot 10^{30})^{1/2} \approx 620 \text{ km/s}$$

$$\Rightarrow H/R_* \approx 2.5 \cdot 10^{-4}, \quad H \approx 100 \text{ km}$$

Total pressure

Alternative solution

had also

$$\frac{1}{g} \frac{dp}{dr} = -g + \text{grad}$$

$$\text{grad} = -\frac{1}{g} \nabla \cdot P \quad (\rightarrow \text{Chap. 4})$$

$$\Rightarrow \frac{1}{g} \frac{dP_{\text{tot}}}{dr} = -g, \quad P_{\text{tot}} = P_{\text{gas}} + P_{\text{rad}},$$

$\nabla \cdot P$ only comp. in rad. direct.

define column density in analogy to $dm = -g dr$
 $d\tau = -\chi dr$ optical depth

$$\Rightarrow \frac{dP_{\text{tot}}}{dm} = g, \quad \underline{P_{\text{tot}} = g \cdot m \text{ exact}}$$

or

$$\frac{dP_{\text{gas}}}{dm} = g - g_{\text{rad}} = g - \frac{4\pi}{c g} \int_0^\infty \chi_\nu H_\nu d\nu$$

- solution by numerical integration
- analytic approx: neglect... as before

$$\rightarrow P_{\text{gas}} = g \cdot m$$

$$g = \frac{g \cdot \mu m_H}{k \cdot T} \cdot m = \frac{1}{H} \cdot m$$

or $\log g = \log m - \log H$

Example

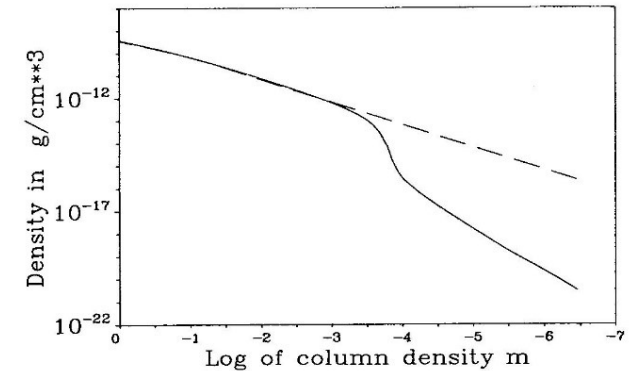


Fig. 16. Mass density ρ as function of logarithm of atmospheric column density m for a typical unified model (solid) and a hydrostatic model (dashed) with similar T_{eff} and $\log g$

Exercise: derive H directly from above figure
 compare with result from
 calculation of H ($T_{\text{eff}} = 40,000 \text{ K}$, $\log g = 3.6$)

Unified atmospheres – density/velocity stratification for stars with winds

photosphere + wind = **unified atmosphere** (Gabler et al. 1989)

Two possibilities:

- a) stratification from theoretical wind models [Castor et al. 1975, Pauldrach et al. 1986, WM-Basic (Pauldrach et al. 2001), see ‘intermezzo’]

Disadvantage: difficult to manipulate if theory not applicable or too simplified

- b) combine quasi-hydrostatic photosphere and empirical wind structure [PHOENIX (Hauschildt 1992), CMFGEN (Hillier & Miller 1998), PoWR (Gräfener et al. 2002), FASTWIND (Puls et al. 2005), see ‘intermezzo’]

Disadvantage: transition regime ill-defined

deep layers: at first $\rho(r)$ calculated (quasi-hydrostatic, with $g_{\text{grav}}(r)$ and $g_{\text{rad}}(r)$)

$$\rightarrow v(r) = \frac{\dot{M}}{4\pi r^2 \rho(r)} \quad \text{for } v \ll v_{\text{sound}} \text{ (roughly: } v < 0.1 v_{\text{sound}} \text{)}$$

outer layers: at first $v(r) = v_{\infty} \left(1 - \frac{bR_*}{r}\right)^{\beta}$, "beta-velocity-law", from observations/theory (b from transition velocity)

$$\rightarrow \rho(r) = \frac{\dot{M}}{4\pi r^2 v(r)}$$

transition zone: smooth transition from deeper to outer stratification

Input/fit parameters: \dot{M} , v_{∞} , β , location of transition zone

Unified atmospheres – density/velocity stratification for stars with winds

abscissa: τ_{Ross} Rosseland optical depth (frequency averaged opacity, see page 105)

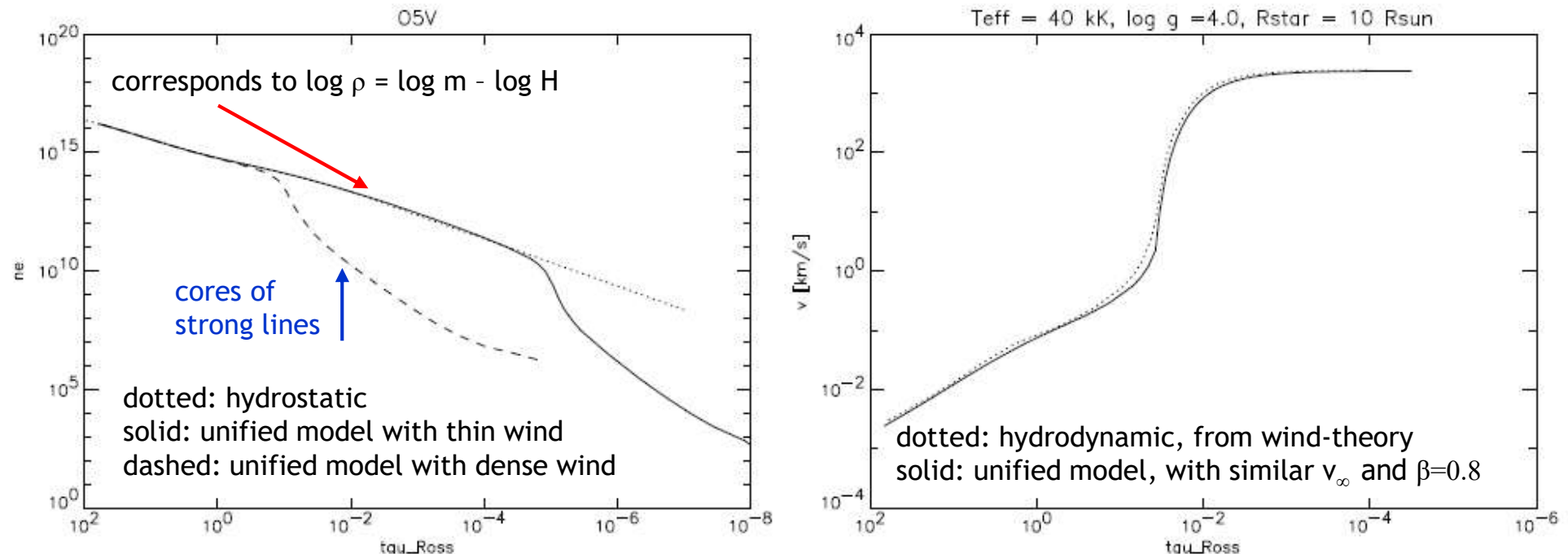


Figure : (Left) Electron-density as a function of the Rosseland optical depth, τ_{Ross} , for different atmospheric models of an O5-dwarf. Dotted: hydrostatic model atmosphere; solid, dashed: unified model with a thin and a moderately dense wind, respectively. In case of the denser wind, the cores of optical lines ($\tau_{\text{Ross}} \approx 10^{-1} - 10^{-2}$) are formed at significantly different densities than in the hydrostatic model, whereas the unified, thin-wind model and the hydrostatic one would lead to similar results.

Figure : (Right) Velocity fields in unified models of an O-star with a thin wind. Dotted: hydrodynamic solution; solid: analytical velocity law with similar terminal velocity and $\beta = 0.8$ (see text).

NOTE: at same τ or m , wind-density (for $v \geq v_{\text{sound}}$) lower than if in hydrostatic equilibrium

Plane-parallel or unified model atmospheres?

- Unified models required if $\tau_{\text{Ross}} \geq 10^{-2}$ at transition between photosphere and wind (roughly at $0.1 \cdot v_{\text{sound}}$)
- **rule of thumb** using a typical velocity law ($\beta=1$)

$$\dot{M}_{\text{max}} = \dot{M}(\tau_{\text{Ross}} = 10^{-2} \text{ at } 0.1 v_{\text{sound}}) \approx 6 \cdot 10^{-8} M_{\odot} \text{yr}^{-1} \cdot \frac{R_*}{10 R_{\odot}} \cdot \frac{v_{\infty}}{1000 \text{km s}^{-1}}$$

- if $\dot{M}(\text{actual}) < \dot{M}_{\text{max}}$ for considered object,
then (most) diagnostic features formed in quasi-hydrostatic part of atmosphere
- plane-parallel, hydrostatic models possible for **optical** spectroscopy of late O-dwarfs and B-stars up to luminosity classes II (early subtypes) or Ib (mid/late subtypes)
- **check required!**

Eddington limit



The Eddington limit

$$-\frac{1}{\rho} \frac{dp}{dr} = g - g_{\text{rad}} = g_{\text{eff}} \quad \text{for } v=0, \text{ no rotation}$$

\uparrow \uparrow
 inwards outwards

- $g_{\text{rad}} = \frac{4\pi}{c^3} \int_0^\infty \chi_\nu H_\nu d\nu$ in static atmospheres (χ_ν isotropic)
- minimum value (\cong main part of total continuum rad. acceleration in outer atmospheres of hot stars)

Thomson scattering

$$g_{\text{rad}}^{\text{Thomson}} = \frac{4\pi}{c^3} \int_0^\infty \sigma^{\text{TH}} H_\nu d\nu = \frac{4\pi}{c} \underbrace{\frac{n_e \sigma_e}{S}}_{\substack{\text{ne}\sigma_e, \text{freq.} \\ \text{independent}}} H(r)$$

σ_e $\begin{cases} 0.34 \text{ H/He fully ionized} \\ 0.4 \text{ pure H, fully ionized} \end{cases}$

Define $\Gamma_e = \frac{g_{\text{rad}}^{\text{TH}}}{g_{\text{grav}}} = \frac{\frac{4\pi}{c} \sigma_e \frac{L}{4\pi r^2}}{\frac{GM}{r^2}} = \text{const (for } \sigma_e = \text{const)}$

$$= \frac{L}{4\pi c GM} \sigma_e = 7.64 \cdot 10^{-5} \cdot \sigma_e \cdot \frac{L/L_\odot}{M/M_\odot}$$

- $\Gamma_e = 1$ defines "Eddington limit": unstable atmosphere
- $g_{\text{eff}} = g - g_{\text{rad}} = g(1 - \Gamma_e)$ ($-g_{\text{rad}}^{\text{rest}}$)
defines "effective" gravity
- NOTE • bound-free + free-free absorption has similar contribution (in intermediate layers)
- bound-bound absorption dominates the radiative acceleration in hot, luminous stars \Rightarrow "line driven winds"

Summary: stellar atmospheres - the solution principle

THUS problem of stellar atmospheres solved (in principle, without convection, p-p geometry, static)
 Given log g*, T_{eff}, abundances

(A) hydrostatic equilibrium

$$\frac{dp_{\text{gas}}}{dz} = -g(g_* - g_{\text{rad}}) ; \quad g_{\text{rad}} = \frac{4\pi}{c} \int_0^\infty \chi_\nu H_\nu d\nu = \frac{4\pi}{c} \left(\sigma^{\text{TH}} H(z) + \int_0^\infty \chi_\nu^{\text{rest}} H_\nu d\nu \right)$$

$$\Rightarrow \frac{dp_{\text{gas}}}{dz} = -g g_* + \sigma^{\text{TH}} \frac{\sigma_B T_{\text{eff}}^4}{c} + \frac{4\pi}{c} \int_0^\infty \chi_\nu^{\text{rest}} H_\nu d\nu$$

$H = \frac{1}{4\pi} \sigma_B T_{\text{eff}}^4 \quad (= \frac{1}{4\pi} F)$

(B) equation of rad. transfer

$$\mu \frac{dI_\nu}{dz} = \chi_\nu (S_\nu - I_\nu) \quad \forall \nu, \mu \quad \Rightarrow \quad J_\nu = \frac{1}{2} \int_{-1}^{+1} I_\nu(\mu) d\mu ; \quad H_\nu = \frac{1}{2} \int_{-1}^{+1} I_\nu(\mu) \mu d\mu$$

(C) a) radiative equilibrium

$$\int_0^\infty (\chi_\nu - \chi_\nu^{\text{rest}}) J_\nu d\nu = \int_0^\infty \left\{ \left(\sigma^{\text{TH}} J_\nu + \chi_\nu^{\text{rest}} S_\nu^{\text{rest}} \right) - \left(\sigma^{\text{TH}} + \chi_\nu^{\text{rest}} \right) J_\nu \right\} d\nu = \int_0^\infty \chi_\nu^{\text{rest}} (S_\nu^{\text{rest}} - J_\nu) d\nu \stackrel{?}{=} 0$$

scattering terms cancel, since conservative

b) flux-conservation: $4\pi \int_0^\infty H_\nu(z) d\nu = 4\pi H(z) \stackrel{?}{=} \sigma_B T_{\text{eff}}^4 \Rightarrow \Delta T(z) \rightarrow \Delta \chi_\nu(z) \text{ etc}$

(D) equation of state $p_{\text{gas}}(z) = \frac{k_B}{\mu m_H} \rho(z) T(z)$

solution by iteration!

Solution of differential equations A and B by **discretization**
 differential operators => finite differences
 all quantities have to be evaluated on suitable grid

Eq. of radiative transfer (B)
 usually solved by the so-called
 Feautrier and/or Rybicki scheme

Grey temperature stratification

- for iteration, we need initial values
 - analytic understanding
- ⇒ "grey" approximation

assume $\chi_\nu = \chi$, freq. independent opacities
(corresponds to suitable averages)

$$\Rightarrow \mu \frac{dI_\nu}{d\tau} = I_\nu - S_\nu \quad \Rightarrow \text{radiative eq.}$$

$$\frac{dH_\nu}{d\tau} = J_\nu - S_\nu \quad \left\{ \begin{array}{l} \text{(freq. integr.)} \\ J = \int_0^\infty J_\nu d\nu \\ \text{etc} \end{array} \right. \quad \frac{dH}{d\tau} = J - S (=0)$$

$$\frac{dK_\nu}{d\tau} = H_\nu \quad \frac{dK}{d\tau} = H$$

⇒ $\frac{dK}{d\tau} = H$, i.e. $K = H \cdot \tau + C$

For large $\tau \gg 1$, we know from diff. approx. that $K_\nu / J_\nu = \frac{1}{3}$

Eddington's approx. $K/J = \frac{1}{3}$ everywhere

⇒ $J = 3H(\tau + c)$

- From rad. equilibrium
 $J = S$, $S = 3H(\tau + c)$

- remember Λ -operator

$$J = \Lambda \tau(S)$$

- analogous

$H = \phi \tau(S)$, in particular

$$H(0) = \frac{1}{2} \int_0^\infty S(t) E_2(t) dt \quad E_2 \text{ 2nd Exp. integral}$$

$$\Rightarrow H(0) = \frac{1}{2} \int_0^\infty (3H(t+c)) E_2(t) dt = \dots$$

$$\dots H \left(\frac{1}{2} + c \frac{3}{4} \right)$$

But $H(0) = H$, i.e., $\left(\frac{1}{2} + c \frac{3}{4} \right) = 1$

$c = \frac{2}{3}$ in Eddington approx

Exact sol. $c = q(\tau)$, "Hopf function",
 $0.51 < q(\tau) < 0.71$

- $J = 3H(\tau + 2/3)$

$$H = \frac{\sigma T_{\text{eff}}^4}{4\pi} \quad ; \quad J \xrightarrow{\text{LTE}} B = \frac{\sigma_B T^4}{\pi}$$

Finally

$$T^4 = \frac{3}{4} T_{\text{eff}}^4 (\tau + 2/3)$$

grey temp. in Eddington approx!

consequences

- $T = T_{\text{eff}}$ at $\tau = 2/3$

- $T(0)/T_{\text{eff}} = \left(\frac{1}{2} \right)^{1/4} = 0.841$

grey temp. in spherical symmetry

basic difference

$J_\nu H \sim \frac{1}{r^2}$ for $r \gg R_x$ quadratic dilution

$J/K = 1$ for $r \gg R_x$

result

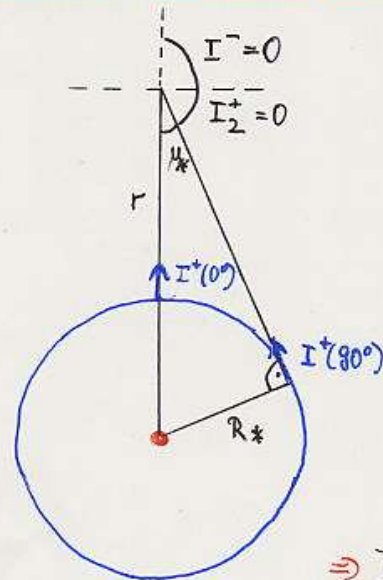
$T^4(r) = \tau_{\text{eff}}^4 (W + \frac{3}{4} \tau')$

W dilution factor, $\frac{1}{2} [1 - (1 - (\frac{R_x}{r})^2)^{\frac{1}{2}}]$

$\tau' = \int_r^\infty \chi(r) (\frac{R_x}{r})^2 dr$

NOTE
 $T^{\text{sph}}(r) \xrightarrow{r \rightarrow R_x} T^{\text{PP}}(\tau)$

Radiation field in optically thin envelopes



- assume
- envelope optically thin $\Rightarrow I = \text{const}$
 - radiation field leaving photosphere isotropic $\Rightarrow I_{\text{phot}}^+(\mu) = \text{const}$

$\Rightarrow J_\nu(r) = \frac{1}{2} \int_{-1}^{+1} I_\nu(r) d\mu \rightarrow$
 $= \frac{1}{2} \int_{\mu_x}^1 I_\nu^+(R_x) d\mu + \frac{1}{2} \int_0^{\mu_x} I_2^+ d\mu + \frac{1}{2} \int_{-1}^0 I^- d\mu$
 $= \frac{1}{2} I_\nu^+(R_x) (1 - \mu_x)$

$\sin \theta = \frac{R_x}{r} \Rightarrow \mu_x = \cos \theta = \sqrt{1 - (\frac{R_x}{r})^2}$

$J_\nu(r) = W \cdot I_\nu^+(R_x)$, $W = \frac{1}{2} [1 - (1 - \frac{R_x^2}{r^2})^{\frac{1}{2}}]$
 "Dilution factor"

exercise: show that for $r \gg R_x$,
 $J_\nu(r) \approx H_\nu(r) \approx K_\nu(r)$

Rosseland opacities



Rosseland opacities

grey approximation $\chi_\nu \equiv \chi$

BUT ionization edges, lines, bf-opacities $\sim \nu^{-3}, \dots$

Question can we define suitable means which might replace the grey opacity?

answer not generally, but in specific cases

most important Rosseland mean

(\rightarrow T-stratification, stellar structure, ...)

$$\frac{dk_\nu}{dz} = -\chi_\nu H_\nu \quad \text{exact}$$

- require, that freq. integration results in correct flux

$$\rightarrow -\int_0^\infty \frac{1}{\chi_\nu} \frac{dk_\nu}{dz} d\nu = \int_0^\infty H_\nu d\nu = H = -\frac{1}{\bar{\chi}} \frac{dk}{dz}$$

Problem: to calculate $\bar{\chi}$, we have to know K_ν

- thus, use additionally diffusion approximation

$$K_\nu = \frac{1}{3} B_\nu \quad \text{and} \quad H_\nu = \frac{1}{3} \frac{dB_\nu}{d\tau_\nu}$$

$$\Rightarrow \frac{1}{\bar{\chi}_R} = -\frac{H}{dK/dz} \rightarrow \frac{\int_0^\infty \frac{1}{3} \frac{1}{\chi_\nu} \frac{\partial B_\nu}{\partial T} \frac{dT}{dz} d\nu}{\int_0^\infty \frac{1}{3} \frac{\partial B_\nu}{\partial T} \frac{dT}{dz} d\nu} = \frac{\int_0^\infty \frac{1}{\chi_\nu} \frac{\partial B_\nu}{\partial T} d\nu}{\int_0^\infty \frac{\partial B_\nu}{\partial T} d\nu} = \frac{\int_0^\infty \frac{1}{\chi_\nu} \frac{\partial B_\nu}{\partial T} d\nu}{\frac{4\sigma_B T^3}{\pi}}$$

$$\left[\text{since } \int B_\nu d\nu = \frac{\sigma_B}{\pi} T^4 \rightarrow \frac{\partial}{\partial T} = \frac{4\sigma_B}{\pi} T^3 \right]$$

- \Rightarrow Rosseland opacity

$$\bar{\chi}_R = \frac{\frac{4\sigma_B T^3}{\pi}}{\int_0^\infty \frac{1}{\chi_\nu} \frac{\partial B_\nu}{\partial T} d\nu}$$

- can be calculated without radiative transfer
- harmonic weighting: maximum flux transport where χ_ν is small!

- alternatively, from construction (for $\tau_\nu \gg 1$)

$$\frac{1}{\bar{\chi}_R} = -\frac{H}{dK/dz} \rightarrow -\frac{H}{\int_0^\infty \frac{1}{3} \frac{\partial B_\nu}{\partial z} d\nu} = -\frac{H}{\frac{1}{3} \frac{dT}{dz} \int_0^\infty \frac{\partial B_\nu}{\partial T} d\nu} = -\frac{H}{\frac{1}{3} \frac{4\sigma_B}{\pi} T^3 \frac{dT}{dz}}$$

⇒

i) $F = 4\pi H = \frac{16\sigma_B}{3} T^3 \frac{dT}{d\tau_R}$

ii) in spherical geometry

$$\frac{L(r)}{4\pi r^2} = -\frac{16\sigma_B}{3\bar{\chi}_R} T^3 \frac{dT}{dr} \quad (\text{used for stellar structure})$$

iii) integrate i), $+ F = \sigma_B T_{\text{eff}}^4$

$$\rightarrow T^4 = T_{\text{eff}}^4 \frac{3}{4} (\tau_{\text{Ross}} + \text{const}), \quad \text{as in grey case, but now with } \tau_{\text{Ross}}$$

THUS possibility to obtain initial (or approx.) values for temperature stratification (\approx exact for large optical depths)

calculate (LTE) opacities χ_ν	} again, iteration required
calculate $\bar{\chi}_R, \tau_R$	
calculate $T(\tau_R)$	

Now we define the stellar radius via

$$R_* = R(\tau_{\text{Ross}} = 2/3)$$

as the average layer ("stellar surface") where the observed UV/optical radiation is created.

Furthermore, if we approximate $\text{const} = 2/3$ as in the (approx.) grey case, i.e.,

$$T^4(\tau_{\text{Ross}}) \approx T_{\text{eff}}^4 \frac{3}{4} (\tau_{\text{Ross}} + 2/3)$$

then we obtain $T(\tau_{\text{Ross}} = 2/3) = T(R_*) = T_{\text{eff}}$ and the definition $L = 4\pi R_*^2 \sigma_B T_{\text{eff}}^4$ has also a **physical meaning** (at least for LTE conditions): "the effective temperature is the atmospheric temperature of a star at its surface".

Note: in reality, $T(\tau_{\text{Ross}} = 2/3)$ deviates (slightly) from T_{eff} , since $\text{const} \neq 2/3$, and because of deviations from LTE

... back to Milne Eddington Model (page 90)

had $B_\nu(\tau_\nu) = a_\nu + b_\nu \tau_\nu$ linear approx

and $J_\nu(0) = \frac{b_\nu}{T^3}$ for $\epsilon_\nu = 0$ pure scattering
 $= a_\nu + \frac{b_\nu \sqrt{3} - a_\nu}{2}$ for $\epsilon_\nu = 1$ purely thermal

$$\epsilon_\nu = \frac{\kappa_\nu^+}{\kappa_\nu^+ + \sigma_{\nu e} u_e}$$

- since temperature stratification known by u_e , can perform some estimates concerning continuum fluxes

had $T^4 \approx T_{\text{eff}}^4 \frac{3}{4} (\tau_R + 2/3)$
 $T(0)^4 = T_{\text{eff}}^4 \frac{3}{4} \cdot 2/3$ } $T^4 = T(0)^4 (1 + \frac{3}{2} \tau_R)$

$B_\nu(\tau_R) \approx B_\nu(\tau_0) + \left(\frac{\partial B_\nu}{\partial \tau_R}\right)_0 \tau_R = B_0 + B_1 \tau_R$

$\Rightarrow B_1 = \frac{\partial B_\nu}{\partial T} \Big|_{T_0} \cdot \frac{\partial T}{\partial \tau_R} \Big|_{\tau_0} = B_\nu \frac{h\nu/kT \cdot \frac{1}{T} e^{-h\nu/kT}}{(e^{h\nu/kT} - 1)} \Big|_{T_0} \frac{\partial T}{\partial \tau_R} \Big|_{\tau_0}$

$= B_\nu \frac{u_0}{1 - e^{-u_0}} \frac{1}{T_0} \frac{\partial T}{\partial \tau_R} \Big|_0$ with $u_0 = \frac{h\nu}{kT_0}$

$4T^3 \frac{\partial T}{\partial \tau_R} = T^4(0) \frac{3}{2}$, $\frac{\partial T}{\partial \tau_R} \Big|_{\tau_0} = \frac{3}{8} T_0$

Thus $B_1 = B_0 \frac{u_0}{1 - e^{-u_0}} \frac{3}{8} \rightarrow$ (Rayleigh-Jeans) $B_1 = \frac{3}{8} B_0$
 \rightarrow (Wien) $B_1 = \frac{3}{8} u_0 B_0$

example $T_{\text{eff}} = 40000 \text{ K}$, $\lambda = 500, 912 \text{ \AA}$
 $T_0 = 33600 \text{ K}$ [Hydrogen Lyman continuum, $\epsilon_\nu \ll 1$]
 $u_0 = \frac{8.56}{4.70} \rightarrow B_1 \approx \frac{3.21}{1.76} B_0$

\rightarrow if $(\kappa_\nu^+ + \sigma_\nu) \approx \bar{\chi}_R$ $J_\nu(0, \epsilon_\nu = 1) \approx \frac{1.42}{1.0} B_0$

$H_\nu(0) = \frac{1}{\sqrt{3}} J_\nu(0)$

$J_\nu(0, \epsilon_\nu \rightarrow 0) \approx \frac{1.85}{1.01} B_0$

can look down deeper into atm.

- additional effect 1

T-stratification with respect to $\tau_R(\bar{\chi}_R)$, but radiation transfer with respect to freq. τ_ν

$J_\nu = B_\nu + \dots = a_\nu + b_\nu \tau_\nu + \dots$

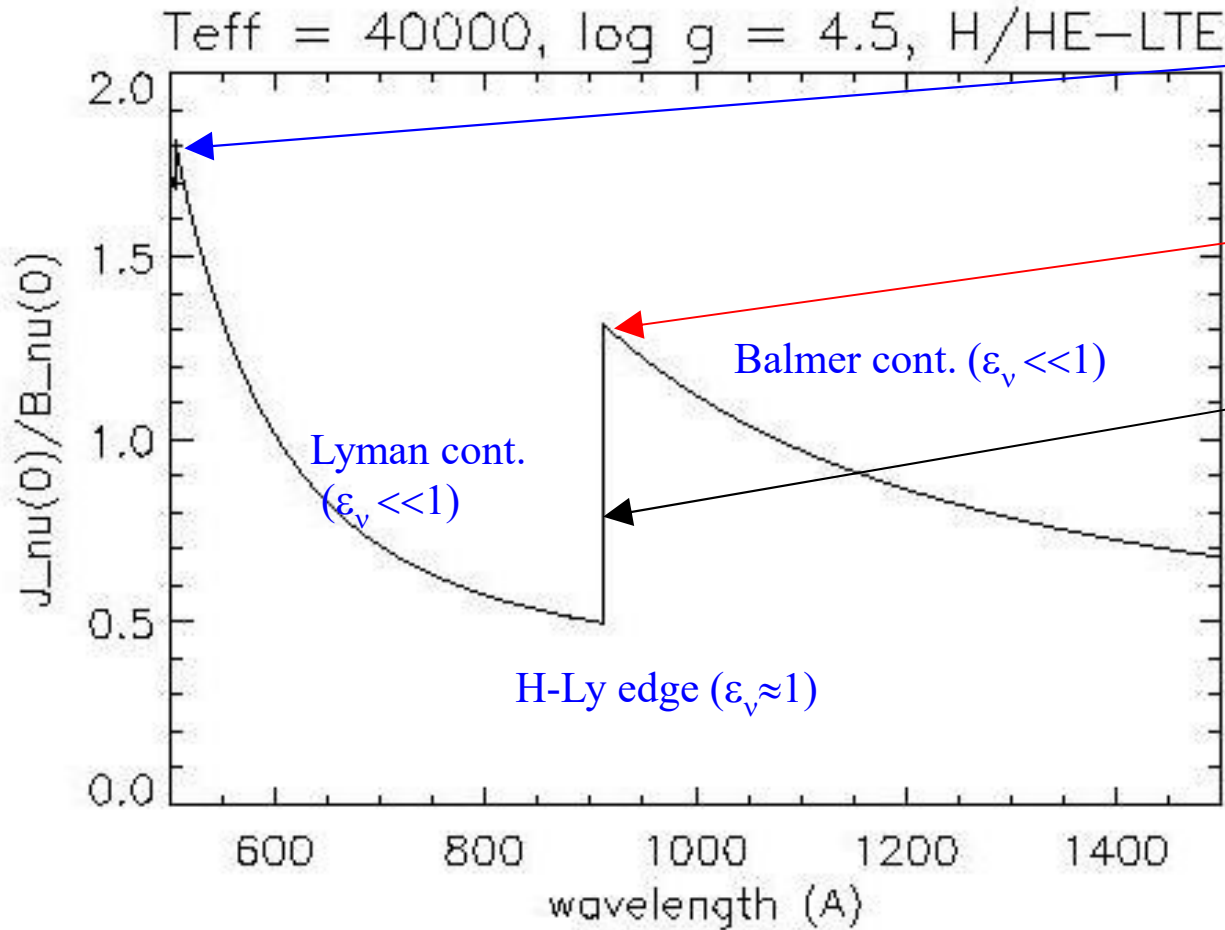
$B_\nu = B_{\nu 0} + B_1 \tau_R = B_{\nu 0} + B_1 \tau_\nu \frac{\tau_R}{\tau_0} \approx B_{\nu 0} + B_1 \frac{\bar{\chi}_R}{\chi_\nu} \tau_\nu$
 effective gradient increased, if κ_ν small compared to $\bar{\chi}_R$

- additional effect 2

far away from ionization edges (where ϵ_ν is small, anyway), also χ_ν small

$(\kappa_\nu^+ \sim (\frac{v_e}{v})^3, \text{ cf Chapter 5}) \rightarrow$ additional enhancement

H/He continuum of a hot star around 1000 Å



Predictions

Lyman cont: $J_\nu / B_\nu \geq 1.85$, **OK**
(at 500 Å) ($\chi_\nu \approx \chi_R$)

Balmer cont: $J_\nu / B_\nu \geq 1.01$, **OK**
(at 912 Å) ($\chi_\nu < \chi_R$)

Lyman edge: $J_\nu / B_\nu \leq 1.0$, **OK**
(911 Å) ($\chi_\nu > \chi_R$)

note: large opacity leads to very small effective T-gradient, minimum value $J_\nu / B_\nu = 0.5$, (cf. page 91)

Convection (simplified)

Convection

energy transport not only by radiation, however also by

- waves
 - heat conduction
 - convection
- not efficient in typical stellar atmospheres, but ... coronae, chromospheres, white dwarfs

Thus

total flux = const

$$\nabla \cdot (\underline{F}^{\text{rad}} + \underline{F}^{\text{conv}}) = 0 \quad (\text{in quasi-hydrostatic atmospheres})$$

or

$$\frac{dF^{\text{conv}}}{dz} = -\frac{dF^{\text{rad}}}{dz} = -4\pi \int_0^\infty \nu \chi_\nu (S_\nu - J_\nu)$$

energy transport by

radiation

convection

most efficient way is chosen

early
O → (A)

spectral type

late
M → F



convective core

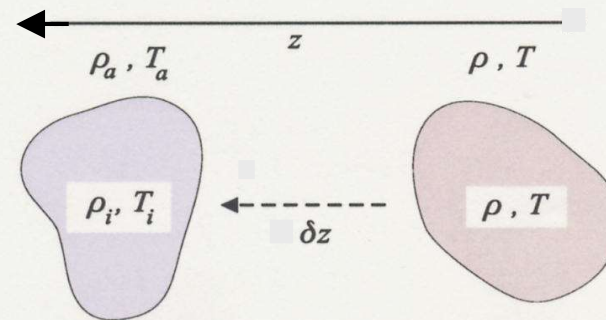
Why???

later



outer convection zone

The Schwarzschild Criterion



assume mass element in photosphere, which moves upwards (by perturbation). Ambient pressure decreases, and "bubble" expands

Thus

$\rho \rightarrow \rho_i, T \rightarrow T_i$ in bubble ($i = \text{internal}$)

$\rho \rightarrow \rho_a, T \rightarrow T_a$ in ambient medium

two possibilities

$\rho_i > \rho_a$ bubble falls back **stable**

$\rho_i < \rho_a$ bubble rises further **unstable**

buoyancy as long as $\rho_i(r+\Delta r) < \rho_a(r+\Delta r)$ since

$$F_b = -g(\rho_i - \rho_a) > 0, \text{ i.e., for } \Delta \rho = (\rho_i - \rho_a) < 0$$

The Schwarzschild criterion



assumption 1

movement so slow, that pressure equilibrium
($\bar{v} < v_{\text{sound}}$)

$$\Rightarrow p_i = p_a \quad \text{and} \quad (gT)_i = (gT)_a \quad \text{over } \Delta r$$

$$\Rightarrow \Delta g = \left[\frac{dg_i}{dr} - \frac{dg_a}{dr} \right] \Delta r = \left(\left| \frac{dg_a}{dr} \right| - \left| \frac{dg_i}{dr} \right| \right) \Delta r$$

Instability, if density inside bubble drops faster

$$\boxed{\left| \frac{dg_i}{dr} \right| > \left| \frac{dg_a}{dr} \right| \quad \text{or} \quad \left| \frac{dT_i}{dr} \right| < \left| \frac{dT_a}{dr} \right|}$$

assumption 2

no energy exchange between bubble and ambient medium (will be modified later)

\Rightarrow adiabatic change of state in bubble

$$s_i = a \cdot p_i^{1/\gamma} \quad , \quad \gamma = c_p/c_v$$

$$\rightarrow \frac{ds_i}{dr} = a \frac{1}{\gamma} p_i^{1/\gamma - 1} \frac{dp_i}{dr} = \frac{1}{\gamma} \frac{s_i}{p_i} \frac{dp_i}{dr} = \frac{1}{\gamma} s_i \frac{d \ln p_i}{dr}$$

\Rightarrow ambient medium ideal gas

$$g_a = a' \frac{p_a}{T_a}$$

$$\rightarrow \frac{dg_a}{dr} = a' \left(\frac{1}{T_a} \frac{dp_a}{dr} - \frac{p_a}{T_a^2} \frac{dT_a}{dr} \right) = g_a \left(\frac{d \ln p_a}{dr} - \frac{d \ln T_a}{dr} \right)$$

\Rightarrow instability for

$$\frac{1}{\gamma} s_i \frac{d \ln p_i}{dr} < g_a \left(\frac{d \ln p_a}{dr} - \frac{d \ln T_a}{dr} \right) \quad , \quad \begin{aligned} s_i(r_0) &= g_a(r_0) \\ \frac{d \ln p_i}{dr} &= \frac{d \ln p_a}{dr} \end{aligned}$$



$$\frac{1}{\gamma} \frac{d \ln p}{dr} < \left(\frac{d \ln p}{dr} - \frac{d \ln T}{dr} \right)$$

$$\Rightarrow \left(\frac{d \ln p}{dr} < 0 \right) \frac{1}{\gamma} > 1 - \frac{d \ln T}{d \ln p}$$

$$\nabla_a = \frac{d \ln T_a}{d \ln p} > 1 - \frac{1}{\gamma} = \nabla_{ad} \quad \text{Schwarzschild criterion}$$

convection, if $\nabla_a > \nabla_{ad}$

- ∇_a : if no convection, radiative stratification

$$\nabla_a = \nabla_{rad} = \frac{d \ln T / dr}{d \ln p / dr} = \frac{3}{16} \frac{\bar{\kappa} \cdot F_{rad}}{\sigma_B T^4} \cdot \frac{1}{\frac{g_{eff} \mu m H}{k T}}$$

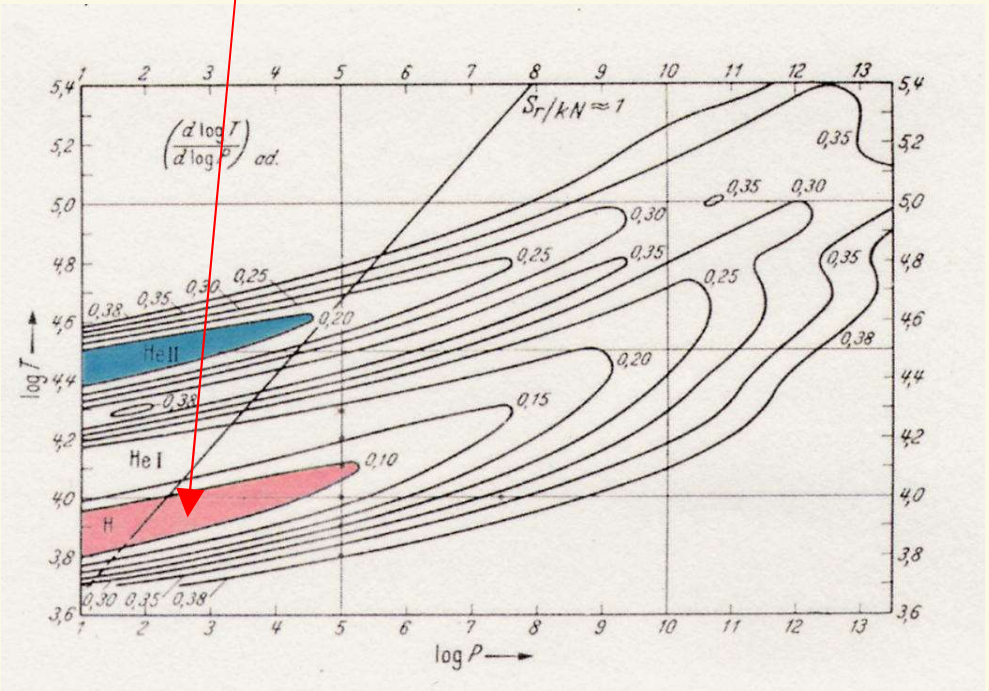
$$= \frac{3}{16} \left(\frac{T_{eff}}{T} \right)^4 \cdot (\bar{\kappa} H) \leq \frac{3}{16} \left(\frac{T_{eff}}{T} \right)^4$$

- $\nabla_{ad} = \left(\frac{d \ln T}{d \ln p} \right)_{ad} = \frac{\gamma - 1}{\gamma} \leq 1$ in photosphere

mono-atomic gas: $\nabla_{ad} = 0.4$, and $\frac{3}{16} \approx 0.19$

- must include ionization effects (number of particles!) and radiation pressure (weak influence in atmosph.)
- pure hydrogen, fully ionized
 $\nabla_{ad} = 0.4 \Rightarrow \nabla_{rad}$
 \Rightarrow hot star atmospheres (convectively) stable!

- pure hydrogen: minimum for 50% ionization
 $\nabla_{ad} \approx 0.07 < \nabla_{rad}$ solar convection zone, $T = 9000 \text{ K}$!



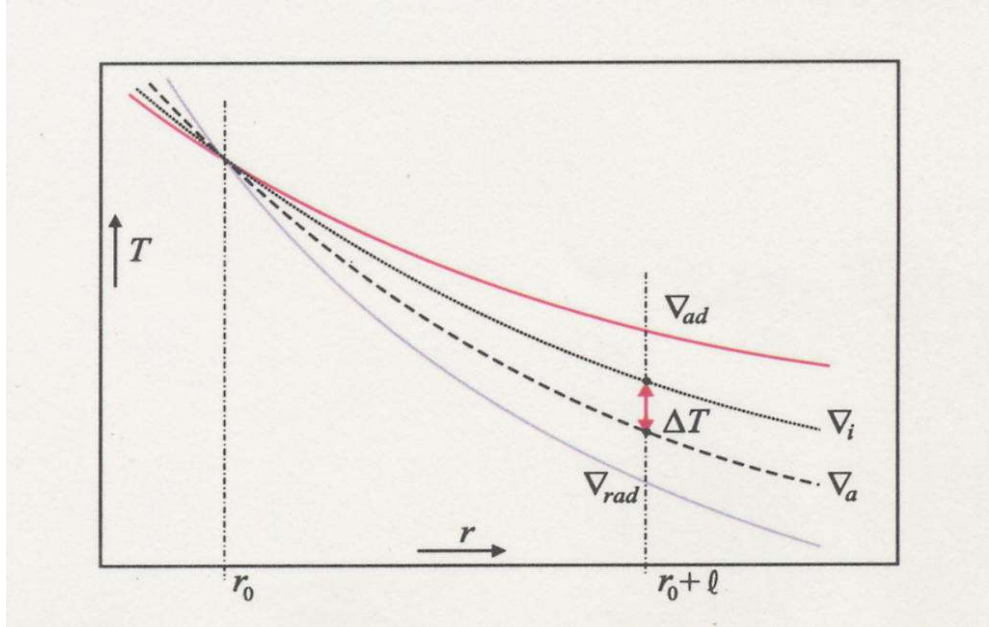
∇_{ad} as function of T and p

Mixing length theory

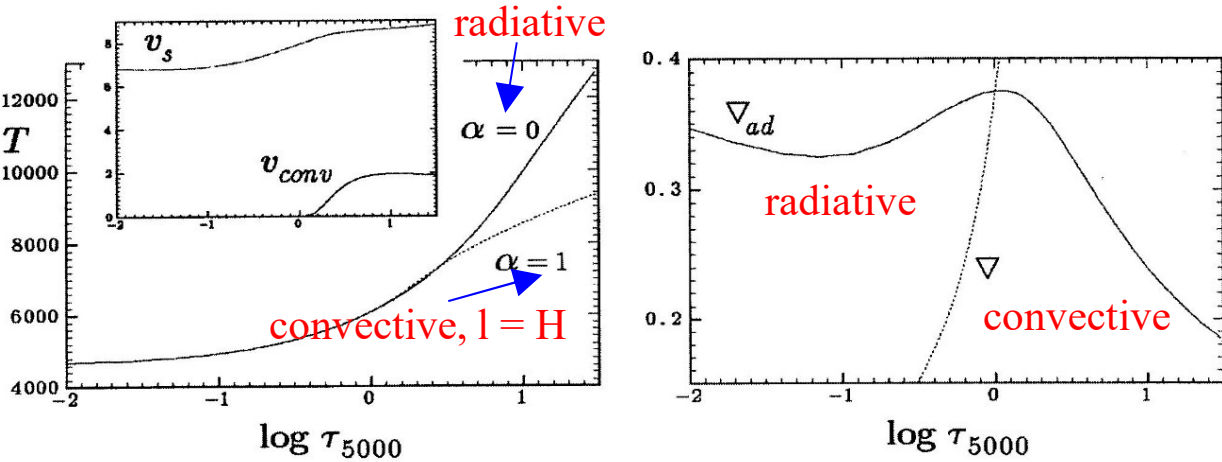
Note:

- mixing length theory only 0th order approach
- modern approach: calculate consistent hydrodynamic solution (e.g., solar convective layer+photosphere, Asplund+, see 'Intermezzo')

radiative vs. adiabatic T-stratification



Model for solar photosphere



- most simplistic approach, however frequently used (reality is much too complex)
- suggested by Prandtl (1925)
- **idea** :-if atmosphere convective unstable at r_0 , assume mass element rises until $r_0 + l$ (mixing length)
 - at $r_0 + l$, excess energy $\Delta E = c_p g \Delta T$ is released into ambient medium, and temperature is increased. Always valid $\nabla_{ad} \leq \nabla_i < \nabla_a < \nabla_{rad}$
 - bubble cools, sinks down, absorbs energy, rises, etc...
- ⇒ Energy is transported, temperature gradient becomes smaller

- $\bar{\tau}$ flux, temperature etc. calculated from simple arguments, $l = \alpha \cdot H$, $\alpha = 1, \dots, 2$
- have to account for radiative losses during lifetime of element until energy is released
 - ⇒ efficiency $\gamma = \frac{\text{excess energy lost}}{\text{radiative losses}}$
- γ large $\rightarrow \nabla_a \approx \nabla_{ad}$; γ small $\rightarrow \nabla_a \approx \nabla_{rad}$

Mixing length theory – some details

$\Delta E = \rho C_p \delta T$ is excess energy density delivered to ambient medium when bubble merges with surroundings.
 C_p is specific heat per mass.

$\Rightarrow F_{conv} = \Delta E \bar{v} = C_p \delta T \rho \bar{v}$ is convective flux (transported energy) with \bar{v} average velocity of rising bubble over distance Δr ($\rho \bar{v}$ mass flux).

δT is temperature difference between bubble and ambient medium.

$$\delta T = \left[\left(-\frac{dT}{dr} \right)_a - \left(-\frac{dT}{dr} \right)_i \right] \Delta r > 0 \text{ when convective unstable,}$$

since then $[(-\Delta T)_a - (-\Delta T)_i] > 0$

From the definition of ∇ ,

$$-\frac{dT}{dr} = -\frac{T}{p} \frac{dp}{dr} \nabla = \frac{T}{H} \nabla, \text{ with pressure scale height } H, \text{ since}$$

$$p = \frac{k \rho T}{\mu m_H}, \quad \frac{dp}{dr} = -g \rho \text{ and } \frac{1}{p} \frac{dp}{dr} = -\frac{\mu m_H g}{kT} = -\frac{1}{H}$$

(assuming hydrostatic equilibrium and neglecting radiation pressure; inclusion of p_{rad} possible, of course)

Defining l as the **mixing length** after which element dissolves, and averaging over all elements (distributed randomly over their paths), we may write $\Delta r = \frac{l}{2}$.

$$\Rightarrow F_{conv} = C_p \rho \bar{v} (\nabla_a - \nabla_i) \frac{T}{H} \frac{l}{2} = \frac{1}{2} C_p \rho \bar{v} T (\nabla_a - \nabla_i) \alpha, \text{ with}$$

mixing length parameter $\alpha = \frac{l}{H}$ (from fits to observations, $\alpha = O(1)$)

The average velocity is calculated by assuming that the work done by the buoyant force is (partly) converted to kinetic energy, where the average of this work might be calculated via

$$\bar{w} = \int_0^{l/2} F_b(\Delta r) d(\Delta r),$$

and the upper limit results from averaging over elements passing the point under consideration. The buoyant force is given by (see page 109)

$$F_b = -g \delta \rho = -g(\rho_i - \rho_a) > 0$$

Using the equation of state, and accounting for pressure equilibrium ($p_i = p_a$),

we find $\frac{\delta \rho}{\rho} = -Q \frac{\delta T}{T}$ with $Q = \left(1 - \frac{\partial \ln \mu}{\partial \ln T} \right)_p$, to account for ionization effects.

$$\Rightarrow F_b = -g \delta \rho = g Q \frac{\rho}{T} \delta T = g Q \frac{\rho}{T} \left[\left(-\frac{dT}{dr} \right)_a - \left(-\frac{dT}{dr} \right)_i \right] \Delta r =$$

$g Q \frac{\rho}{H} (\nabla_a - \nabla_i) \Delta r := A \Delta r$. Thus, F_b is linear in Δr , and

$$\bar{w} = \int_0^{l/2} A \Delta r d(\Delta r) = A \frac{l^2}{8} = g Q \rho \frac{H}{8} (\nabla_a - \nabla_i) \left(\frac{l}{H} \right)^2$$

Mixing length theory – some details

Let's assume now that 50% of the work is lost to friction (pushing aside the turbulent elements), and 50% is converted into kinetic energy of the bubbles, i.e.,

$$\frac{1}{2} \bar{w} = \frac{1}{2} \rho \bar{v}^2 \quad \Rightarrow \quad \bar{v} = \left(\frac{\bar{w}}{\rho} \right)^{1/2} = \left(\frac{gQH}{8} \right)^{1/2} (\nabla_a - \nabla_i)^{1/2} \alpha,$$

and the convective flux is finally given by

$$F_{conv} = \left(\frac{gQH}{32} \right)^{1/2} (\rho C_p T) (\nabla_a - \nabla_i)^{3/2} \alpha^2.$$

NOTE : different averaging factors possible and actually found in different versions!

Remember that still $\nabla_{ad} \leq \nabla_i < \nabla_a < \nabla_{rad}$.

The gradients ∇_i and ∇_a are calculated from the efficiency γ and the condition that the *total* flux remains conserved (outside the nuclear energy creating core), i.e.,

$$r^2 (F_{conv} + F_{rad}) = r^2 F_{tot} = R_*^2 F_{rad}(R_*) = R_*^2 \sigma_B T_{eff}^4 = \frac{L}{4\pi}$$

or from the condition that

$$(F_{conv} + F_{rad}) = \frac{L_r}{4\pi r^2} \text{ with } L_r \text{ the luminosity at } r.$$

Usually, a tricky iteration cycle is necessary.

Convective vs. radiative energy transport

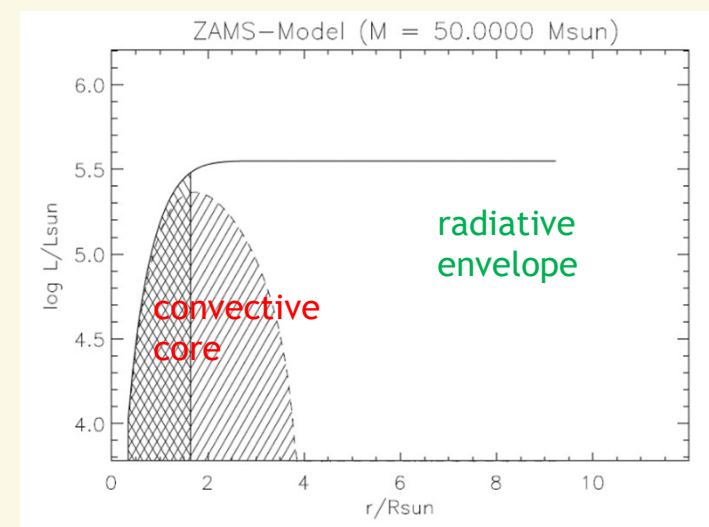
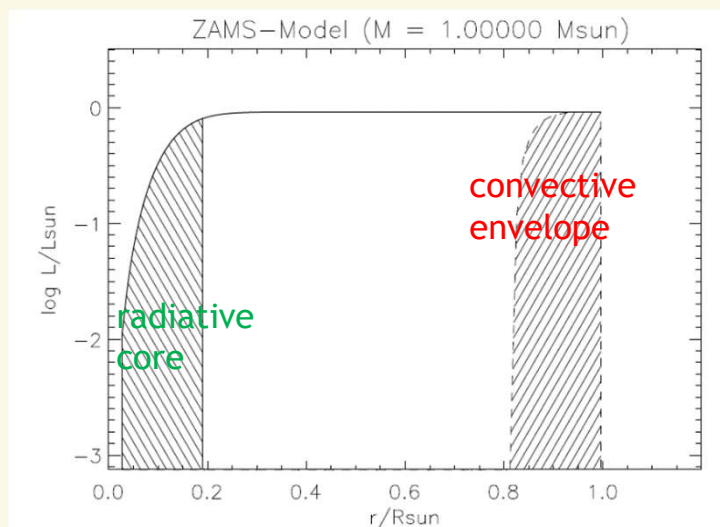


- ▶ major difference in internal structure at MS – **convective** vs. **radiative** energy transport:
 - ▶ if T-stratification shallow (compared to adiabatic gradient) → radiative energy transport;
 - ▶ else convective energy transport
- ▶ cool (low-mass stars) during MS:
 - ▶ interior: p-p chain, shallow dT/dr → **radiative core**
 - ▶ outer layers: H/He recombines → large opacities → steep dT/dr , low adiabatic gradient → **convective envelope**
- ▶ hot (massive) stars during MS:
 - ▶ interior: CNO cycle, steep dT/dr → **convective core**
 - ▶ outer layers: H/He ionized → low opacities → shallow dT/dr , large adiabatic gradient → radiative envelope

Note: (i) transition from p-p chain to CNO cycle around 1.3 to $1.4 M_{\text{sun}}$ at ZAMS

(ii) most massive stars have a sub-surface convection zone due to iron opacity peak

(iii) evolved objects (red giants and supergiants) and brown dwarfs are **fully convective**



Chap. 7 Microscopic theory



Absorption- and emission coefficients

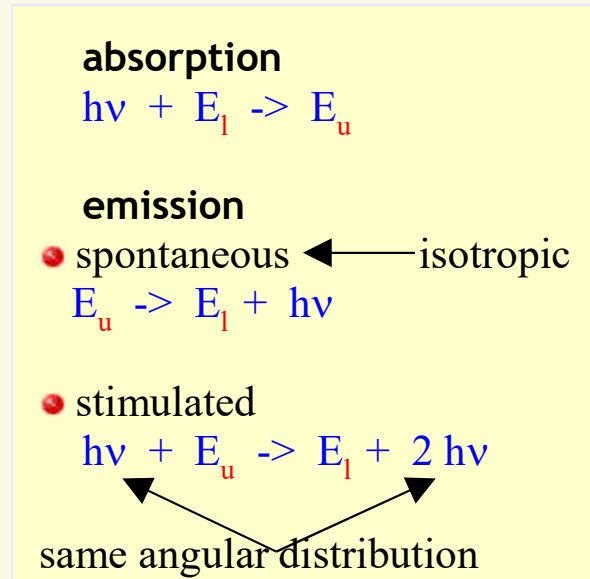
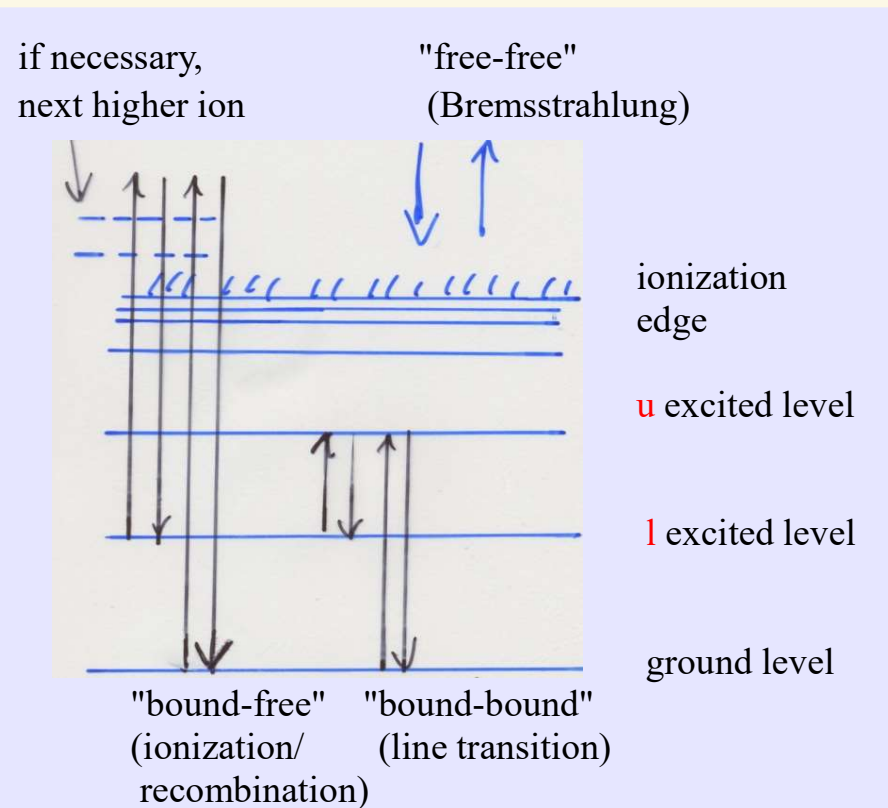
• can calculate now a lot, if absorption- and emission-coefficients given, e.g.

$$\chi_\nu \sim \sigma_{lu} \cdot \phi(\nu) \cdot n_l(r)$$

cross-section
(quantum mech.)
profile function
(normalized)
occupation
numbers

LTE
Saha-Boltzmann

NLTE
detailed calculation



Line transitions

- Einstein coefficients
probability, that photon with energy $\sim [v, v+dv]$ is absorbed by atom in state E_l with resulting transition $l \rightarrow u$, per second

$$dW_{abs}(v, \Omega, l, u) = B_{lu} \cdot I_v(\Omega) \int \psi(v) dv \frac{d\Omega}{4\pi}$$

\swarrow atomic property \downarrow prop. to number of incident photons \downarrow probability that $v \in [v, v+dv]$

$\underbrace{\hspace{10em}}$ prob. for $l \rightarrow u$

\leftarrow prob. that $\Omega \in [\Omega, \Omega+d\Omega]$

B_{lu} Einstein coefficient for absorption

analogously $\psi_v \neq g_v$ without further assumpt.

$$dW^{sp}(v, \Omega, u, l) = A_{ul} \psi(v) dv \frac{d\Omega}{4\pi}$$

$$dW^{stim}(v, \Omega, u, l) = B_{ul} I_v(\Omega) \psi(v) dv \frac{d\Omega}{4\pi}$$

compare absorbed energy

$$dE_v^{abs} = n_l dW_{abs}, \quad h\nu dV - \underbrace{n_u dW^{stim} h\nu dV}_{\text{stimulated emission delivers part of absorbed energy, with same angular distrib. as } I_v(\Omega)}$$

and emitted energy

$$dE_v^{em} = n_u dW^{sp} h\nu dV$$

with definition of opacity and emissivity

$$\Rightarrow \chi_v^{line} = \frac{h\nu}{4\pi} g(v) [n_l B_{lu} - n_u B_{ul} \frac{\psi(v)}{g(v)}]$$

$$\eta_v^{line} = \frac{h\nu}{4\pi} \psi(v) n_u A_{ul}$$

$\psi = 1$ for "complete redistribution"

- Einstein coefficients are atomic properties, must NOT depend on thermodynamic state of matter

Thus assume thermodynamic equilibrium

- from chap 4, we know $S_v^* = \frac{\eta_v^*}{\chi_v^*} = B_v(T)$

(and $\psi_v^* = g_v$)

$$\Rightarrow S_v^* = \frac{n_u A_{ul}}{n_l B_{lu} - n_u B_{ul}}$$

freq. independent
(also valid in (N) LTE, if "complete redistribution")

$$= \frac{A_{ul}}{B_{ul}} \frac{1}{\left(\frac{n_l}{n_u}\right)^* \frac{B_{lu}}{B_{ul}} - 1}$$

- TE: Boltzmann excitation, $\left(\frac{n_l}{n_u}\right)^* = \frac{g_l}{g_u} e^{-h\nu_{lu}/kT}$

$$B_v = \frac{2h\nu^3}{c^2} \frac{1}{e^{h\nu/kT} - 1} = S_v^* = \frac{A_{ul}}{B_{ul}} \frac{1}{\left(\frac{g_l B_{lu}}{g_u B_{ul}}\right) e^{h\nu/kT} - 1}$$

stat. weights

$$\Rightarrow \boxed{g_l B_{lu} = g_u B_{ul}, \quad A_{ul} = \frac{2h\nu^3}{c^2} B_{ul}}$$

ONLY ONE EINSTEIN COEFF. HAS TO BE CALCULATED!



- has to be calculated from quantum mechanics (from 'dipole operator')

- result

$$\frac{h\nu}{4\pi} B_{lu} = \frac{\pi e^2}{m_e c} f_{lu}$$

f "oscillator strength",
dimensionless

↑
classical result, from
electrodynamics

"strong" transitions have $f \approx 0.1 \dots 10$

and "selection rules", e.g. $\Delta l = \pm 1$

"forbidden transitions": magnetic dipole, electr.
quadrupole: f very low,
 10^{-5} and lower

• THUS
$$\chi_\nu = \frac{\pi e^2}{m_e c} f_{lu} \left(n_l - \frac{g_l}{g_u} n_u \right) \cdot g_\nu$$

$$= \frac{\pi e^2}{m_e c} (gf)_{lu} \cdot \left(\frac{n_l}{g_l} - \frac{n_u}{g_u} \right) \cdot g_\nu$$

↑
"gf-value" = $g_l f_{lu}$

with $\int_{-\infty}^{\infty} g(\nu) d\nu = 1$

$$\frac{\pi e^2}{m_e c} \approx 0.02654 \frac{\text{cm}^2}{\text{s}}$$

Profile function?

Line broadening

1. Radiation damping ("natural" line broadening)

- QED effect
- heuristic finite life time with respect to spontaneous emission

$$\tau = \frac{1}{A_{ul}} \quad (\text{e.g., } 10^{-8} \text{ s for } H2 \rightarrow 1)$$

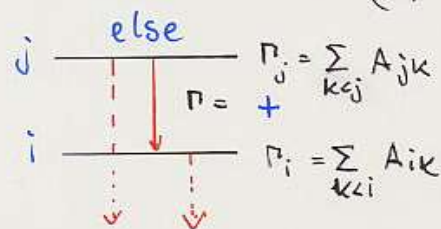
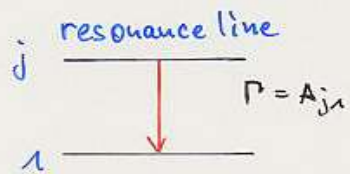
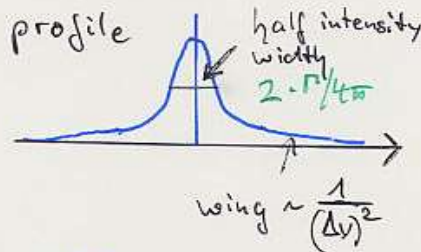
and uncertainty principle

$$\Delta E \cdot \tau \approx \hbar$$

⇒ broadening (classical theory: damping by radiation)

→ dispersion (Lorentzian) profile

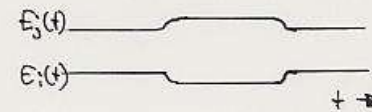
$$g(\nu) = \frac{\Gamma/4\pi^2}{(\nu - \nu_0)^2 + (\Gamma/4\pi)^2}$$



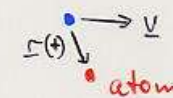
- of primary importance for strong lines (res. lines) in low density environment (no other broadening mechanisms), e.g. $L\alpha$ in interstellar medium

2. Collisional broadening

- radiating atoms perturbed by passing particles
- brief perturbation, close perturbers



"impact theory"



$$\Delta E(t) \sim \frac{1}{r^4(t)}$$

n=2 linear Stark effect

for levels with degenerate angular momentum, e.g., $H I$, $He II$

$$\Delta E \sim F = \frac{q}{r^2}$$

↑
field strength

very important, if many electrons:

photospheres of hot stars, $n_e \approx 10^{12} \text{ cm}^{-3}$

n=3 resonance broadening

atom A is perturbed by atom A' of same species in "cool" stars, e.g. Balmer lines in sun

n=4 quadratic Stark effect

metal ions in photospheres of hot stars $\Delta E \sim F^2$

n=6 van der Waals broadening

atom A perturbed by atom B in cool stars, e.g. Na perturbed by H in sun

resulting profiles are dispersion profiles!



- impact theory fails for (far) wings
 \Rightarrow statistical description (mean field of ensemble of perturbers)
 + q.m.

approximate behaviour for linear Stark broadening

$$f(\Delta\nu \rightarrow \infty) \sim \frac{1}{(\Delta\nu)^{5/2}} \quad (\text{instead of } \frac{1}{(\Delta\nu)^2})$$

3. Thermal velocities : Doppler broadening

- radiating atoms have thermal velocity (so far assumed as zero)

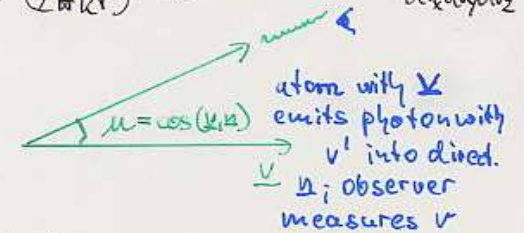
Maxwellian distribution

$$P(v_x, v_y, v_z) dv_x dv_y dv_z = \left(\frac{m}{2\pi kT}\right)^{3/2} e^{-\frac{m}{2kT}(v_x^2 + v_y^2 + v_z^2)} dv_x dv_y dv_z$$

+ Doppler effect

$$v \approx v' + v_0 \frac{u \cdot v}{c}$$

observer's frame atomic frame



\Rightarrow convolution; as long as isotropic emission:

$$\phi(\nu) = \frac{1}{\pi^{1/2}} \int_{-\infty}^{+\infty} e^{-v^2} g(\nu - \nu_0 - \Delta\nu_0 \frac{v}{c}) dv$$

profile function
in atomic frame

"Doppler width"
 $v_{th} = \left(\frac{2kT}{m_A}\right)^{1/2}$ therm. velocity



i) assume sharp line, i.e. $f(\nu - \nu_0) = \delta(\nu - \nu_0)$

$$\rightarrow \phi(\nu) = \frac{1}{\Delta\nu_D} \frac{1}{\sqrt{\pi}} e^{-\left(\frac{\nu - \nu_0}{\Delta\nu_D}\right)^2}$$

Doppler profile, valid in line cores

ii) assume dispersion (Lorentzian) profile with Γ

$$\rightarrow \phi(\nu) = \frac{1}{\Delta\nu_D \sqrt{\pi}} \frac{a}{\pi} \int_{-\infty}^{+\infty} \frac{e^{-y^2} dy}{\left(\frac{\nu - \nu_0}{\Delta\nu_D} - y\right)^2 + a^2}$$

$$= \frac{1}{\Delta\nu_D \sqrt{\pi}} H\left(a, \frac{\nu - \nu_0}{\Delta\nu_D}\right), \quad a = \frac{\Gamma}{4\pi\Delta\nu_D} \text{ damping parameter}$$

Voigt function, can be calculated numerically

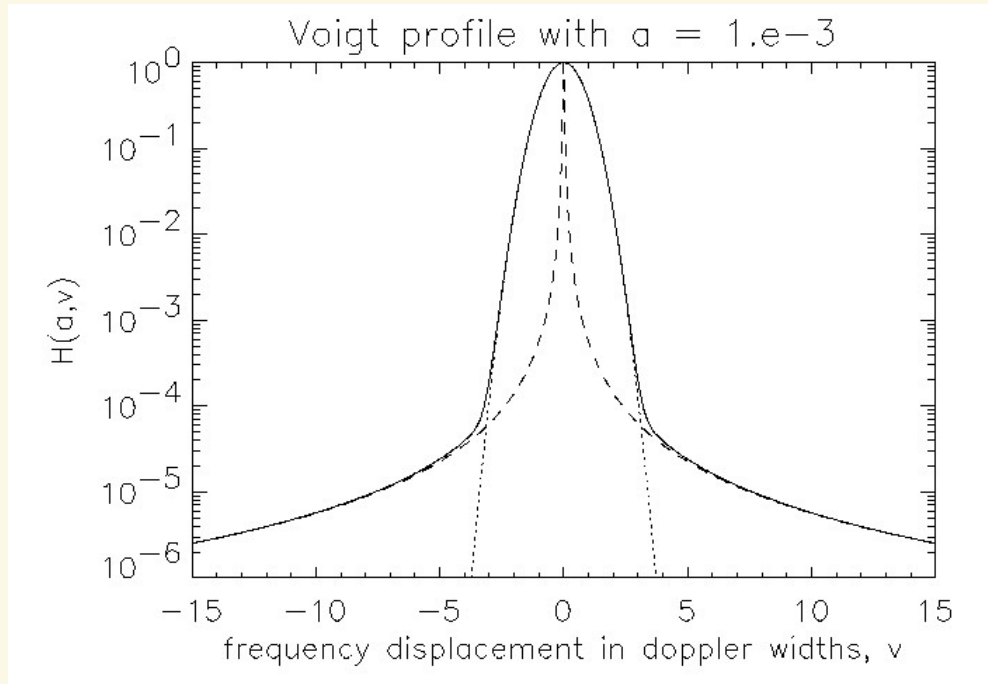
NOTE $H\left(a, \frac{\nu - \nu_0}{\Delta\nu_D}\right) \approx e^{-\left(\frac{\nu - \nu_0}{\Delta\nu_D}\right)^2} + \frac{a}{\sqrt{\pi}} \frac{1}{\left(\frac{\nu - \nu_0}{\Delta\nu_D}\right)^2}$

↑
↑
 line core wings

iii) assume other "intrinsic" profile functions

$\phi(\nu)$ from (numerical) convolution

(e.g., with fast Fourier transformation)



fully drawn: Voigt profile $H(a, \nu)$
 dotted: $\exp(-\nu^2)$, Doppler profile (core)
 dashed: $a / (\sqrt{\pi} \nu^2)$, dispersion profile (wings)

Curve of growth method

Theoretical curve of growth

- standard diagnostic tool to determine metal abundances in cool stars in a simple way
 - assumptions
 - pure absorption line
 - Milne Eddington model, LTE, $\epsilon_v = 1$ (no scattering)
- $$\chi_v = \chi_c + \underbrace{\bar{\chi}_L}_{\chi_v^{line}} \phi_v = \chi_c (1 + \beta_v), \quad \beta_v = \frac{\bar{\chi}_L}{\chi_c} \phi_v$$
- \uparrow
depth independent

$$\begin{aligned} \beta_v(\tau) &= a + b \tau_c \quad \text{defined on continuum scale} \\ &= a + b \frac{\chi_c}{\chi_v} \tau_v = a + b \frac{1}{1 + \beta_v} \tau_v \\ &\Rightarrow b_v \text{ in Milne-Edd. model} \end{aligned}$$

- From Milne Edd. model we have (page 90/91)

$$H_v^{line}(0), \epsilon_v = 1 = \frac{1}{\sqrt{3}} J_v(0) = \frac{1}{\sqrt{3}} \left(a + \frac{1 + \beta_v}{2} \frac{b}{\sqrt{3}} - a \right)$$

$$H_v^{cont}(0), \epsilon_v = 1 = (\beta_v = 0) = \frac{1}{\sqrt{3}} \left(a + \frac{b/\sqrt{3} - a}{2} \right)$$

\Rightarrow residual intensity ("line profile")

$$R_v = \frac{H_v^{line}}{H_v^{cont}} = \frac{b \frac{1}{1 + \beta_v} + \sqrt{3} a}{b + \sqrt{3} a}$$

$$\beta_v = \frac{\pi e^2}{m_e c} f_{lu} \frac{n_e}{\chi_c} (1 - e^{-h\nu/kT}) \phi(\nu) = \beta_0 \phi(\nu) \quad \leftarrow \text{Voigt profile!}$$

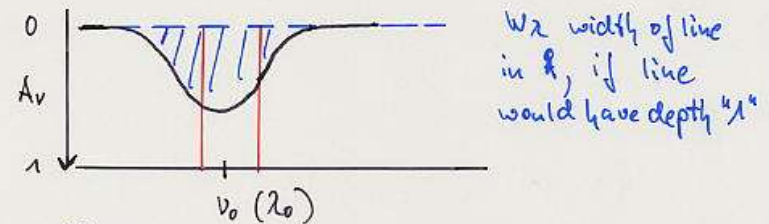
line depth $A_v = 1 - R_v$

$$= \frac{\beta_0 \phi_v}{1 + \beta_0 \phi_v} \underbrace{\left(\frac{b}{b + \sqrt{3} a} \right)}$$

A_0 central depth of line with $\beta_0 \rightarrow \infty$

$$A_v = A_0 \beta_0 \frac{\phi_v}{1 + \beta_0 \phi_v}$$

equivalent width $w_v = \int_0^\infty A_v d\nu$ area below (see also continuum p.8.3)



$$\Rightarrow w_v = A_0 \beta_0 \int_0^\infty \frac{\phi_v}{1 + \beta_0 \phi_v} d\nu$$

$$w_\lambda = \int_0^\infty A(\lambda) d\lambda \approx \left(\int_0^\infty A_v d\nu \right) \frac{\lambda_0^2}{c} \quad w_\lambda = \frac{\lambda_0^2}{c} \cdot w_v$$

with Voigt profile H (Doppler core + Lorentz wings)

$$w_v = A_0 \beta_0 \frac{1}{\Gamma \pi \Delta\nu_D} \int_0^\infty \frac{H\left(\frac{\nu - \nu_0}{\Delta\nu_D}\right) d\nu}{1 + \frac{\beta_0}{\Gamma \pi \Delta\nu_D} H\left(\frac{\nu - \nu_0}{\Delta\nu_D}\right)}$$

$v = \frac{\nu - \nu_0}{\Delta\nu_D}$
 $d\nu = d\nu \Delta\nu_D$

$$W_\nu = \frac{A_0 \beta_0}{\Gamma \pi} \int_{-\infty}^{+\infty} \frac{H(\nu) d\nu}{1 + \frac{\beta_0}{\Gamma \pi \Delta \nu_D} H(\nu)}$$

3 regimes

a) linear regime: Doppler core not saturated, $H(a, \nu) = e^{-\nu^2}$

$$\Rightarrow W_\nu \approx \frac{A_0 \beta_0}{\Gamma \pi} \int_{-\infty}^{+\infty} \frac{e^{-\nu^2} d\nu}{1 + \frac{\beta_0}{\Gamma \pi \Delta \nu_D} e^{-\nu^2}}$$

$$\rightarrow (\beta_0 / \Delta \nu_D < 1) \quad \frac{A_0 \beta_0}{\Gamma \pi} \int_{-\infty}^{+\infty} e^{-\nu^2} \left(1 - \frac{\beta_0}{\Delta \nu_D \Gamma \pi} e^{-\nu^2} + \dots \right) d\nu$$

$\approx A_0 \beta_0 \sim \beta_0$, independent on $\Delta \nu_D$

b) saturation part: line reaches maximum depth ($\approx A$), however wings still unimportant

as above, i.e. $\phi_\nu \sim e^{-\nu^2}$, however $\beta_0 / \Delta \nu_D > 1$

\Rightarrow (integration tricky)

$$W_\nu = 2 A_0 \Delta \nu_D \sqrt{\ln \beta^*} \left(1 - \left(\frac{\pi^2}{24} (\ln \beta^*)^2 - \dots \right) \right)$$

with $\beta^* = \beta_0 / \Gamma \pi \Delta \nu_D$

flat growth with $\sqrt{\ln \beta^*}$, $W_\nu \sim \Delta \nu_D$

c) damping (square-root) part
line wings dominate equivalent width

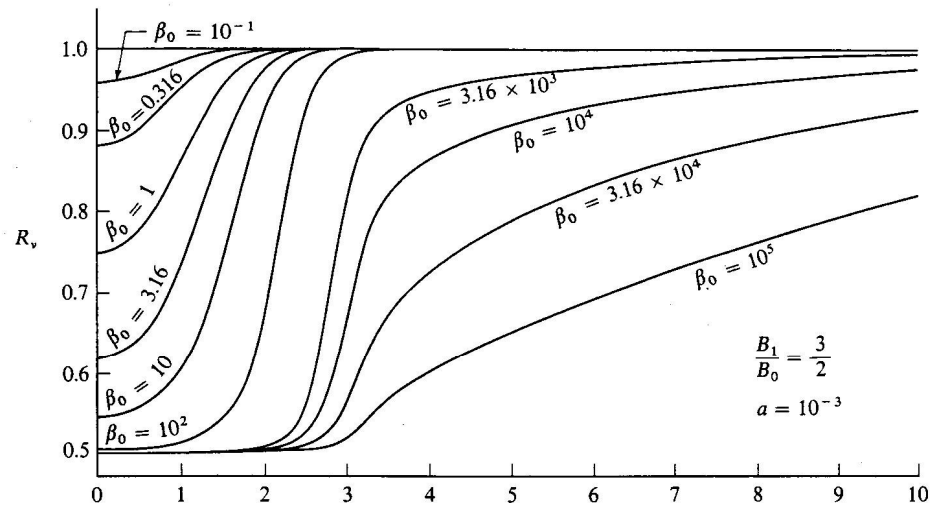
$$\Rightarrow W_\nu \approx \frac{A_0 \beta_0}{\Gamma \pi} \int_{-\infty}^{+\infty} \frac{a / (\Gamma \pi \nu^2) d\nu}{1 + \frac{\beta_0}{\Gamma \pi \Delta \nu_D} \frac{a}{\Gamma \pi \nu^2}} \quad \text{a damping parameter}$$

$$= \frac{A_0 \beta_0}{\pi} a \int_{-\infty}^{+\infty} \frac{d\nu}{\nu^2 + \frac{\beta_0 a}{\pi \Delta \nu_D}}$$

$$= A_0 (a \pi \Delta \nu_D \beta_0)^{\frac{1}{2}} \quad (\text{attention: typo in Mihalas})$$

growth with $\beta_0^{\frac{1}{2}}$

in total, we have $W_\nu = f(\beta_0)$ or $f\left(\frac{\beta_0}{\Delta \nu_D \Gamma \pi}\right) = f(\beta^*)$



Voigt profile with $A_0 = 0.5$, $\beta_0 = \beta^*$

Development of a spectrum line with increasing number of atoms along the line of sight. The line is assumed to be formed in pure absorption. For $\beta_0 \lesssim 1$, the line strength is directly proportional to the number of absorbers. For $30 \lesssim \beta_0 \lesssim 10^3$ the line is saturated, but the wings have not yet begun to develop. For $\beta_0 \gtrsim 10^4$ the line wings are strong and contribute most of the equivalent width.

Now:

$$\beta^* = \frac{\pi e^2}{m c} f_{lu} \frac{n_e}{\chi_c} (1 - e^{-h\nu/kT_e}) \frac{1}{\Delta\nu_D \sqrt{\pi}}$$

$$\chi_c = \chi_c^0 (1 - e^{-h\nu/kT_e}) \quad \text{LTE, next section}$$

$$n_e = n_1 \frac{g_e}{g_1} e^{-E_{ex}/kT_e} \quad \text{Boltzmann excitation, next section}$$

$$\Delta\nu_D = \frac{v_0 v_{th}}{c} = \sqrt{\frac{2kT}{m}} \frac{1}{\lambda}$$

$$\Rightarrow \log \beta^* = \log (g_e f_{lu} \cdot \lambda) + \log (e^{-E_{ex}/kT_e}) + \log \left(\frac{n_1}{g_1 \chi_c^0} \frac{\pi e^2}{m c} \sqrt{\frac{m}{2kT_e}} \right)$$

$$= \log (g_e f_{lu} \cdot \lambda) - \frac{5040 \cdot E_{ex}}{T_e} + \log C$$

in one ionization stage and if E in eV

- in one ionization stage, $C \approx \text{const}$
- lines belonging to one ionization stage should form curve of growth, since β^* varies as function of considered transition

- if T_e and χ_c^0 known
- shift "observed" $W_\nu(\beta^*)$ horizontally until curve matches theoretical curve
- $n_1 \Rightarrow$ (using Saha-Boltzmann equation for ionization, next section) abundances

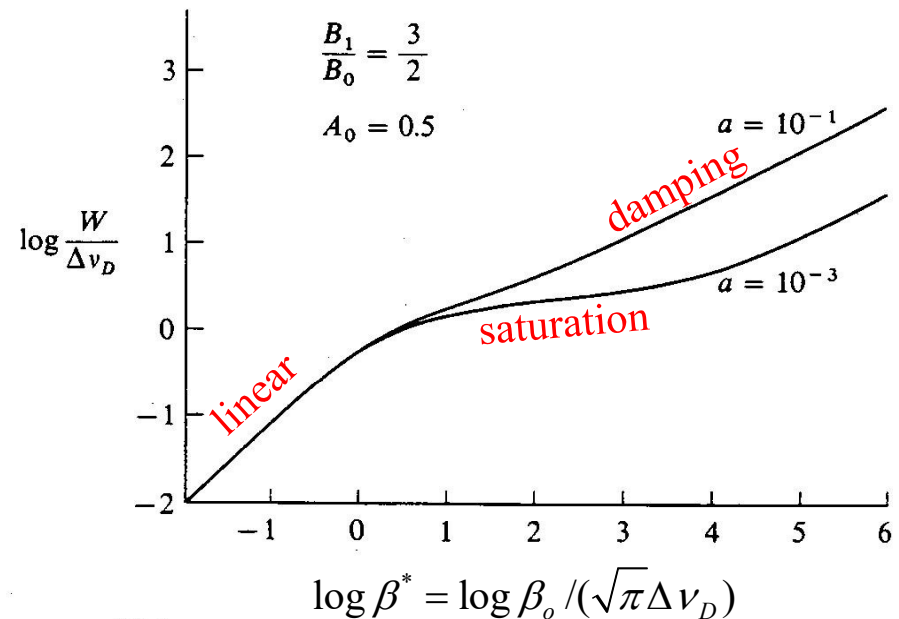
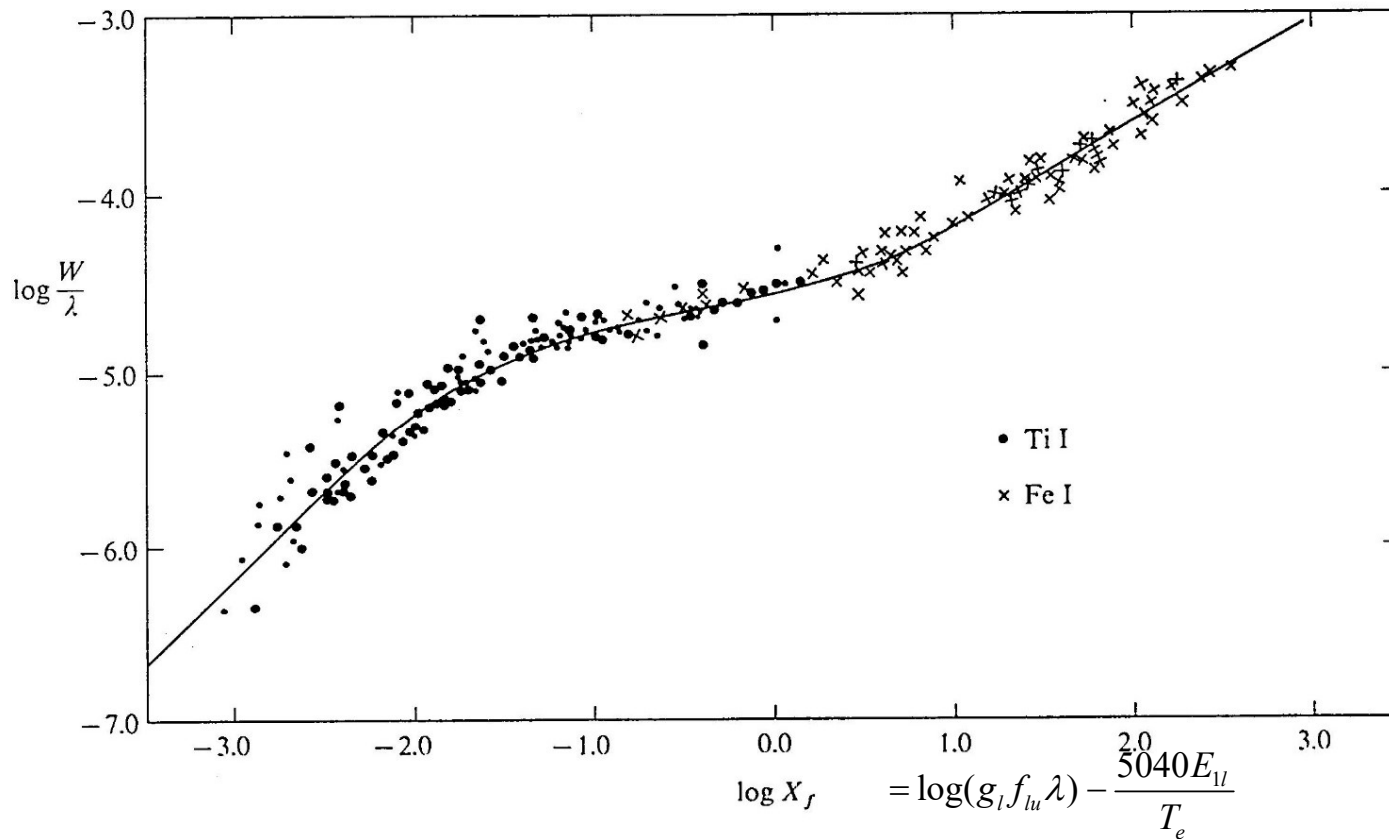


FIGURE 10-2
Curves of growth for pure absorption lines. Note that the larger the value of a , the sooner the square-root part of the curve rises away from the flat part.

measure $W(\lambda)$ for different lines (with different strengths) of one ionization stage

plot as function of $\log(g_l f_{lu} \lambda) - \frac{5040 E_{1l}}{T_e} + \log C$, with "C" fit-quantity

shift horizontally until *theoretical curve of growth* $W(\beta^*)$ is matched $\Rightarrow \log C \Rightarrow \frac{n_1}{\chi_c^0} \Rightarrow n_1$

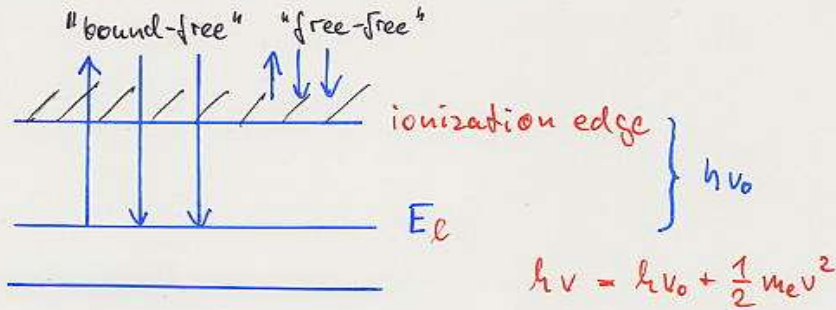


Empirical curve of growth for solar Fe I and Ti I lines. Abscissa is based on laboratory f -values. From (686).
Ti I lines shifted horizontally to define a unique relation

Continuous processes



Continuous absorption/emission and scattering



- bound free processes

"one" transition: $\chi_{\nu}^{bf} = n_e \sigma_{\ell k}(\nu)$, $\nu > \nu_0$

\uparrow absorption cross section \uparrow threshold

in total: many processes at one frequency

$$\chi_{\nu}^{bf} = \sum_{\text{elements}} \sum_{\text{ions}} \sum_{\ell} n_{\ell} \sigma_{\ell k}(\nu)$$

hydrogenic ions $\sigma_{\ell k}(\nu) = \sigma_0(\ell) \left(\frac{\nu_0}{\nu}\right)^3 \cdot g_{bf}(\nu)$

\uparrow "giant-factor" ≈ 1

EINSTEIN-MILNE relations

$$\chi_{\nu}^{bf} = \sum_{\substack{\text{elements,} \\ \text{ions}}} \sum_{\ell} \sigma_{\ell k}(\nu) \left(n_{\ell} - n_{\ell}^* e^{-h\nu/kT} \right)$$

\uparrow stim. emission

$$\eta_{\nu}^{bf} = \sum_{\ell} \sum_{\ell} \sigma_{\ell k}(\nu) \frac{2h\nu^3}{c^2} n_{\ell}^* e^{-h\nu/kT}$$

\uparrow spontaneous emission

$n_{\ell}^* = \text{LTE value}$

NOTE: $n_e = n_{\ell}^* \rightarrow S_{\nu}^{bf} = \frac{\eta_{\nu}^{bf}}{\chi_{\nu}^{bf}} = B_{\nu}(T)!$

free-free processes

(emission process: "bremsstrahlung", decelerated charges radiate!)

$$\chi_{\nu}^{ff} = n_e n_{\text{ion}} \sigma_{kk}(\nu) (1 - e^{-h\nu/kT})$$

\uparrow stim. emission

$$\sigma_{kk} \sim \frac{Z^3}{T}, \text{ important in IR and radio!}$$

$$\eta_{\nu}^{ff} = n_e n_{\text{ion}} \sigma_{kk}(\nu) \frac{2h\nu^3}{c^2} e^{-h\nu/kT}$$

NOTE $S_{\nu}^{ff} = B_{\nu}(T)$ always!

Scattering

1. electron scattering

- important for hot stars
- difference to f-f processes

f-f: photon interacts with e^- in ion's central field
 \Rightarrow absorption \Rightarrow photon destruction, i.e. "true" process

scattering: without influence of central field, i.e., no "third" partner in collisional process
 \Rightarrow no absorption possible, since energy and momentum conservation cannot be fulfilled simultaneously

\Rightarrow scattering

- very high energies (many MeVs)
Klein Nishina (Q.E.D.)
- high energies
Compton / inverse Compton scattering
- low energies ($< 12.4 \text{ keV} \approx 1 \text{ \AA}$)
Thomson scattering

classical e^- radius

$$\sigma^{\text{TH}} = n_e \sigma_T; \quad \sigma_T = \sigma_{\text{class}} = \frac{8\pi}{3} r_0^2 = \frac{8\pi}{3} \frac{e^4}{m_e^2 c^4}$$

$$= 6.65 \cdot 10^{-25} \text{ cm}^2$$

2. Rayleigh-scattering

actually: line absorption/emission of atoms/molecules far from resonance frequency

\Rightarrow from q.m., Lorentzprofile with $|v-v_0| \gg v_0$

$$\sigma(v) = f c n \sigma_T \cdot \left(\frac{v}{v_0}\right)^4 \sim \lambda^{-4} \quad \text{for } v \ll v_0$$

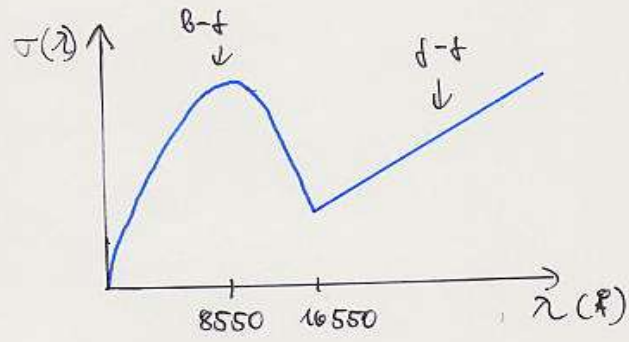
- if line transition strong, λ^{-4} decrease of far wings can be of major importance

example: Rayleigh wings of Ly-alpha in metal-poor, cool stars (G/K-type, few electrons, thus few H^- , see next paragraph) become important opacity source, even in the optical

The H^- ion

- for cool stars (e.g., the sun), one bound state of H^- ($1p + 2e^-$)
- dominant bf-opacity (also ff component)
- only by inclusion of H^- (Pannekoek + Wildt, 1935) the solar continuum could be explained

$$\frac{hc}{\lambda} \approx 0.75 \text{ eV} \approx 16550 \text{ \AA}$$



Total opacities and emissivities

$$\chi_{\nu}^{\text{tot}} = \chi_{\nu}^{\text{line}} \phi(\nu) + \sum \chi_{\nu}^{\text{bf}} + \sum \chi_{\nu}^{\text{ff}} + n_e \sigma_T$$

$$\eta_{\nu}^{\text{tot}} = \chi_{\nu}^{\text{line}} \phi(\nu) S_L + \sum \eta_{\nu}^{\text{bf}} + \sum \eta_{\nu}^{\text{ff}} + n_e \sigma_T J_{\nu}$$

NOTE: for LTE ($n_i = n_i^*$) and $J_{\nu} = B_{\nu}$

we have always

$$\frac{\eta_{\nu}^{\text{tot}}}{\chi_{\nu}^{\text{tot}}} = B_{\nu}(T), \quad \text{good test!}$$

Ionization and Excitation

had $\chi_{\nu}^{\text{line}} = \frac{\pi e^2}{m_e c} g f_{lu} \left(\frac{n_e}{g_l} - \frac{n_u}{g_u} \right) \phi(\nu)$

$$\chi_{\nu}^{\text{bf}} = \sum_l (n_l e^{-u_l} - n_l^* e^{-h\nu/kT}) \sigma_{\text{ex}}(\nu)$$

$$\sigma^{\text{TH}} = n_e \sigma_T$$

How to determine occupation numbers and electron densities?

Local Thermodynamic Equilibrium (LTE)

- each volume element in TE, with temperature $T_e(r)$

Hypothesis: collisions ($e^- \leftrightarrow$ ions) adjust equilibrium

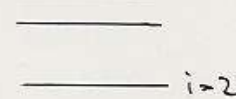
problem: interaction with non-local photons
LTE valid, if

- influence of photons small or
- radiation field Planckian at $T_e(r)$ (and isotropic)

Excitation

- Fermi statistics \rightarrow low density, high temperat.
 \rightarrow Boltzmann statistics

- distribution of level occupation n_{ij}
(per dU , ionization stage j)



$$\frac{n_{ij}}{n_{1j}} = \frac{g_{ij}}{g_{1j}} e^{-E_{ij}/kT}$$

(if $E_1 = 0$)

- g_i statistical weights (number of degen. states)
- for hydrogen $g_i = 2i^2$, i - princ. quant. number
* LS coupling $g = (2S+1)(2L+1)$
- if E_i excitation energy with resp. to ground state

$$\frac{n_u}{n_l} = \frac{g_u}{g_l} e^{-E_{ul}/kT} \quad \text{with} \quad E_{ul} = E_u - E_l$$



Ionization

- from generalization of Boltzmann formula for ratio of two (neighbouring) ionic species j and $j+1$

$$n_{ij} \text{ with } g_{ij} \rightarrow n_{i,j+1} \text{ with } g_{i,j+1} \cdot g_{el} \text{ (weight of final state)}$$

+ free e^-

g_{el} : Number of available elements in phase space for free e^- ,

$$\frac{d^3 \Gamma d^3 p}{h^3} \cdot 2 \text{ (spin)}, \quad d^3 \Gamma = dV = \frac{1}{n_e} \text{ (} 1 e^- \text{ per } dV)$$

$$\Rightarrow \frac{n_{i,j+1}}{n_{ij}} = \frac{1}{n_e} 2 \frac{g_{i,j+1}}{g_i} \left(\frac{2\pi m k T}{h^2} \right)^{3/2} e^{-E_{i,j+1}/kT}$$

Saha eq., 1920

- ratio (i.e., ionization) grows with T (clear!) falls with n_e (recomb!)
- generalization for arbitrary levels: calculate n_{ij} , then $n_{ij} = n_j \frac{g_{ij}}{g_j} e^{-E_{ij}/kT}$

- all levels

$$N_j = \sum_{i=1}^{\infty} n_{ij}, \quad N_{j+1} = \sum_{i=1}^{\infty} n_{i,j+1}$$

- Boltzmann excitation

$$\sum_{i=1}^{\infty} n_{ij} = \frac{n_{ij}}{g_{ij}} \underbrace{\sum_{i=1}^{\infty} g_{ij} e^{-E_{ij}/kT}}_{U_j(T)} = N_j$$

$U_j(T)$ partition function

$$\Rightarrow \frac{n_{ij}}{g_{ij}} = \frac{N_j}{U_j(T)}, \quad \frac{n_{i,j+1}}{g_{i,j+1}} = \frac{N_{j+1}}{U_{j+1}(T)}$$

$$\Rightarrow \frac{N_{j+1} \cdot n_e}{N_j} = \left(\frac{2\pi m k T}{h^2} \right)^{3/2} 2 \frac{U_{j+1}(T)}{U_j(T)} e^{-E_{i,j+1}/kT}$$

Note: Summation in partition function until finite maximum, to account for extent of atom

$$\frac{4\pi}{3} r_{\max}^3 = \Delta V = \frac{1}{n}$$

example hydrogen $r_i = a_0 i^2 = r_{\max} \Rightarrow i_{\max}$

An Example: Pure Hydrogen Atmosphere in LTE

given: temperature + density (here: total particle density)

$$N = n_p + n_e + \sum_{i=1}^{i_{\max}} n_i$$

$$= n_p + n_e + \frac{n_1}{g_1} U(T)$$

only hydrogen: $n_p = n_e$

$$\frac{n_e n_p}{n_1} = \left(\frac{2\pi m k T}{h^2} \right)^{3/2} \frac{2 \cdot g_p}{g_1} e^{-E_{ion}/kT}$$

$$\Rightarrow \frac{n_1}{g_1} = \frac{n_e^2}{2} \left(\frac{h^2}{2\pi m k T} \right)^{3/2} e^{E_{ion}/kT}$$

$$N = 2n_e + n_e^2 \underbrace{\frac{1}{2} \left(\frac{h^2}{2\pi m k T} \right)^{3/2} e^{E_{ion}/kT} U(T)}_{\alpha(T)}$$

$$= 2n_e + n_e^2 \alpha(T)$$

$$\Rightarrow n_e = -\frac{1}{\alpha(T)} + \sqrt{\frac{1}{\alpha^2(T)} + \frac{N}{\alpha(T)}}$$

$$= n_p \xrightarrow{\text{Saha}} n_1 \xrightarrow{\text{Boltzmann}} n_i; \text{ finished!}$$

for mixture of elements, analogously!

LTE bf and ff opacities for hydrogen

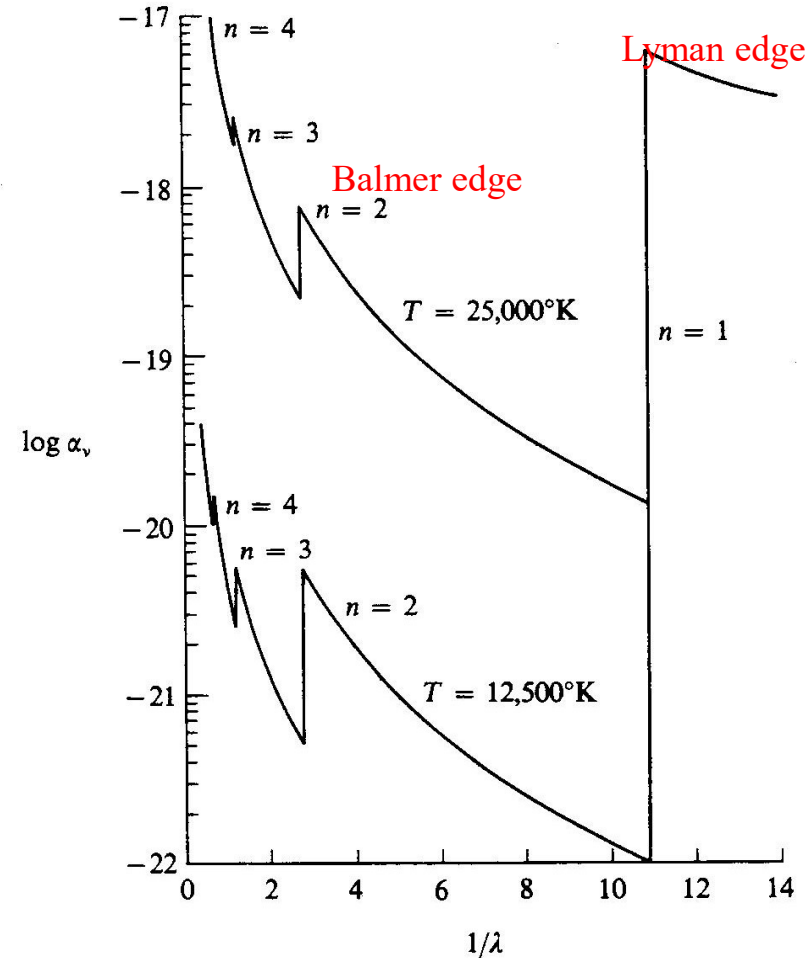


FIGURE 4-1
Opacity from neutral hydrogen at $T = 12,500^\circ\text{K}$ and $T = 25,000^\circ\text{K}$, in LTE; photoionization edges are labeled with the quantum number of state from which they arise/neutral atom
Ordinate: sum of bound-free and free-free opacity in cm^2/atom ;
abscissa: $1/\lambda$ where λ is in microns.



LTE and NLTE

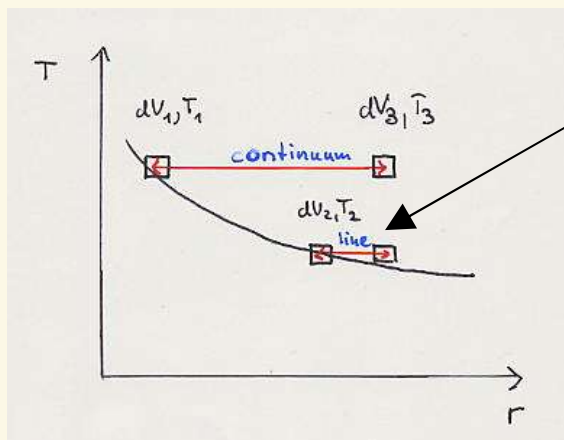


(L)TE: for **each** process, there exists an inverse process with **identical transition rate**

LTE = ‘detailed balance’ for all processes!

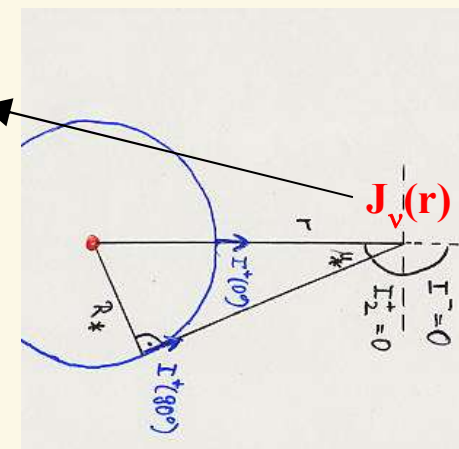
processes = radiative + collisional

- **collisional** processes (and those which are essentially collisional in character, e.g., radiative recombination, ff-emission) in detailed balance, if velocity distribution of colliding particles is **Maxwellian (valid in stellar atm., see below)**
- **radiative** processes: photoionization, photoexcitation (= bb absorption) in detailed balance only if radiation field **Planckian and isotropic (approx. valid only in innermost atmosphere)**



radiative processes couple regions with different temperatures, as a function of frequency: $\Delta\tau_\nu \leq 1$

$$J_\nu(r) = W(r) B_\nu$$



anisotropy



Question: is $f(v) dv$ Maxwellian?

- elastic collisions -> establish equilibrium
- inelastic collisions/recombinations disturb equilibrium
 - inelastic collisions: involve electrons only in certain velocity ranges, tend to shift them to lower velocities
 - recombinations : remove electrons from the pool, prevent further elastic collisions
- can be shown: in *typical* stellar plasmas, $t_{el} / t_{rec} \approx 10^{-5} \dots 10^{-7} \approx t_{el} / t_{inel}$
=> **Maxwellian distribution**
- under certain conditions (solar chromosphere, corona), certain deviations in high-energy tail of distribution possible

Question: is $T(\text{electron}) = T(\text{atom/ion})$?

- equality can be proven for stellar atmospheres with $5,000 \text{ K} < T_e < 100,000 \text{ K}$

When is LTE valid???

roughly: **electron collisions**
 $\propto n_e T^{1/2}$

>> **photoabsorption rates**
 $\propto I_\nu(T) \propto T^x, x \geq 1$

LTE: T low, n_e high
NLTE: T high, n_e low

dwarfs (giants), late B and cooler
all supergiants + rest

however:
NLTE-effects also in cooler stars, e.g.. iron in **sun**

TE - LTE - NLTE : a summary



USM

	TE	LTE	NLTE
velocity distribution of particles Maxwellian ($T_e=T_i$)	✓	✓	✓
excitation Boltzmann	✓	✓	no
ionization Saha	✓	✓	no
source function	$B_\nu(T)$	$B_\nu(T)$, except scattering component	only $S_\nu^{ff} = B_\nu(T)$
radiation field	$J_\nu = B_\nu(T)$	$J_\nu \neq B_\nu(T)$, equality only for $\tau_\nu \geq \left(\frac{1}{\epsilon_\nu}\right)^{1/2}$	$J_\nu \neq B_\nu(T)$ dito

Kinetic equilibrium



USM

NLTE – Kinetic equilibrium (or statistical equilibrium)

- do NOT use Saha-Boltzmann, however calculate occupation numbers by assuming statistical equilibrium
- for stationarity ($d/dt=0$) and as long as kinematic time-scale \gg atomic transition time scales (usually valid)

$$\sum_{j \neq i} n_j P_{ji} = \sum_{j \neq i} n_i P_{ij} \quad \forall i$$

n_i occupation number (atomic species, ionization stage, level)

P_{ij} transition rate from level $i \rightarrow j$ ($\dim P_{ij} = s^{-1}$)

- in words: the number of all possible transitions from level i into other states j is balanced by the number of transitions from all other states j into level i .

\Rightarrow linear equation system for n_i , has to be closed by abundance equation

$$\sum n_{ik} = n_k$$

if n_{ik} the occupation numbers of species k and n_k the total particle density of k

Transition rates

- collisional processes bb , ionization/rec.
- radiative processes bb , ionization/rec.

Radiative processes depend on radiation field
radiation field depends on opacities
opacities depend on occupation numbers

Iteration required!

... not so easy, however possible

Note: to obtain reliable results, order of

30 species

3-5 ionization stages / species

20...1000 level/ion

100,000... some 10^6 transitions

to be considered in parallel

requires large data base of atomic quantities (energies, transitions, cross sections)
fast algorithm to calculate radiative transfer!

Solution of the rate equations – a simple example

HAD: for each atomic level, the sum of all populations must be equal to the sum of all depopulations (for stationary situations)

example: 3-niveau atom with continuum

assume: all rate coefficients are known (i.e., also the radiation field)

\Rightarrow **rate equations** (equations of statistical equilibrium)

$$-n_1 [R_{1k} + C_{1k} + R_{12} + C_{12} + R_{13} + C_{13}] + n_2 (R_{21} + C_{21}) + n_3 (R_{31} + C_{31}) + n_k (R_{k1} + C_{k1}) = 0$$

$$n_1 (R_{12} + C_{12}) - n_2 [R_{2k} + C_{2k} + R_{21} + C_{21} + R_{23} + C_{23}] + n_3 (R_{32} + C_{32}) + n_k (R_{k2} + C_{k2}) = 0$$

$$n_1 (R_{13} + C_{13}) + n_2 (R_{23} + C_{23}) - n_3 [R_{3k} + C_{3k} + R_{31} + C_{31} + R_{32} + C_{32}] + n_k (R_{k3} + C_{k3}) = 0$$

$$n_1 (R_{1k} + C_{1k}) + n_2 (R_{2k} + C_{2k}) + n_3 (R_{3k} + C_{3k}) - n_k [R_{k1} + C_{k1} + R_{k2} + C_{k2} + R_{k3} + C_{k3}] = 0$$

with

R_{ij} , radiative bound-bound transitions (lines!)

R_{ik} radiative bound-free transitions (ionizations)

R_{ki} radiative free-bound transitions (recombinations)

C_{ij} collisional bound-bound transitions

C_{ik} collisional bound-free transitions

C_{ki} collisional free-bound transitions

in matrix representation \Rightarrow

$$P = \begin{pmatrix} -(R_{1k} + C_{1k} + R_{12} + C_{12} + R_{13} + C_{13}) & (R_{21} + C_{21}) & (R_{31} + C_{31}) & (R_{k1} + C_{k1}) \\ (R_{12} + C_{12}) & -(R_{2k} + C_{2k} + R_{21} + C_{21} + R_{23} + C_{23}) & (R_{32} + C_{32}) & (R_{k2} + C_{k2}) \\ (R_{13} + C_{13}) & (R_{23} + C_{23}) & -(R_{3k} + C_{3k} + R_{31} + C_{31} + R_{32} + C_{32}) & (R_{k3} + C_{k3}) \\ (R_{1k} + C_{1k}) & (R_{2k} + C_{2k}) & (R_{3k} + C_{3k}) & -(R_{k1} + C_{k1} + R_{k2} + C_{k2} + R_{k3} + C_{k3}) \end{pmatrix}$$

rate matrix, diagonal elements sum of all depopulations

Rate matrix is **singular**, since, e.g., last row linear combination of other rows (negative sum of all previous rows)

THUS: **LEAVE OUT** arbitrary line (mostly the last one, corresponding to ionization equilibrium) and **REPLACE** by inhomogeneous, linearly independent equation for all n_i , to obtain unique solution

particle number conservation for considered atom:

$$\sum_{i=1}^N n_i = \alpha_k N_H, \text{ with } \alpha_k \text{ the abundance of element k}$$

NOTE 1: numerically stable equation solver required, since typically hundreds of levels present, and (rate-) coefficients of highly different orders of magnitude

NOTE 2: occupation numbers n_i depend on radiation field (via radiative rates), and radiation field depends (non-linearly) on n_i (via opacities and emissivities)
=> Clever iteration scheme required!!!!

Example for extreme NLTE condition

Nebulium (= [OIII] 5007, 4959) in Planetary Nebulae

mechanism suggested by *I. Bowen* (1927):

- low-lying meta-stable levels of OIII(2.5 eV) **collisionally excited** by free electrons (resulting from photoionization of hydrogen via "hot", *diluted* radiation field from central star)
- Meta-stable levels become **strongly populated**
- **radiative decay** results in **very strong** [OIII] emission lines
- impossible to observe suggested process in laboratory, since *collisional deexcitation* (no photon emitted) *much stronger than radiative decay under terrestrial conditions*.
- Thus, after detection new element proposed , "nebulium"

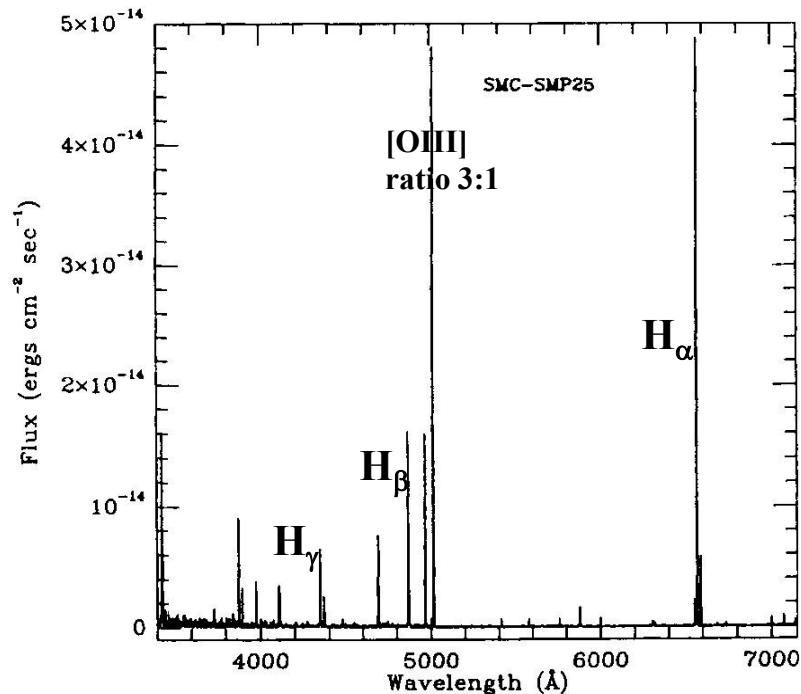


FIG. 1a

Condition for radiative decay

NOTE: $A_{ml} \leq 10^{-2}$ (typical values are 10^7)

$n_m A_{ml} \gg n_m n_e q_{ml}(T_e)$, with metastable level m
 $\rightarrow n_e \ll n_e(\text{crit})$,

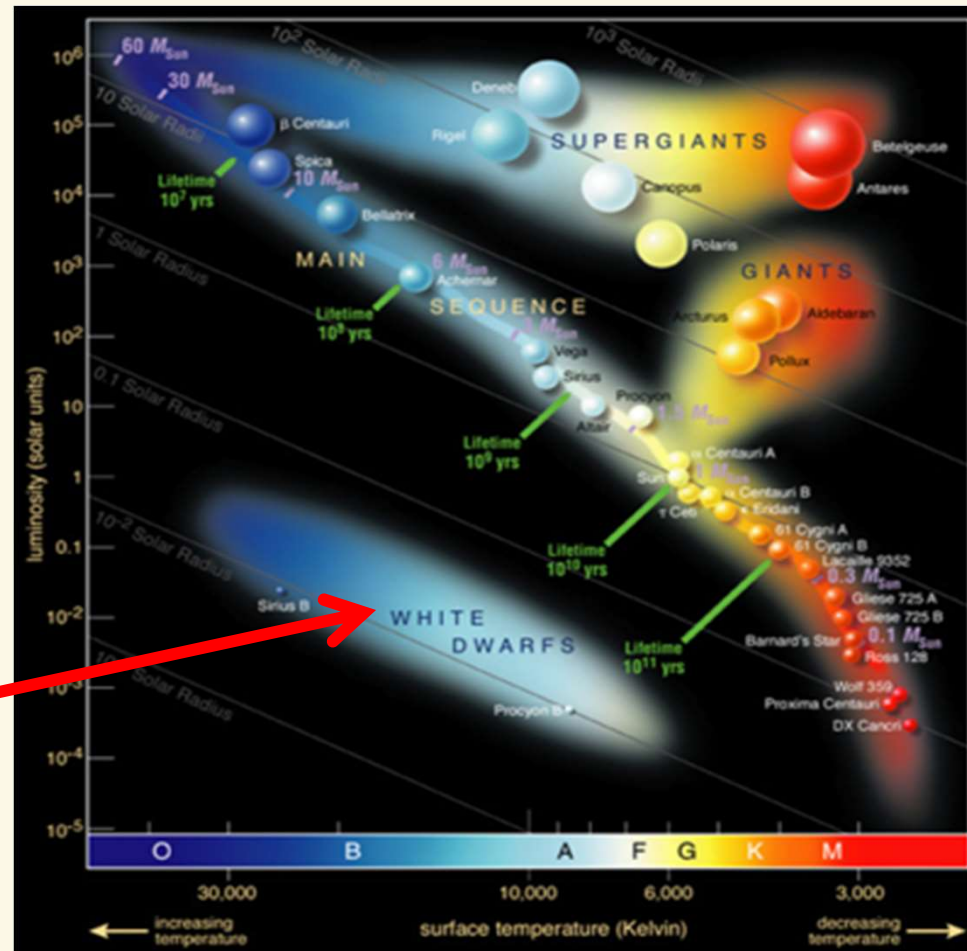
$$n_e(\text{crit}) = \frac{A_{ml}}{q_{ml}(T_e)}, \quad q_{ml} = 8.63 \cdot 10^{-6} \frac{\Omega(l, m)}{g_m \sqrt{T_e}}$$

$\Omega(l, m)$ collisional strength, order unity

for typical temperatures $T_e \approx 10,000\text{K}$ and [OIII] 5007,
we have $n_e(\text{crit}) \approx 4.9 \cdot 10^5 \text{cm}^{-3}$,
much larger than typical nebula densities

Intermezzo: Stellar Atmospheres in practice

A tour de modeling and analysis of stellar atmospheres throughout the HRD



except for
white dwarfs

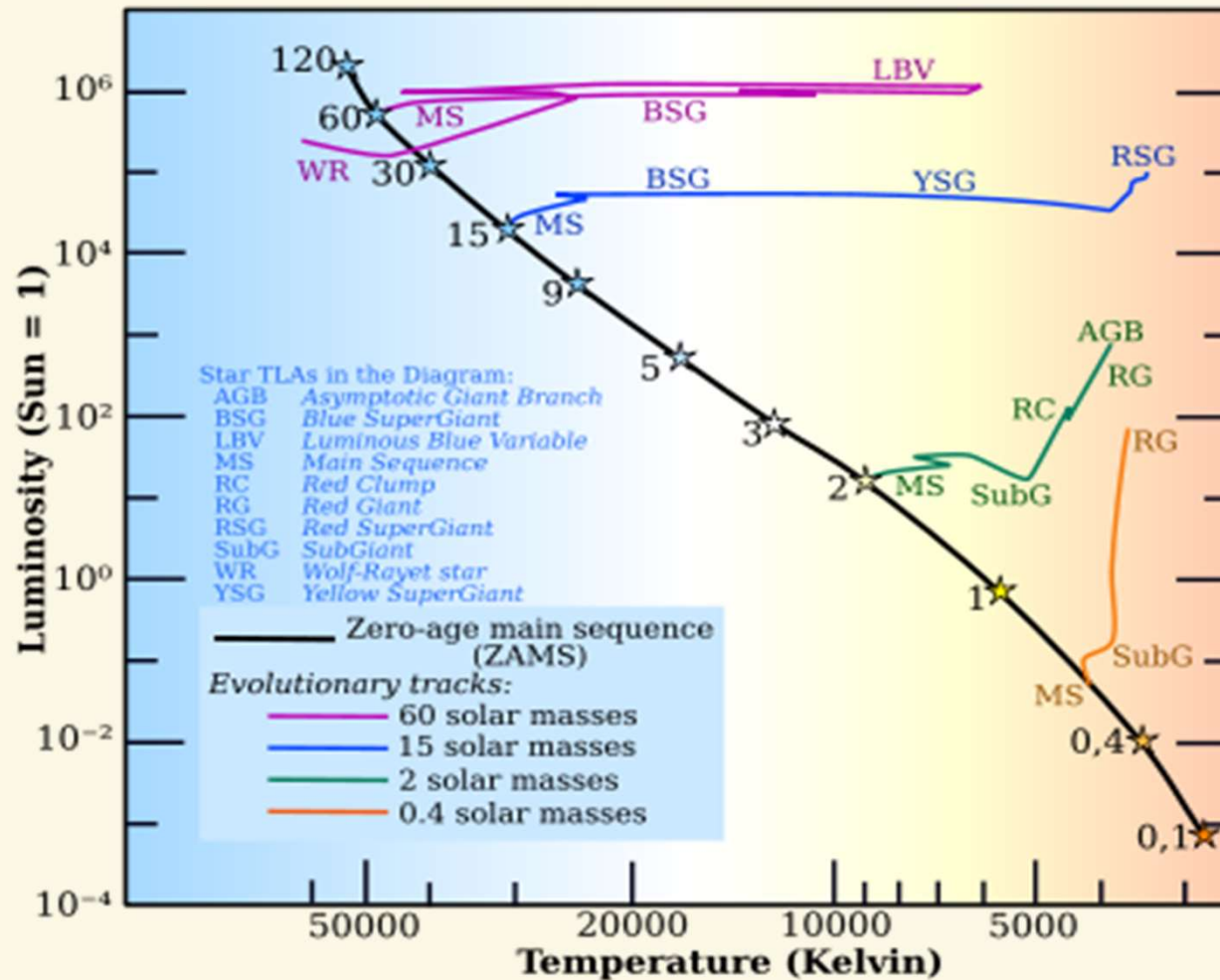


Stellar Atmospheres in practice



Some different types of stars...

Hot luminous stars:
 Massive, main-sequence (MS, $\sim 10 R_{\text{sun}}$) or evolved, ($\sim 20 \dots 100 R_{\text{sun}}$).
 Strong, fast stellar winds



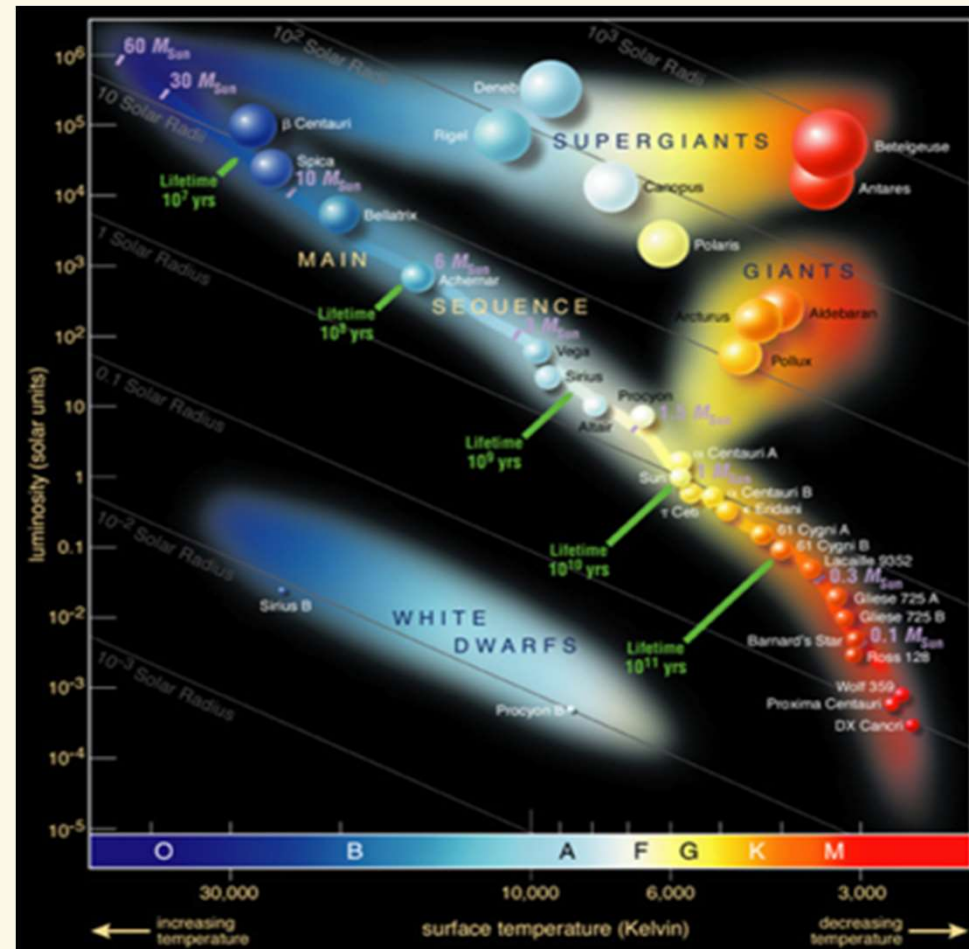
Cool, luminous stars (RSG, AGB):
 Massive or low/intermediate mass, evolved, several 100 (!) R_{sun} .
 Strong, slow stellar winds

Solar-type stars:
 Low-mass, on or near MS, hot surrounding coronae, weak stellar winds (e.g., solar wind)



A tour de modeling and analysis of stellar atmospheres throughout the HRD

Different regimes require different key input physics and assumptions



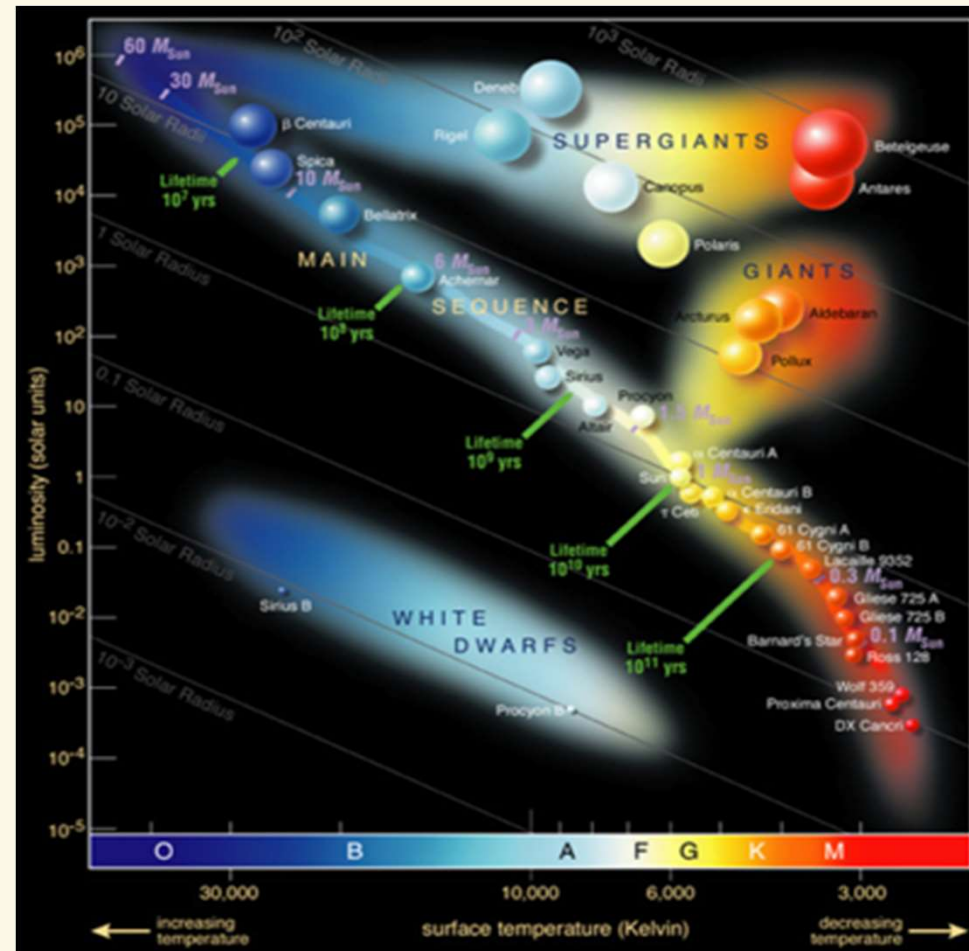
- LTE or NLTE
- Spectral line blocking/blanketing
- (sub-) Surface convection
- Geometry and dimensionality
- Velocity fields and outflows



Spectroscopy and Photometry

ALSO:
Analysis
of different
WAVELENGTH
BANDS
is different

(X-ray, UV,
optical, infra-
red...)



Depends on where in
atmosphere light
escapes from

Question: Why is this
“formation depth”
different for different
wavebands and
diagnostics?



Spectroscopy/photometry (see Chap. 2)

...gives insight into and understanding of our cosmos

- ▶ provides
 - ▶ **stellar properties**, mass, radius, luminosity, energy production, chemical composition, properties of outflows
 - ▶ **properties of (inter) stellar plasmas**, temperature, density, excitation, chemical comp., magnetic fields
- ▶ INPUT for stellar, galactic and cosmologic **evolution** and for stellar and galactic structure
- ▶ requires
 - ▶ **plasma physics**, plasma is "normal" state of atmospheres and interstellar matter (plasma diagnostics, line broadening, influence of magnetic fields,...)
 - ▶ **atomic physics/quantum mechanics**, interaction light/matter (micro quantities)
 - ▶ **radiative transfer**, interaction light/matter (macroscopic description)
 - ▶ **thermodynamics**, thermodynamic equilibria: TE, LTE (local), NLTE (non-local)
 - ▶ **hydrodynamics**, atmospheric structure, velocity fields, shockwaves,...

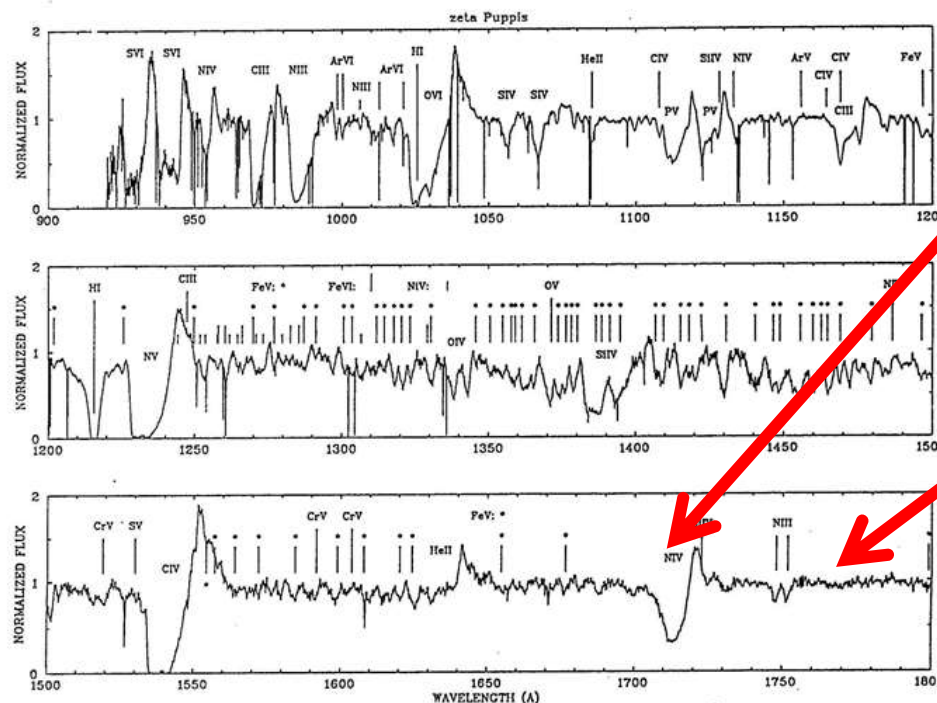


Spectroscopy (see Chap. 2)

UV “P-Cygni” lines formed in rapidly accelerating, hot stellar winds
 (quasi-) continuum formed in (quasi-) hydrostatic photosphere

advanced reading

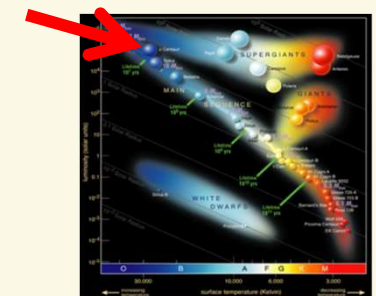
UV spectrum of the O4I(f) supergiant ζ Pup



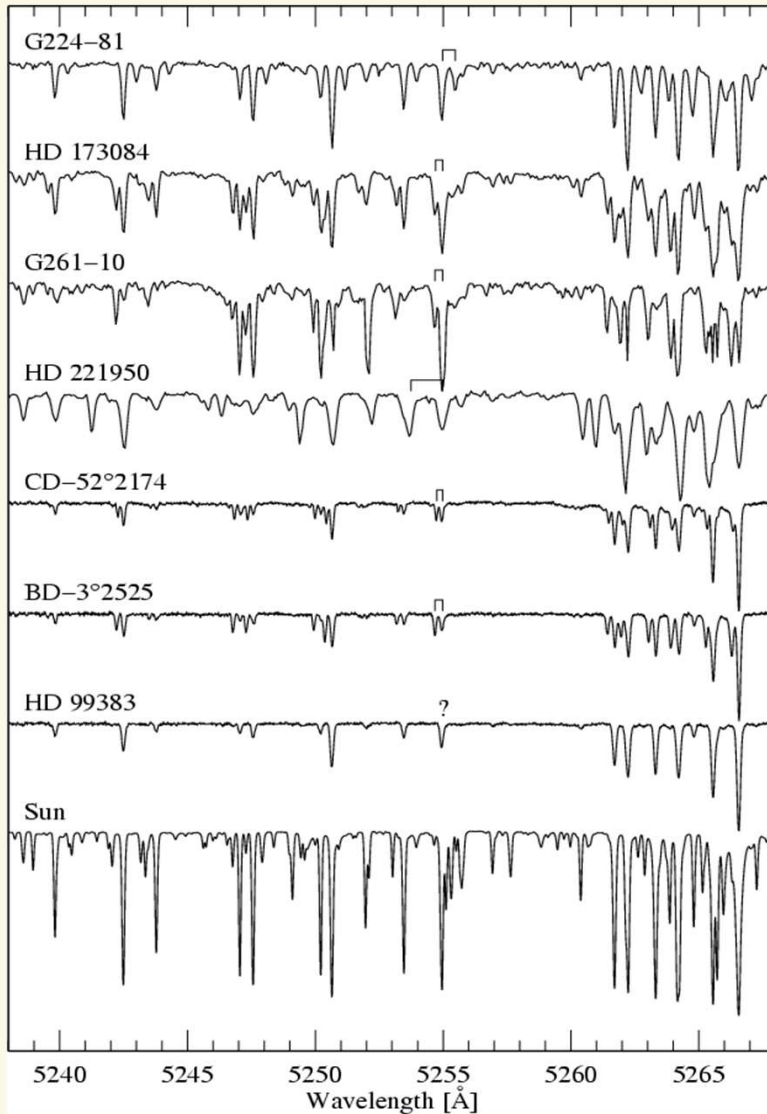
montage of **Copernicus** ($\lambda < 1500 \text{ \AA}$, high res. mode, $\Delta\lambda \approx 0.05 \text{ \AA}$, Morton & Underhill 1977) and **IUE** ($\Delta\lambda \approx 0.1 \text{ \AA}$) observations

IMPRS advanced course - Radiative transfer, stellar atmospheres and winds

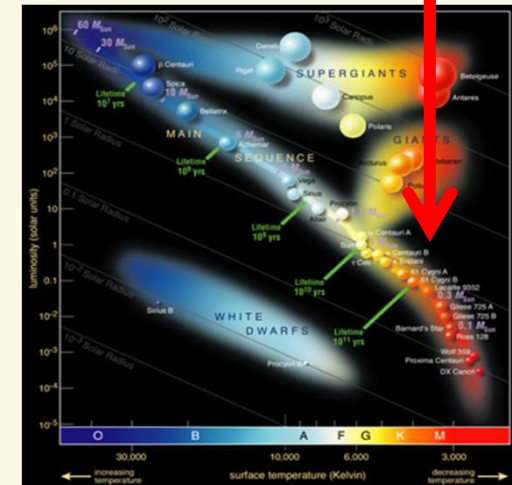
38



Spectroscopy



Lines and continuum in the **optical** around 5200 Å, in cool, solar-type stars, formed in the photosphere





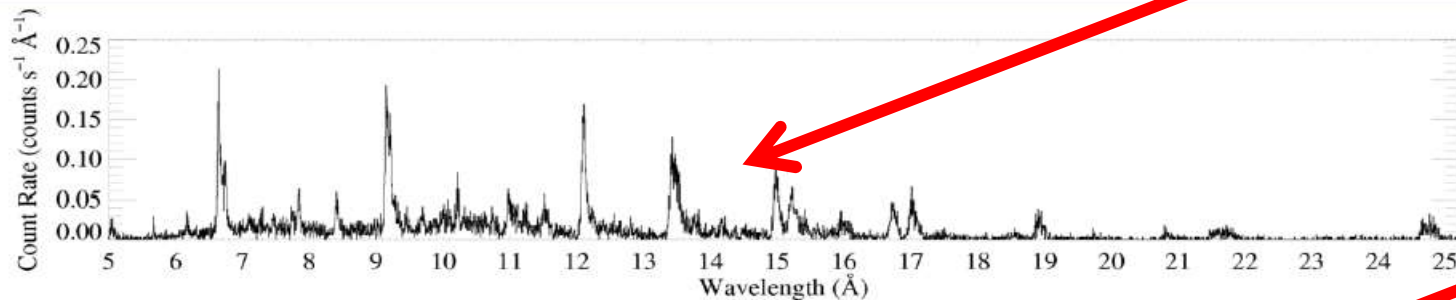
Stellar Atmospheres in practice



Spectroscopy

Chandra grating (HETGS/MEG) spectra

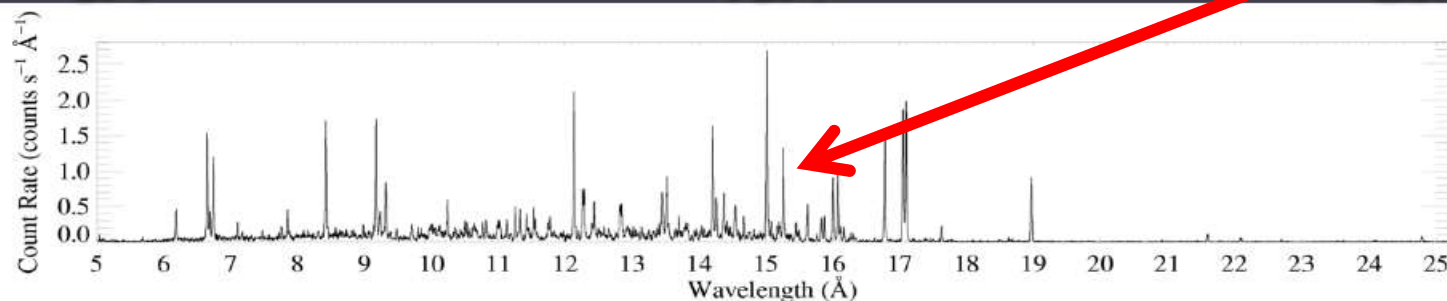
ζ Pup (O4 If)



5Å

15Å

25Å



Capella (G5 III)

X-rays from hot stars, formed in shocks in stellar wind

X-rays from cool stars, formed in hot coronae

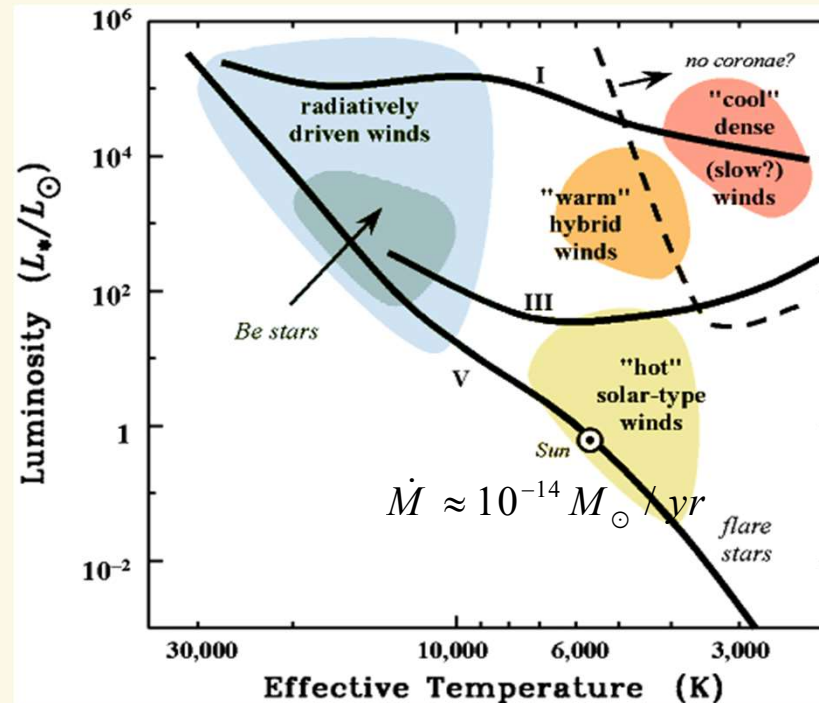


A tour de modeling and analysis of stellar atmospheres throughout the HRD

Stellar Winds (see Chap. 8)

KEY QUESTION:
What provides the force able to overcome gravity?

$$\dot{M} \approx 10^{-4} \dots 10^{-8} M_{\odot} / yr$$



- LTE or NLTE
- Spectral line blocking/blanketing
- (sub-) Surface convection
- Geometry and dimensionality
- Velocity fields and outflows

A tour de modeling and analysis of stellar atmospheres throughout the HRD

KEY QUESTION: What provides the force able to overcome gravity?

Pressure gradient

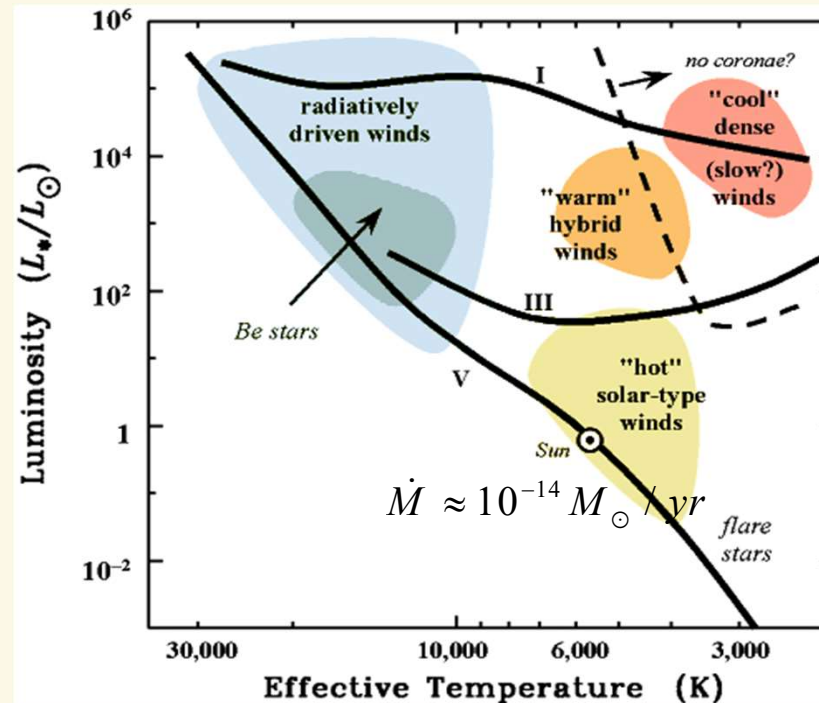
in hot coronae of solar-type stars

Radiation force:

Dust scattering (in pulsation-levitated material, see Chap. 8) in cool AGB stars (S. Höfner and colleagues)

Same mechanism in cool RSGs?

$$\dot{M} \approx 10^{-4} \dots 10^{-8} M_{\odot} / yr$$



- LTE or NLTE
- Spectral line blocking/blanketing
- (sub-) Surface convection
- Geometry and dimensionality
- **Velocity fields and outflows**



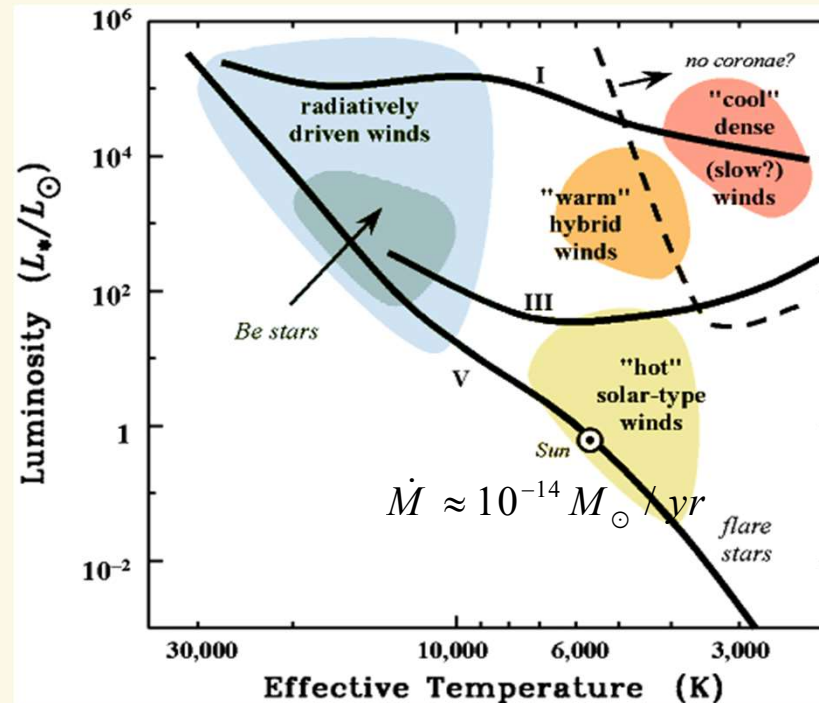
A tour de modeling and analysis of stellar atmospheres throughout the HRD

KEY QUESTION: What provides the force able to overcome gravity?

$$\dot{M} \approx 10^{-4} \dots 10^{-8} M_{\odot} / yr$$

Radiation force:

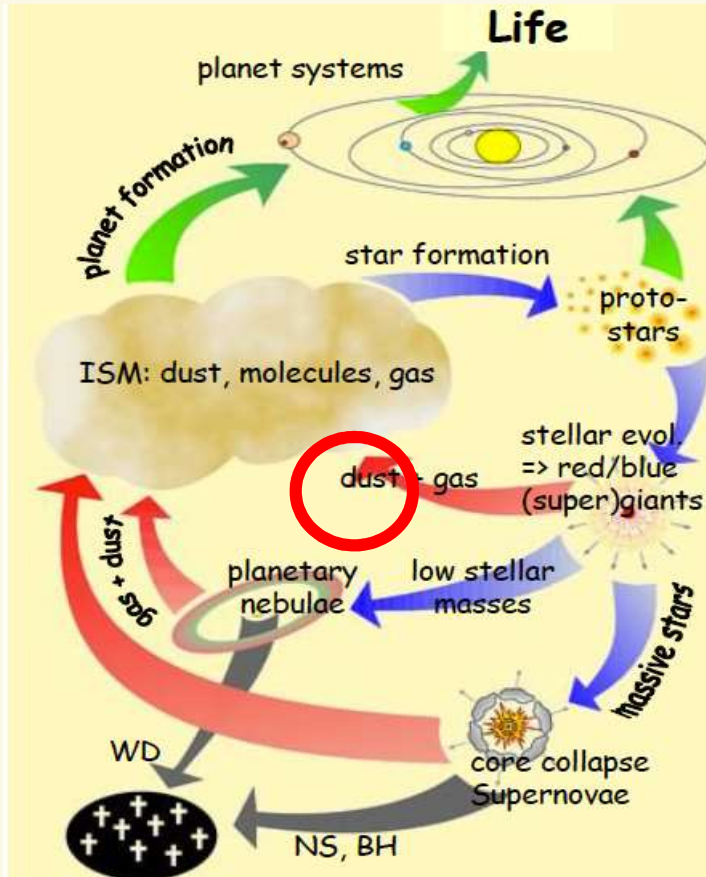
line scattering in hot, luminous stars
→ done at USM, more to follow in Chap. 8



- LTE or NLTE
- Spectral line blocking/blanketing
- (sub-) Surface convection
- Geometry and dimensionality
- **Velocity fields and outflows**

Question: How do you think the high mass loss of stars with high luminosities affects the evolution of the star and its surroundings?

from introductory slides ...



Feedback

- massive stars determine energy (kinetic and radiation) and momentum budget of surrounding ISM
- kinetic energy and momentum budget via winds (of different strengths, in dependence of evolutionary status)
- massive stars enrich environment with metals, via winds and SNe, determine chemo-dynamical evolution of Galaxies (exclusively before onset of SNe Ia)
 - in particular: first chemical enrichment of Universe by First (VMS) Stars

→“FEEDBACK”



Bubble Nebula (NGC 7635) in Cassiopeia

wind-blown bubble around BD+602522 (O6.5III_f)

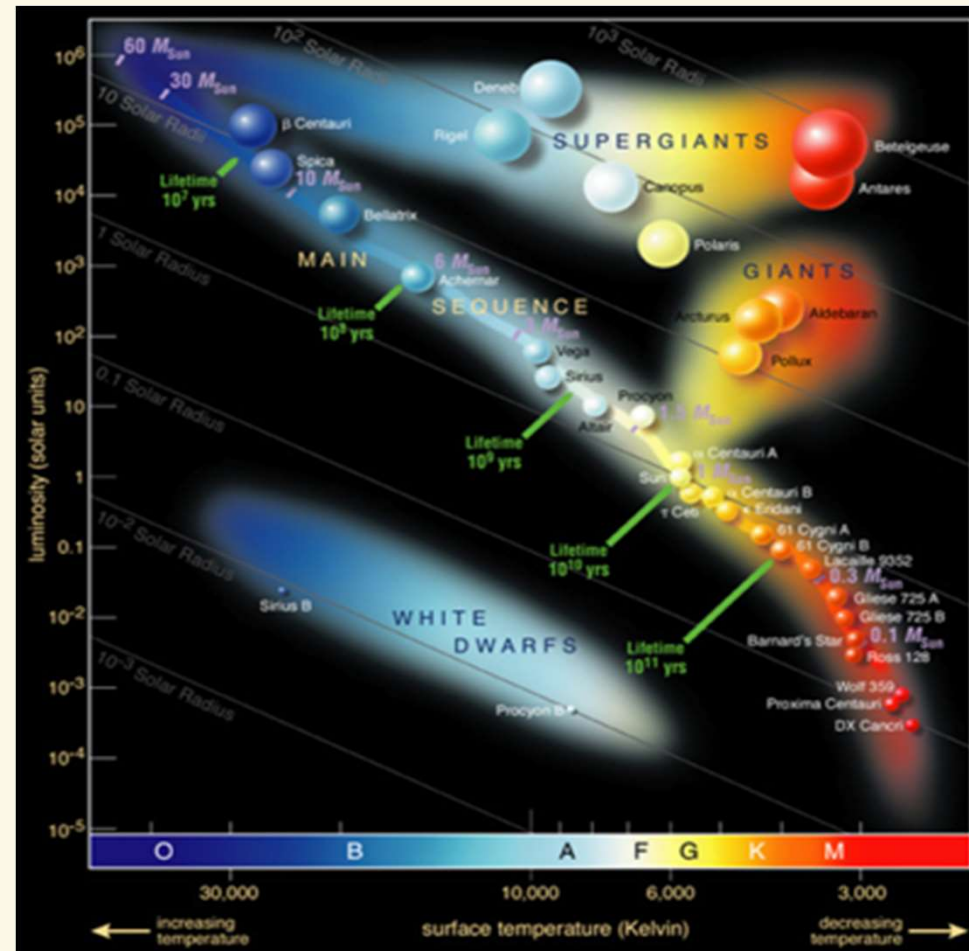
IMPRS advanced course - Radiative transfer, stellar atmospheres and winds

31

Stellar Winds from hot/evolved cool stars control evolution/late evolution, and feed the ISM with nuclear processed material

A tour de modeling and analysis of stellar atmospheres throughout the HRD

In the following,
we focus on stellar
photospheres



From Chap. 6

Summary: stellar atmospheres - the solution principle

THUS problem of stellar atmospheres solved (in principle, without convection, p-p geometry, static)
 Given $\log g_*$, T_{eff} , abundances

(A) hydrostatic equilibrium

$$\frac{dp_{\text{gas}}}{dz} = -g(g_* - g_{\text{rad}}); \quad g_{\text{rad}} = \frac{4\pi}{c} \int_0^\infty \chi_\nu H_\nu d\nu = \frac{4\pi}{c} \left(\sigma^{\text{TH}} H(z) + \int_0^\infty \chi_\nu^{\text{rest}} H_\nu d\nu \right)$$

$$\Rightarrow \frac{dp_{\text{gas}}}{dz} = -g g_* + \sigma^{\text{TH}} \frac{\sigma_B T_{\text{eff}}^4}{c} + \frac{4\pi}{c} \int_0^\infty \chi_\nu^{\text{rest}} H_\nu d\nu \quad H = \frac{1}{4\pi} \sigma_B T_{\text{eff}}^4 \quad (= \frac{1}{4\pi} F)$$

(B) equation of rad. transfer

$$\mu \frac{dI_\nu}{dz} = \chi_\nu (S_\nu - I_\nu) \quad \forall \nu, \mu \Rightarrow J_\nu = \frac{1}{2} \int_{-1}^{+1} I_\nu(\mu) d\mu; \quad H_\nu = \frac{1}{2} \int_{-1}^{+1} I_\nu(\mu) \mu d\mu$$

(C) a) radiative equilibrium

$$\int_0^\infty (\chi_\nu - \chi_\nu^{\text{rest}}) J_\nu d\nu = \int_0^\infty \left\{ \sigma^{\text{TH}} J_\nu + \chi_\nu^{\text{rest}} S_\nu^{\text{rest}} - (\sigma^{\text{TH}} + \chi_\nu^{\text{rest}}) J_\nu \right\} d\nu = \int_0^\infty \chi_\nu^{\text{rest}} (S_\nu^{\text{rest}} - J_\nu) d\nu \stackrel{?}{=} 0$$

scattering terms cancel, since conservative

b) flux-conservation: $4\pi \int_0^\infty H_\nu(z) d\nu = 4\pi H(z) \stackrel{?}{=} \sigma_B T_{\text{eff}}^4 \Rightarrow \Delta T(z) \rightarrow \Delta \chi_\nu(z) \text{ etc}$

(D) equation of state $p_{\text{gas}}(z) = \frac{k_B}{\mu m_H} \rho(z) T(z)$

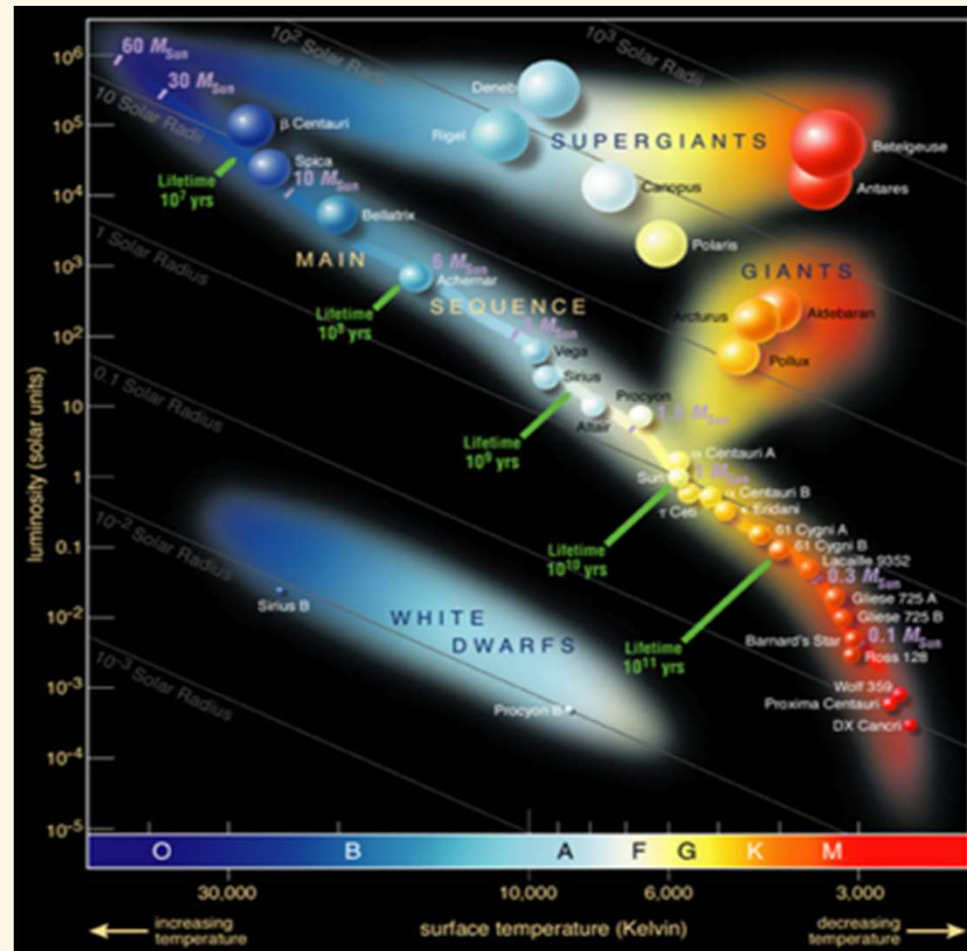
solution by iteration!

Solution of differential equations A and B by **discretization**
 differential operators \Rightarrow finite differences
 all quantities have to be evaluated on suitable grid

Eq. of radiative transfer (B)
 usually solved by the so-called
 Feautrier and/or Rybicki scheme

OBSERVATIONS!!!

A tour de modeling and analysis of stellar atmospheres throughout the HRD



- LTE or NLTE
- Spectral line blocking/blanketing
- (sub-) Surface convection
- Geometry and dimensionality
- Velocity fields and outflows



LTE or NLTE? (see Chap. 7)

When is LTE valid???

roughly: **electron collisions**
 $\propto n_e T^{3/2}$

>> photoabsorption rates
 $\propto I_\nu(T) \propto T^x, x \geq 1$

LTE: T low, n_e high
NLTE: T high, n_e low

dwarfs (giants), late B and cooler
all supergiants + rest

however:
NLTE-effects also
in cooler
stars, e.g..
iron in **sun**

HOT STARS:

Complete model atmosphere and synthetic spectrum must be calculated in NLTE

NLTE calculations for various applications (including Supernovae remnants) within the expertise of USM

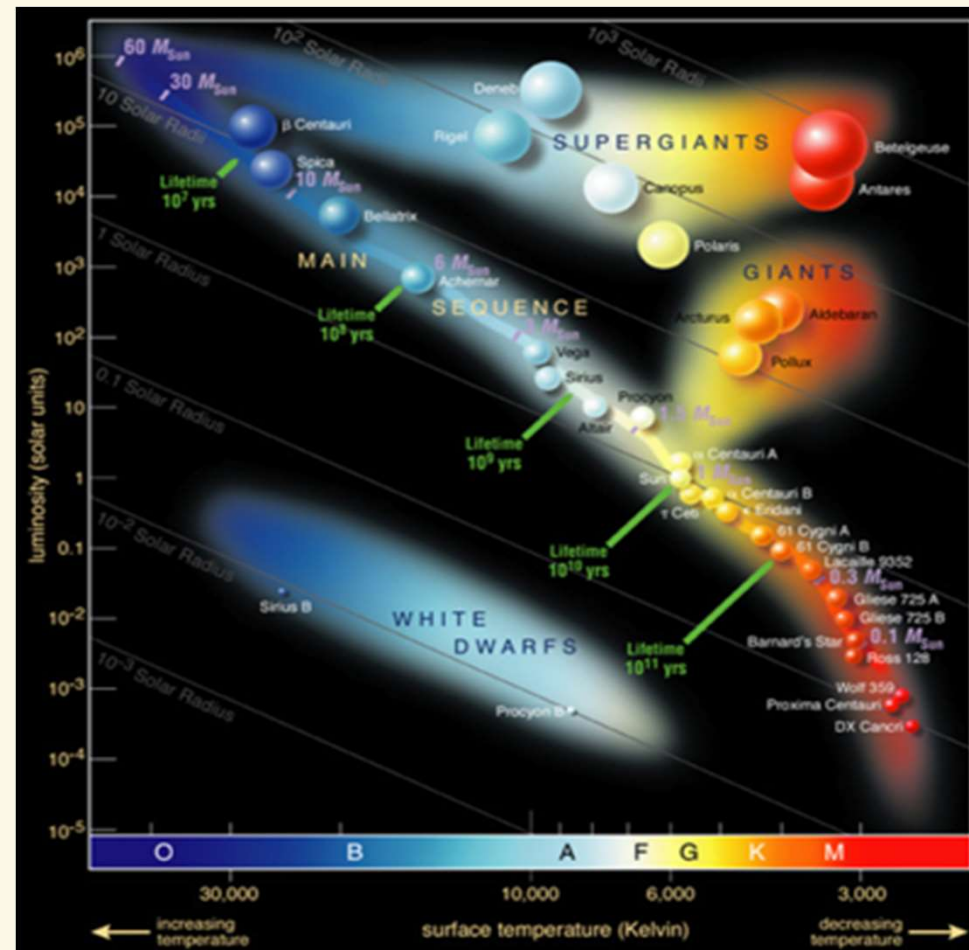
COOL STARS:

Standard to neglect NLTE-effects on atmospheric structure, might be included when calculating line spectra for individual “trace” elements (typically used for chemical abundance determinations)

BUT: See work by Phoenix-team (Hauschildt et al.)
ALSO: RSGs still somewhat open question



A tour de modeling and analysis of stellar atmospheres throughout the HRD



- LTE or NLTE
- Spectral line blocking/blanketing
- (sub-) Surface convection
- Geometry and dimensionality
- Velocity fields and outflows



Spectral line blocking/blanketing

- Effects of numerous -- literally millions -- of (primarily metal) spectral lines upon the atmospheric structure and flux distribution
- **Q: Why is this tricky business?**

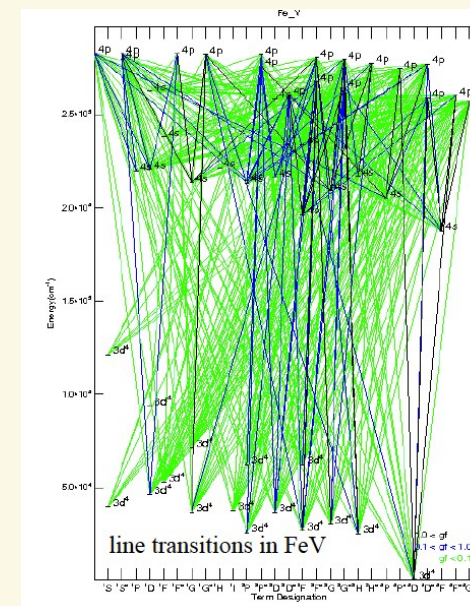


Spectral line blocking/blanketing

- Effects of numerous -- literally millions -- of (primarily metal) spectral lines upon the atmospheric structure and flux distribution
- **Q: Why is this tricky business?**
 - Lots of atomic data required (thus atomic physics and/or experiments)
 - LTE or NLTE?
 - What lines are relevant?
(i.e., what ionization stages? Are there molecules present?)

Techniques:

- Opacity Distribution Functions
- Opacity-Sampling
- Direct line by line calculations





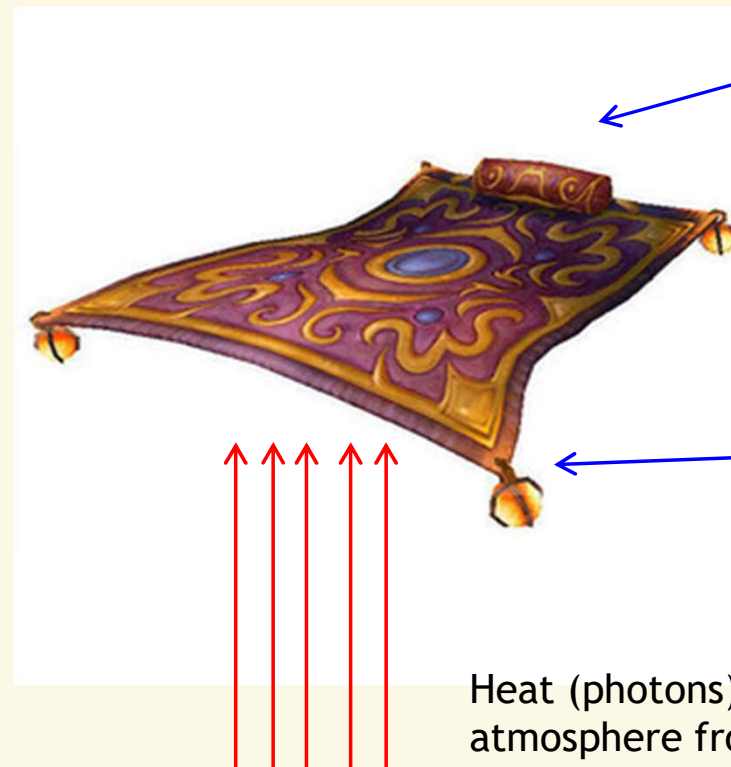
Spectral line blocking/blanketing

Back-warming (and surface-cooling)

Numerous absorption lines
“block” (E)UV radiation
flux

Total flux conservation
demands these photons be
emitted elsewhere →
redistributed to
optical/infra-red

Lines act as “blanket”,
whereby back-scattered
line photons are (partly)
thermalized and thus heat
up deeper layers



“Blanket” typically cools
uppermost layers

“Blanket” warms deep
layers

Heat (photons) enters
atmosphere from
sub-photospheric layers



Spectral line blocking/blanketing

Back-warming and flux redistribution

...occur in stars of all spectral types

$$\Delta T = T_{\text{no lines}} - T_{\text{with lines}}$$

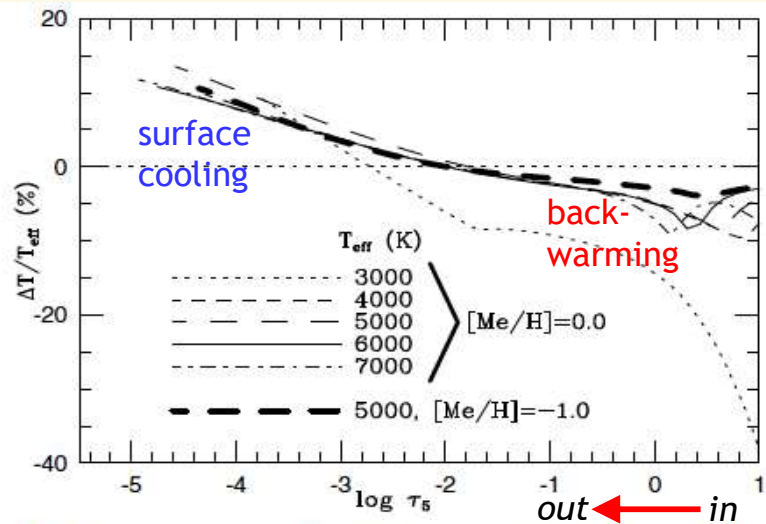


Fig. 4. The effects of switching off line absorption on the temperature structure of a sequence of models with $\log g = 3.0$ and solar metallicity. Note that $\Delta T \equiv T(\text{no lines}) - T(\text{lines})$. It is seen that the blanketing effects are fairly independent of effective temperature for models with $T_{\text{eff}} \geq 4000$.

Back warming in cool stars
(from Gustafsson et al. 2008)

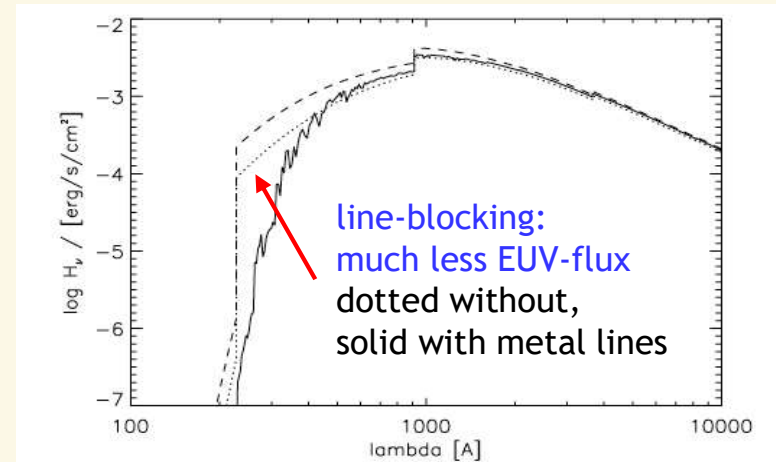


Fig.10. Emergent Eddington flux H_ν as function of wavelength. Solid line: Current model of HD 15629 (O5V((f)) with parameters from Table 1 ($T_{\text{eff}} = 40\,500$ K, $\log g = 3.7$, "model 1"). Dotted: Pure H/He model without line-blocking/blanketing and negligible wind, at same T_{eff} and $\log g$ ("model 2"). Dashed: Pure H/He model, but with $T_{\text{eff}} = 45\,000$ K and $\log g = 3.9$ ("model 3").

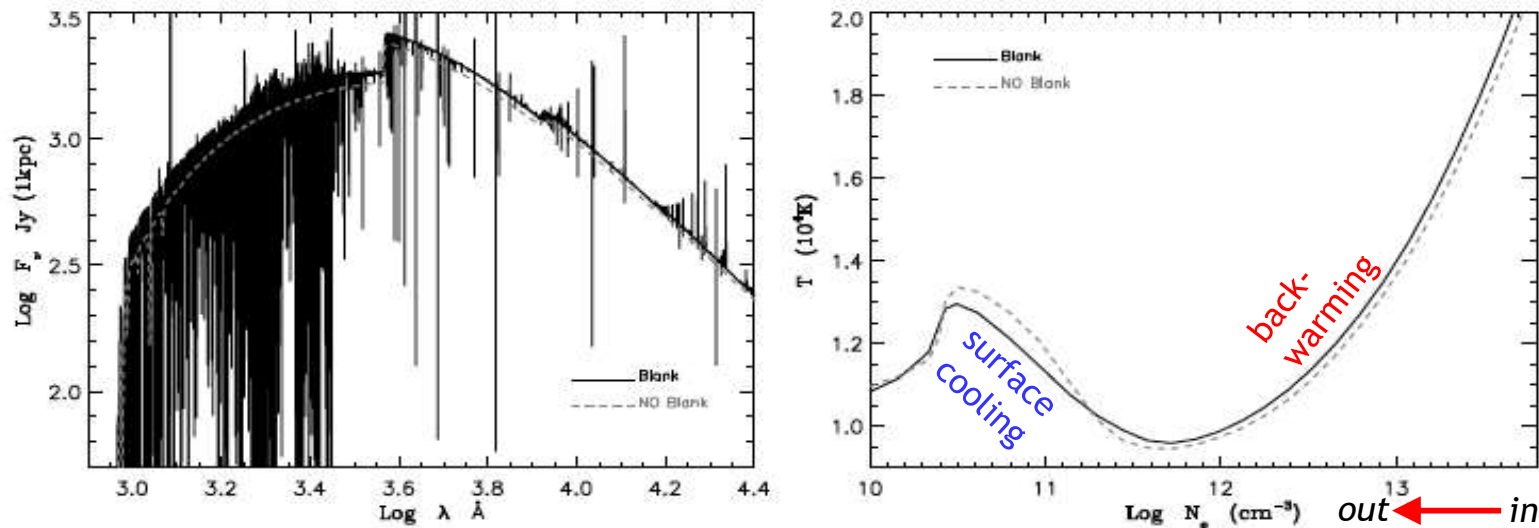
UV to optical flux redistribution in hot stars
(from Repolust, Puls & Hererro 2004)



Spectral line blocking/blanketing

Back-warming and flux redistribution

...occur in stars of all spectral types



From Puls et al. 2008

Fig. 9 Effects of line blanketing (solid) vs. unblanketed models (dashed) on the flux distribution ($\log F_\nu$ (Jansky) vs. $\log \lambda$ (Å), left panel) and temperature structure (T (10^4 K) vs. $\log n_e$, right panel) in the atmosphere of a late B-hypergiant. Blanketing blocks flux in the UV, redistributes it towards longer wavelengths and causes back-warming.



Spectral line blocking/blanketing

in line/continuum forming regions, blanketed models at a certain T_{eff} have a plasma temperature corresponding to an unblanketed model with higher T'_{eff}

Back-warming – effect on effective temperature

RECALL: T_{eff} -- or total flux (plane-parallel) -- fundamental input parameter in model atmosphere!

$$F = \sigma_B T_{\text{eff}}^4$$

T_{eff} in cool stars derived, e.g., by optical photometry

From Gustafsson et al. 2008: Estimate effect by assuming a blanketed model with T_{eff} such that the deeper layers correspond to an unblanketed model with effective temperature $T'_{\text{eff}} > T_{\text{eff}}$

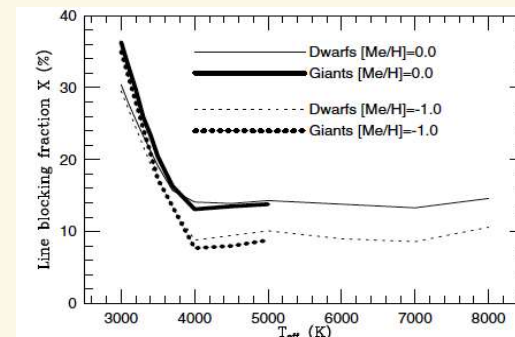


Fig. 3. The blocking fraction X in percent for models in the grid with two different metallicities. The dwarf models all have $\log g = 4.5$ while the giant models have $\log g$ values increasing with temperature, from $\log g = 0.0$ at $T_{\text{eff}} = 3000$ K to $\log g = 3.0$ at $T_{\text{eff}} = 5000$ K.

Question: Why does the line blocking fraction increase for very cool stars?

$$T'_{\text{eff}} = (1 - X)^{-\frac{1}{4}} \cdot T_{\text{eff}}, \quad (35)$$

where X is the fraction of the integrated continuous flux blocked out by spectral lines,

$$X = \frac{\int_0^{\infty} (F_{\text{cont}} - F_{\lambda}) d\lambda}{\int_0^{\infty} F_{\text{cont}} d\lambda}. \quad (36)$$



Spectral line blocking/blanketing

Back-warming – effect on effective temperature

RECALL: T_{eff} -- or total flux (plane-parallel) -- fundamental input parameter in model atmosphere!

Previous slide were LTE models. In hot stars, everything has to be done in NLTE...

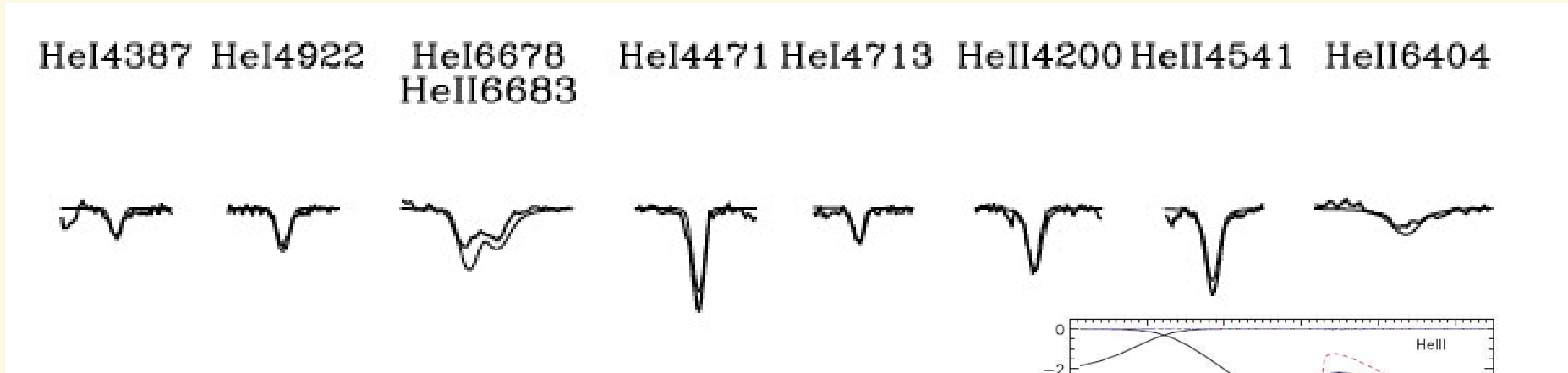
$$F = \sigma_{\text{B}} T_{\text{eff}}^4$$

Question: Why is optical photometry generally NOT well suited to derive T_{eff} in hot stars?



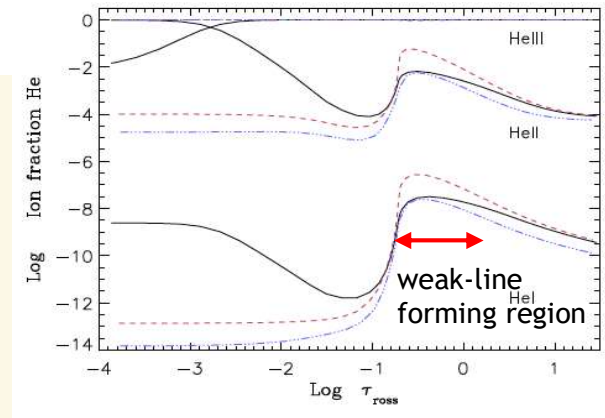
Spectral line blocking/blanketing

Instead, He ionization-balance is typically used
(or N for the very hottest stars, or, e.g., Si for B-stars)



Simultaneous fits to observed HeI and HeII lines
-- from Repolust, Puls, Hererro (2004)

- Back-warming shifts ionization balance toward more completely ionized Helium in blanketed models
→ thus fitting the same observed spectrum requires **lower T_{eff}** than in unblanketed models



- black - blanketed $T_{\text{eff}}=45$ kK
- red - unblanketed $T_{\text{eff}}=45$ kK
- blue - unblanketed $T_{\text{eff}}=50$ kK

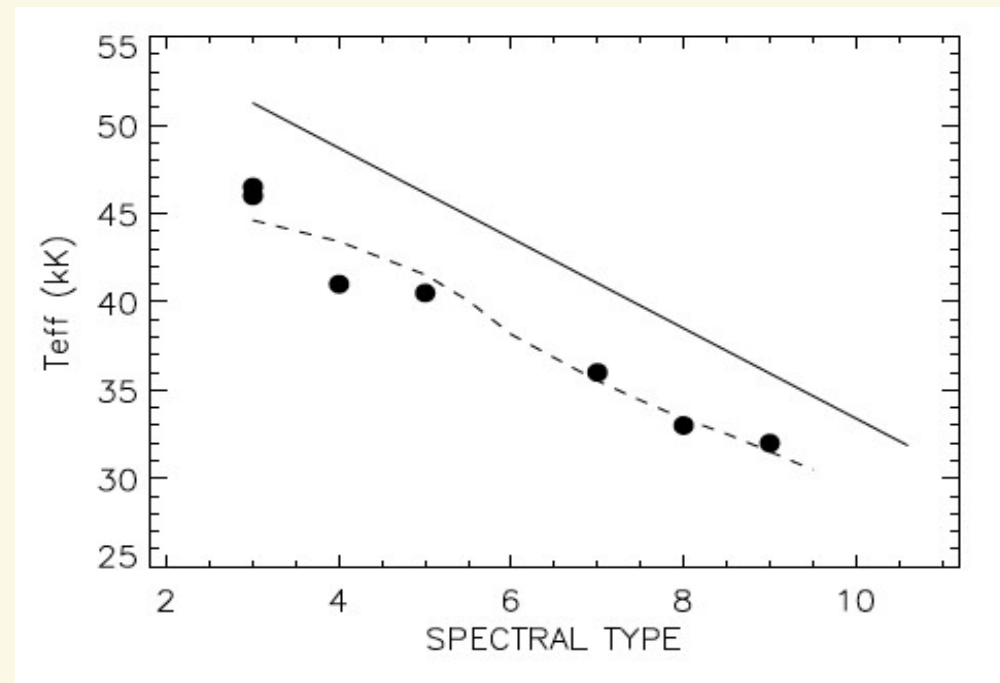
black and blue have similar (low) HeI/II ionization fractions in weak-line forming region, thus similar line profiles



Spectral line blocking/blanketing

Instead, He ionization-balance is typically used
(or N for the very hottest stars, or, e.g., Si for B-stars)

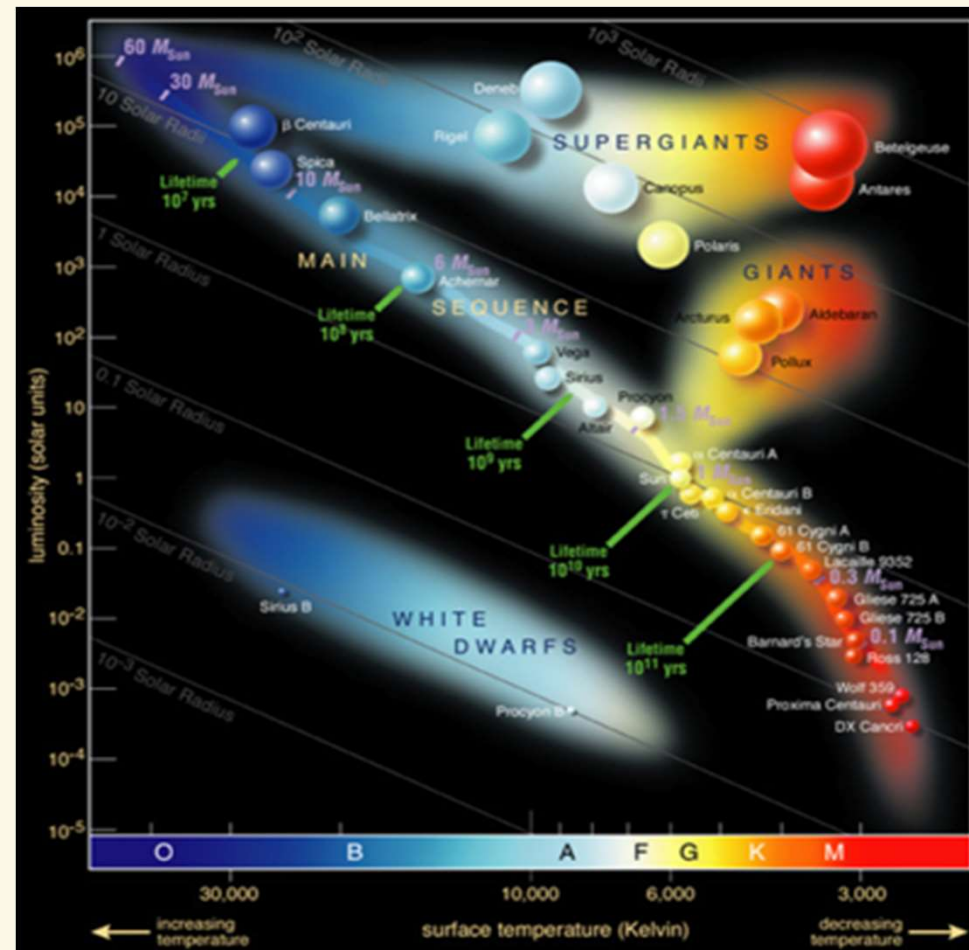
Result: In hot O-stars with $T_{\text{eff}} \sim 40,000$ K, back-warming can lower the derived T_{eff} as compared to unblanketed models by several thousand degrees!
(~ 10 %)



New T_{eff} scale for O-dwarf stars. Solid line - unblanketed models. Dashed - blanketed calibration, dots - observed blanketed values (from Puls et al. 2008)



A tour de modeling and analysis of stellar atmospheres throughout the HRD



- LTE or NLTE
- Spectral line blocking/blanketing
- (sub-) Surface convection
- Geometry and dimensionality
- Velocity fields and outflows



Surface Convection

from Chap. 6

Convection

energy transport not only by radiation,
however also by

- waves
 - heat conduction
 - convection
- } not efficient in typical stellar atmospheres, but ... coronae, chromospheres, white dwarfs

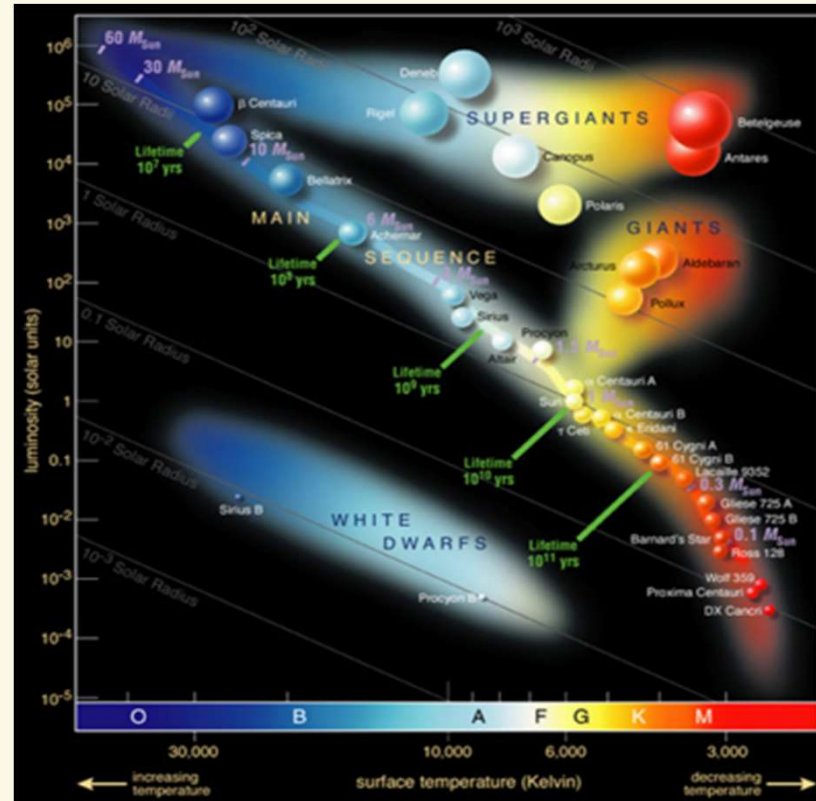
Thus

$$\nabla \cdot (\underline{F}^{\text{rad}} + \underline{F}^{\text{conv}}) \stackrel{\text{total flux = const}}{\downarrow} = 0 \quad (\text{in quasi-hydrostatic atmospheres})$$

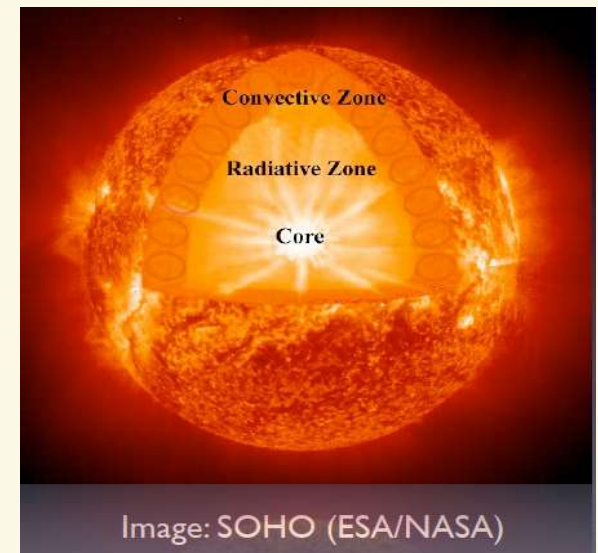


Surface Convection

OBSERVATIONS:
 “Sub-surface”
 convection in layers
 $T \sim 160,000$ K (due to
 iron-opacity peak)
 currently discussed
 also in hot stars



- H/He recombines in atmospheres of cool stars
- Provides MUCH opacity
- Convective Energy transport





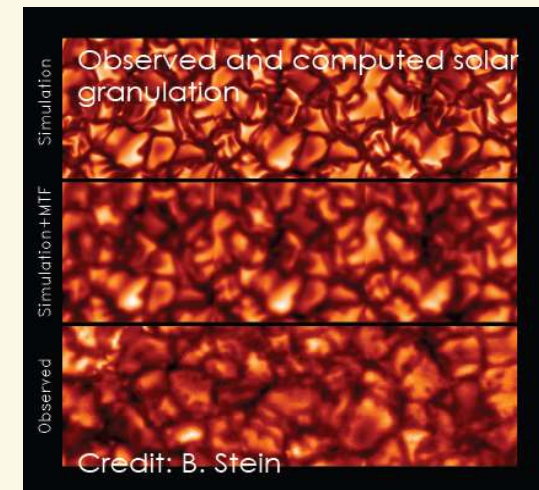
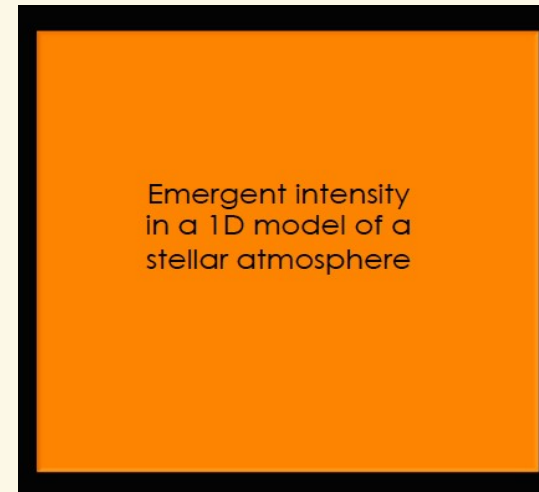
Surface Convection

Traditionally accounted for by rudimentary “mixing-length theory” (see Chap. 6) in 1-D atmosphere codes

BUT:

- Solar observations show very dynamic structure
- Granulation and lateral inhomogeneity

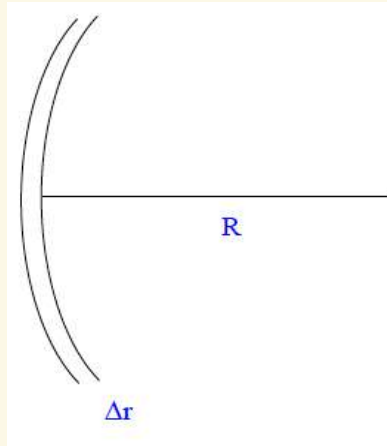
→ Need for full 3-D radiation-hydrodynamics simulations in which convective motions occur spontaneously if required conditions fulfilled (all physics of convection ‘naturally’ included)





Surface Convection

Solar-type stars:
Photospheric extent \ll stellar radius
Small granulation patterns



example: the sun

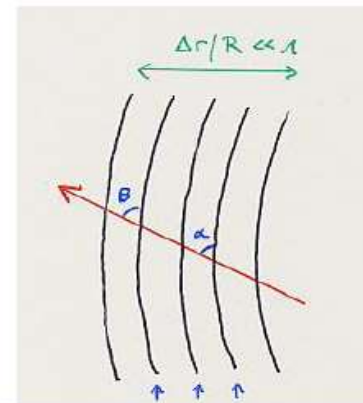
$R_{\text{sun}} \approx 700,000 \text{ km}$
 $\Delta r (\text{photo}) \approx 300 \text{ km}$

$\Rightarrow \Delta r / R \approx 4 \cdot 10^{-4}$

BUT corona
 $\Delta r / R (\text{corona}) \approx 3$

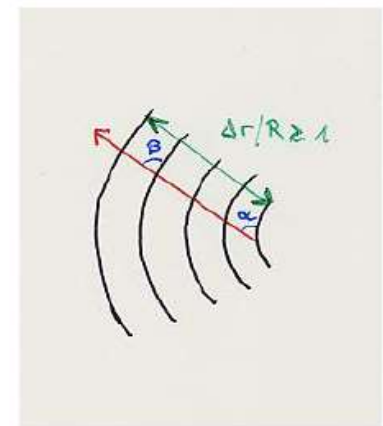
as long as $\Delta r / R \ll 1 \Rightarrow$ plane-parallel symmetry

light ray through atmosphere



lines of constant temperature and density (isocontours)

curvature of atmosphere insignificant for photons' path: $\alpha = \beta$



significant curvature: $\alpha \neq \beta$, spherical symmetry

examples

solar photosphere / cromosphere
atmospheres of
main sequence stars
white dwarfs
giants (partly)

solar corona
atmospheres of
supergiants
expanding envelopes (stellar winds)
of OBA stars, M-giants and supergiants

from Chap. 3

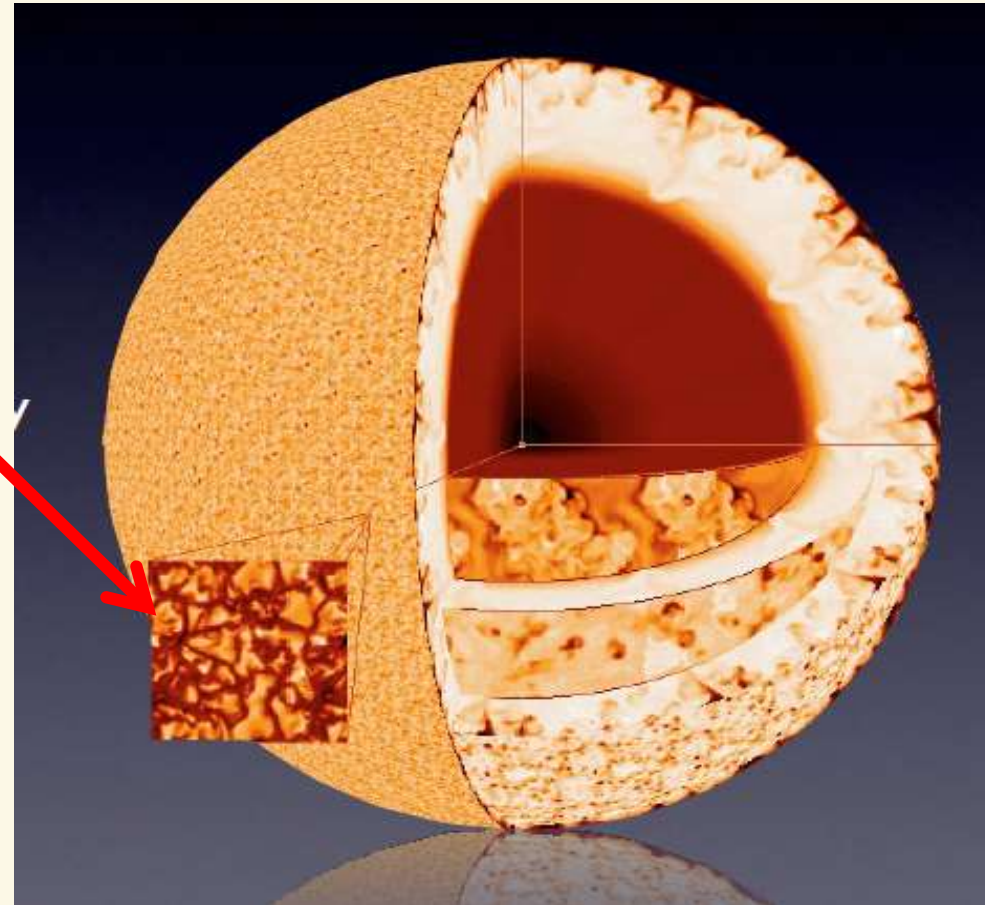


Surface Convection

Solar-type stars:
Atmospheric extent \ll stellar radius
Small granulation patterns

→
**Box-in-a-star
Simulations**

(cmp. plane-parallel approximation)



From Wolfgang Hayek

Surface Convection

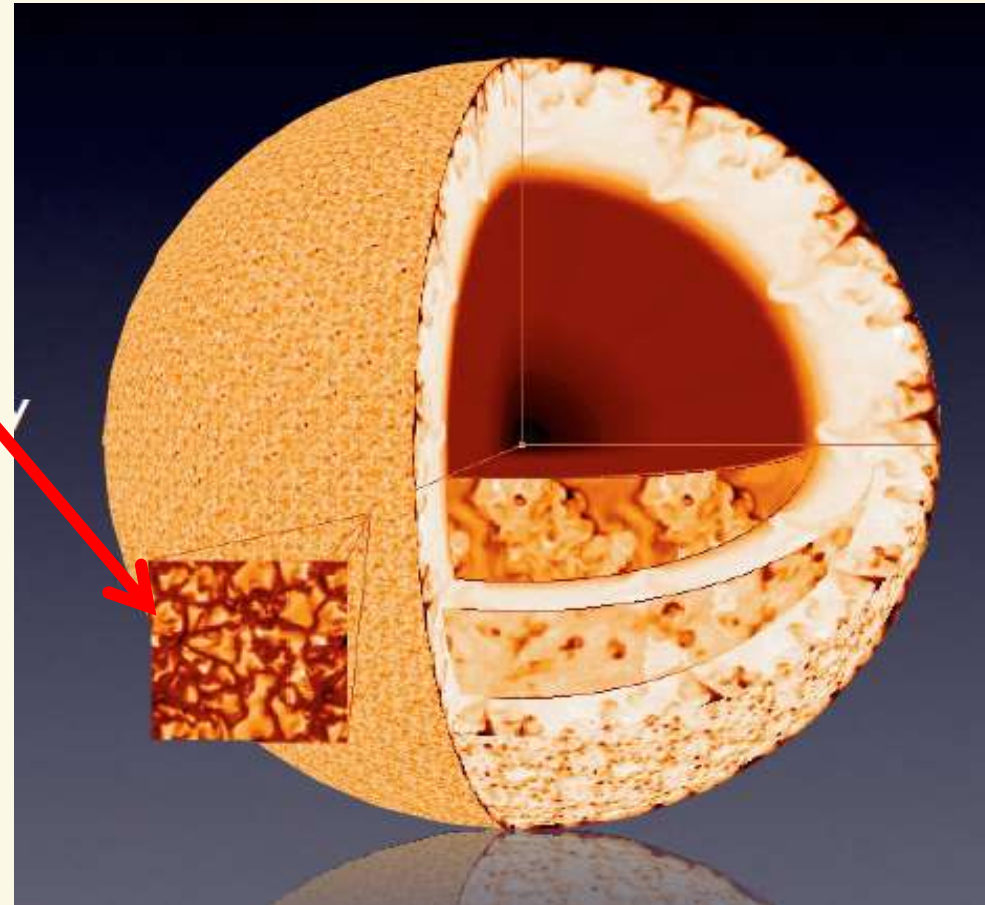
Approach
(teams by Nordlund, Steffen):

Solve radiation-hydrodynamical conservation equations of mass, momentum, and energy (closed by equation of state).

3-D radiative transfer included to calculate net radiative heating/cooling q_{rad} in energy equation, typically assuming LTE and a very simplified treatment of line-blanketing

$$q_{\text{rad}} = 4\pi\rho \int_{\lambda} \kappa_{\lambda} (J_{\lambda} - S_{\lambda}) d\lambda,$$

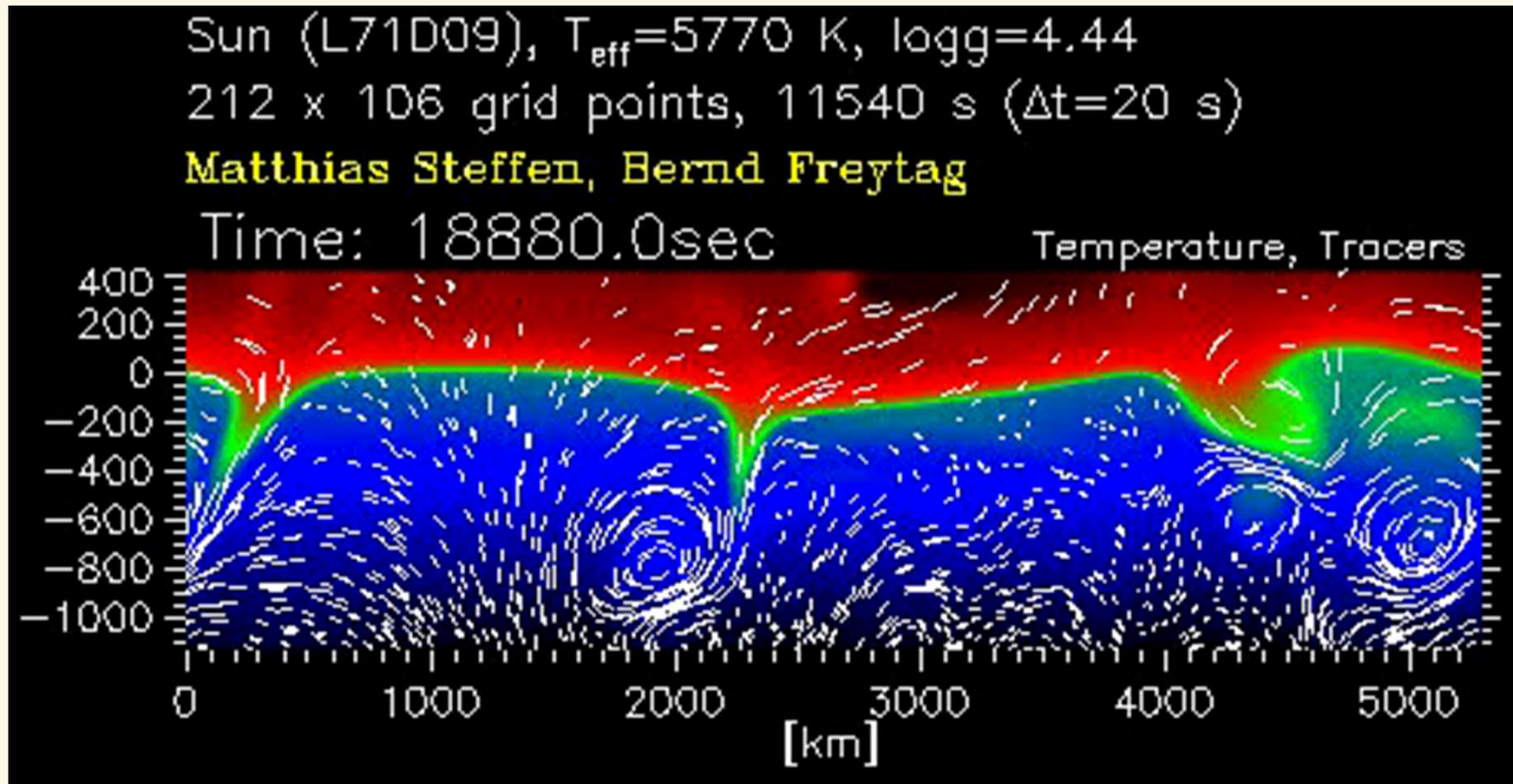
(= 0 in case of radiative equilibrium)



From Wolfgang Hayek



Surface Convection



From Berndt Freytag's homepage:

<http://www.astro.uu.se/~bf/>

Stellar Atmospheres in practice

Surface Convection

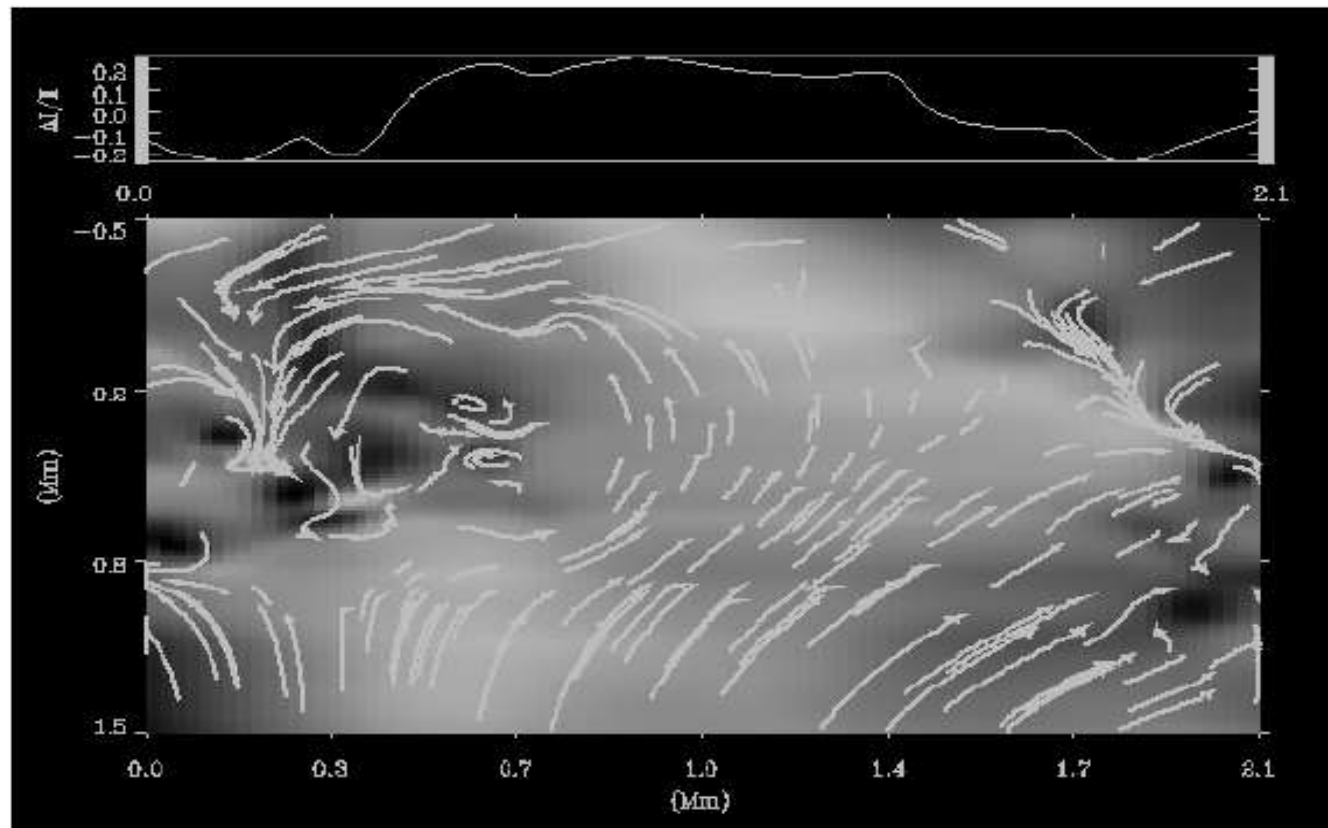


FIG. 4.—Pressure fluctuations about the mean hydrostatic equilibrium and the velocity field in an xz slice through a granule. The pressure is high above the centers of granules, which decelerates the warm upflowing fluid and diverts it horizontally. High pressure also occurs in the intergranular lanes where the horizontal motions are halted and gravity pulls the now cool, dense fluid down into the intergranular lanes. Horizontal rolls of high vorticity occur at the edges of the intergranular lanes. The emergent intensity profile across the slice is shown at the top.

From Stein & Nordlund (1998)



Surface Convection

Some key features:

Slow, broad upward motions, and
faster, thinner downward
motions

Non-thermal velocity fields

Overshooting from zone where
convection is efficient
according to stability criteria
(see Chap. 6)

Energy balance in upper layers not
only controlled by radiative
heating/cooling, but also by
cooling from adiabatic
expansion

See Stein & Nordlund (1998);
Collet et al. (2006), etc.

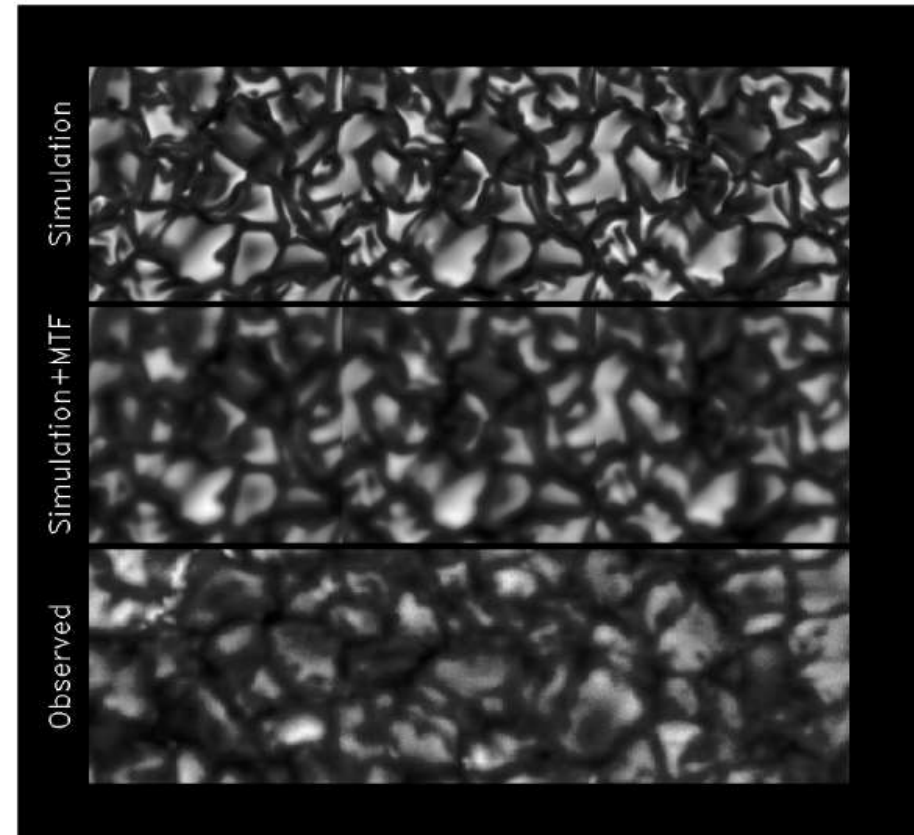


FIG. 19.—Comparison of granulation as seen in the emergent intensity from the simulations and as observed by the Swedish Vacuum Solar Telescope on La Palma. The top row shows three simulation images at 1 minute intervals, which together make a composite image 18×6 Mm in extent. The middle row shows this image smoothed by an Airy plus exponential point-spread function. The bottom row shows an 18×6 Mm white-light image from La Palma. Note the similar appearance of the smoothed simulation image and the observed granulation. The common edge brightening in the simulation is reduced when smoothed. Images by (Title 1996, private communication) taken in the CH G-band have much more contrast than white light and clearly reveal the edge brightening of granules.

Question: This does not look much like the traditional 1-D models we've discussed during the previous lecture! - Do you think we should throw them in the garbage?

Surface Convection

blue: mean temperature from 3D hydro-model (scatter = dashed)

red: from 1D semi-empirical model (Holweger & Müller, see Chap. 5)

green: from 1D theoretical model atmospheres (MARCS)

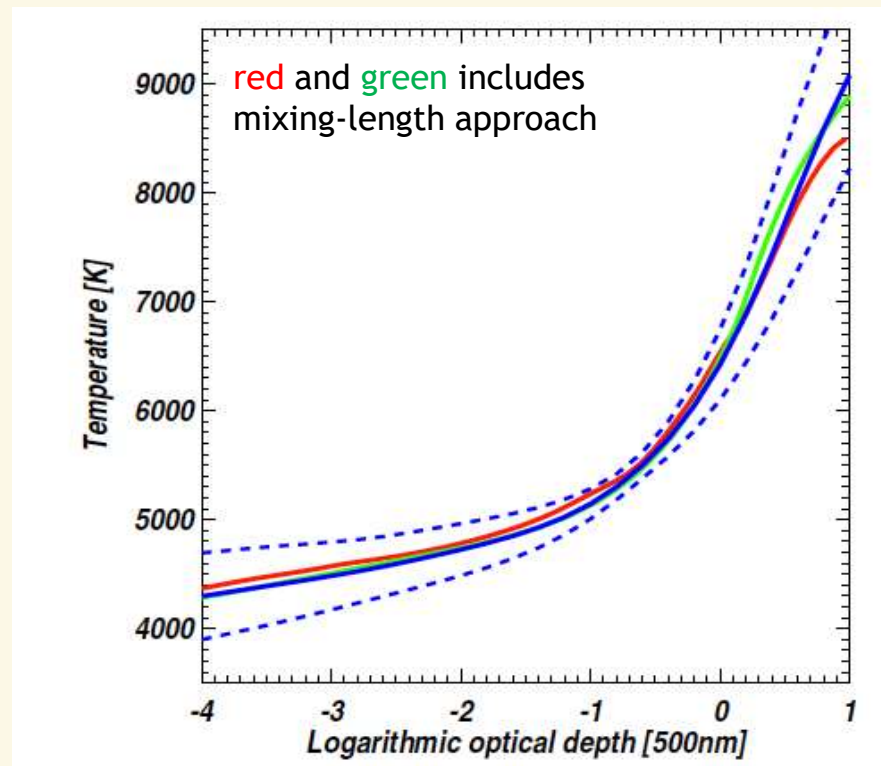


Figure 1: The mean temperature structure of the 3D hydrodynamical model of Trampedach et al. (2009) is shown as a function of optical depth at 500 nm (blue solid line). The blue dashed lines correspond to the spatial and temporal rms variations of the 3D model, while the red and green curves denote the 1D semi-empirical Holweger & Müller (1974) and the 1D theoretical MARCS (Gustafsson et al. 2008) model atmospheres, respectively.

In many (though not all) cases, AVERAGE properties still quite OK:

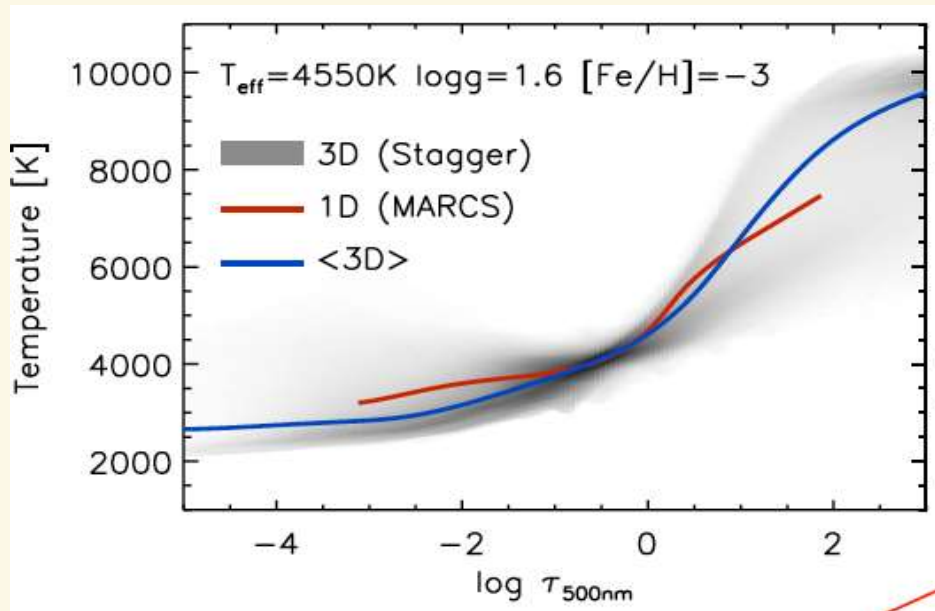
Convection in energy balance approximated by “mixing-length theory”
Non-thermal velocity fields due to convective motions included by means of so-called “micro-” and “macro-turbulence”

BUT quantitatively we always need to ask:
To what extent can average properties be modeled by traditional 1-D codes?

Unfortunately, a general answer very difficult to give, need to be considered case by case



Surface Convection



Metal-poor red giant, simulation by Remo Collet, figure from talk by M. Bergemann

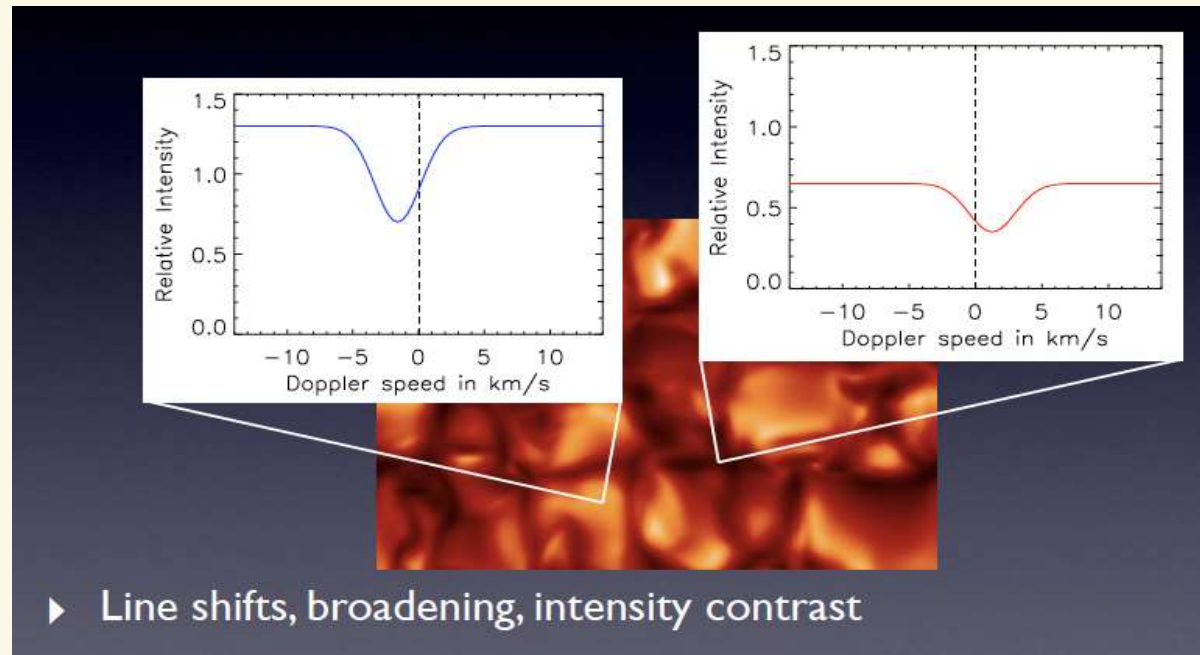
For example:

In metal-poor cool stars spectral lines are scarce (Question: Why?), and energy balance in upper photosphere controlled to a higher degree by adiabatic expansion of convectively overshoot material.

In classical 1-D models though, these layers are convectively stable, and energy balance controlled only by radiation (radiative equilibrium, see Chap. 4).



Surface Convection



From talk by Hayek

3-D radiation-hydro models successful in reproducing many solar features (see overview in Asplund et al. 2009), e.g:

Center-to-limb intensity variation

Line profiles and their shifts and variations (without micro/macroturbulence)

Observed granulation patterns

Surface Convection

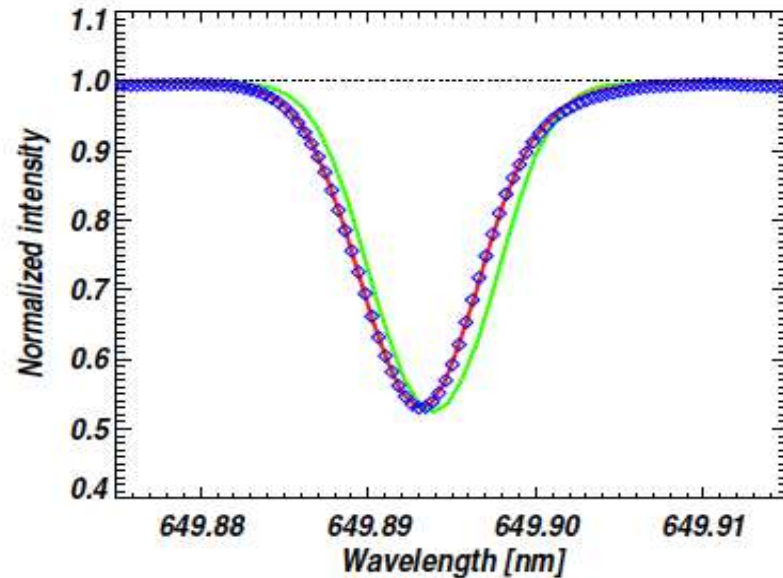


Figure 3: The predicted spectral line profile of a typical Fe I line from the 3D hydrodynamical solar model (red solid line) compared with the observations (blue rhombs). The agreement is clearly very satisfactory, which is the result of the Doppler shifts arising from the self-consistently computed convective motions that broaden, shift and skew the theoretical profile. For comparison purposes also the predicted profile from a 1D model atmosphere (here Holweger & Müller 1974) is shown; the 1D profile has been computed with a microturbulence of 1 km s^{-1} and a tuned macroturbulence to obtain the right overall linewidth. Note that even with these two free parameters the 1D profile can neither predict the shift nor the asymmetry of the line.

affects chemical abundance
(determined by means of line profile fitting to observations)

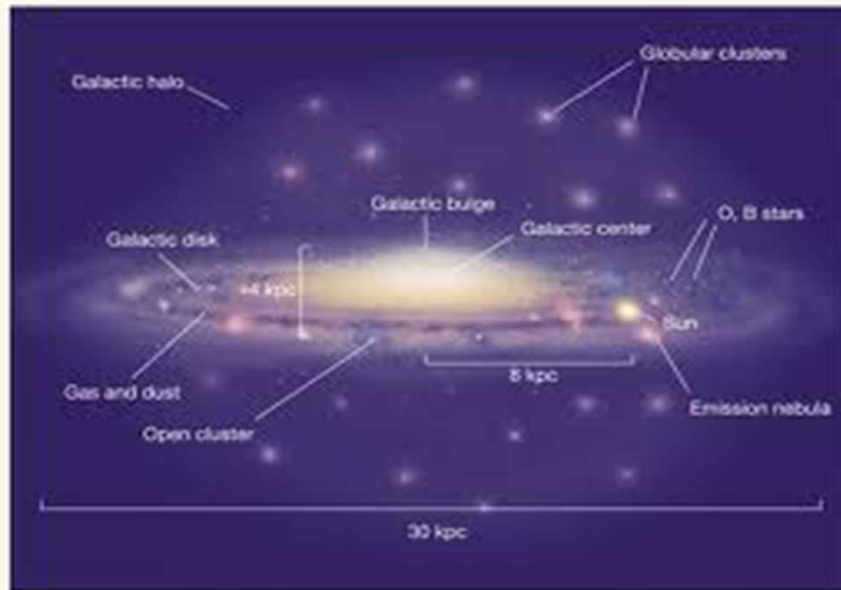
One MAJOR result:
Effects on line formation has led to a downward revision of the CNO solar abundances and the solar metallicity, and thus to a revision of the *standard cosmic chemical abundance scale*

Fig. from Asplund et al. (2009) - "The Chemical Composition of the Sun"



Surface Convection

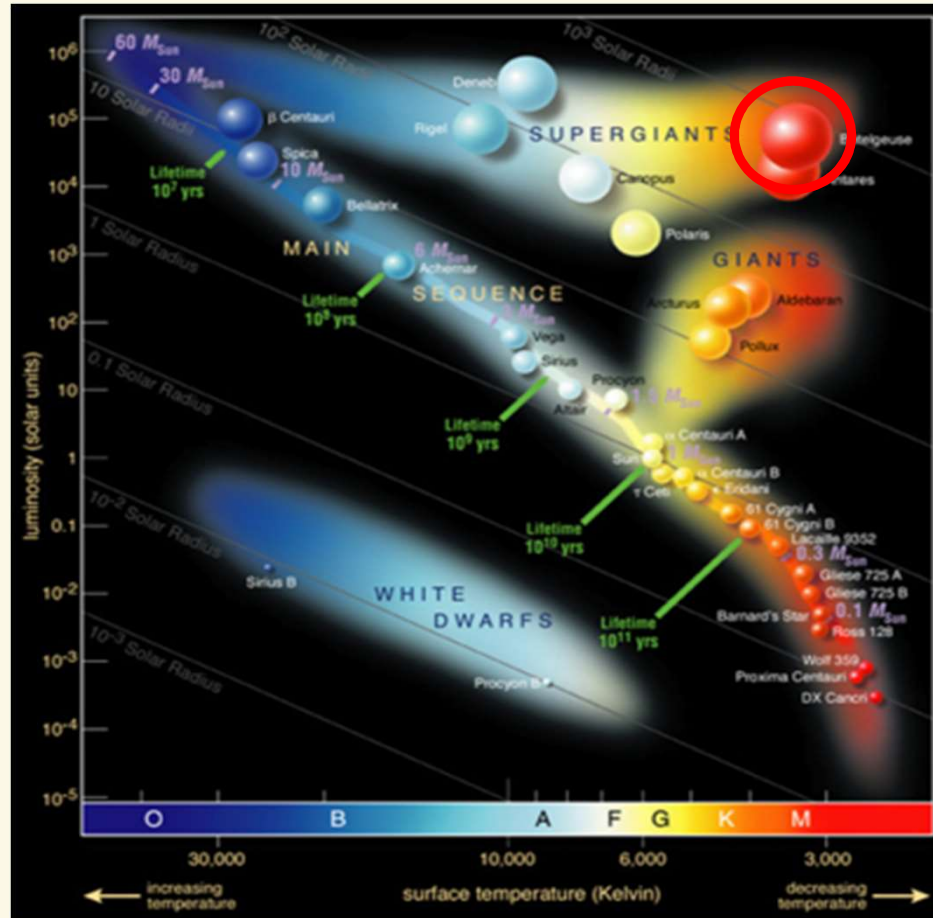
Also potentially critical for **Galactic archeology**...



...which traces the chemical evolution of the Universe by analyzing VERY old, metal-poor Globular Cluster stars -- relics from the early epochs (e.g., A. Frebel and collaborators)



Surface Convection



- giant convection cells in the low-gravity, extended atmospheres of Red Supergiants
- **Question: Why extended?**

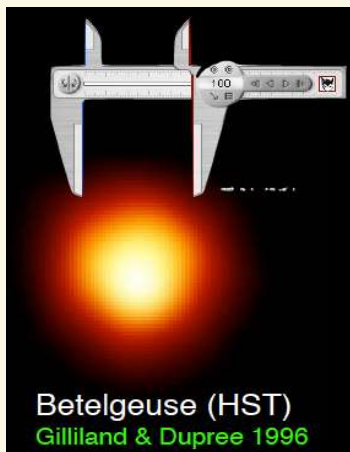
$$H = a^2 / g \quad (\text{with } a = v_s \text{ the isothermal speed of sound})$$

$$a^2_{\text{RSG}} / a^2_{\text{sun}} \approx T_{\text{RSG}} / T_{\text{sun}} = 0.5 \dots 0.6$$

$$g_{\text{RSG}} / g_{\text{sun}} \approx 10^{-4} !$$

(see Chap. 6)

Out to Jupiter...



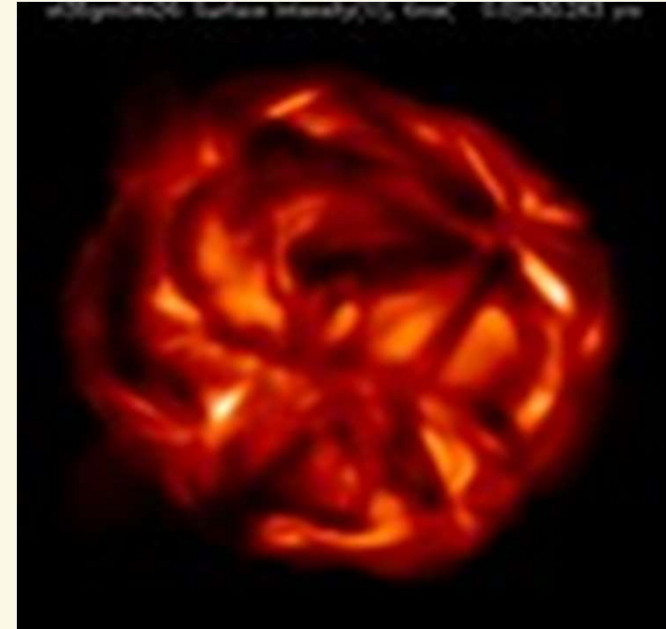


Surface Convection

Supergiants (or models including a stellar wind):
Atmospheric extent > stellar radius:

Box-in-a-star → Star-in-a-box

(1D: Plane-parallel → Spherical symmetry,
see Chap. 3)



Star to model: Betelgeuse

Mass: 5 solar masses

Radius: $600 R_{\text{sun}}$

Luminosity: $41400 L_{\text{sun}}$

Grid: Cartesian cubical grid with 171^3 points

Edge length of box 1674 solar radii

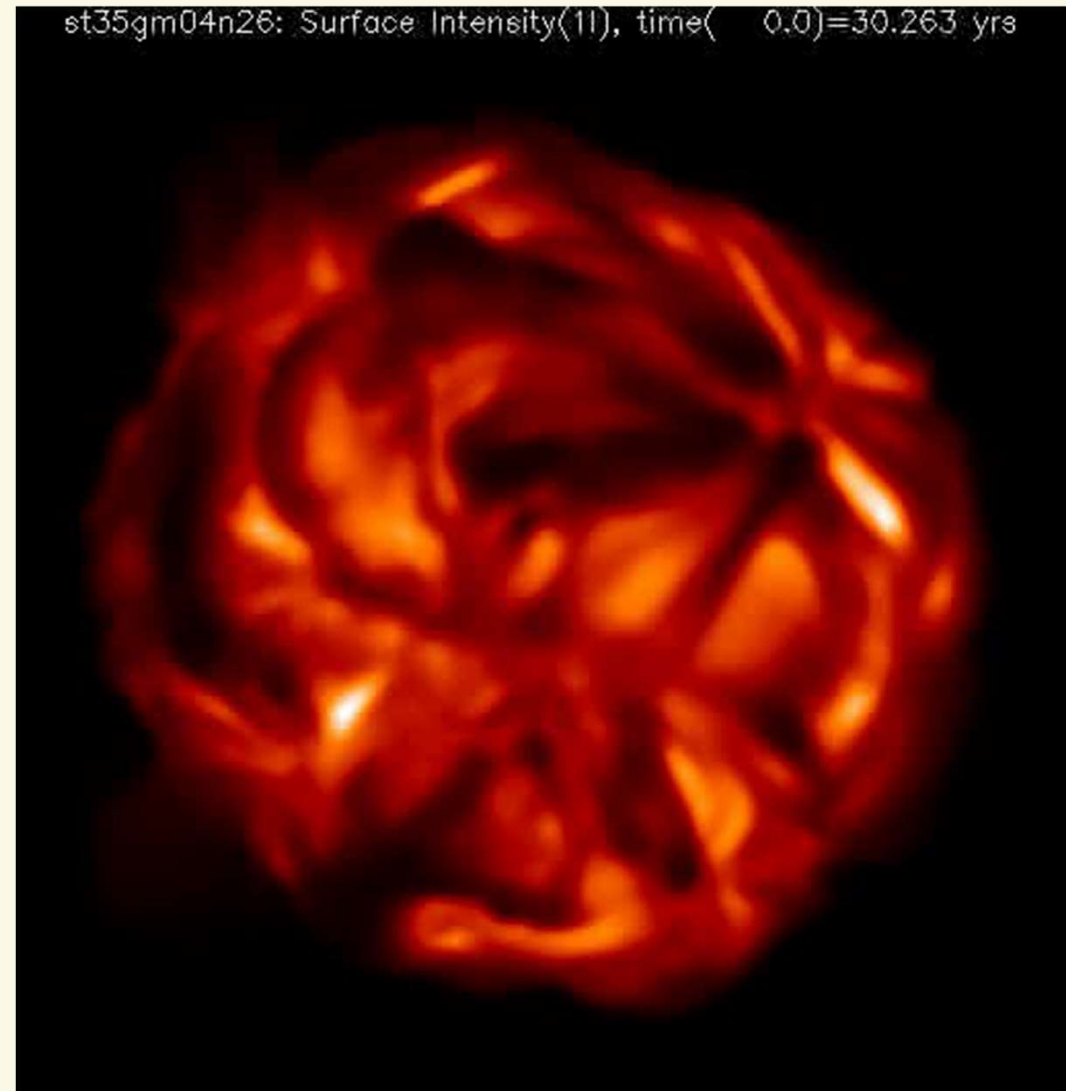
Model by Berndt Freytag, note the **HUGE** convective cells visible in the emergent intensity map!!



Surface Convection

Star to model: Betelgeuse
Mass: 5 solar masses
Radius: $600 R_{\text{sun}}$
Luminosity: $41400 L_{\text{sun}}$
Grid: Cartesian cubical grid with 171^3 points
Edge length of box 1674 solar radii
Movie time span: 7.5 years

[http://www.astro.uu.se/~bf/movie/dst35gm04n26/
movie.html](http://www.astro.uu.se/~bf/movie/dst35gm04n26/movie.html)



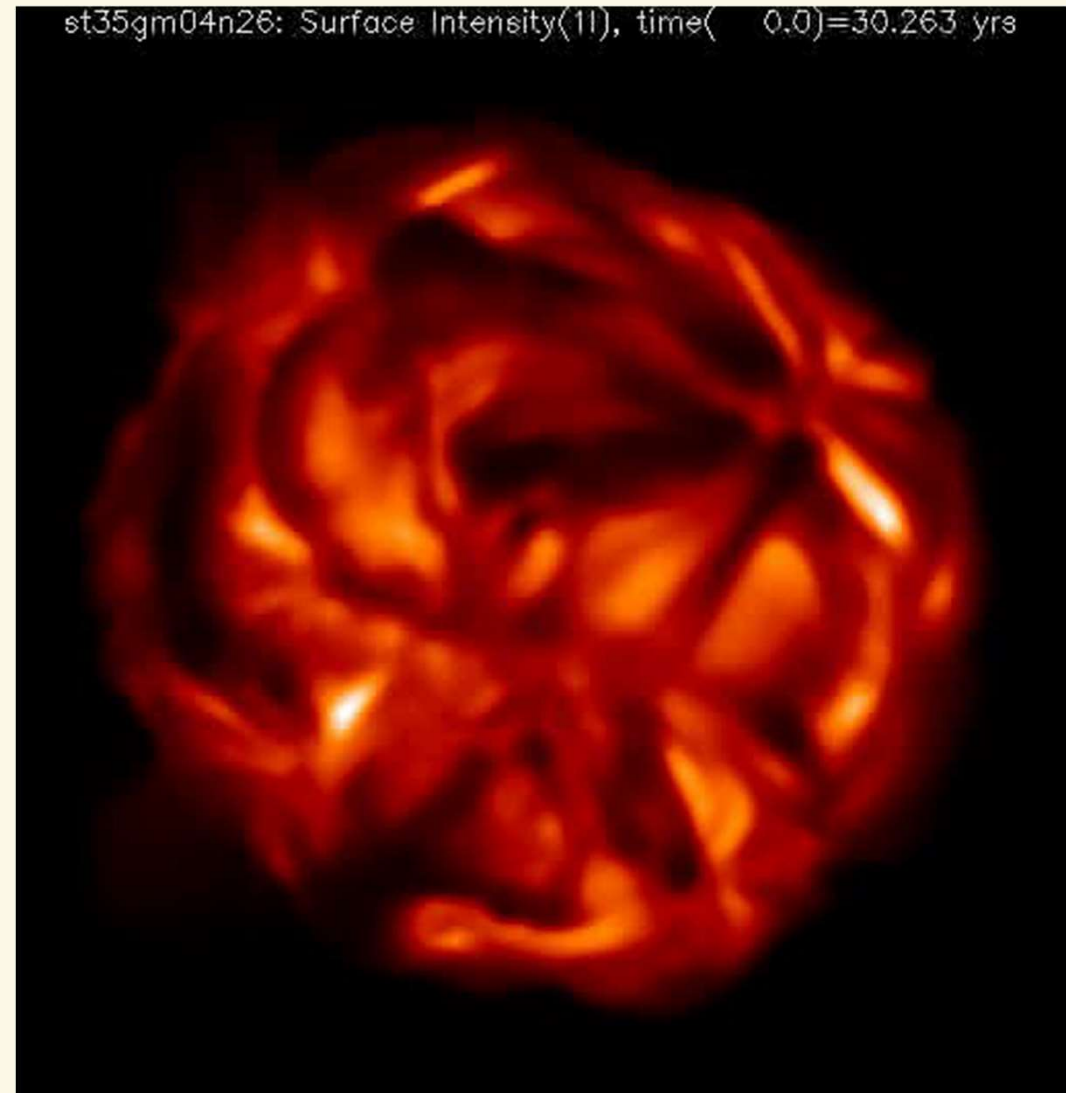


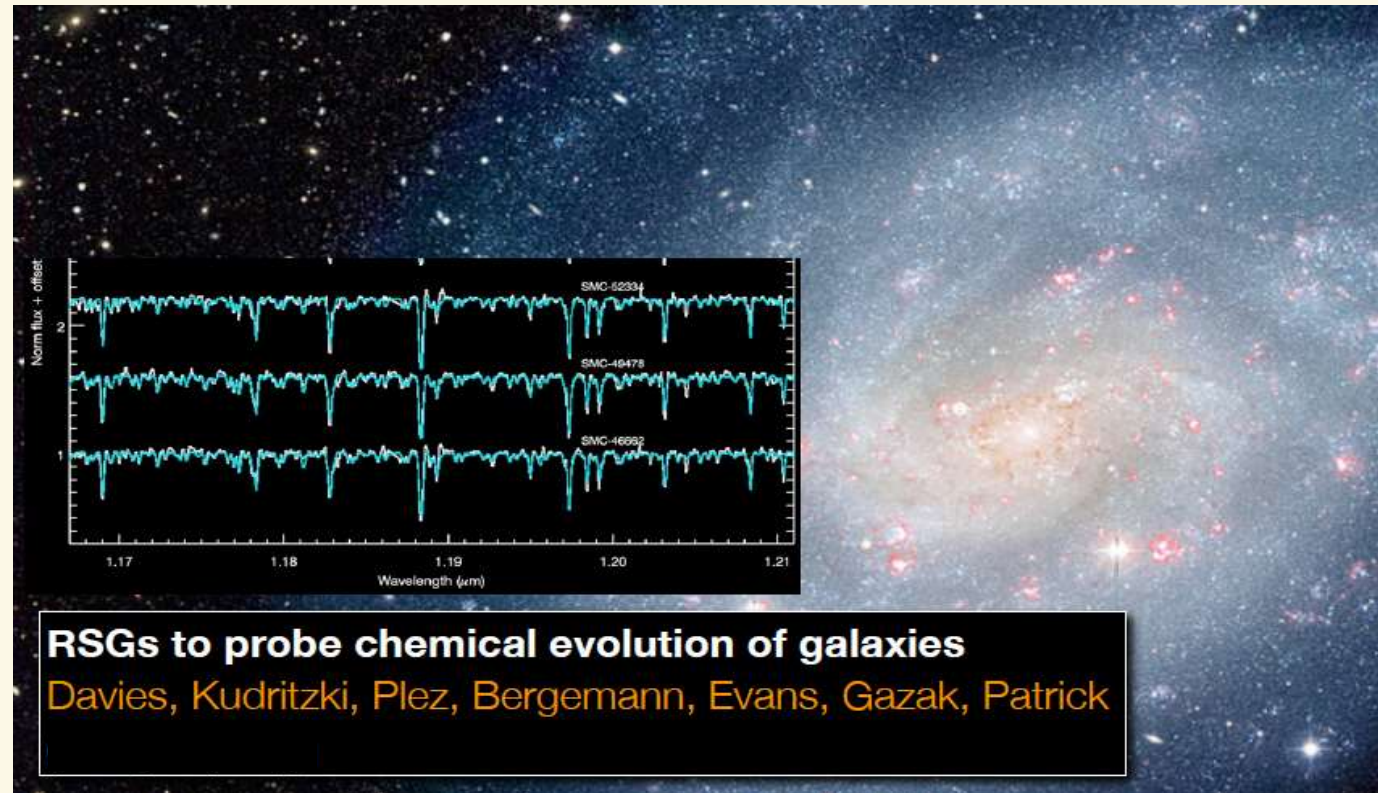
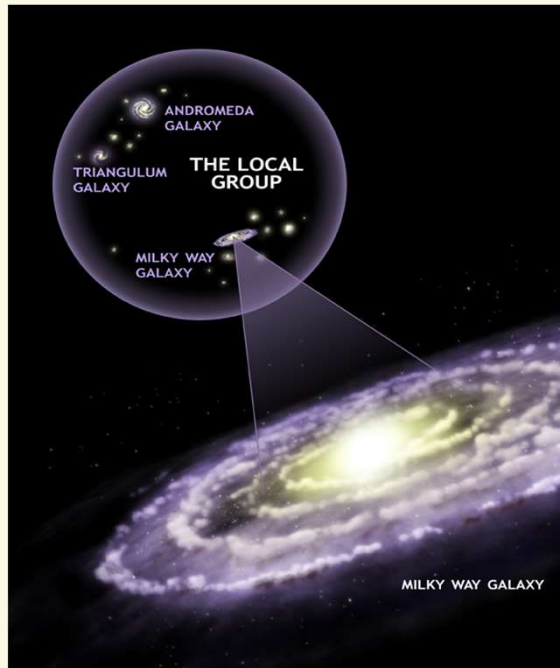
Surface Convection

Extremely challenging,
models still in their infancies.
LOTS of exciting physics to explore, like

- Pulsations
- Convection
- Numerical radiation-hydrodynamics
- Role of magnetic fields
- Stellar wind mechanisms

Also, to what extent can main effects
be captured by 1-D models?
For quantitative applications like....





Question: Why are RSGs ideal for observational extragalactic stellar astrophysics, particularly in the near future?

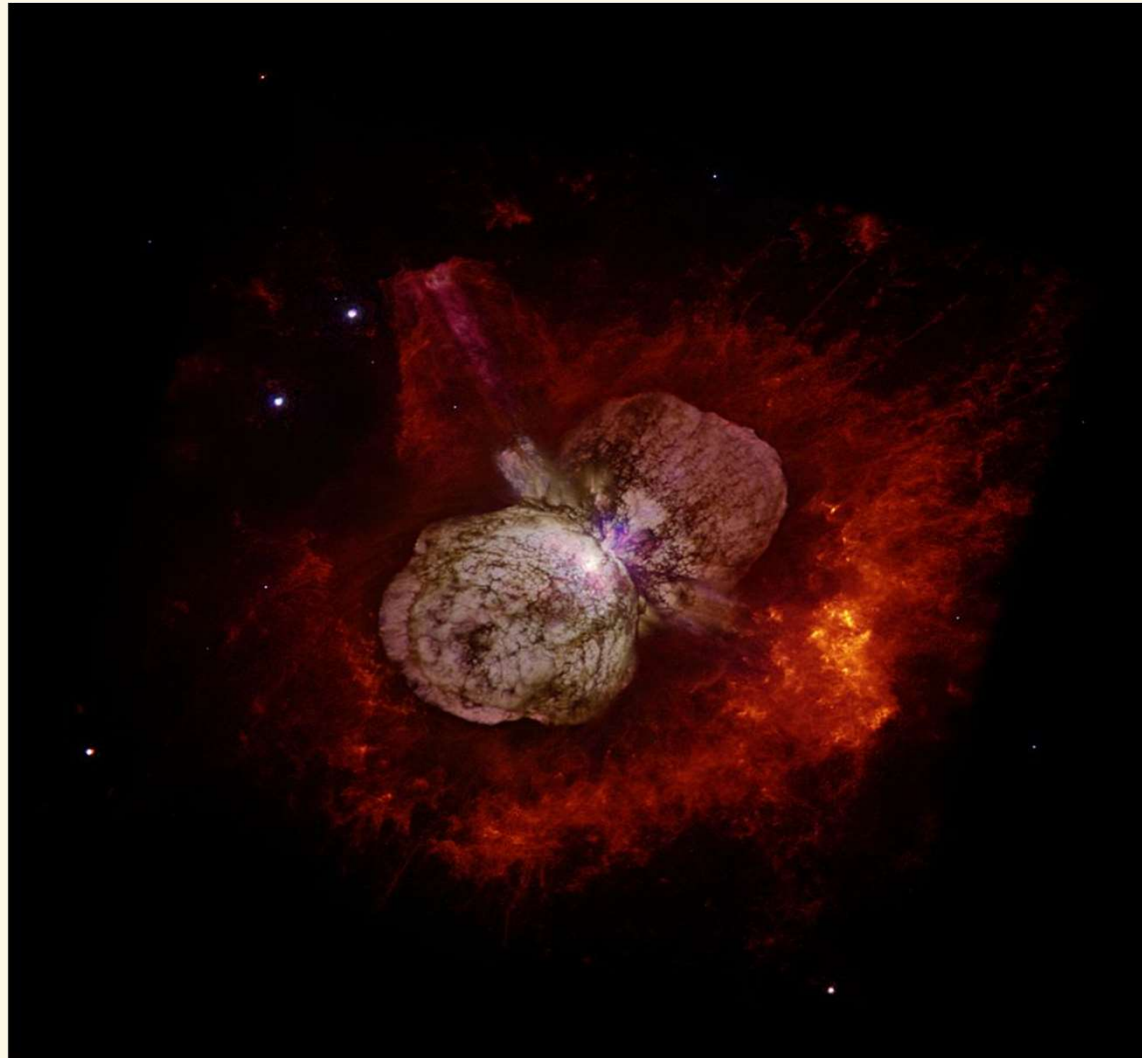


important codes (not complete) and their features

Codes	FASTWIND CMFGEN PoWR	WM-basic	TLUSTY Detail/Surface	Phoenix	MARCS Atlas	CO5BOLD STAGGER
geometry	1-D spherical	1-D spherical	1-D plane-parallel	1-D/3-D spherical/ plane-parallel	1-D plane-parallel (MARCS also spherical)	3-D Cartesian
LTE/NLTE	NLTE	NLTE	NLTE	NLTE/LTE	LTE	LTE simplified
dynamics	quasi-static photosphere + prescribed supersonic outflow	time-independent hydrodynamics	hydrostatic	hydrostatic or allowing for supersonic outflows	hydrostatic	hydrodynamic
stellar wind	yes	yes	no	yes	no	no
major application	hot stars with winds	hot stars with dense winds, ion. fluxes, SNRs	hot stars with negligible winds	cool stars, brown dwarfs, SNRs	cool stars	cool stars
comments	CMFGEN also for SNRs; FASTWIND using approx. line- blocking	line-transfer in Sobolev approx. (see part 2)	Detail/Surface with LTE- blanketing	convection via mixing-length theory	convection via mixing-length theory	very long execution times, but model grids start to emerge



And then there are, e.g.,



- Luminous Blue Variables (LBVs) like Eta Carina,
- Wolf-Rayet Stars (WRs)
- Planetary Nebulae (and their Central Stars)
- Be-stars with disks
- Brown Dwarfs
- Pre main-sequence T-Tauri and Herbig stars

...and many other interesting objects

Stellar astronomy alive and kicking! Very rich in both

Physics

Observational applications



A first application – The D4000 break in early type galaxies



- ▶ spectroscopic study of region around 4000 Å: useful tool to investigate stellar populations in composite stellar systems

$$D_{4000} = \frac{(\lambda_2^- - \lambda_1^-) \int_{\lambda_1^+}^{\lambda_2^+} F_\nu d\lambda}{(\lambda_2^+ - \lambda_1^+) \int_{\lambda_1^-}^{\lambda_2^-} F_\nu d\lambda},$$

where $(\lambda_1^-, \lambda_2^-, \lambda_1^+, \lambda_2^+) = (3750, 3950, 4050, 4250)$ Å.

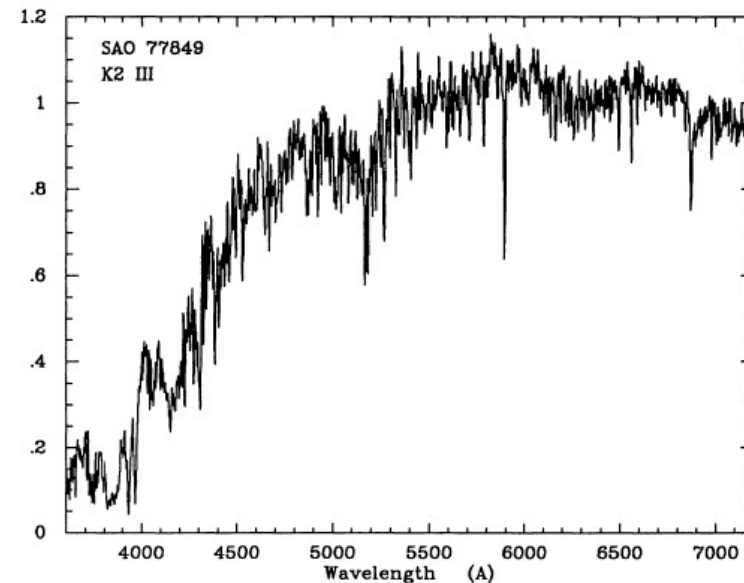
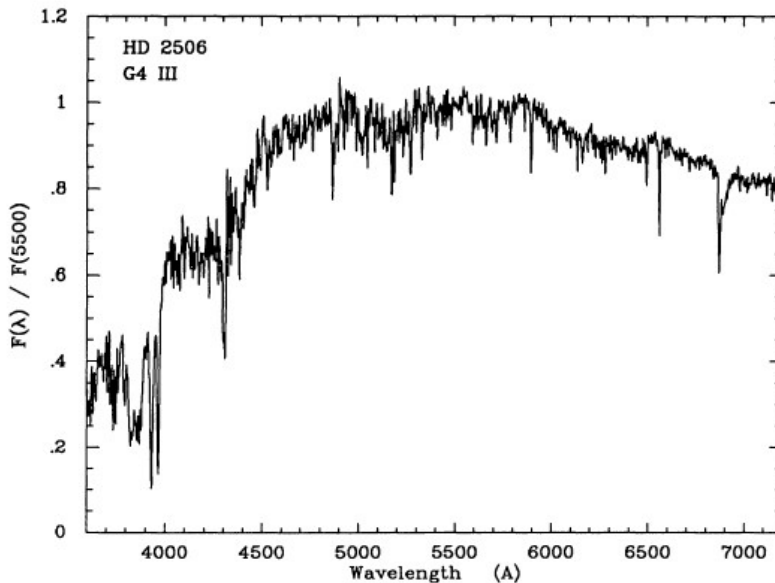
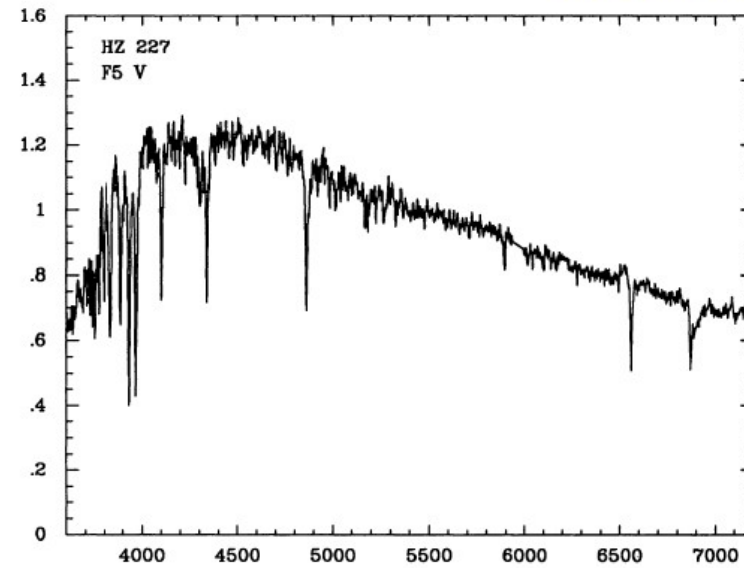
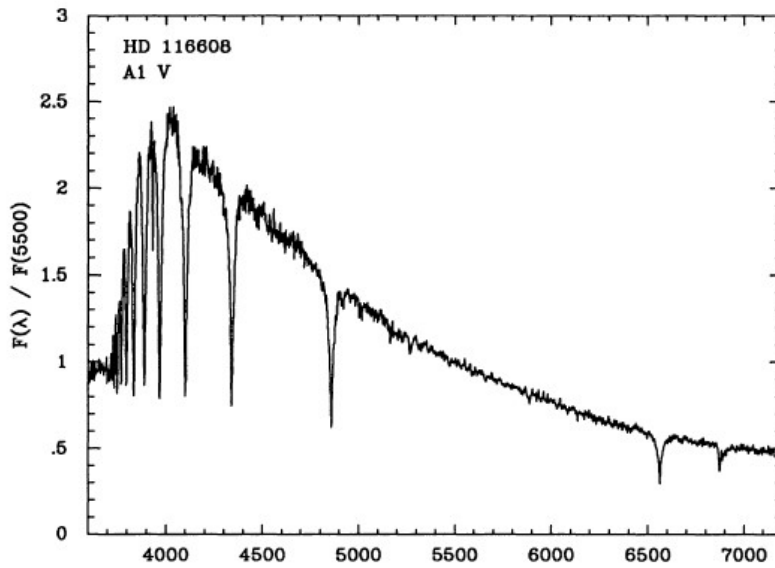
definition by Bruzual (1983)

D4000 pseudo color
(combination of λ and ν ,
not logarithmically defined)

- ▶ star formation history (e.g., easy detection of young populations “contaminating” the break)
- ▶ distinct indicator of stellar population ages (Kauffmann, 2003) and metallicities (Maraston 2005)
- ▶ Balmer decrement (“jump”, “break”) and D4000 break often used as a single feature to detect high redshift “quiescent” galaxies

- ▶ **D4000 break in early type galaxies**
 - ▶ only low signal to noise required
 - ▶ only weakly contaminated by reddening
 - ▶ no absolute fluxes required
 - ▶ same def. for red-shifted objects, only int. range has to be modified → photometric parallaxes
 - ▶ BUT: many lines contribute to break, complex behavior

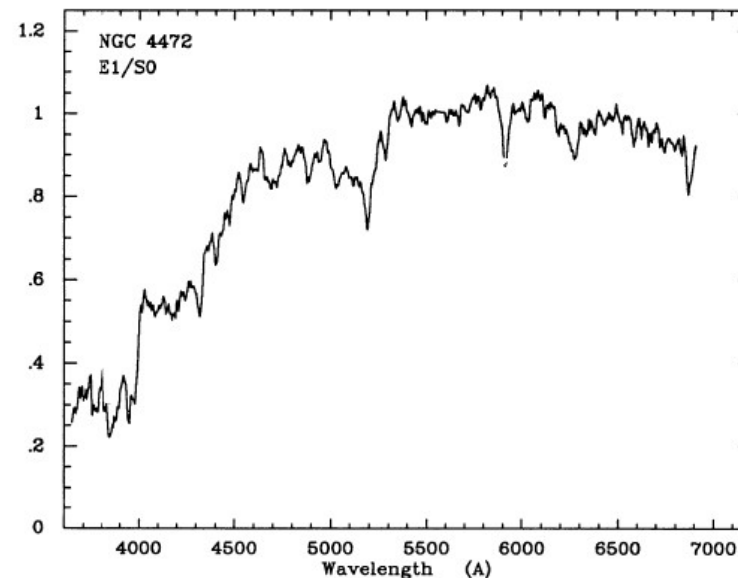
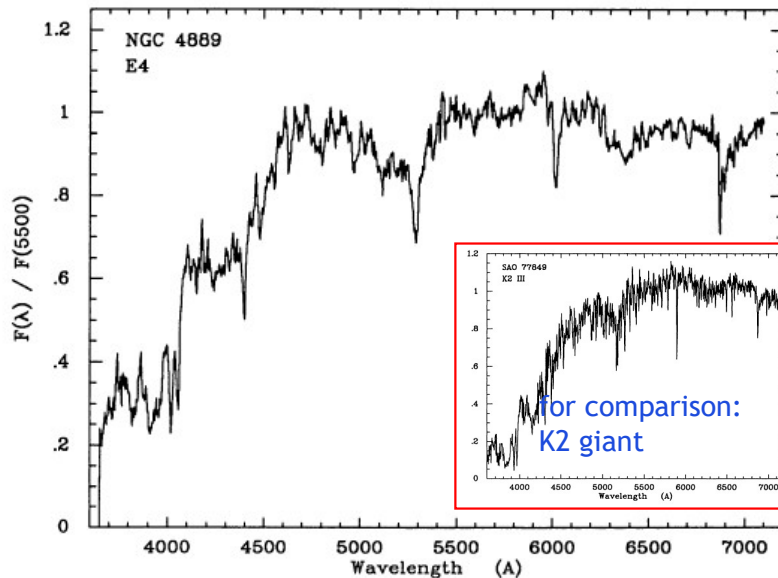
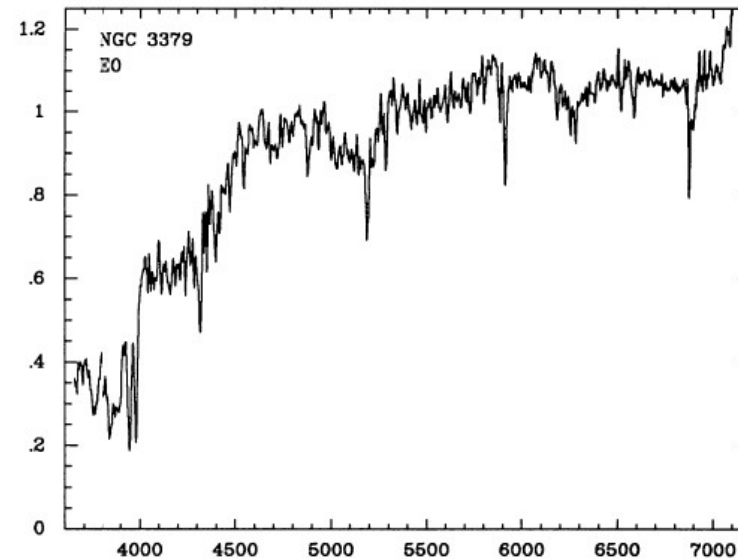
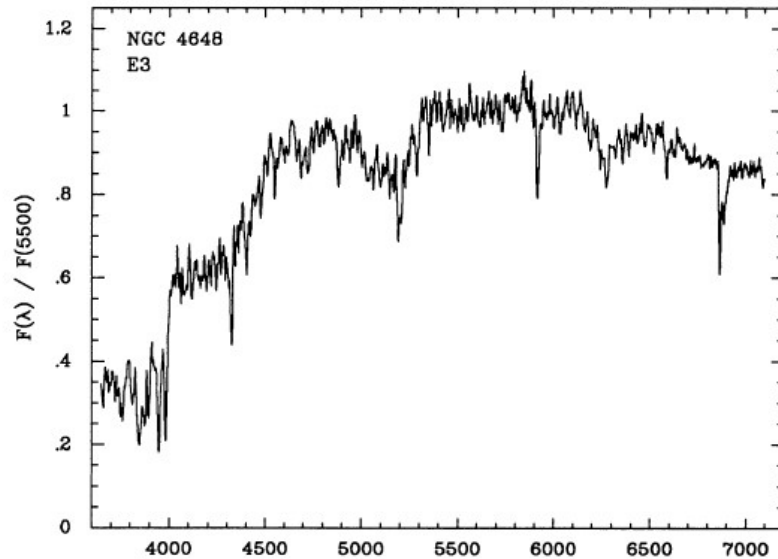
Spectral energy distribution of A-K stars



Note the change in the energy distribution as a function of spectral type (T_{eff})

FIG. 4.—Spectra of four Galactic stars, taken from the spectral library of Jacoby et al. (1984). These spectra can be used to identify some of the major stellar absorption features in the galaxy spectra.

Spectral energy distribution of elliptical galaxies



D4000 break
clearly visible,
Mg/MgH (5000-
5500 \AA) complex
strong
 \Rightarrow dominated by
G/K-giants

FIG. 5.—Integrated spectra of four elliptical galaxies. The spectrum of NGC 4472 (lower right) was obtained at lower resolution with the IRS scanner.

from Kennicutt,
1992, ApJS 79

Spectral energy distribution of spiral galaxies



USM

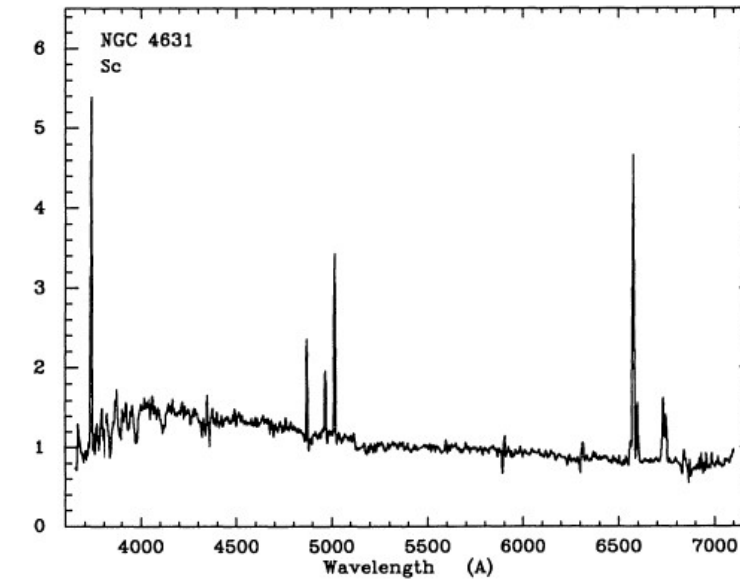
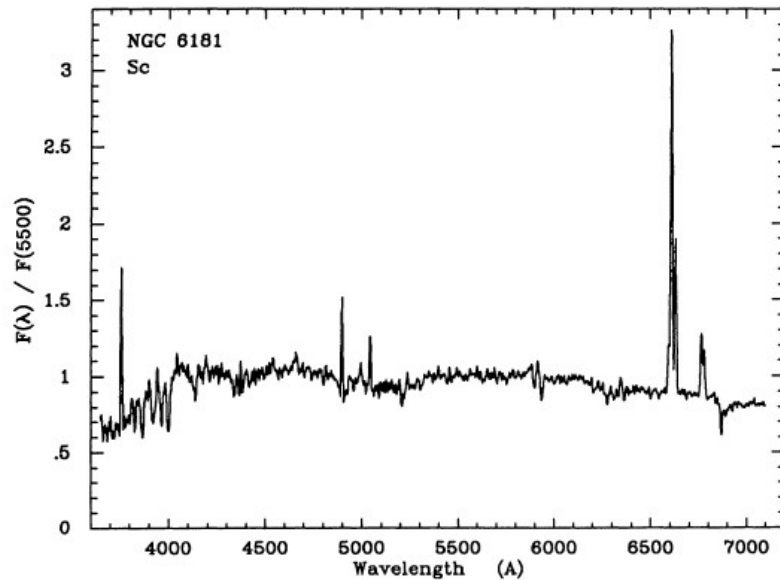
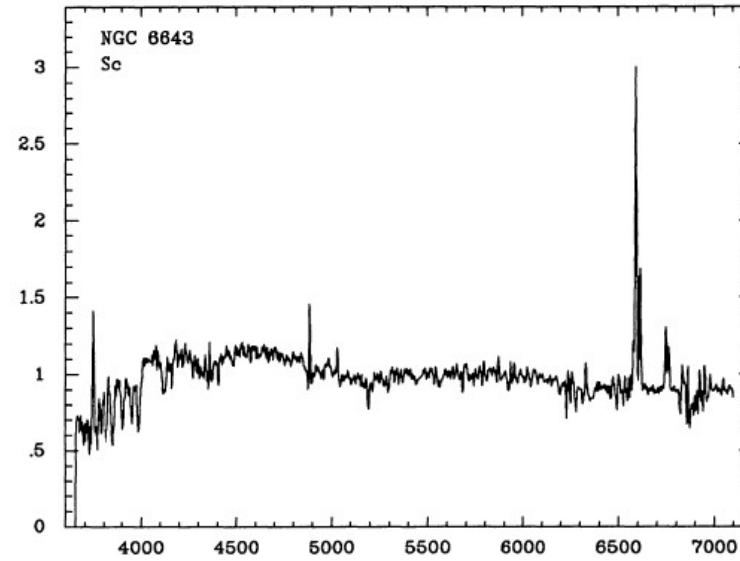
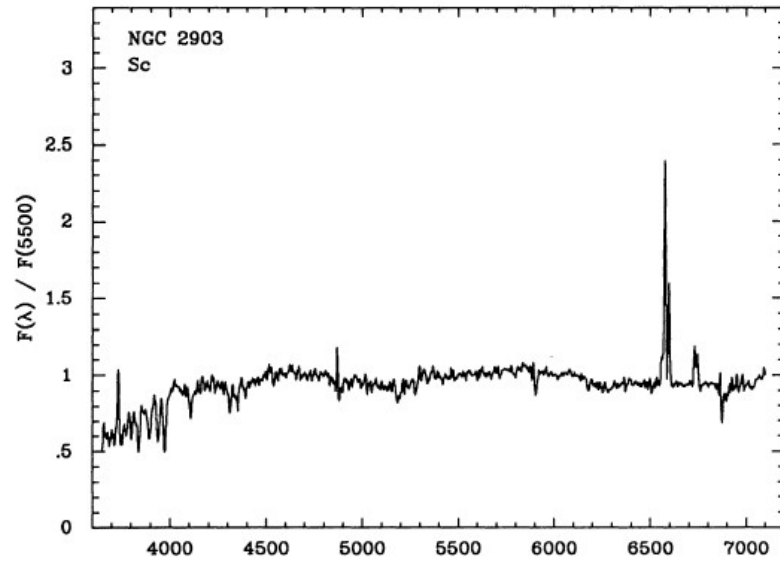
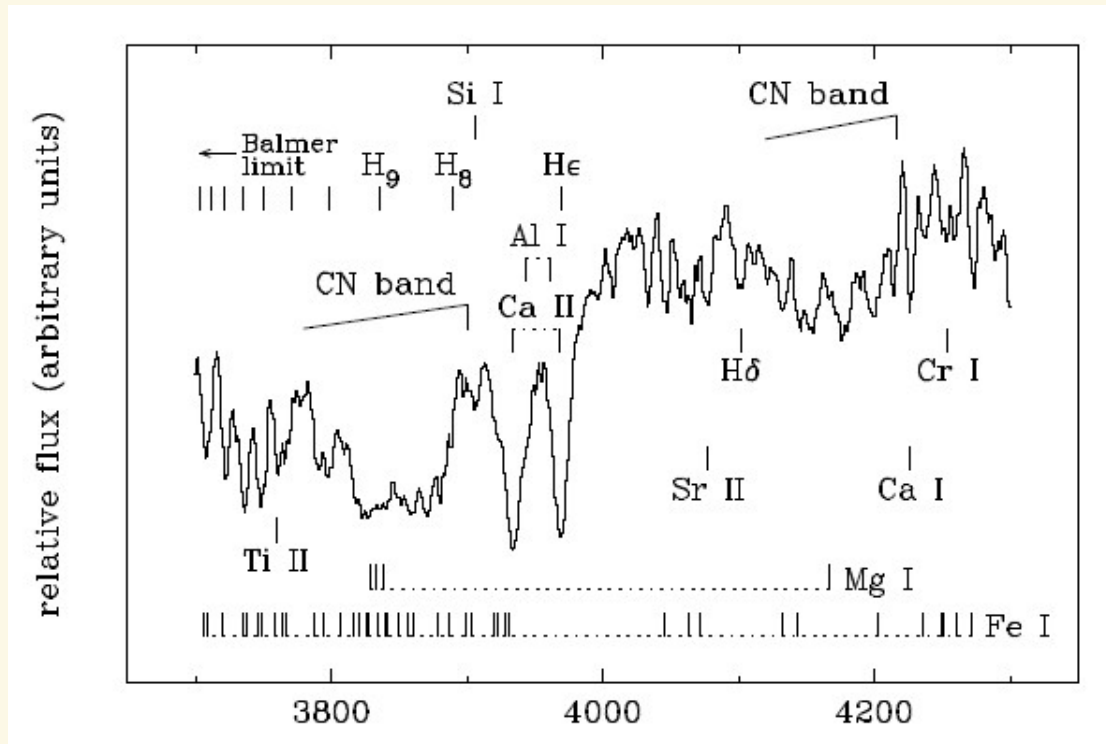


FIG. 10.—Integrated spectra of four Sbc–Sc galaxies, selected to illustrate the range in excitation in the emission-line spectra. See Fig. 9 for other examples.

no break,
Balmer decrement,
nebular emission
lines (H α ,
H β , [OIII 4959,
5007],...)

\Rightarrow presence of
early type stars
plus HII-regions

The 4000 Å region: a closer inspection



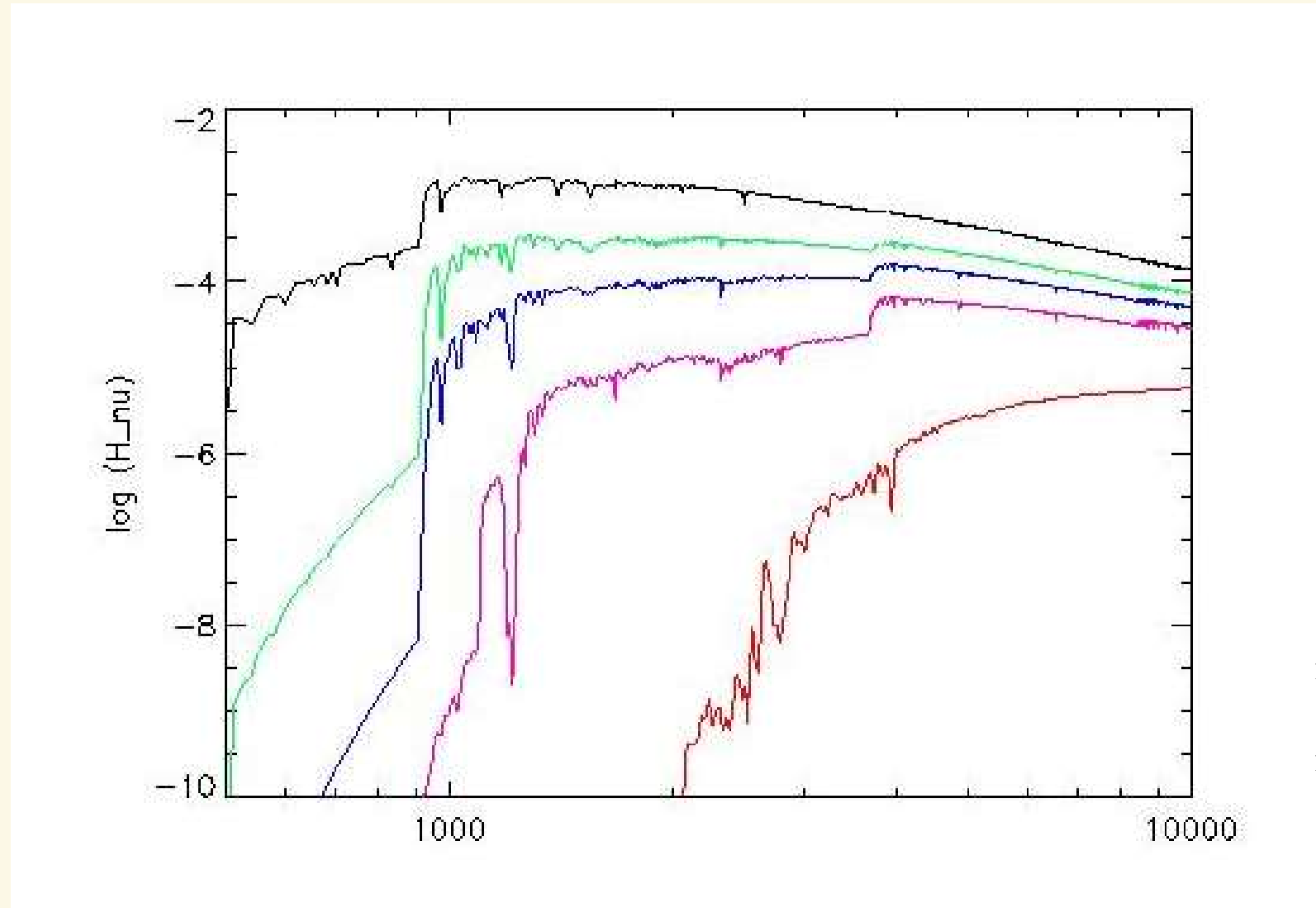
From Gorgas et al., 1999, A&A

spectrum of HD72324(G9 III)

- ▶ very strong CaII H/K lines
 - ▶ major ion, resonance lines (almost all Ca-atoms are in ground-state of CaII)
=> very strong lines
- ▶ weaker Balmer lines (almost all hydrogen in ground-state)
- ▶ multitude of FeI and MgI lines
- ▶ + CN band lines
- => **Strong D4000 break**



Theoretical energy distributions of (super)giants

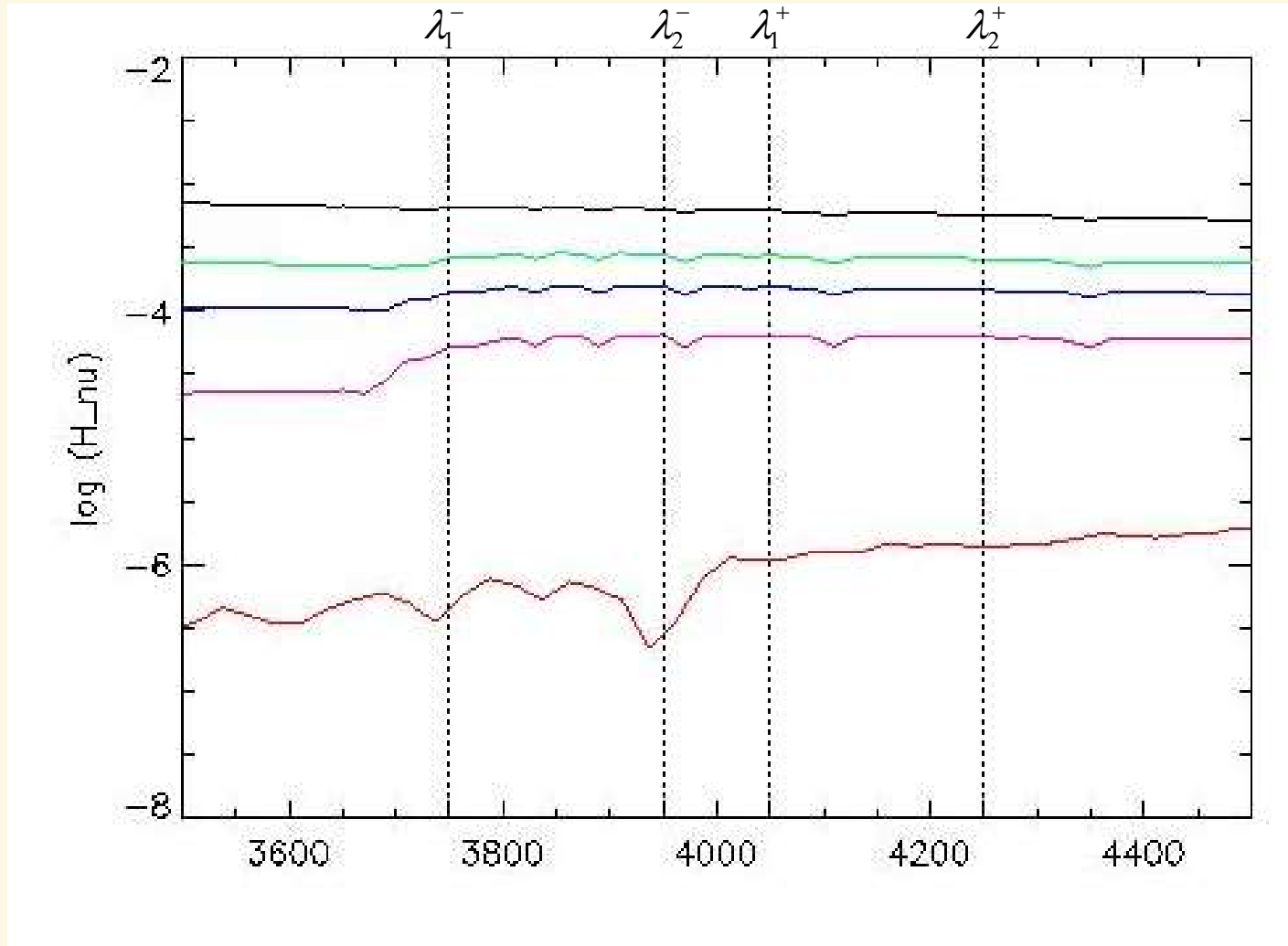


Teff [K] =

- 30000
- 20000
- 15000
- 10000
- 5000

calculated by
means of
'Atlas' (Kurucz)
model atmospheres
(LTE)

Theoretical energy distributions of (super)giants: zoom into the 4000 Å region



$T_{\text{eff}} [\text{K}] =$

30000

20000

15000

10000

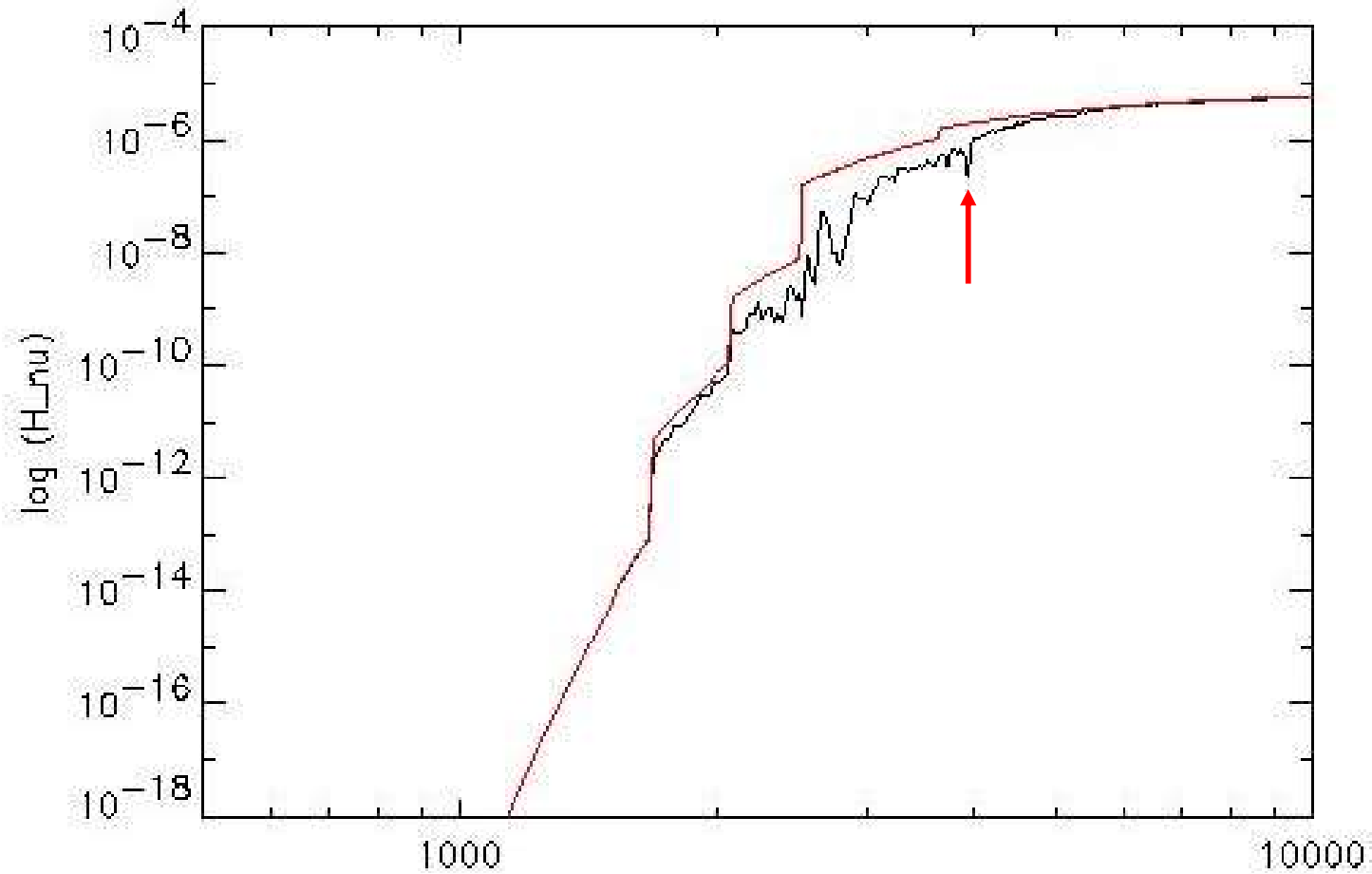
5000

calculated by
means of
'Atlas' (Kurucz)
model atmospheres
(LTE)

The D4000 break: consequence of line-blocking



$T_{\text{eff}} = 5000 \text{ K}$, $\log g = 1.5$



pure continuum

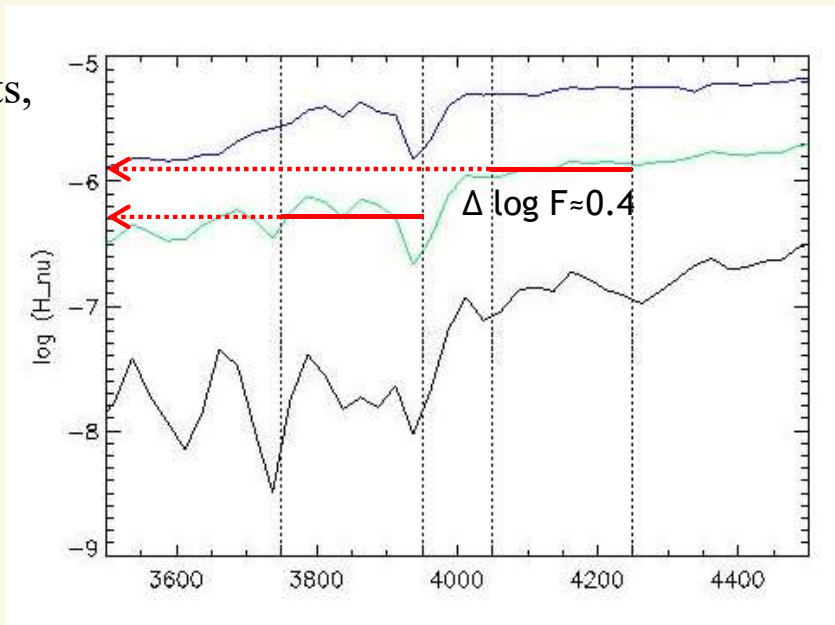
including multitude
of lines:
line-blocking

The D4000 break: dependence on parameters



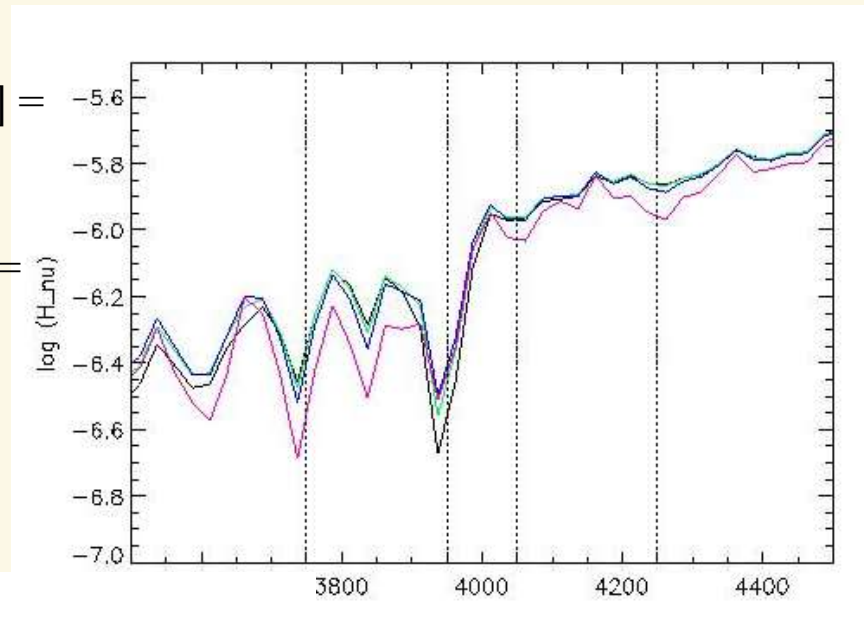
supergiants,
Teff [K] =

6000
5000
4000

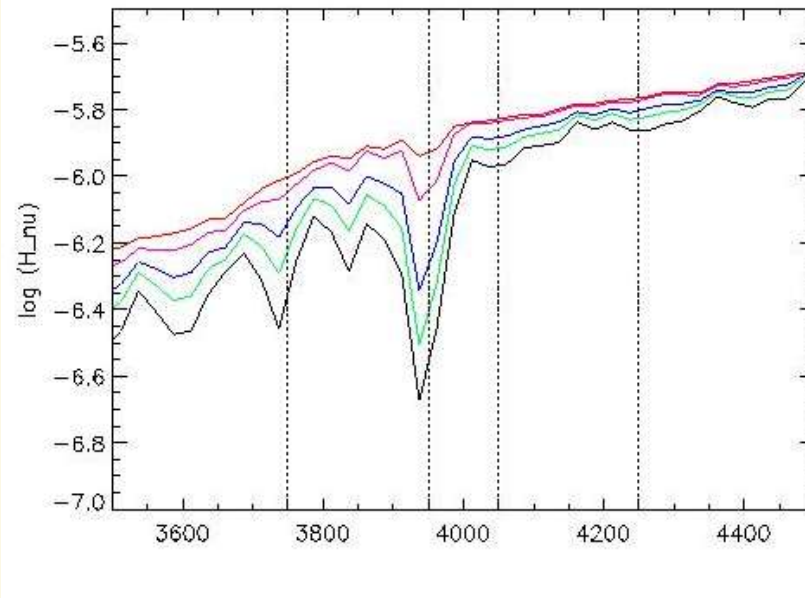


Teff [K] =
5000

log g =
1.50
2.25
3.00
4.50



- ✓ dependence on T_{eff} : strong
- ✓ dependence on log g: weak
- ✓ dependence on Z: strong



Teff [K] = 5000
log g = 1.50

metallicity ($\log Z/Z_{\text{sun}}$)
0.00
-0.50
-1.00
-2.00
-3.00

The D4000 break: empirical calibration



factor 2.5
corresponds to
 $\Delta \log F = 0.4$
(see previous
slide)

18

J. Gorgas et al.: Empirical calibration of the $\lambda 4000 \text{ \AA}$ break

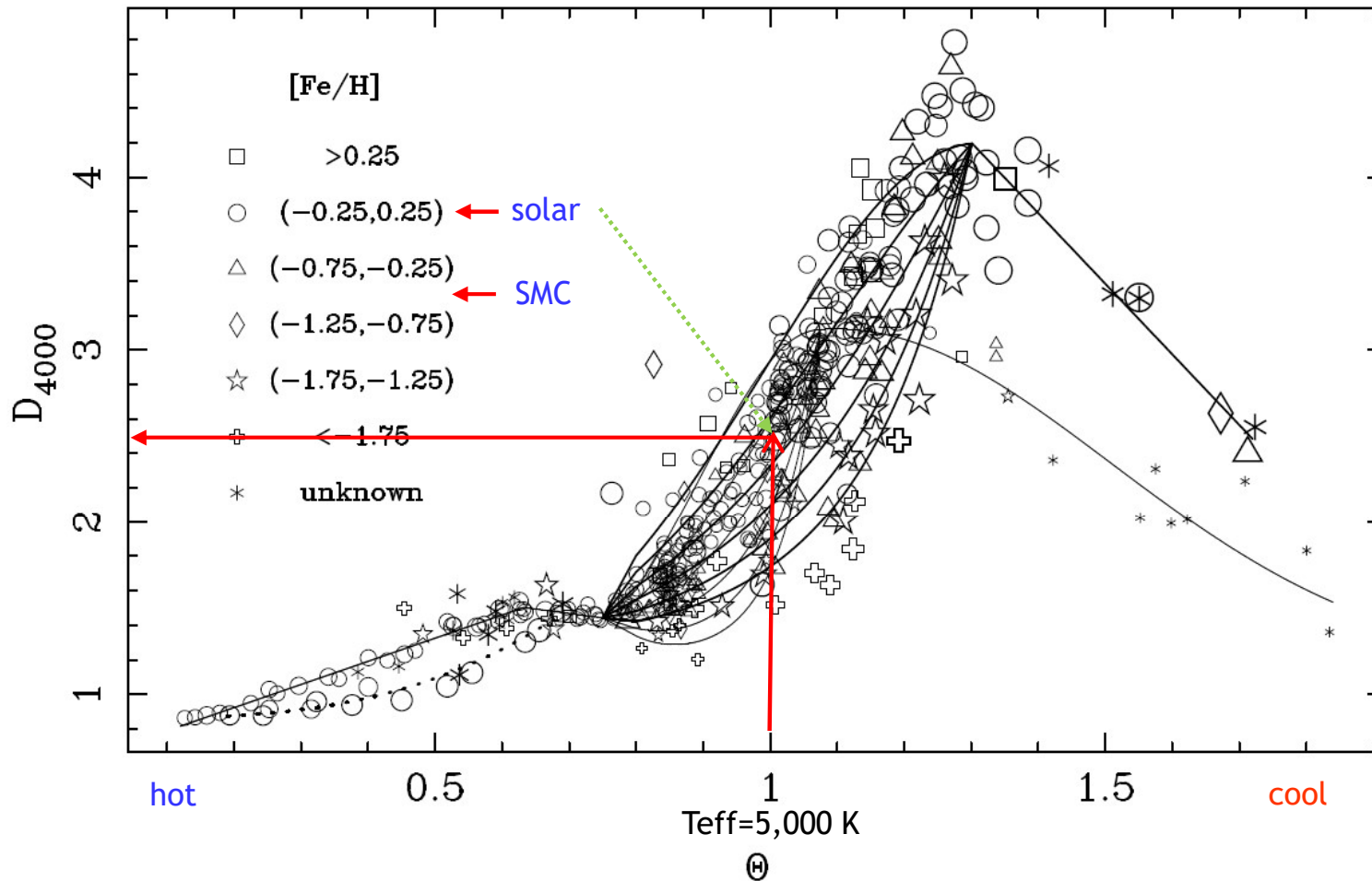
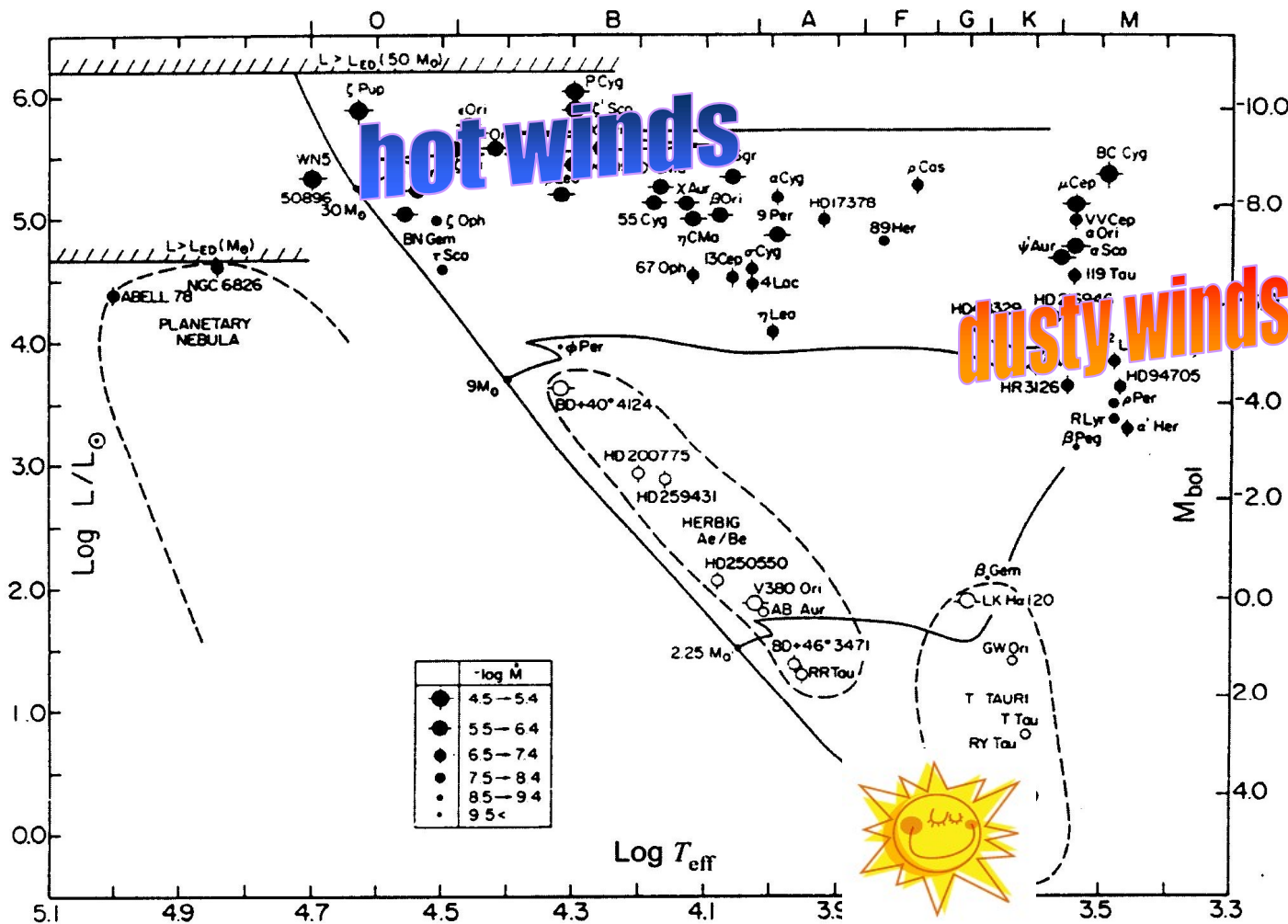


Fig. 5. D_{4000} as a function of $\theta \equiv 5040/T_{\text{eff}}$ for the sample, together with the derived fitting functions. Stars of different metallicities are shown with different symbol types, with sizes giving an indication of the surface gravity (in the sense that low-gravity stars, i.e. giants, are plotted with larger symbols). Concerning the fitting functions, in the low θ range, the solid line corresponds to dwarf and giant stars, whereas the dashed line is used for supergiants. For lower temperatures, thick and thin lines refer to giant and dwarf stars respectively. For each of these groups in the mid-temperature range, the different lines represent the metallicities $[\text{Fe}/\text{H}] = +0.5, 0, -0.5, -1, -1.5, -2$, from top to bottom.

Chap. 8 – Stellar winds



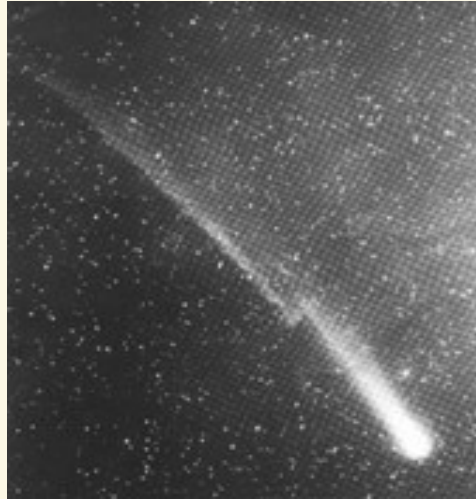
ubiquitous phenomenon

- solar type stars (incl. the sun)
- red supergiants/AGB-stars ("normal" + Mira Variables)
- hot stars (OBA supergiants, Luminous Blue Variables, OB-dwarfs, Central Stars of PN, sdO, sdB, Wolf-Rayet stars)
- T-Tauri stars
- and many more

The solar wind - a suspicion



comet Halley,
with „kink“ in
tail



comet Hale-Bopp
with dust and
plasma tail (blue)

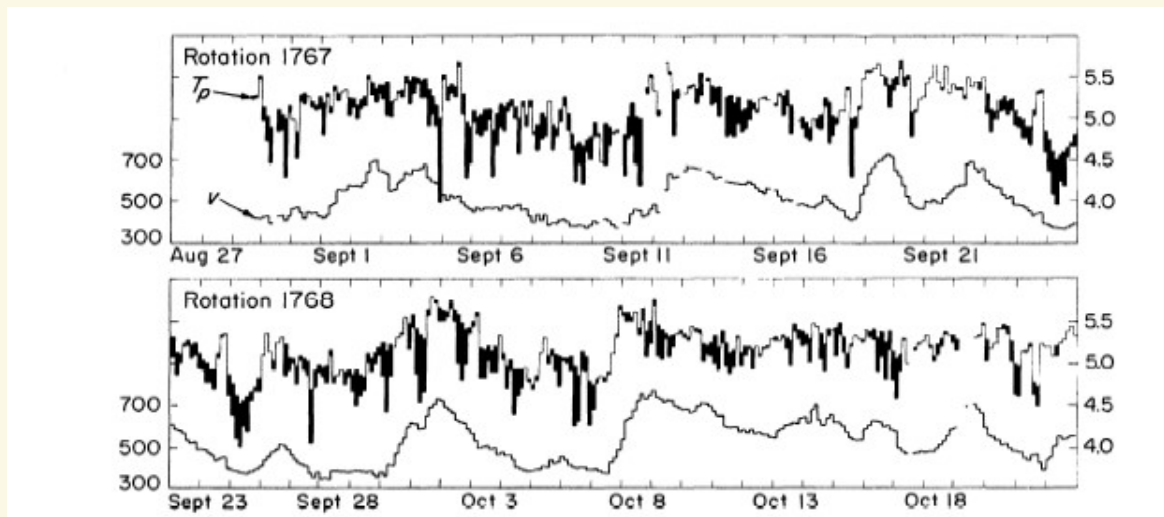


- comet tails *directed away from the sun*
- **Kepler**: influence of solar radiation pressure (-> radiation driven winds)
- *Ionic tail*: emits own radiation, sometimes different direction
- **Hoffmeister** (1943, subsequently Biermann): *solar particle radiation* different direction, since v (particle) comparable to v (comet)

The solar wind - the discovery



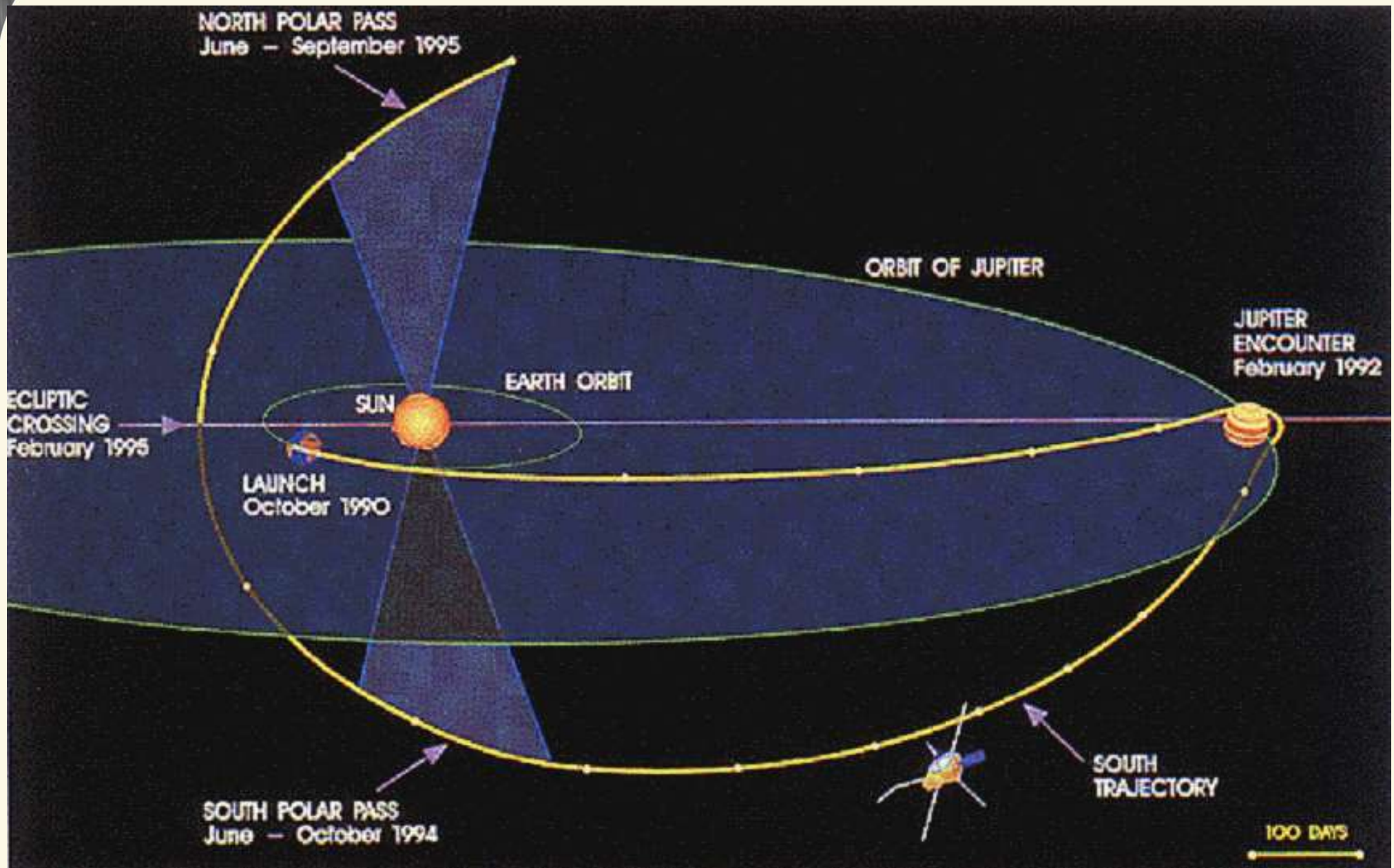
- **Eugene Parker (1958):** theoretical(!) investigation of coronal equilibrium: high temperature leads to (solar) wind (more detailed later on)
- **confirmed by**
 - Soviet measurements (Lunik2/3) with “ion-traps” (1959)
 - Explorer 10 (1961)
 - Mariner II (1962): measurement of fast and slow flows (27 day cycle -> co-rotating, related “coronal holes” and sun spots)



The solar wind - Ulysses ...



... surveying the polar regions



ULYSSES/SWOOPS

Los Alamos
Space and Atmosphere

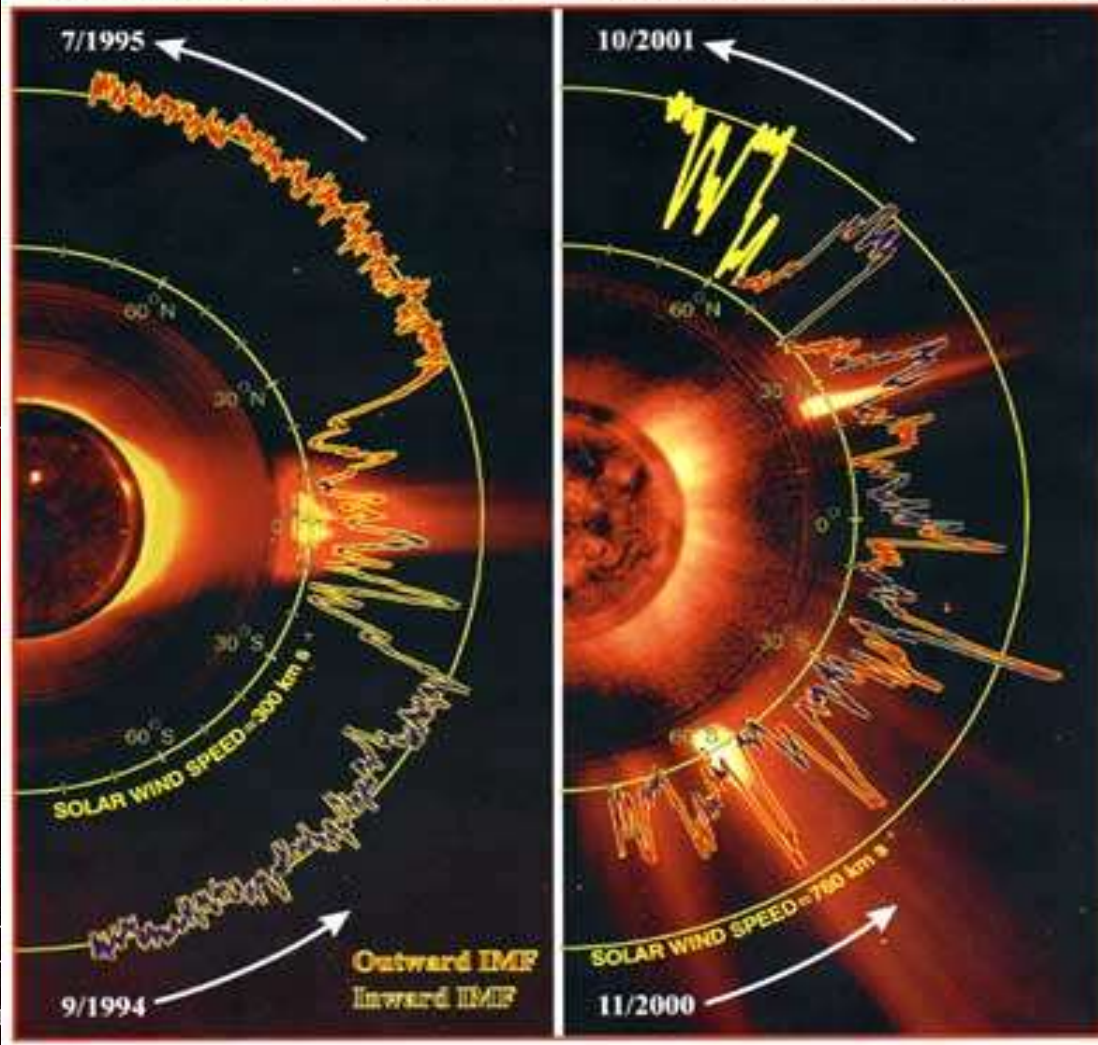
1000

Speed (km s^{-1})

ULYSSES FAST-LATITUDE SCANS

NEARING SOLAR MINIMUM

AROUND SOLAR MAXIMUM



1000

1000

ULYSSES
Imperial

- Outward IMF
- Inward IMF

Outward IMF
Inward IMF

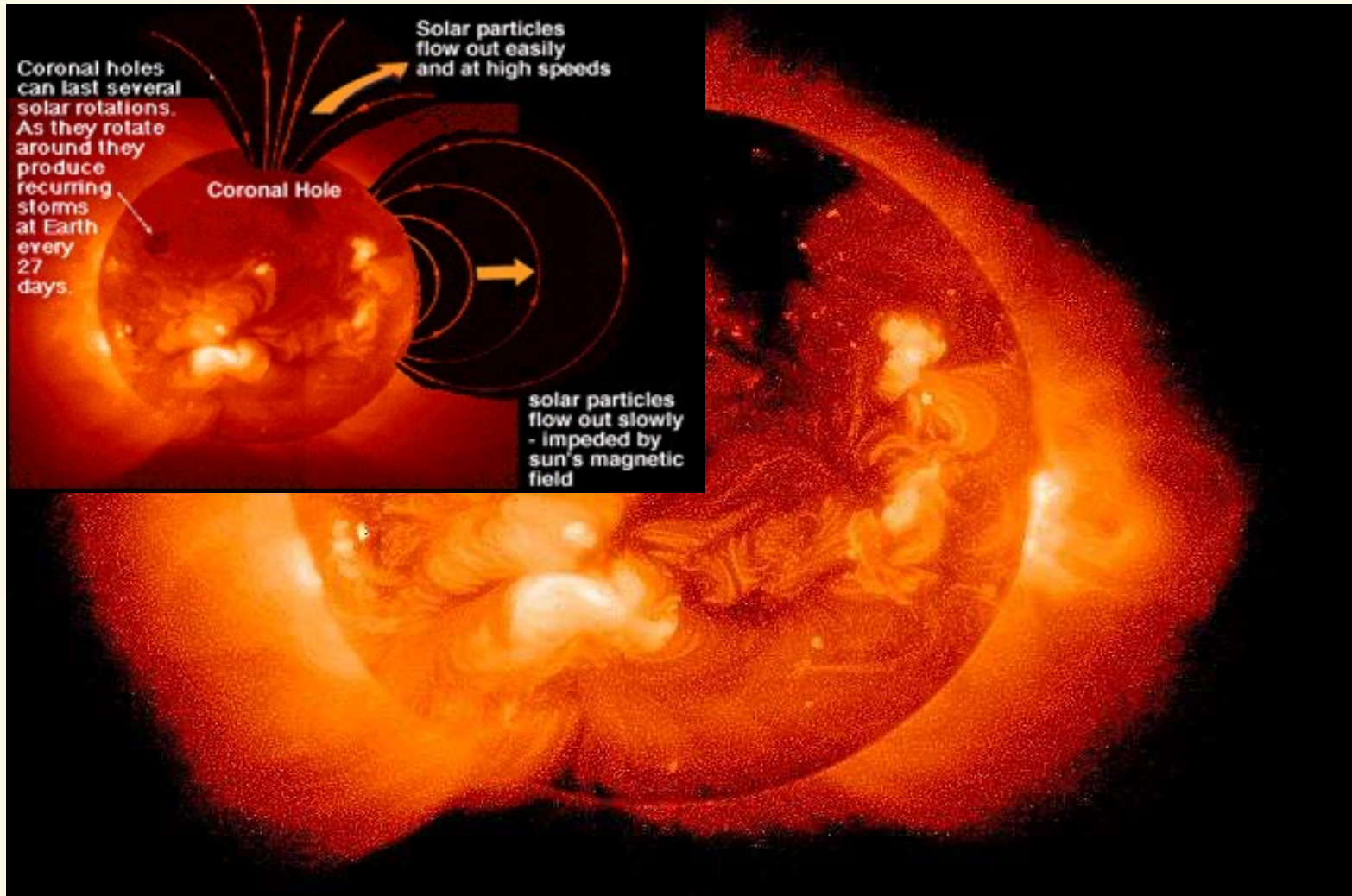
GSFC)
MK3 (HAO)
NRL)

1000

polar wind:
fast and thin

equatorial wind:
slow and dense

The solar wind - coronal holes



fast wind:
over coronal holes
(dark corona, “open”
field lines, e.g., in
polar regions)

coronal X-ray
emission

⇒

**very high
temperatures**

(Yohkoh Mission)

The sun and its wind: mean properties



USM

The sun

radius = 695,990 km = 109 terrestrial radii

mass = $1.989 \cdot 10^{30}$ kg = 333,000 terrestrial masses

luminosity = $3.85 \cdot 10^{33}$ erg/s = $3.85 \cdot 10^{20}$ MW $\approx 10^{18}$ nuclear power plants

effective temperature = 5770 °K

central temperature = 15,600,000 °K

life time approx. $10 \cdot 10^9$ years

age = $4.57 \cdot 10^9$ years

distance sun earth approx. $150 \cdot 10^6$ km ≈ 400 times earth-moon

The solar wind

temperature when leaving the corona: approx. $1 \cdot 10^6$ K

average speed approx. 400-500 km/s (travel time sun-earth approx. 4 days)

particle density close to earth: approx. 6 cm^{-3}

temperature close to earth: $\lesssim 10^5$ K

mass-loss rate: approx 10^{12} g/s (1 Megaton/s) $\approx 10^{-14}$ solar masses/year

\approx one Great-Salt-Lake-mass/day \approx one Baltic-sea-mass/year

\Rightarrow no consequence for solar evolution, since only 0.01% of total mass lost over total life time

Stellar winds - hydrodynamic description



Need mechanism which accelerates material beyond **escape velocity**:

- **pressure driven winds**
- **radiation driven winds**

Note: **red giant** winds still not understood, only scaling relations available (“Reimers-formula”)

remember equation of motion (conservation of momentum + stationarity, cf. Chap. 6, **page 94**)

$$v \frac{dv}{dr} = -\frac{1}{\rho} \frac{dp}{dr} + g^{ext} \quad (\text{in spherical symmetry}), \quad \text{and } p = \rho a^2 \quad (\text{equation of state, with isothermal sound-speed } a)$$

⇒ with mass-loss rate \dot{M} , radius r , density ρ and velocity v

$$\dot{M} = 4\pi r^2 \rho v,$$

equation of continuity:
conservation of mass

$$\left(1 - \frac{a^2}{v^2}\right) v \frac{dv}{dr} = -\frac{GM}{r^2} + g_{rad} + \frac{2a^2}{r} - \frac{da^2}{dr}$$

equation of motion:
from conservation of momentum

vel. field	grav. accel.	radiative accel.	(part of) accel. by pressure gradient
positive for $v > a$	inwards	outwards	outwards
negative for $v < a$			



$$\left(1 - \frac{a^2}{v^2}\right) v \frac{dv}{dr} = -\frac{GM}{r^2} + \cancel{g_{rad}} + \frac{2a^2}{r} - \cancel{\frac{da^2}{dr}}$$

vel. field
grav. accel.
radiative accel.
“pressure”

The solar wind as a proto-type for pressure driven winds

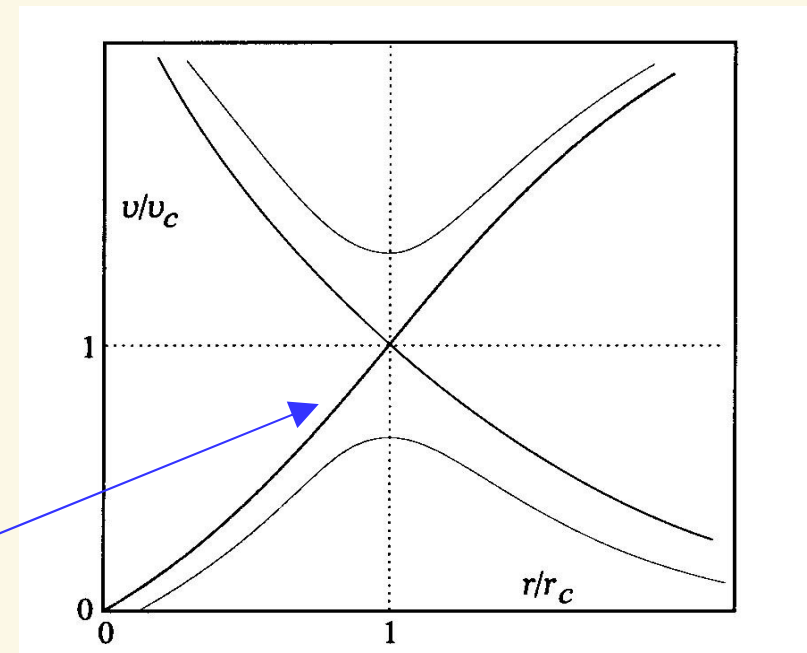
- present in stars which have an (extremely) hot corona ($T \approx 10^6$ K)
- with $g_{rad} \approx 0$ and $T \approx \text{const}$, the rhs of the equation of motion changes sign at

$$r_c = \frac{GM}{2a^2}; \quad \text{with } a (T=1.5 \cdot 10^6 \text{ K}) \approx 160 \text{ km/s,}$$

we find for the sun $r_c \approx 3.9 R_{sun}$

and obtain four possible solutions for v/v_c ("c" = critical point)

- only one (the "transonic") solution compatible with observations
- pressure driven winds as described here rely on the presence of a hot corona (large value of a !)
- Mass-loss rate $\dot{M} \approx 10^{-14} M_{sun} / \text{yr}$, terminal velocity $v_\infty \approx 500$ km/s
- has to be heated (dissipation of acoustic and magneto-hydrodynamic waves)
- not completely understood so far



accelerated by radiation pressure:

$$\left(1 - \frac{a^2}{v^2}\right) v \frac{dv}{dr} = -\frac{GM}{r^2} + g_{rad} + \underbrace{\frac{2a^2}{r} - \frac{da^2}{dr}}_{\text{important only in lowermost wind}}$$

pressure terms only of secondary order
($a \approx 20$ km/s for hot stars,
 ≈ 3 km/s for cool stars)

- ★ cool stars (AGB): major contribution from **dust** absorption; coupling to “gas” by viscous drag force (gas - grain collisions)

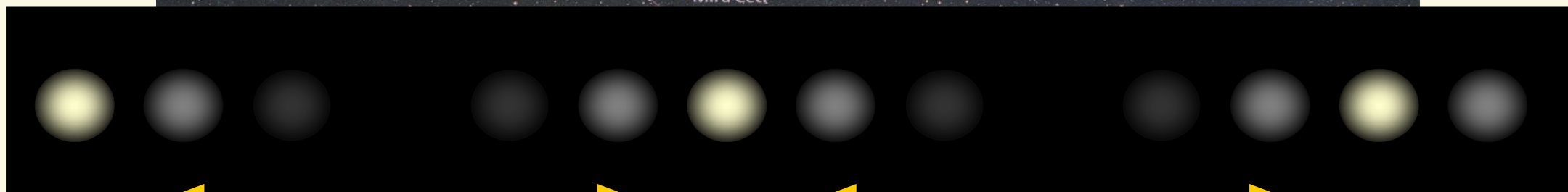
$$\dot{M} \approx 10^{-6} M_{\text{sun}} / \text{yr}, v_{\infty} \approx 20 \text{ km/s}$$

- ★ hot stars: major contribution from **metal line** absorption; coupling to bulk matter (H/He) by Coulomb collisions

$$\dot{M} \approx 10^{-6} \dots 10^{-5} M_{\text{sun}} / \text{yr}, v_{\infty} \approx 2,000 \text{ km/s}$$



dusty
winds



(David Fabricius, 1596)

- brightness variations by 5.5 mag (from 3.5 to 9), corresponding to a factor of 160

Eckhardt Slawik)

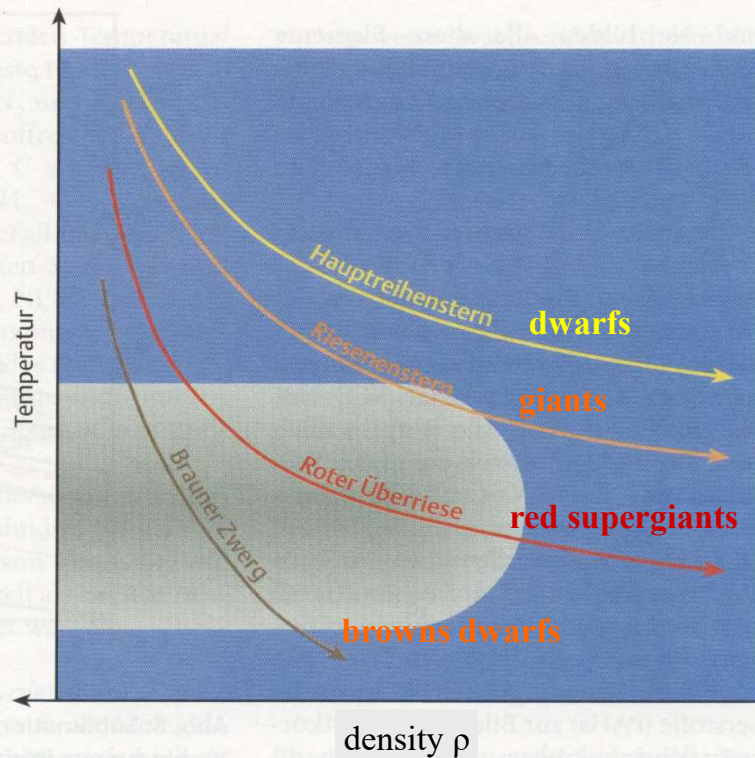


Walfisc (Cetus)

Cool supergiants: The dust-factories of our Universe



USM



dust: approx. 1% of ISM, 70% of this fraction formed in the winds of AGB-stars (cool, low-mass supergiants)

Red supergiants are located in dust-forming “window”

transition from gaseous phase to solid state possible only in **narrow range of temperature and density:**

gas density must be high enough and temperature low enough to allow for the chemical reactions:

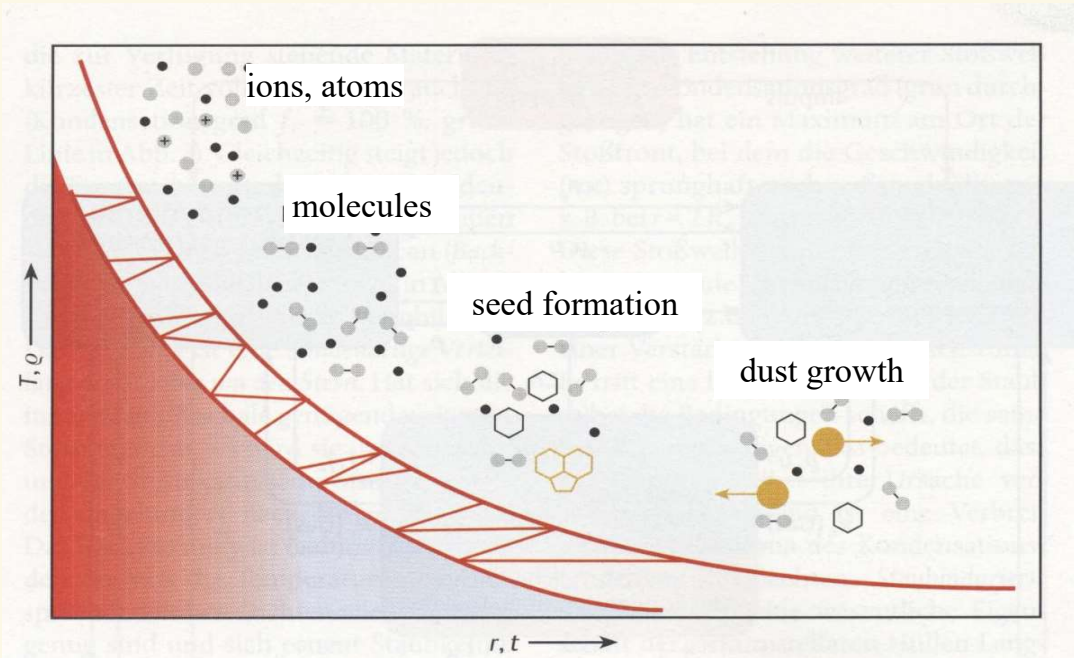
- sufficient number of dust forming molecules required
- the dust particles formed have to be thermally stable

Material on this and following pages from Chr. Helling, *Sterne und Weltraum*, Feb/March 2002

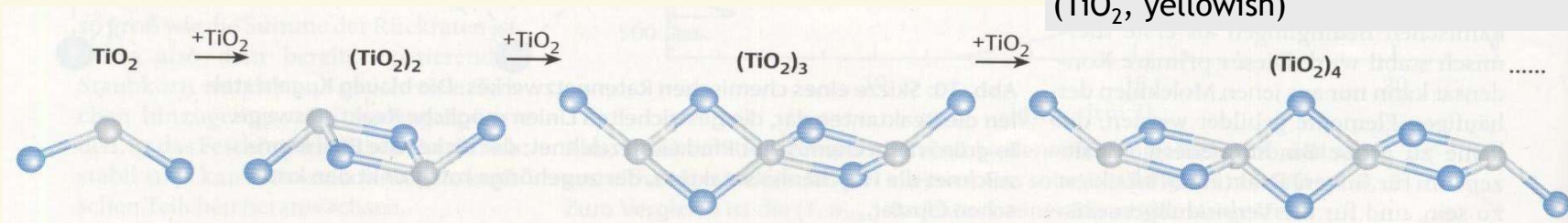
Growth of dust in matter outflow



- decrease of density and temperature
- more and more complex structures are forming
- dust: macroscopic, solid state body, approx. 10^{-7} m (1000 Angstrom), 10^9 atoms



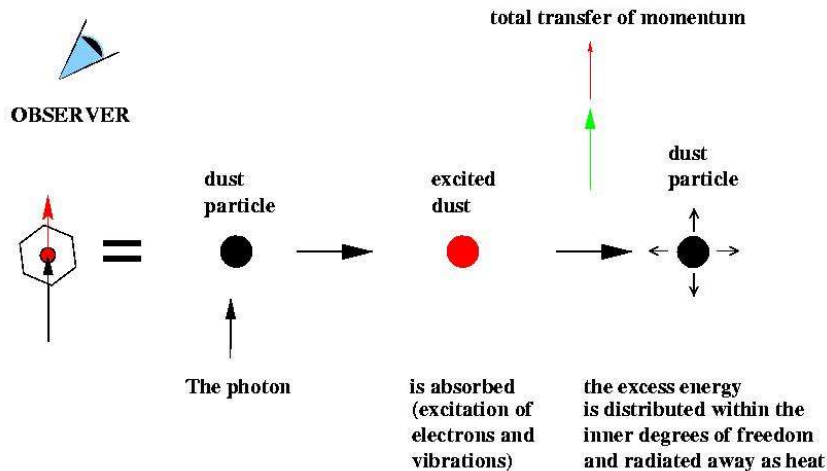
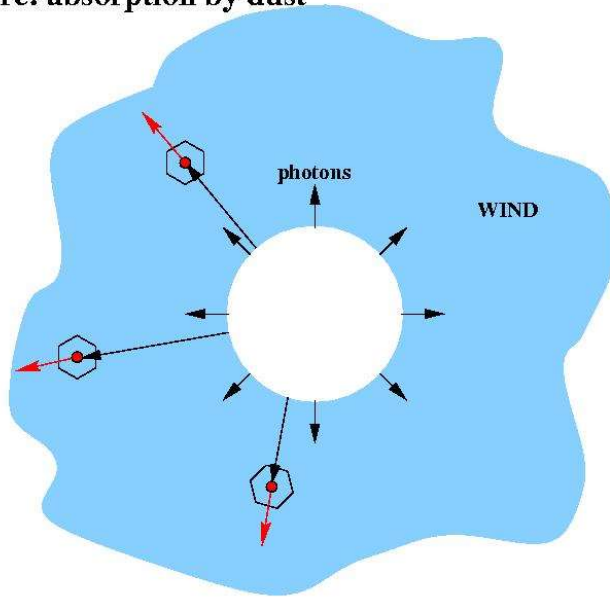
terrestrial, macroscopic rutile crystal (TiO_2 , yellowish)



first steps of a linear reaction chain, forming the seed of $(\text{TiO}_2)_N$

Dust-driven winds: the principle

The principle of radiation driven winds
here: absorption by dust



- star emits photons
- photons absorbed (or scattered) by dust
- momentum transfer accelerates dust
- gas accelerated by viscous drag force due to gas-dust collisions

acceleration

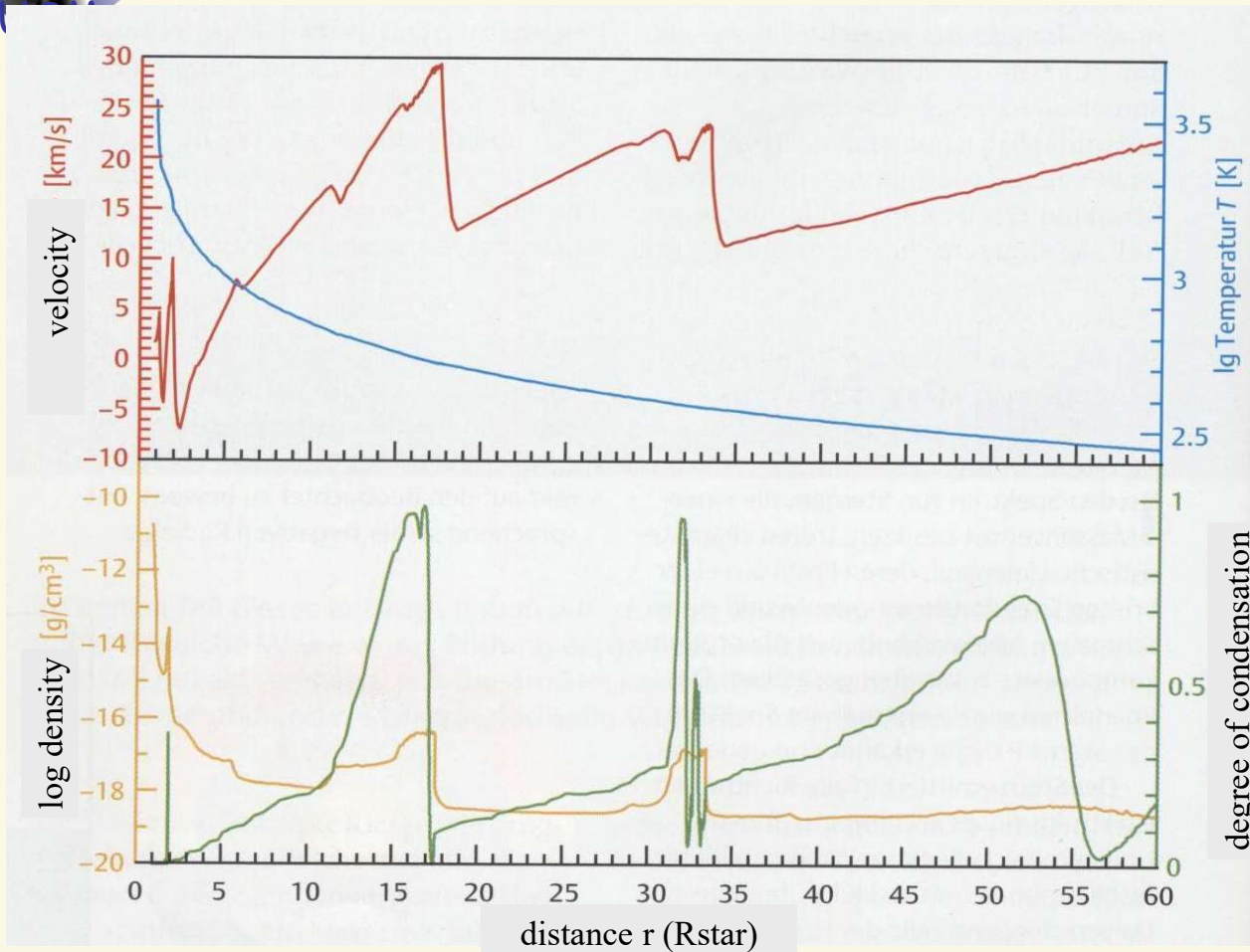
proportional to number of photons, i.e.,
proportional to *stellar luminosity* L

⇒ mass-loss rate $\propto L$

dust driven winds at tip of AGB responsible
for ejection of envelope

⇒ Planetary Nebulae

winds from **massive red supergiants** still
not explained, but maybe similar mechanism

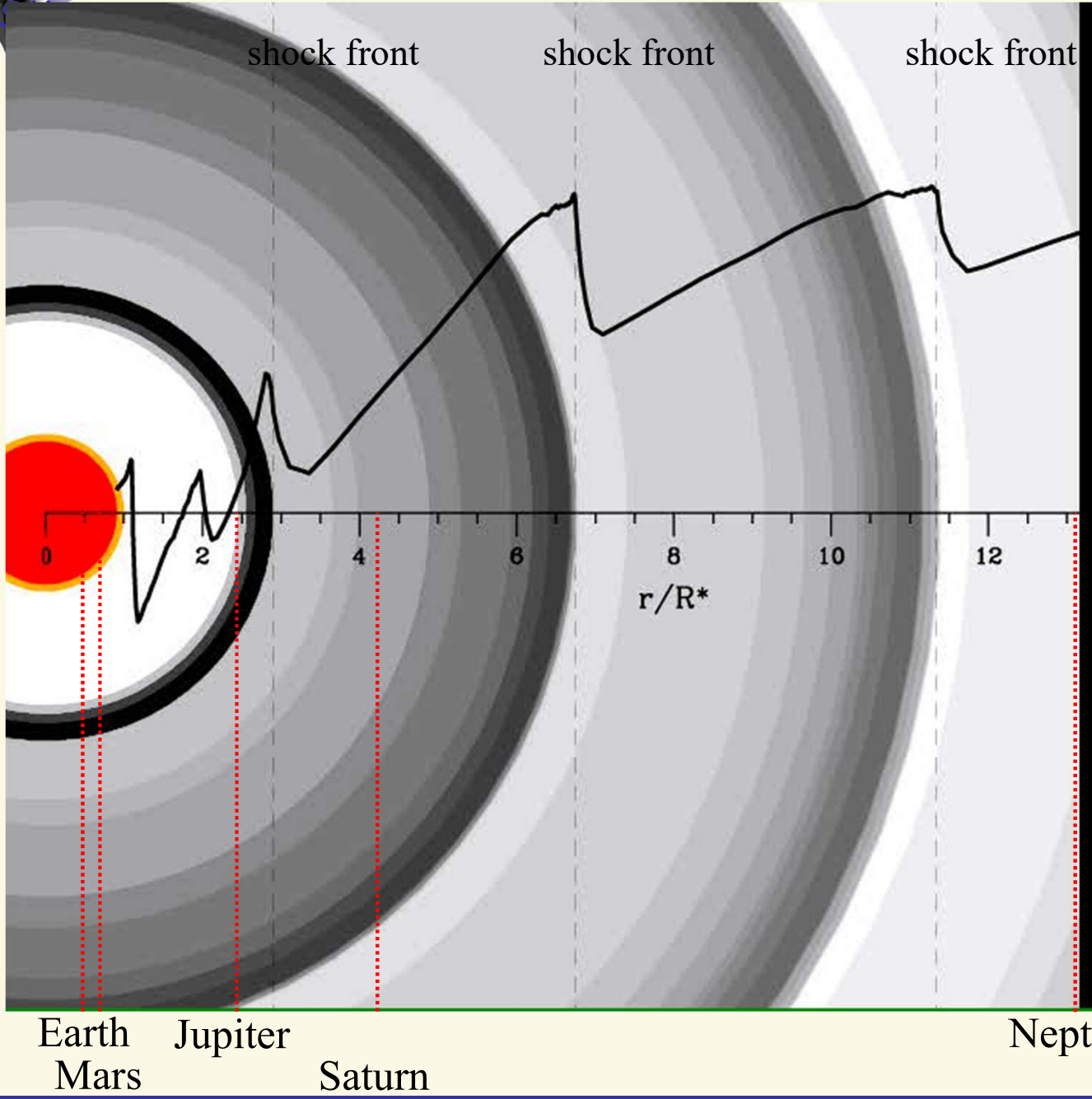


snapshot of a time-dependent hydro-simulation of a carbon-rich circumstellar envelope of an AGB-star. Model parameters similar to next slide.

- star (“surface”) pulsates,
- sound waves are created,
- steepen into shocks;
- matter is compressed,
- dust is formed
- and accelerated by radiation pressure

dust shells are blown away, following the pulsational cycle

- ⇒ periodic darkening of stellar disc
- ⇒ **brightness variations**



dark colors: dust shells

velocity

simulation of a
dust-driven wind
*(previous working group
E. Sedlmayr, TU Berlin)*

$$T = 2600 \text{ K}, L = 10^4 L_{\text{sun}},$$

$$M = 1 M_{\text{sun}}, \Delta v = 2 \text{ km/s}$$

Earth Mars Jupiter Saturn Neptun

Stars and their winds - typical parameters



	The sun	Red AGB-stars	Blue supergiants
mass [M_{\odot}]	1	1 ... 3	10...100
luminosity [L_{\odot}]	1	10^4	$10^5...10^6$
stellar radius [R_{\odot}]	1	400	10...200
effective temperature [K]	5570	2500	$10^4...5 \cdot 10^4$
wind temperature [K]	10^6	1000	8000...40000
mass loss rate [M_{\odot} /yr]	10^{-14}	$10^{-6} ... 10^{-4}$	$10^{-6} ... \text{few } 10^{-5}$
terminal velocity [km/s]	500	30	200...3000
life time [yr]	10^{10}	10^5	10^7
total mass loss [M_{\odot}]	10^{-4}	$\gtrsim 0.5$	up to 90% of total mass

massive stars determine energy (kinetic and radiation)
and momentum budget of surrounding ISM

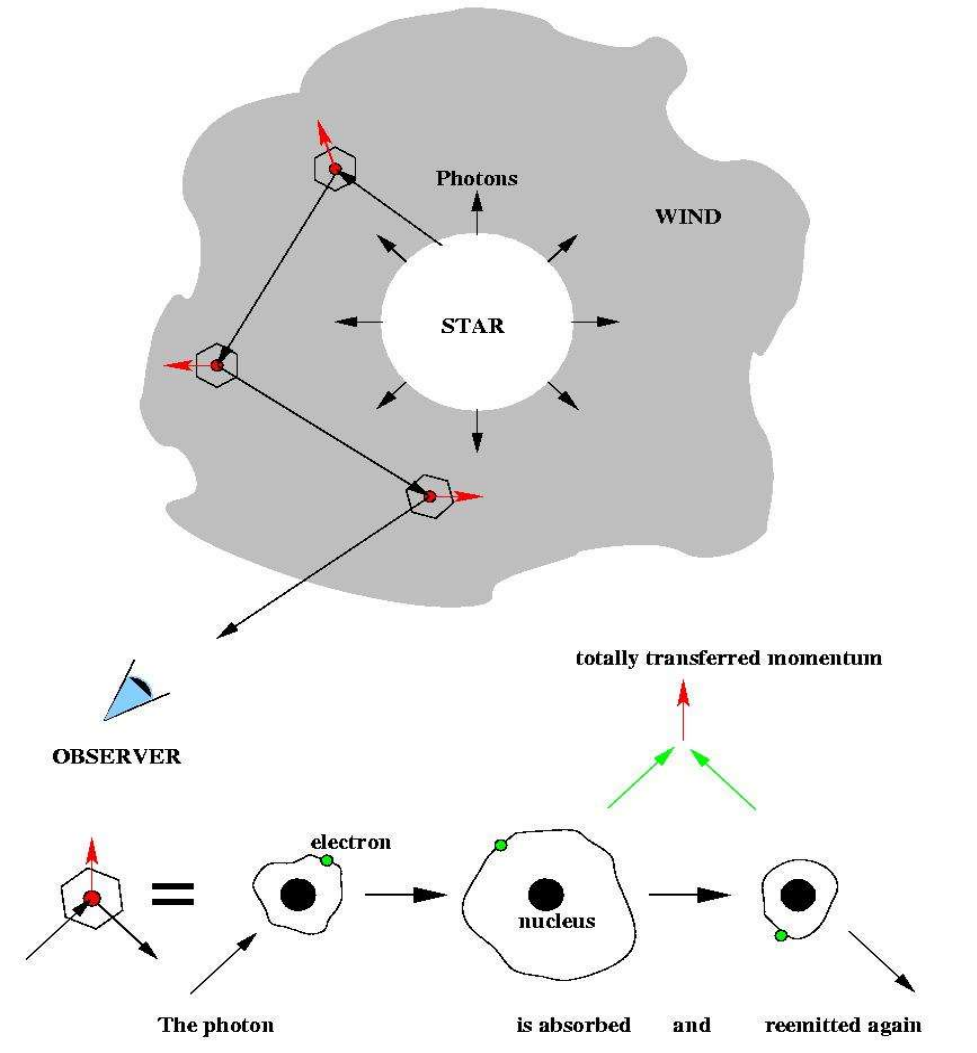


Bubble Nebula
(NGC 7635)
in Cassiopeia

wind-blown
bubble around
BD+602522
(O6.5III f)



The principle of radiatively driven winds



- accelerated by radiation pressure in **lines**
 $M \approx 10^{-7} \dots 10^{-5} M_{\text{sun}} / \text{yr}$, $v_{\infty} \approx 200 \dots 3,000 \text{ km/s}$
- momentum transfer from accelerated species (ions) to bulk matter (H/He) via Coulomb collisions

Prerequisites for radiative driving

- large number of photons => high luminosity
 $L \propto R_*^2 T_{\text{eff}}^4$ => supergiants or hot dwarfs
- line driving:
 large number of lines close to flux maximum (typically some $10^4 \dots 10^5$ lines relevant) with high interaction probability
 (=> mass-loss dependent on metal abundances)
- line driven winds important for chemical evolution of (spiral) Galaxies, in particular for starbursts
- transfer of momentum (=> induces *star formation*, hot stars mostly in *associations*), energy and nuclear processed material to surrounding environment
- dramatic impact on stellar evolution of massive stars (mass-loss rate vs. life time!)

pioneering investigations by

Lucy & Solomon, 1970, ApJ 159

Castor, Abbott & Klein, 1975, ApJ 195 (CAK)

reviews by Kudritzki & Puls, 2000, ARAA 38

Puls et al. 2008 A&Arv 16, issue 3



$$g_{rad} \propto N \text{ (number of absorbed photons)}$$

LINE absorption

absorption only if frequency close to a possible line transition,

$$\kappa_\nu \propto \kappa_0 \text{ if } \nu_0 \pm \delta\nu \text{ (thermal width)}$$

$$\kappa_\nu = 0 \text{ else}$$

- absorption always at *line frequency* $\nu_0 (\pm\delta\nu)$ *in frame of matter*
- matter moves at certain velocity with respect to stellar frame
- matter “sees” stellar photons at different frequency than star itself (Doppler-effect)

$$\nu_{CMF} = \nu_{obs} - \frac{\nu_0 v(r)}{c} =: \nu_0 \text{ (radial photons, } \mu=1, \text{ assumed)}$$

- the larger the velocity of matter, the larger the photon’s stellar frame frequency must be in order to become absorbed at ν_0 (in frame of matter)

$$\left. \begin{aligned} \nu_0 &= \nu_1^{obs} - \frac{\nu_0}{c} v_1(r) \\ \nu_0 &= \nu_2^{obs} - \frac{\nu_0}{c} v_2(r) \end{aligned} \right\} \text{if } v_2(r) > v_1(r), \text{ then } \nu_2^{obs} > \nu_1^{obs}$$

\Rightarrow accelerated matter “sees” photons from a considerably larger band-width than static matter, $\Delta\nu_{obs} = \frac{\nu_0}{c} \Delta v \gg \delta\nu$

shell of matter with spatial extent Δr ,

and velocity $v_0 + \left(\frac{dv}{dr}\right)_1 \Delta r$

absorption of photons at $\nu_0 \pm \delta\nu$

in frame of matter

photons must start at higher (stellar)

frequencies, are "seen" at $\nu_0 \pm \delta\nu$

in frame of matter because of Doppler-effect.

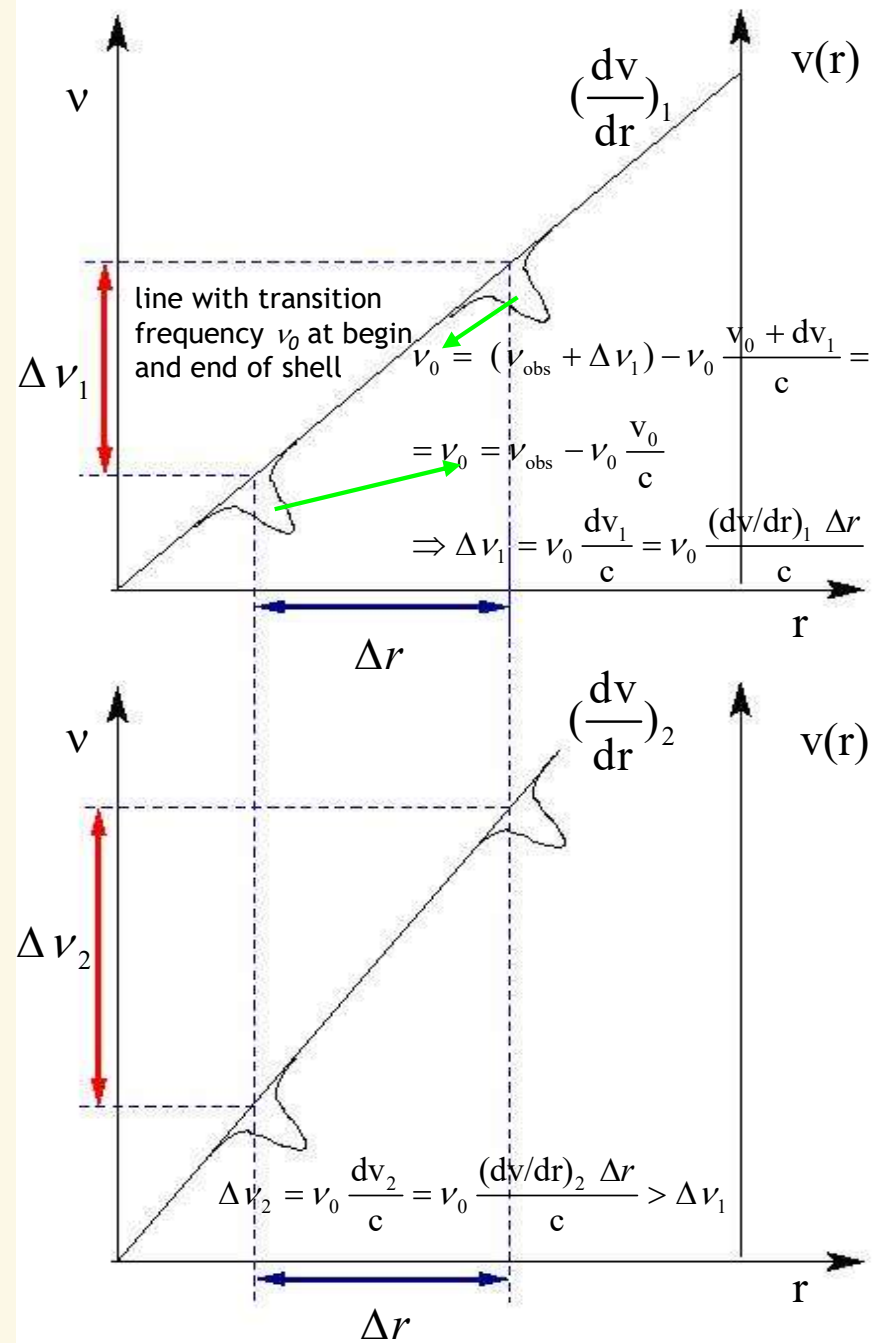
Let $\Delta\nu$ be frequency band contributing to acceleration of matter in Δr

The larger $\frac{dv}{dr}$,

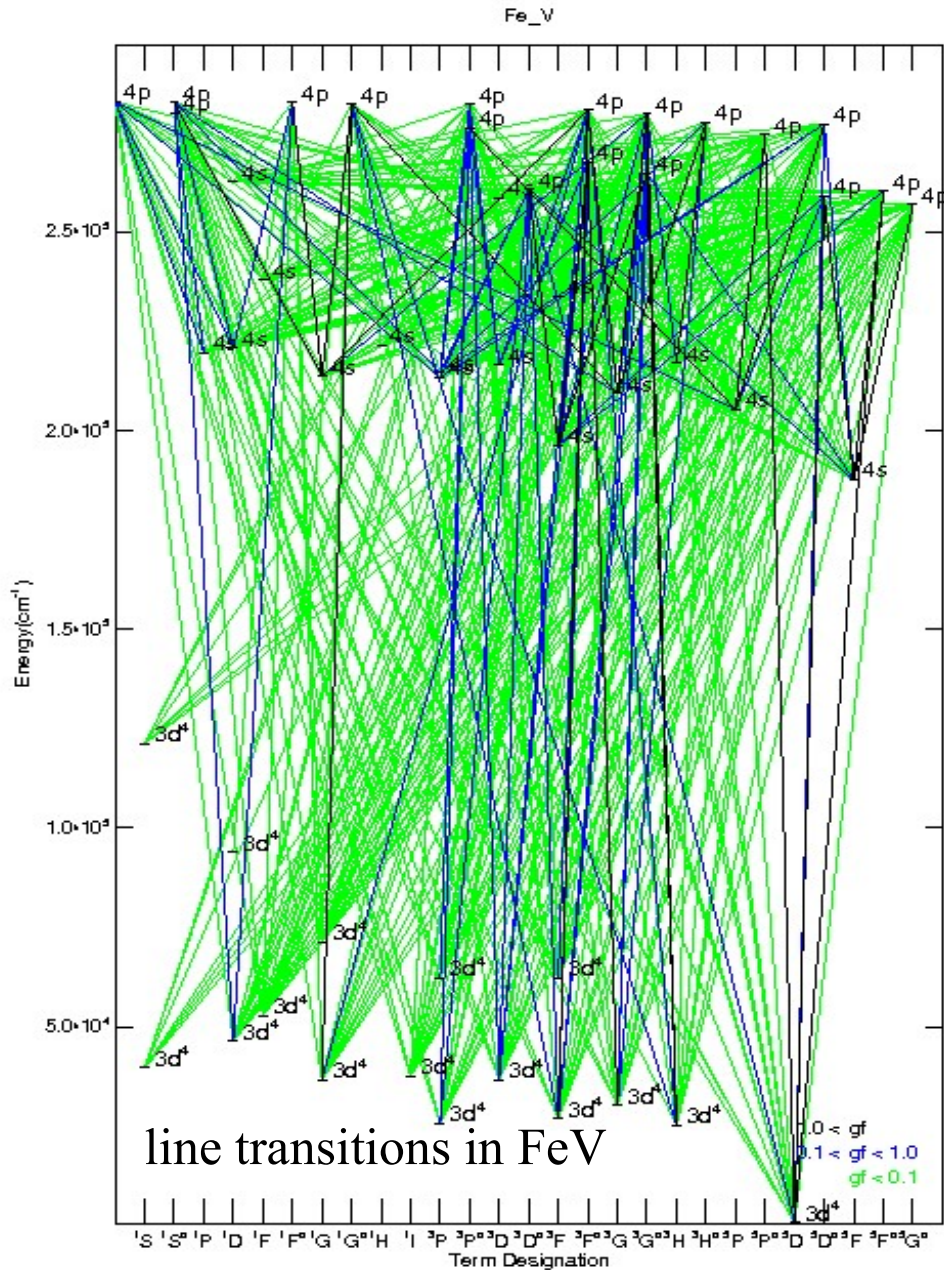
- the larger $\Delta\nu$
- the more photons can be absorbed
- the larger the acceleration

$$g_{\text{rad}} \propto \frac{dv}{dr}$$

(assuming that each photon is absorbed, i.e., acceleration from optically thick lines)



Millions of lines



... are present
... and needed!

Remember (Chapt. 4)

$$g_{rad} = \frac{1}{c\rho} \int \kappa_{\nu} \mathcal{F}_{\nu} d\nu \quad \text{with opacity } \kappa_{\nu}$$

and radiative flux \mathcal{F}_{ν}

summing up the individual contributions
from optically thin and thick lines,

$$g_{rad}^{tot} = \sum_{\text{all lines}} g_{rad}^i,$$

$$g_{rad}^{thin} \propto L_{\nu}^i k^i, \quad k^i \propto \frac{\kappa^i}{\rho} \quad (\text{line-strength})$$

$$g_{rad}^{thick} \propto L_{\nu}^i \frac{dv/dr}{\rho}$$

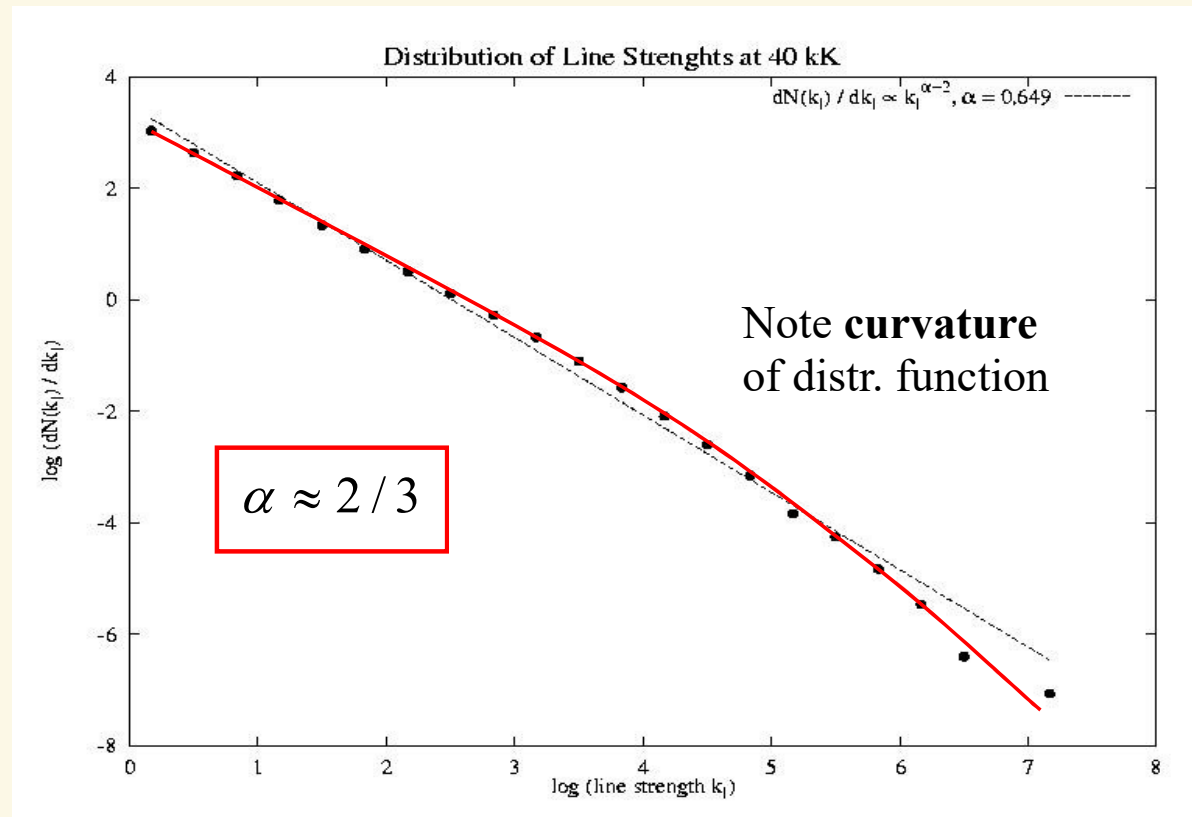
when accounting for interaction probability $(1 - \exp(-\tau^i))$

The line distribution function



USM

- pioneering work by Castor, Abbott & Klein (1975) and by Abbott (1982)
- first realistic line-strength distribution function by Kudritzki et al. (1988)
- NOW: 4.2 Ml (Mega lines), 150 ionization stages (H - Zn), NLTE



$$\frac{dN(k)}{dk} = k^{\alpha-2}, \quad \alpha \approx 0.6...0.7$$

+ 2nd empirical finding:
valid in *each* frequential
subinterval

$$dN(k, \nu) = -N_0 f(\nu) d\nu k^{\alpha-2} dk$$

Logarithmic plot of line-strength distribution function for an O-type wind at 40,000 K and corresponding power-law fit (see Puls et al. 2000, A&AS 141)

$$g_{rad}^{tot} = \sum_{\text{all lines}} g_{rad}^i \Rightarrow \iint g_{rad}^i(v, k) dN(v, k) \propto N_{\text{eff}} L \left(\frac{dv/dr}{\rho} \right)^\alpha,$$

N_{eff} "effective" number of lines

α exponent of line-strength distr. function, also: $\alpha = \frac{g_{rad}^{thick}}{g_{rad}^{tot}}$

Hydrodynamical description

with

mass-loss rate \dot{M} , radius r

$$\dot{M} = 4\pi r^2 \rho v,$$

isothermal soundspeed a

$$g_{rad} = g_{\text{cont}} + g_{\text{lines}}, \quad g_{\text{lines}} \propto N_{\text{eff}} L \left(\frac{dv/dr}{\rho} \right)^\alpha,$$

(approximate) analytical solution possible

equation of continuity

conservation of mass-flux

$$\left(1 - \frac{a^2}{v^2} \right) v \frac{dv}{dr} = -\frac{GM}{r^2} + g_{rad} + \frac{2a^2}{r} - \frac{da^2}{dr}$$

equation of motion

conservation of momentum-flux

velocity field

grav. accel. radiative accel. "pressure"

positive for $v > a$

inwards outwards outwards

negative for $v < a$

Scaling relations for line-driven winds (without rotation)



$$\dot{M} \propto N_{\text{eff}}^{1/\alpha'} L^{1/\alpha'} (M(1-\Gamma))^{1-1/\alpha'}$$

$$v_{\infty} \approx 2.25 \frac{\alpha}{1-\alpha} v_{\text{esc}}, \quad v_{\text{esc}} = \left(\frac{2GM(1-\Gamma)}{R_*} \right)^{1/2}$$

$$v(r) = v_{\infty} \left(1 - \frac{R_*}{r} \right)^{\beta}, \quad \beta = 0.8 \text{ (O-stars) ... } 2 \text{ (BA-SG)}$$

Γ Eddington factor, accounting for acceleration by Thomson-scattering, diminishes effective gravity

N_{eff} number of lines effectively driving the wind, corrected for ionization effects, dependent on metallicity and spectral type

α exponent of line-strength distribution function, $0 < \alpha < 1$
large value: more optically thick lines

$\alpha' = \alpha - \delta$, with δ ionization parameter, typical value for O-stars: $\alpha' \approx 0.6$

- use scaling relations for \dot{M} and v_∞ , calculate modified wind-momentum rate

$$\dot{M} v_\infty R_*^{1/2} \propto N_{\text{eff}}^{1/\alpha'} L^{1/\alpha'} (M(1-\Gamma))^{1-1/\alpha'} (M(1-\Gamma))^{1/2}$$

$$(\alpha' \approx \frac{2}{3}) \propto N_{\text{eff}}^{1/\alpha'} L^{1/\alpha'}, \text{ independent of } M \text{ and } \Gamma$$

$$\Rightarrow \log(\dot{M} v_\infty R_*^{1/2}) \approx \frac{1}{\alpha'} \log L + \text{const}(z, \text{sp.type})$$

(Kudritzki, Lennon & Puls 1995)

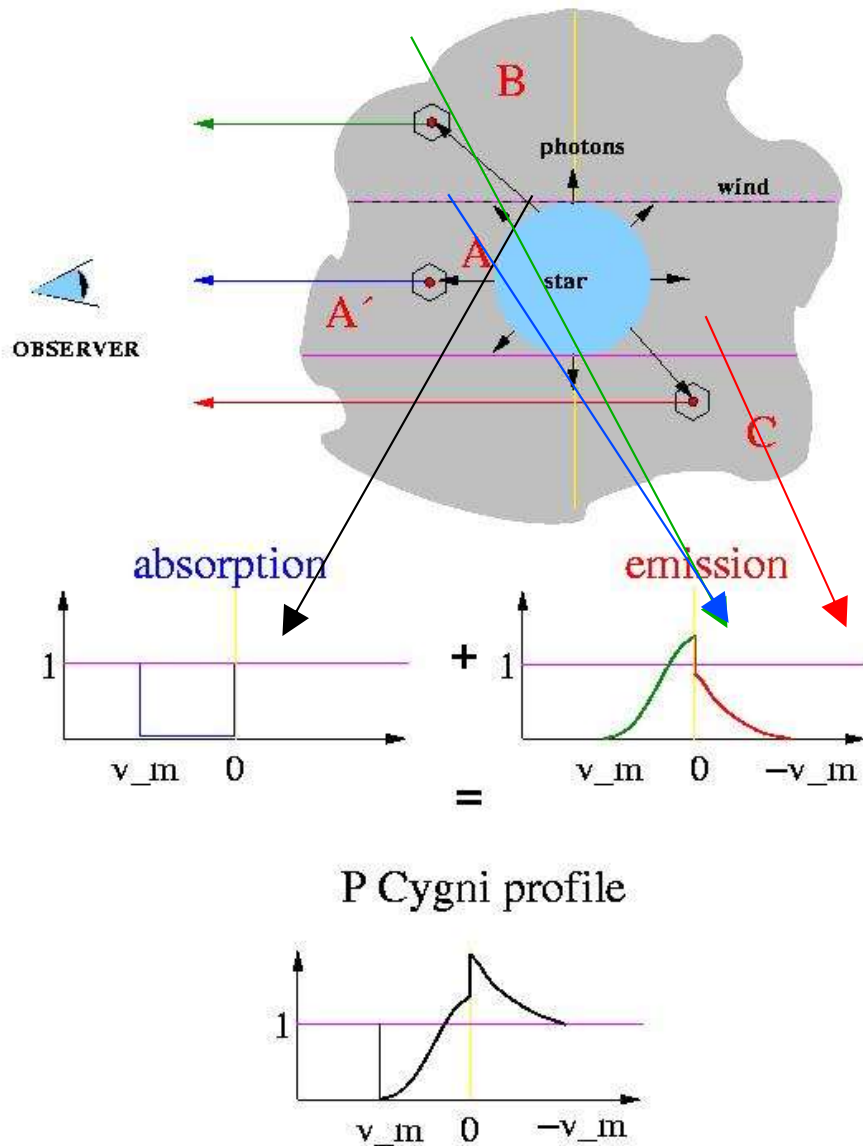
- (at least) two applications

(1) construct **observed** WLR, calibrate as a function of spectral type and metallicity (N_{eff} and α' depend on both parameters)
independent tool to measure extragalactic distances
from *wind-properties*, T_{eff} and metallicity

(2) compare with **theoretical** WLR to test validity of radiation driven wind theory

Determination of wind-parameters: v_∞

P Cygni profile formation



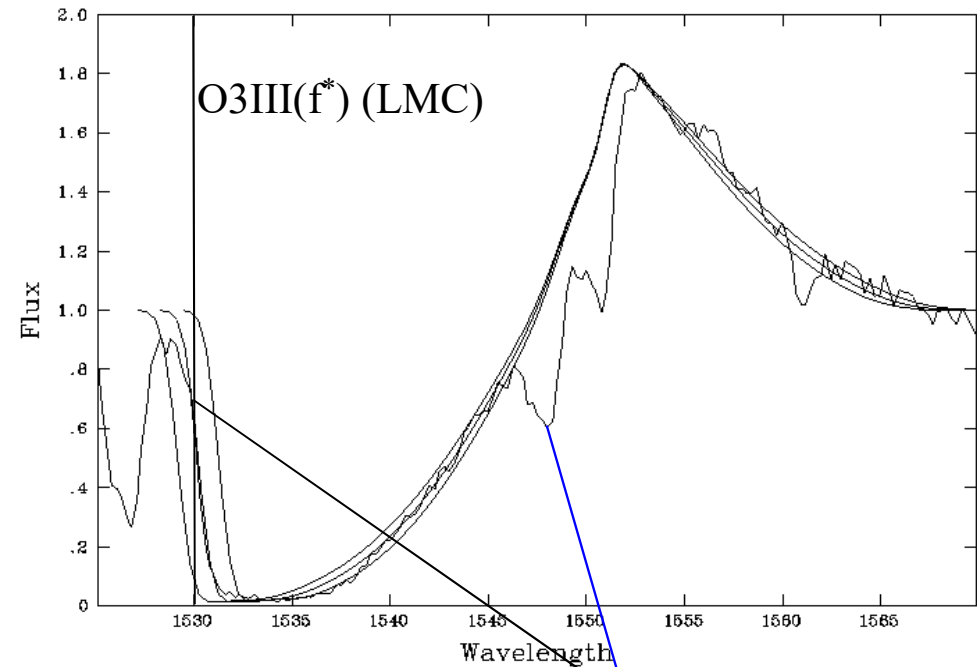
$$v_{\text{obs}} = v_0 \left(1 + \frac{\mu v(r)}{c} \right); \quad v_0 \text{ line frequency in CMF}$$

$$\mu v(r) > 0: \quad v_{\text{obs}} > v_0 \quad \text{blue side}$$

$$\mu v(r) < 0: \quad v_{\text{obs}} < v_0 \quad \text{red side}$$

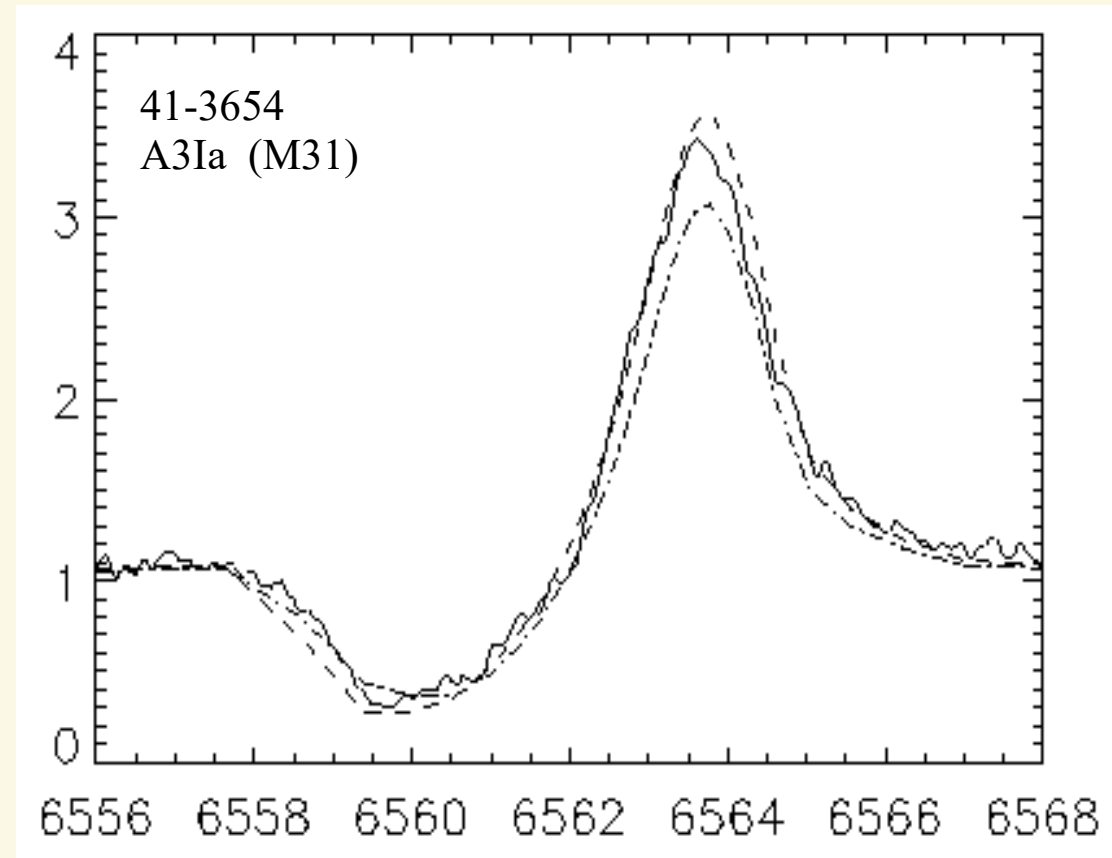
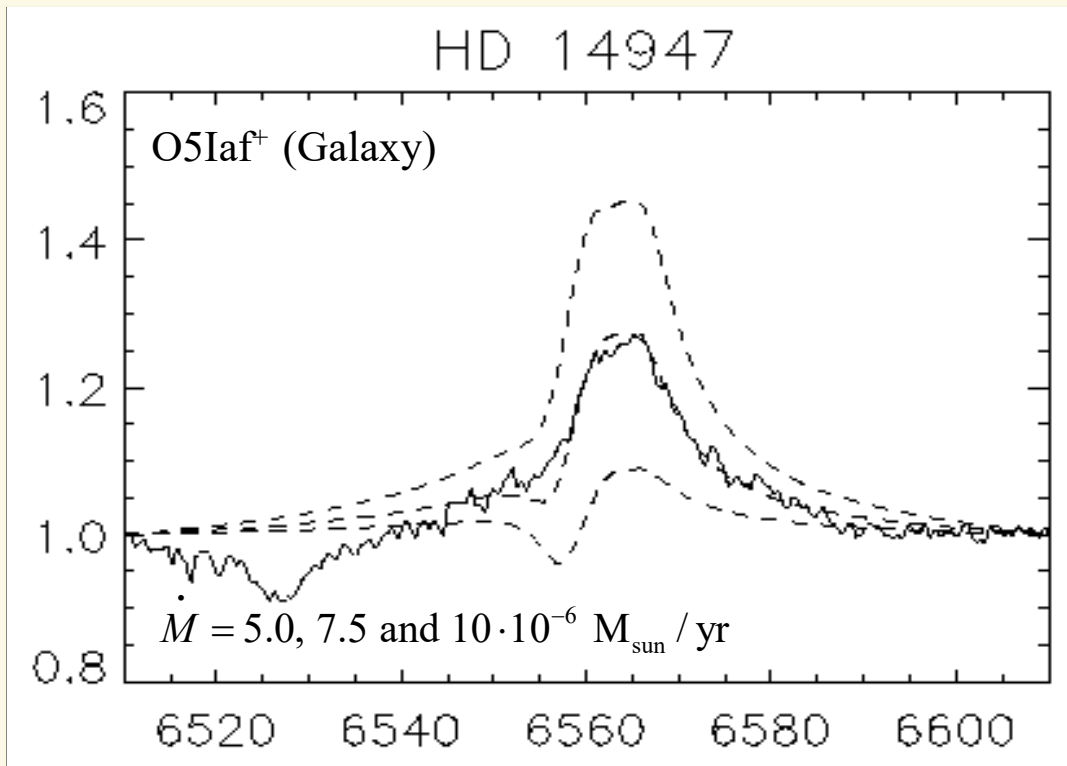
$$\frac{v_m}{c} = \frac{v_{\text{max}} - v_0}{v_0} = 1 - \frac{\lambda_{\text{min}}}{\lambda_0}$$

Sk -68 137 CIV $v_{\text{inf}}=3200/3400/3600$ km/s



$$v_m \approx 2.998 \cdot 10^5 \left(1 - \frac{1530}{1548} \right) \approx 3,480 \text{ km/s}$$

Determination of mass-loss rate from H α



Note: Wind parameters can be cast into one quantity

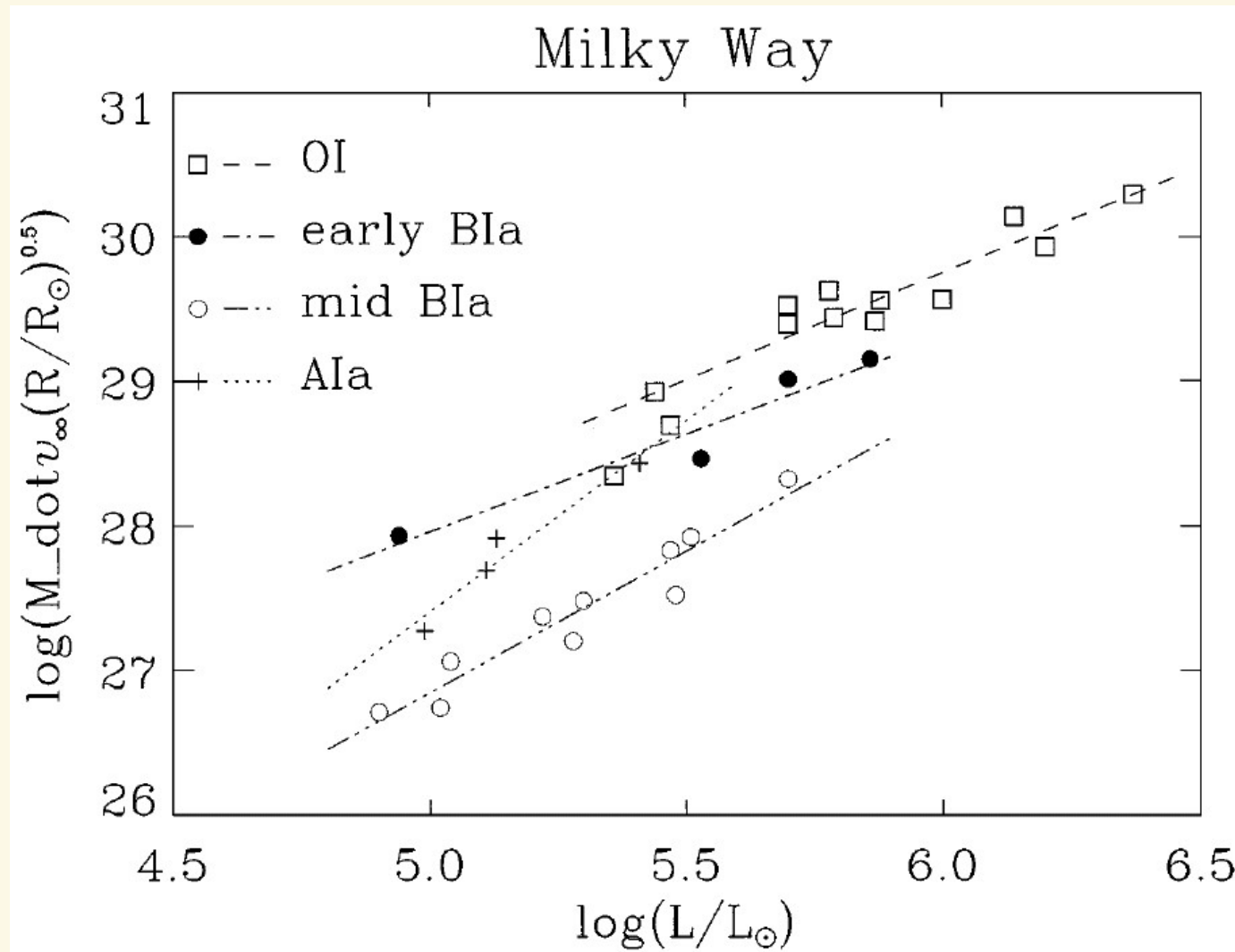
$$Q = \frac{\dot{M}}{(R_* v_\infty)^{1.5}} \quad \text{or} \quad Q' = \frac{\dot{M}}{R_*^{1.5}}$$

For same values of $Q^{(')}$ (albeit different combinations of \dot{M} , v_∞ and R_*), profiles look almost identical!

H α taken with the Keck HIRES spectrograph, compared with two model calculations adopting $\beta = 3$, $v_\infty = 200 \text{ km/s}$ and $\dot{M} = 1.7 \text{ and } 2.1 \times 10^{-6} M_{\text{sun}}/\text{yr}$.



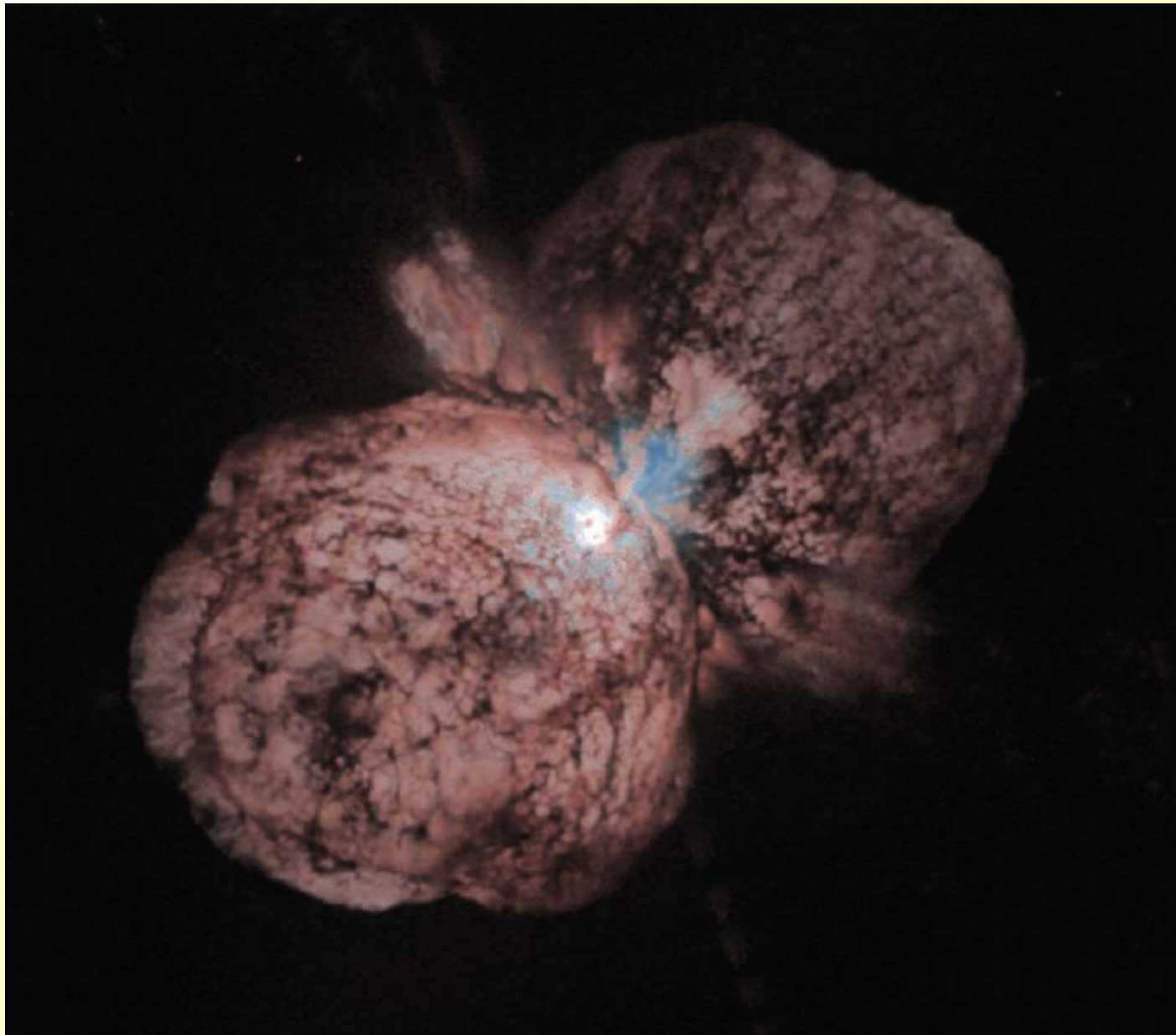
Observed WLR



Modified wind momenta of Galactic O-, early B-, mid B- and A-supergiants as a function of luminosity, together with specific WLR obtained from linear regression. (From Kudritzki & Puls, 2000, ARAA 38).

η Car: Aspherical ejecta

image by HST



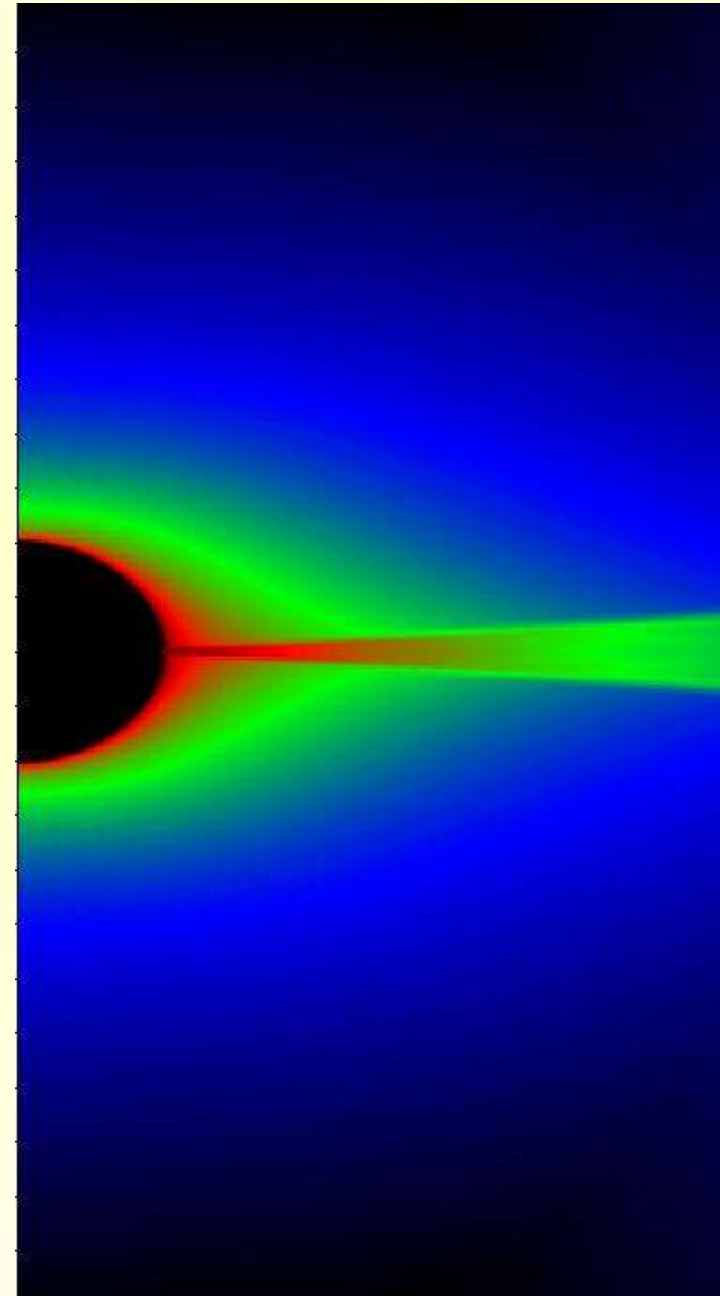
Influence of rotation

hot, massive stars = **young stars**

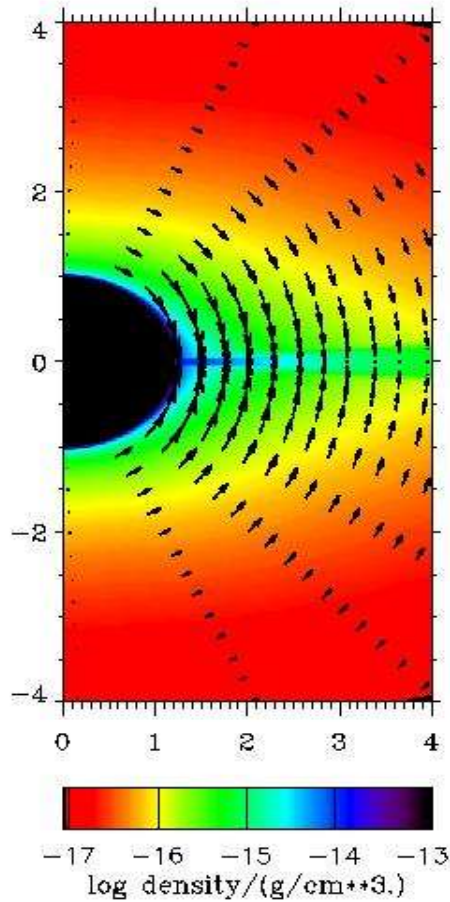
rapidly rotating (up to several 100 km/s)

twofold effect

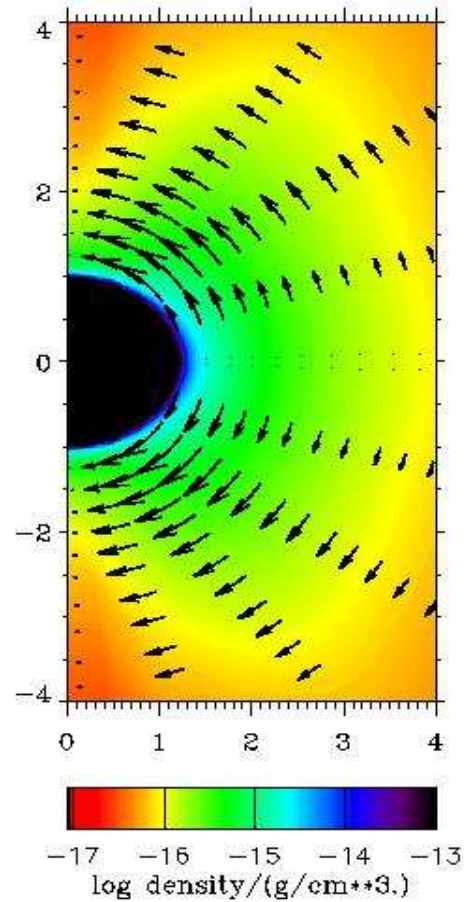
- star becomes “oblate”
- wind has to react on additional **centrifugal acceleration**, large in equatorial, small in polar regions



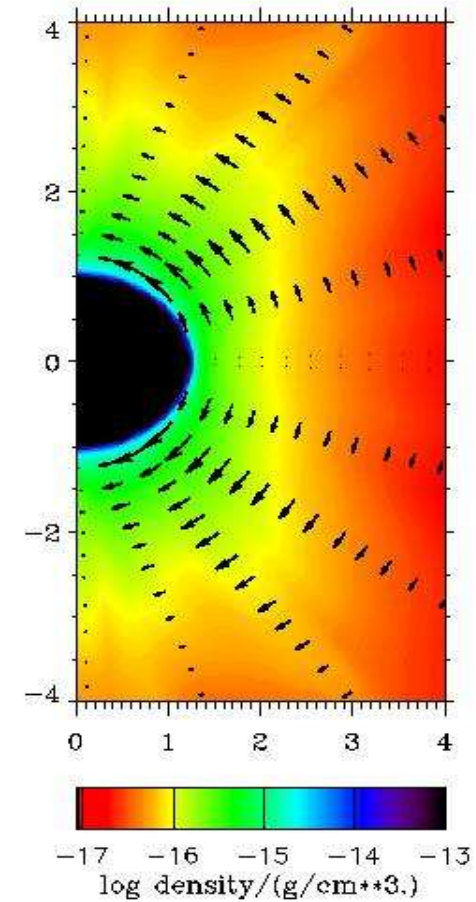
Prolate or oblate wind structure?



purely radial radiative
acceleration:
wind-compressed disk

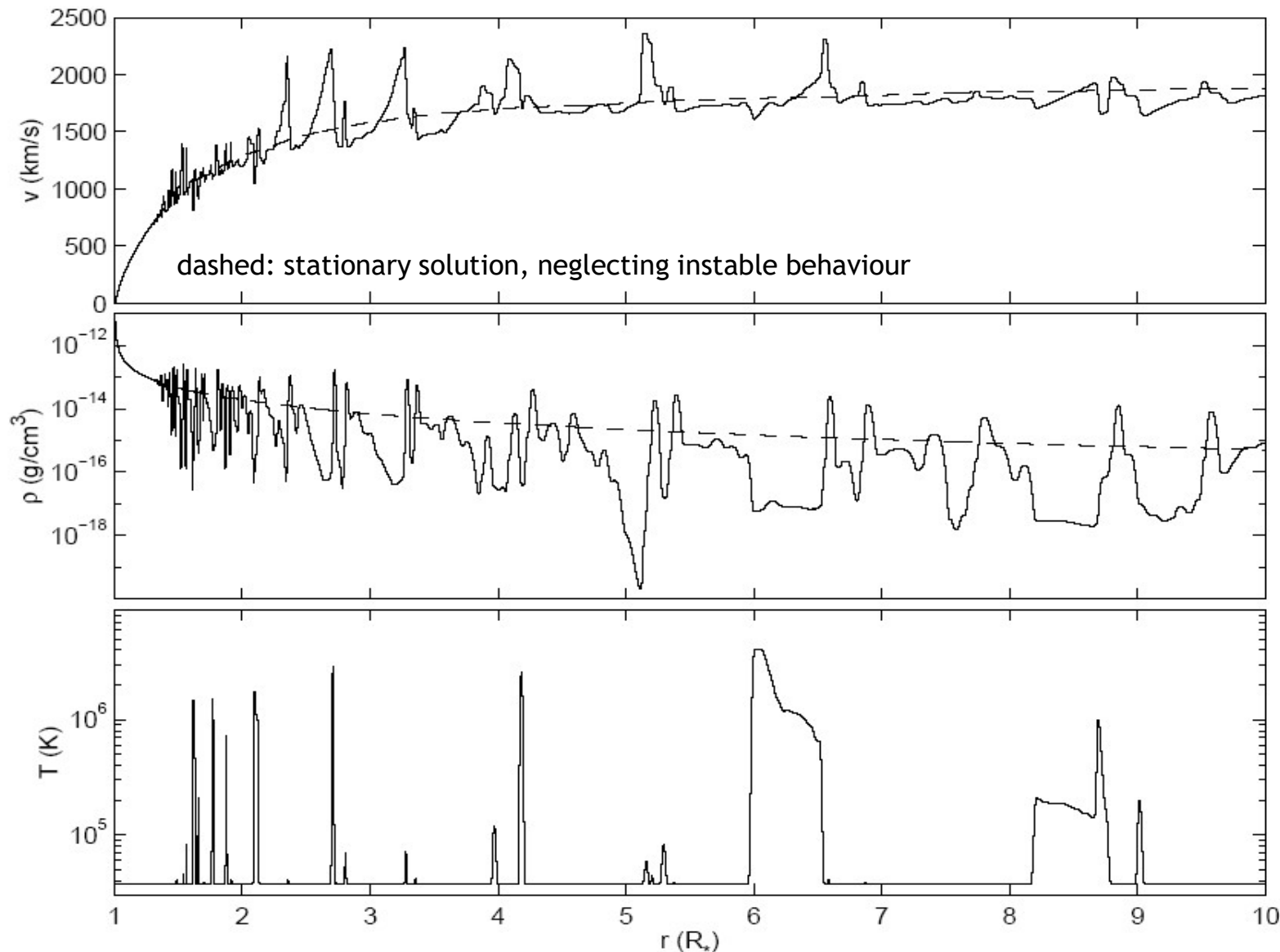


inclusion of non-
radial component
of line-acceleration
(rotation breaks
symmetry)



non-radial line-acceleration
plus „gravity darkening“:
prolate geometry

Time dependent hydro-simulations of line-driven winds: Snapshot of density, velocity and temperature structure



average hydro-structure
not too different from
stationary approx.:
Most line profiles fairly
similar, but effect
("clumping")
needs to be accounted
for in analysis

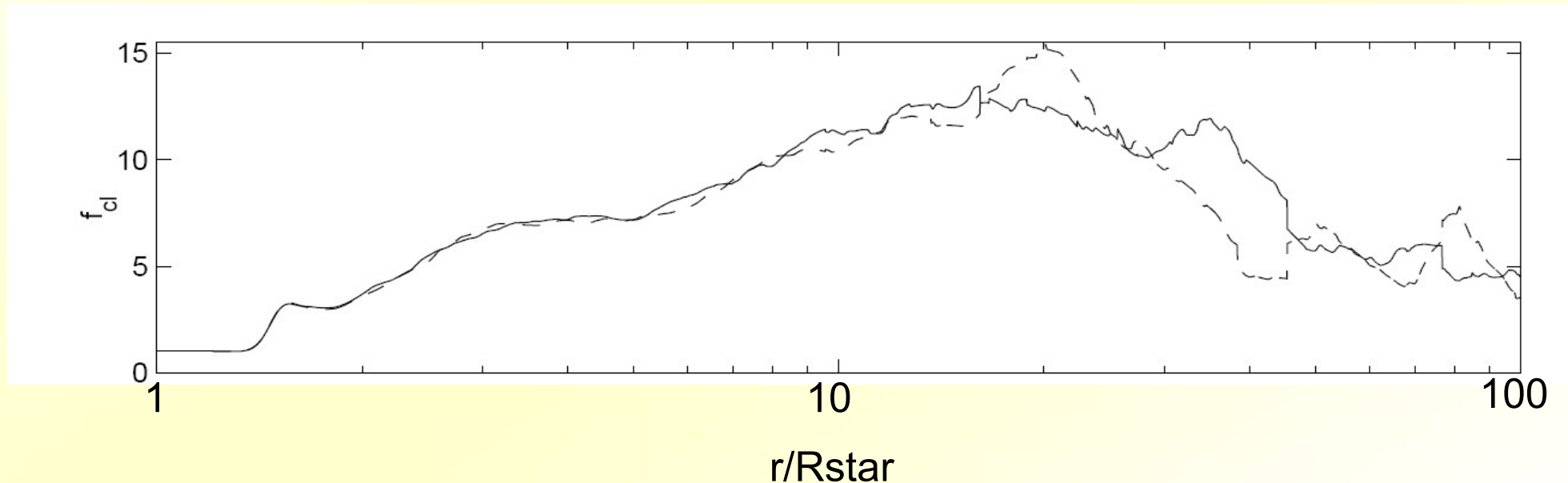
(very) hot gas
→ X-ray emission
(observed!)

From Runacres & Owocki, 2002, A&A 381

The clumping factor

$$f_{\text{cl}} = \frac{\langle \rho^2 \rangle}{\langle \rho \rangle^2} \geq 1 \text{ always! (= 1 only for smooth flows)}$$

brackets denote temporal averages



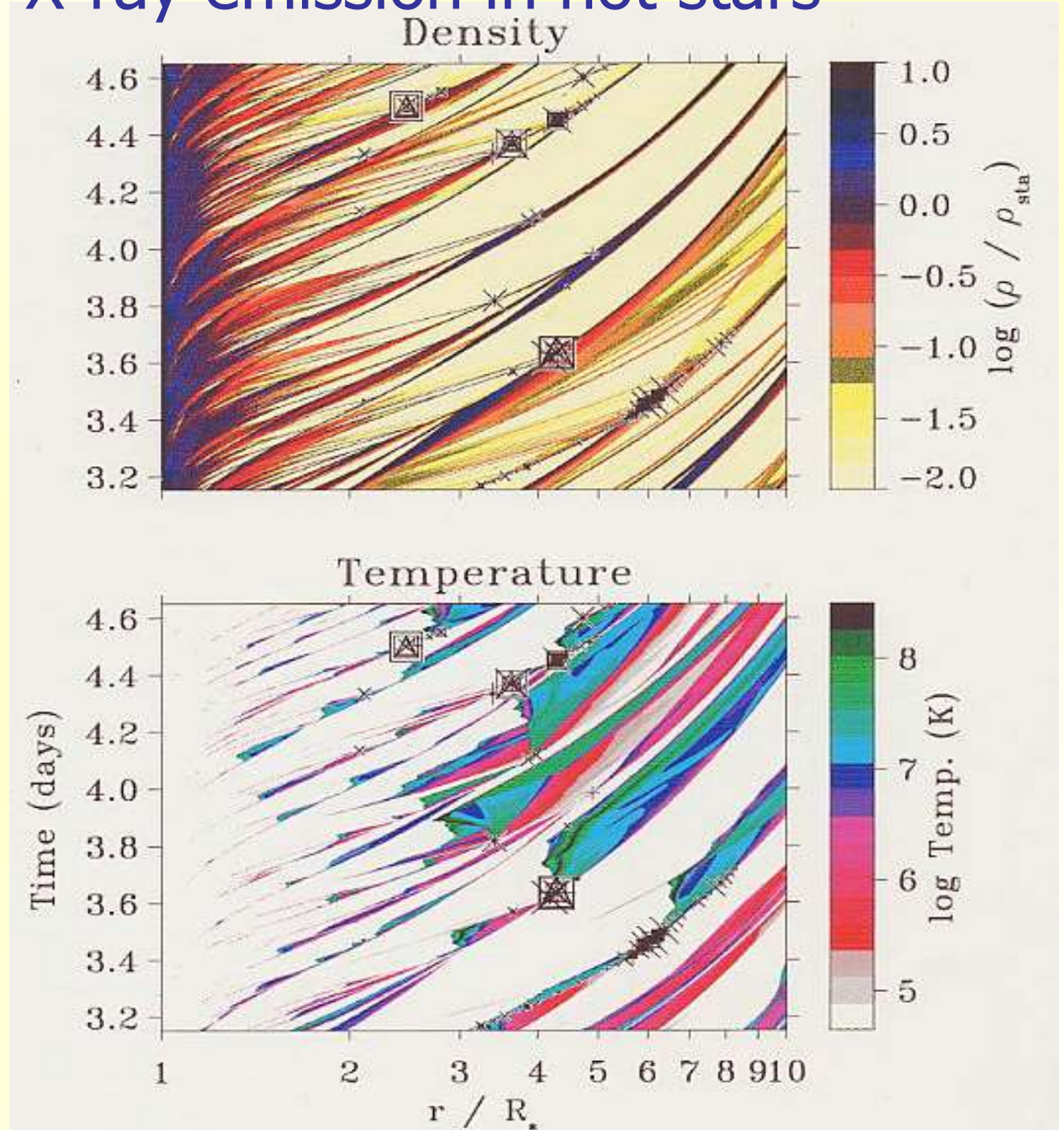
Inhomogeneities have to be accounted for in model atmospheres/spectrum synthesis!

Clumping and X-ray emission in hot stars

density and temperature evolution
as a function of time

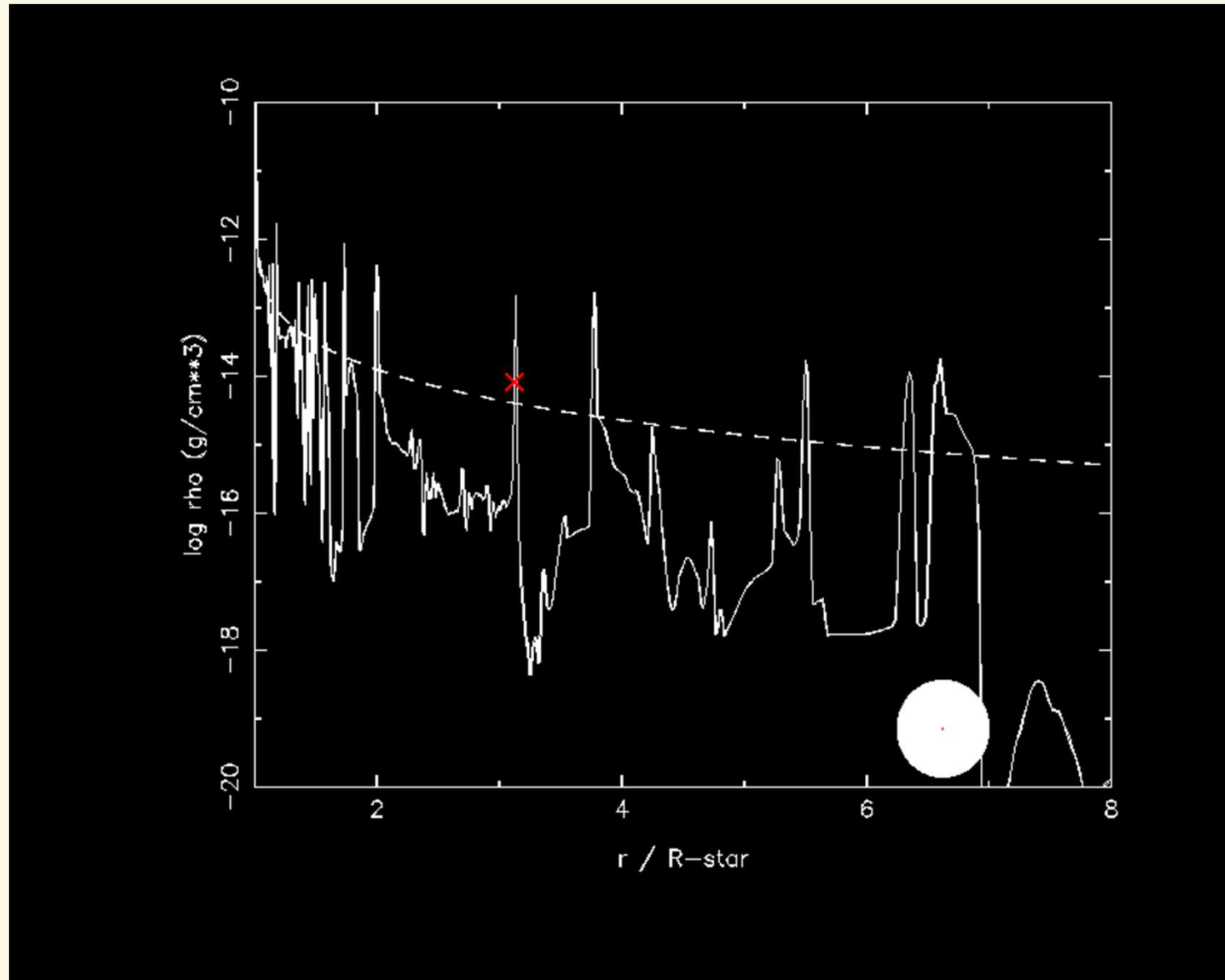
(very) hot gas
→ X-ray emission
(observed!)

hydrodynamical simulations of unstable hot star winds,
from Feldmeier et al., 1997,
A&A 322



Density evolution in an unstable wind

X
X-ray
“flash”



Chap. 9 Quantitative spectroscopy

The exemplary case of hot stars



Determine atmospheric parameters from observed spectrum

Required

T_{eff} , $\log g$, R , Y_{He} , \dot{M} , v_{∞} , β (+ metal abundances)
(R stellar radius at $\tau_R = 2/3$)

also necessary

v_{rad} (radial velocity)
 $v \sin i$ (projected rotational velocity)

Given

- *reduced* optical spectra (eventually +UV, +IR, +X-ray)
- $\lambda/\Delta\lambda$, resolution of observed spectrum
- Visual brightness V
- distance d (from cluster/association membership), partly rather insecure
- NLTE-code(s), "model grid"

1. Rectify spectrum, i.e. divide by continuum (**experience required**)

2. Shift observed spectrum to lab wavelengths (use narrow **stellar** lines as reference):

$$\lambda_{\text{lab}} \approx \lambda_{\text{obs}} \left(1 - \frac{v_{\text{rad}}}{c} \right), \quad v_{\text{rad}} \text{ assumed as positive if object moves away from observer}$$

• Alternative set of parameters

L , M , R *or*
 L , M , T_{eff} *or*
 T_{eff} , $\log g$, R ...

• interrelations

$$L = 4\pi R_*^2 \sigma_B T_{\text{eff}}^4$$

$$g = \frac{GM}{R_*^2}$$

• Useful scaling relations

If L , M , R in *solar units*, then

$$R_* = \frac{L^{0.5}}{T_{\text{eff}}^2} \cdot 3.327 \cdot 10^7$$

$$\log g = \log \left(\frac{M}{R_*^2} \cdot 2.74 \cdot 10^4 \right)$$

$$v_{\text{esc}} = \sqrt{R_* g (1 - \Gamma)} \cdot 1.392 \cdot 10^{11}$$

$$\Gamma = s_e T_{\text{eff}}^4 / g \cdot 1.8913 \cdot 10^{-15}$$

$$s_e = 0.4 \frac{1 + I_{\text{He}} Y_{\text{He}}}{1 + 4Y_{\text{He}}}, \quad \text{cf. page 90}$$

with I_{He} number of free electrons per Helium atom

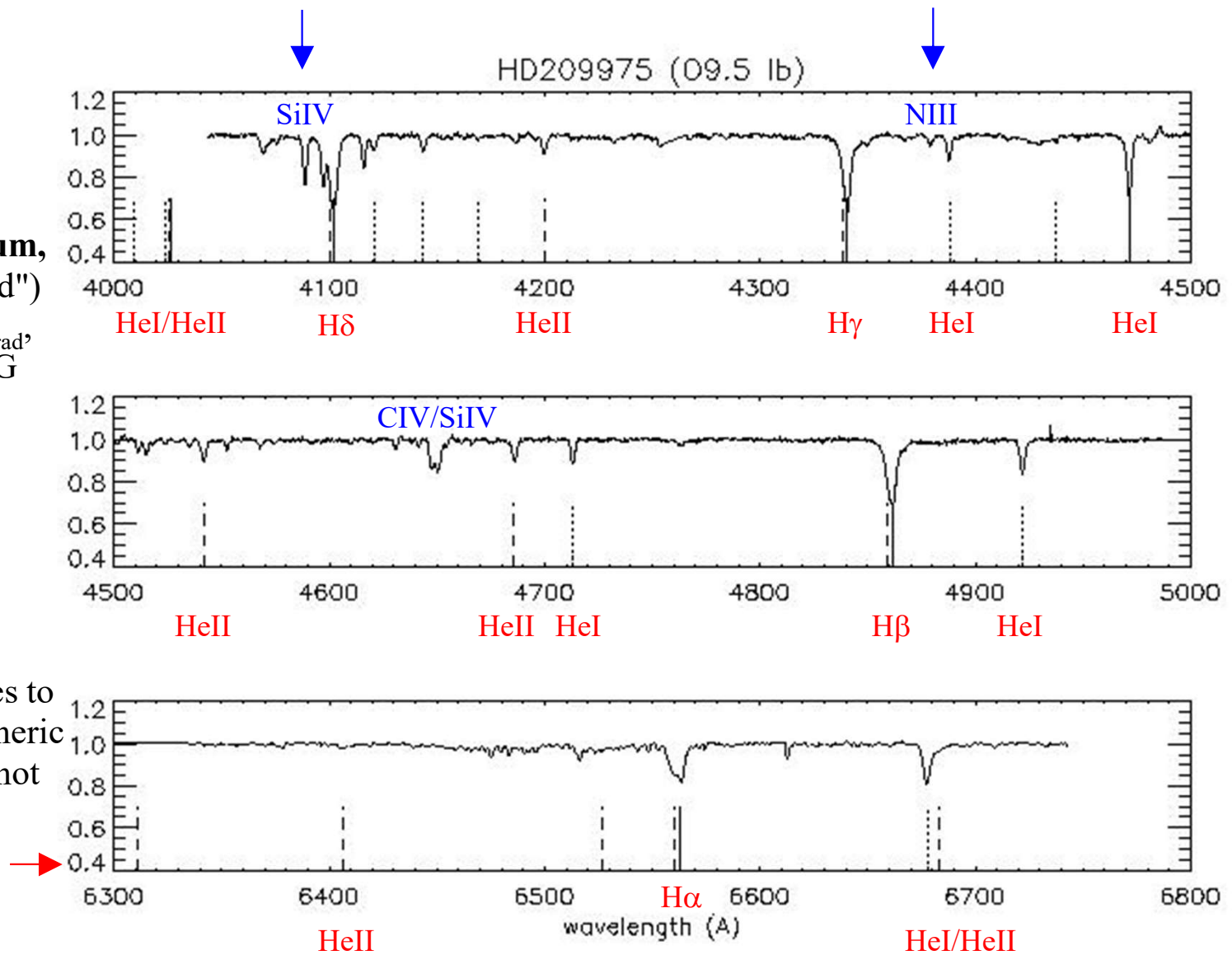
(e.g., =2, if completely ionized)



rectified
optical spectrum,
("blue" and "red")
corrected for v_{rad}
of the late O-SG
19 Cep

— Hydrogen
..... Helium I
- - - Helium II

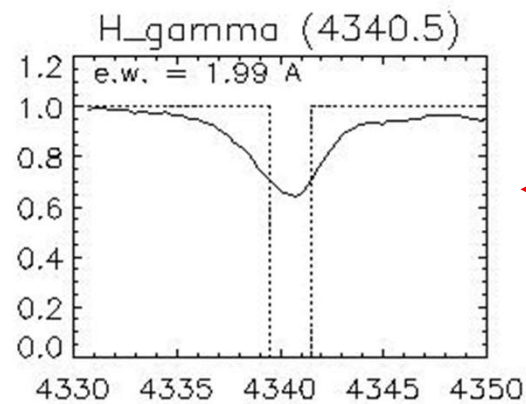
in "red":
"strategic" lines to
derive atmospheric
parameters in hot
stars



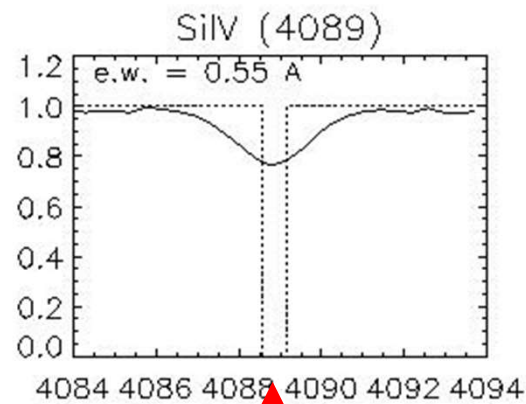


$$\text{Equivalent width } W_\lambda = \int_{\text{line}} \frac{H_{\text{cont}} - H_{\text{line}}(\lambda)}{H_{\text{cont}}} d\lambda = \int_{\text{line}} (1 - R(\lambda)) d\lambda,$$

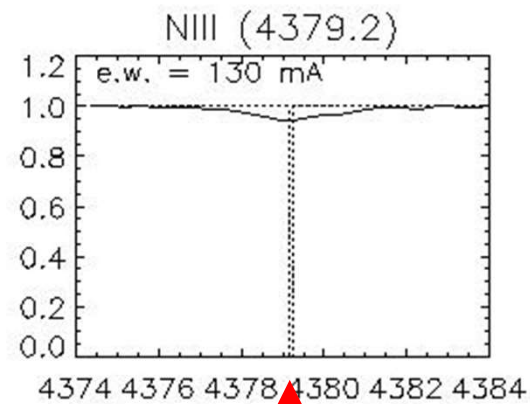
area of profile under continuum, $\text{dim}[W_\lambda] = \text{Angstrom or milliAngstrom, m}\text{\AA}$
corresponds to width of saturated profile ($R(\lambda) = 0$) with same area



← strong line



intermediate line

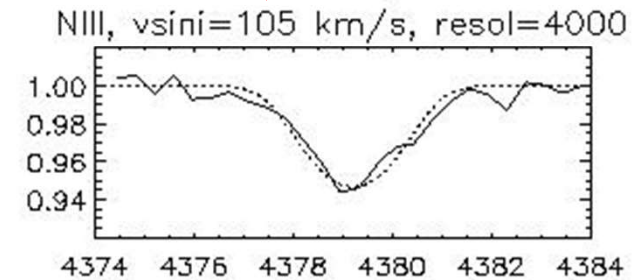
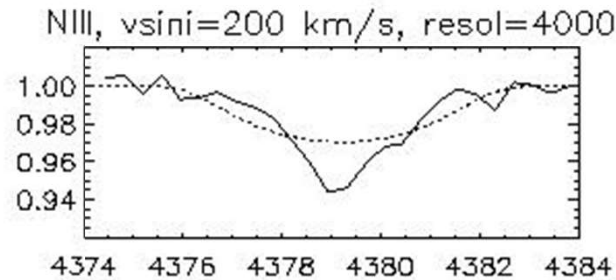
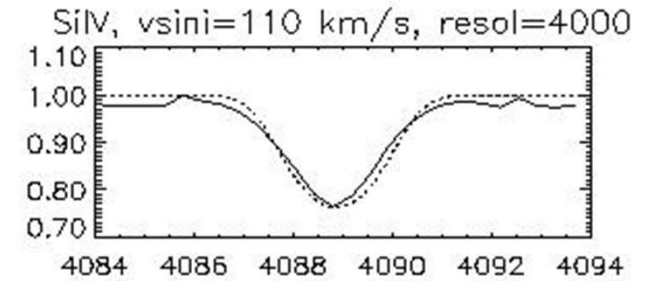
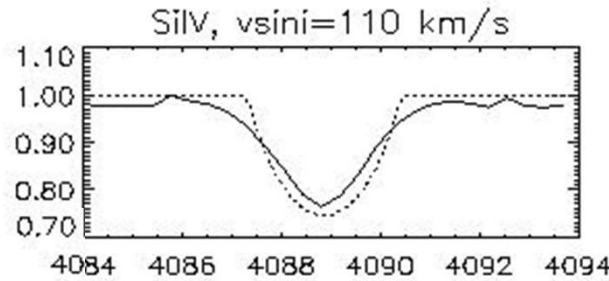
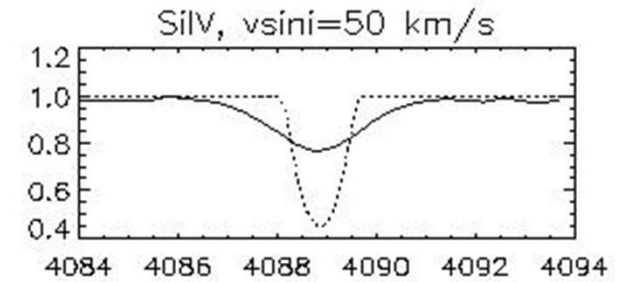
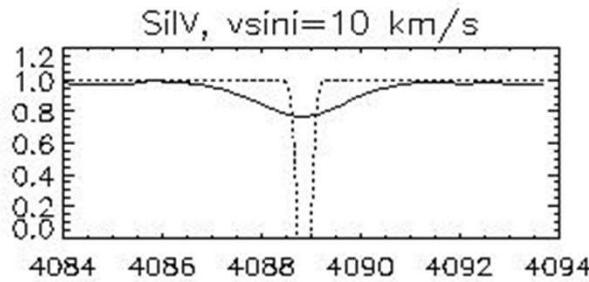


weak line

Determine projected rotational speed $v \sin i$

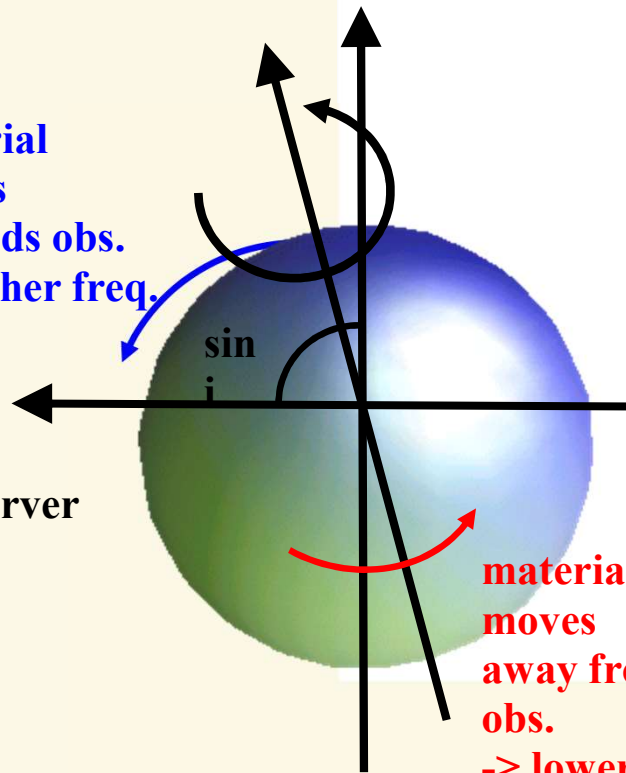
Use **weak metal lines** to derive $v \sin i$:
Convolve theoretical line with rotational profile.

Convolve finally with instrumental profile (~ Gauss) according to **spectral resolution**



material moves towards obs. -> higher freq.

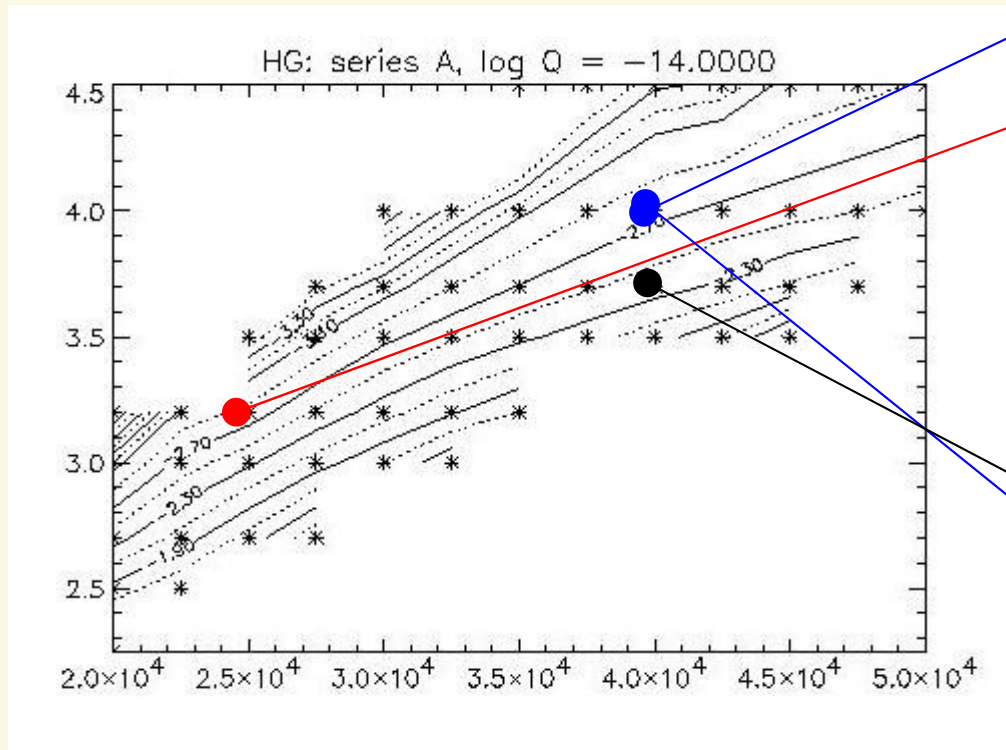
to observer



material moves away from obs. -> lower freq.

Convolution with rotational and instrumental profile conserves equivalent width!!!
Recent methods use a Fourier technique to infer $v \sin i$

H γ - log g and T_{eff}

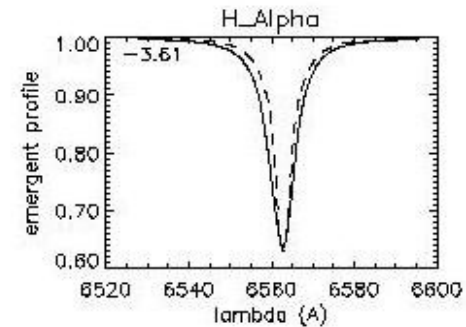
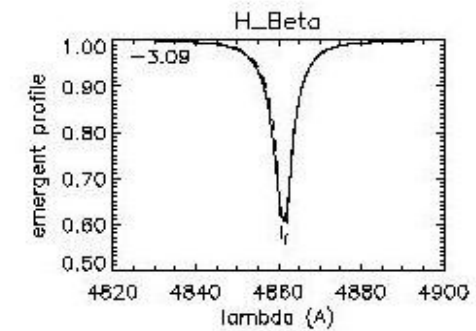
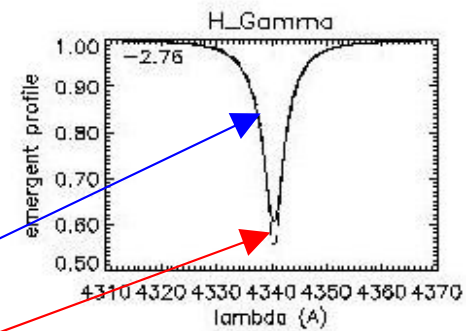


Iso-contours of equiv. widths for H γ (from model grid), for solar Helium abundance and (very) thin winds

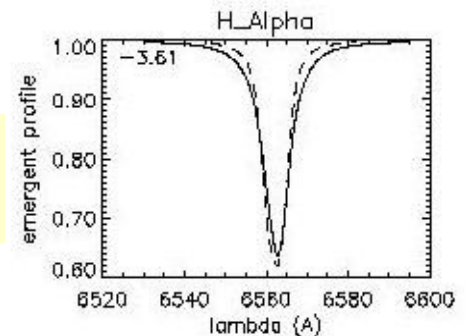
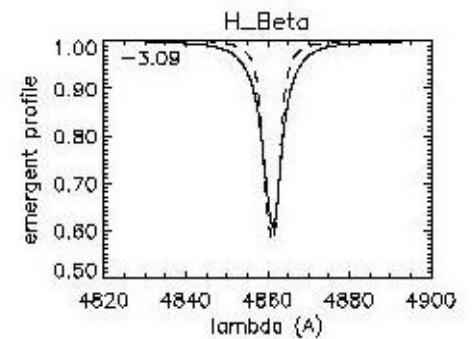
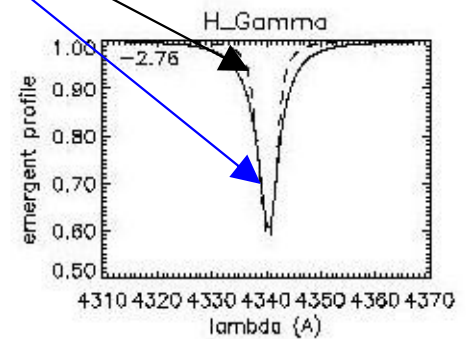
to derive T_{eff}, log g and Y_{He}, at least 3 lines have to be fitted in parallel (if no wind is present):

- H γ defines log g (for given T_{eff})
- HeII/HeI define T_{eff} (for given log g)
- absolute strength of He lines define Y_{He}

usually, wind emission has to be accounted for (profiles shallower)

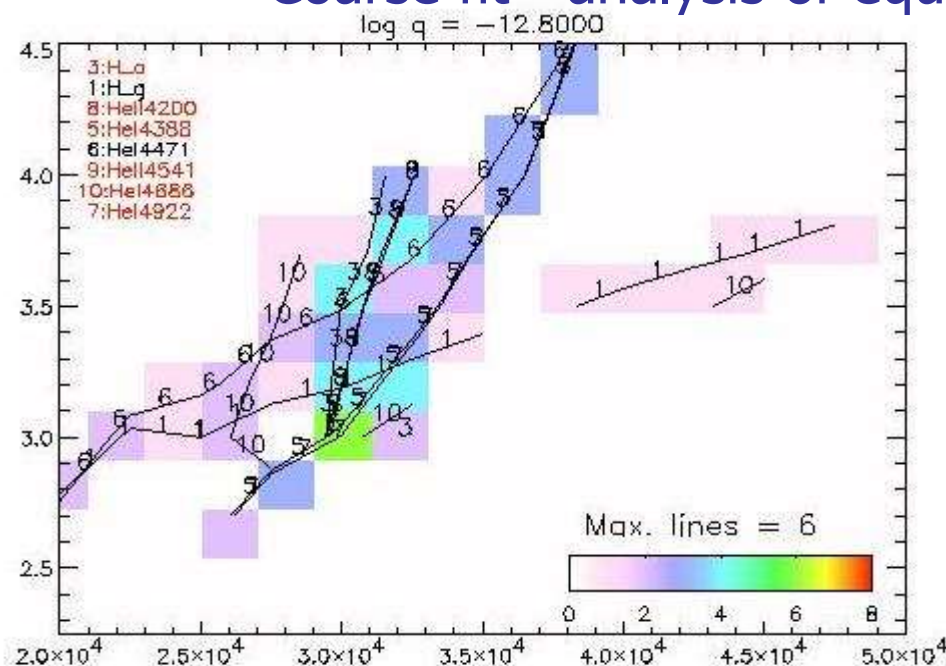


degeneracy of profiles: (almost) identical lines for T_{eff}=40,000 and log g=4.0 and T_{eff}=25,000 and log g=3.2

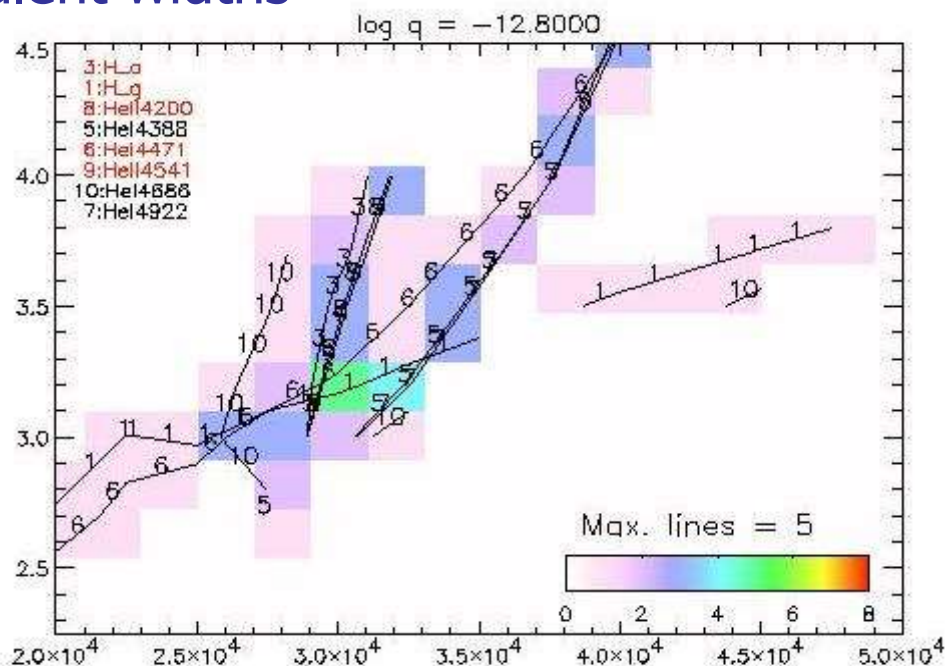


wings of Balmer lines (Stark-broadened) react strongly on electron-density (as a function of τ) => perfect gravity indicator

Coarse fit - analysis of equivalent widths



Fit diagram for $Y_{\text{He}} = 0.1$ (best fit at $\log Q = -12.8$)



Fit diagram for $Y_{\text{He}} = 0.15$ (best fit at $\log Q = -12.8$)

Measured equivalent widths

Balmer lines	HeI	HeII
$H\gamma$ 1.99	4387 0.32	4200 0.25
$H\alpha$ 1.33	4471 0.86	4541 0.31
	4922 0.46	4686 0.27

Note: $H\alpha$ and HeII 4686 mass-loss indicators

Result: $T_{\text{eff}} \approx 30,000 \text{ K}$, $\log g \approx 3.0 \dots 3.2$,
 $Y_{\text{He}} \approx 0.10 \dots 0.15$, $\log Q \approx -12.8$

Fit diagram constructed from model grid with

$20,000 \text{ K} < T_{\text{eff}} < 50,000 \text{ K}$ with $\Delta T = 2,500 \text{ K}$

$2.2 < \log g < 4.5$ with $\Delta \log g = 0.25$

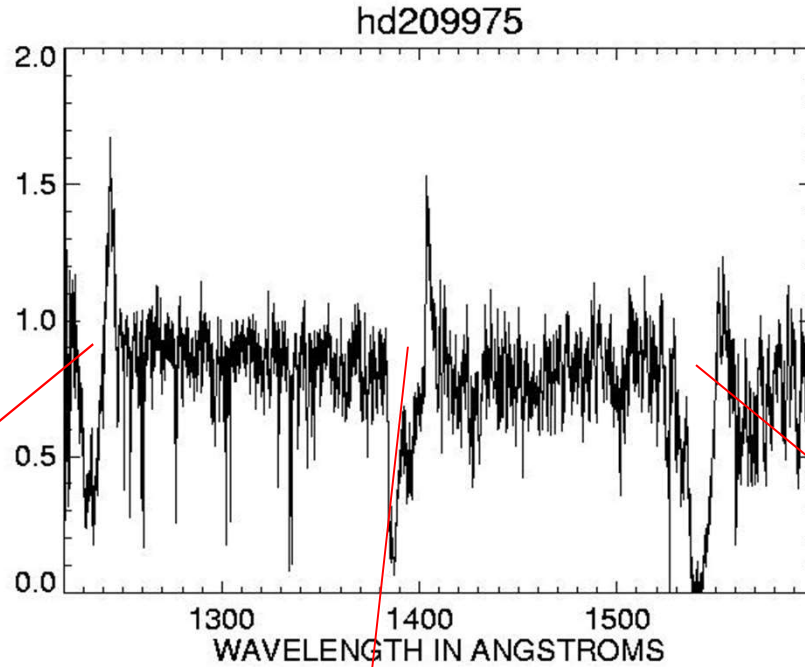
$-14 < \log Q < -11$ with $\Delta \log Q = 0.3$, $Y_{\text{He}} = 0.10, 0.15, 0.20$

Note: Wind parameters can be cast into one quantity

$$Q = \frac{M}{(R_* v_\infty)^{1.5}}$$

For same values of Q (albeit different combinations of \dot{M} , v_∞ and R_*), profiles look almost identical!

Determination of terminal velocity from UV-P Cygni profiles



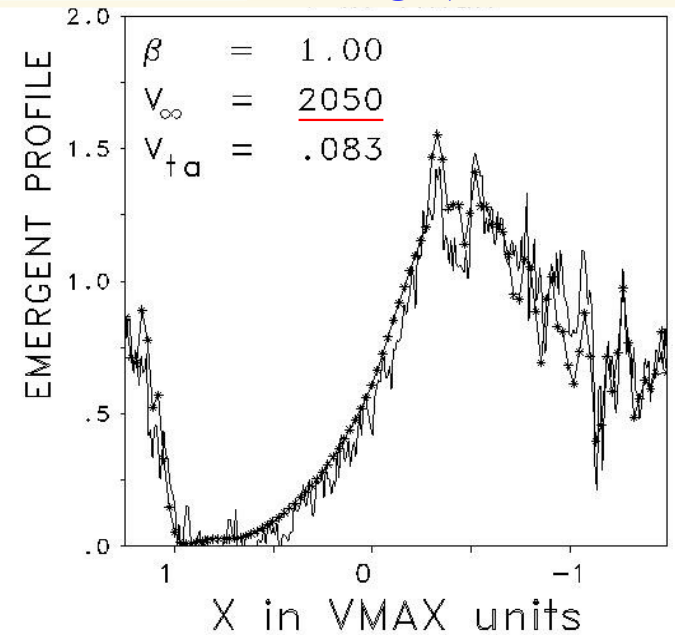
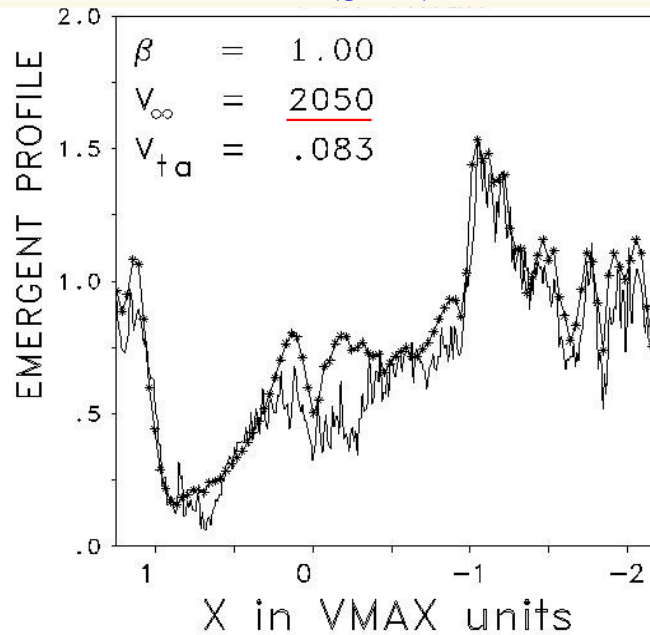
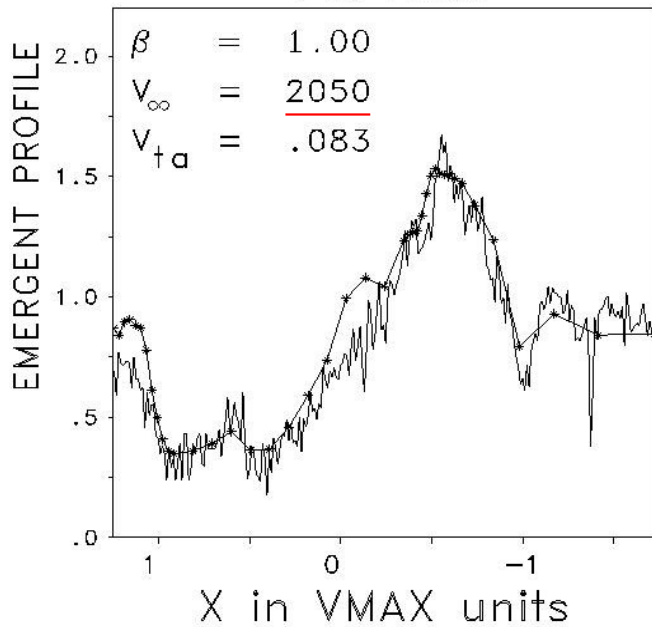
observation with IUE (International Ultraviolet Explorer) no longer active

recent data (archive!) from HST ($\lambda > 1200 \text{ \AA}$) and FUSE ($\lambda > 911 \text{ \AA}$)

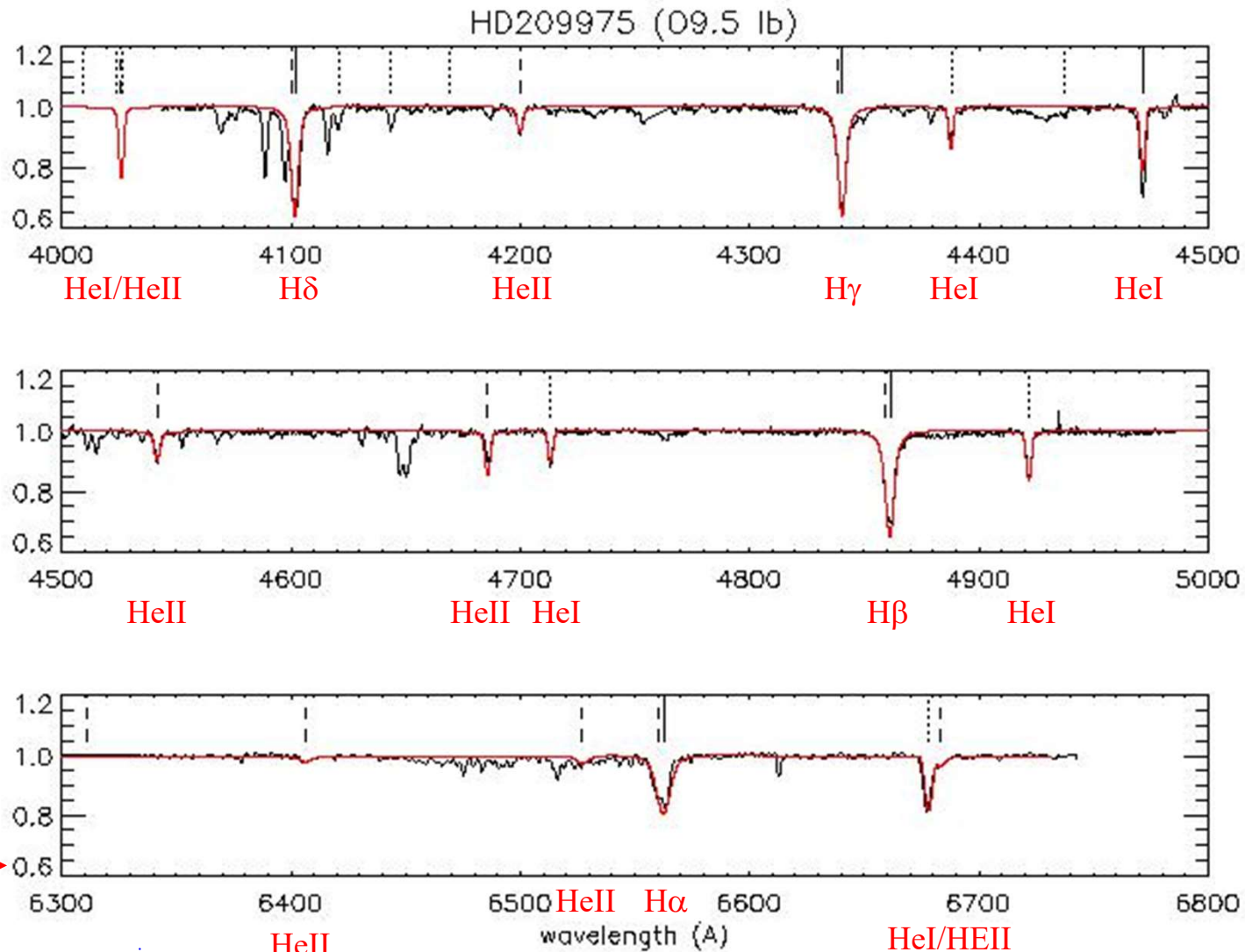
NV

Si IV

CIV



Fine fit - detailed comparison of line profiles



analysis via (semi-) automatic methods, based on high-dimensional model grids or genetic algorithms, to optimize the fit quality for a multitude of lines

derived parameters

$T_{\text{eff}} = 31,000 \text{ K}$
 $\log g = 3.17$
 $\log Q = -12.87$
 $Y_{\text{He}} = 0.10$
 $\beta = 1.0$

with $v_{\infty} = 2050 \text{ km/s}$
 we have

$$\log(M/R_*^{1.5}) = -7.9$$

$$Q = \frac{M}{(R_* v_{\infty})^{1.5}}$$

Determination of stellar radius - if it cannot be resolved



• **IF you believe in stellar evolution**

- ★ use **evolutionary tracks** to derive M from (measured) T_{eff} and $\log g \Rightarrow R$
- ★ transformation of conventional HRD into $\log T_{\text{eff}} - \log g$ diagram required
- ★ for many massive objects, "mass discrepancy":
"spectroscopic masses" and "evolutionary masses" not consistent, discrepancy presumably related to photospheric turbulence pressure and mass-loss rates (Markova et al. 2018)

• **IF you know the distance (e.g., from GAIA) and have theoretical fluxes (from model atmospheres):**

$$V = -2.5 \log \int_{\text{filter}} \mathcal{F}_\lambda S_\lambda d\lambda + \text{const}$$

S_λ spectral response of photometric system

absolute flux calibration

$V = 0$ corresponds to $\mathcal{F}_\lambda = 3.66 \cdot 10^{-9} \text{ erg s}^{-1} \text{ cm}^{-2} \text{ \AA}^{-1}$ at $\lambda_0 = 5,500 \text{ \AA}$ outside earth's atmosphere

λ_0 *isophotal* wavelength such that $\int_{\text{filter}} \mathcal{F}_\lambda S_\lambda d\lambda \approx \mathcal{F}(\lambda_0) \int_{\text{filter}} S_\lambda d\lambda$, $\int_{\text{filter}} S_\lambda d\lambda \approx 2895$ for Johnson V-filter

\Rightarrow

$$\text{const} = -2.5 \log(3.66 \cdot 10^{-9} \cdot 2895) = -12.437$$

$$M_V = -2.5 \log \left[\left(\frac{R_* R_{\text{sun}}}{10 \text{ pc}} \right)^2 \int_{\text{filter}} \mathcal{F}_\lambda S_\lambda d\lambda \right] + \text{const}$$

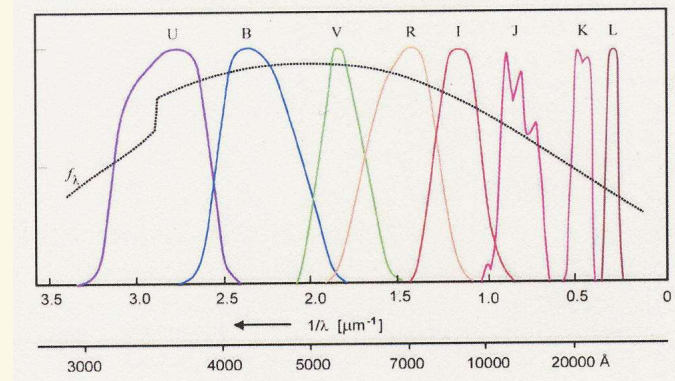
$$5 \log R_* = 29.553 + (V_{\text{theo}} - M_V)$$

if R_* in solar units, M_V the absolute visual brightness (from V(observed), distance and reddening) and

$$V_{\text{theo}} = -2.5 \log \int_{\text{filter}} 4 H_\lambda S_\lambda d\lambda \text{ with } H_\lambda \text{ the theoretical Eddington flux in units of } [\text{erg s}^{-1} \text{ cm}^{-2} \text{ \AA}^{-1}]$$

• **IF you believe in radiation driven wind theory**

- ★ use **wind-momentum luminosity relation**





• **Alternatively**, use bolometric correction (BC)

Calibration **for Galactic O-stars**:

$$BC = M_{\text{Bol}} - M_V \approx 27.58 - 6.8 \log(T_{\text{eff}}) \quad (\text{see Martins et al. 2005, A\&A 436})$$

and definition of M_{Bol}

$$\log \frac{L}{L_{\odot}} = 4 \log \frac{T_{\text{eff}}}{T_{\text{eff}, \odot}} + 2 \log \frac{R_*}{R_{\odot}} = 0.4(M_{\text{Bol}, \odot} - M_{\text{Bol}})$$

$$\log \frac{R_*}{R_{\odot}} = 0.2(4.74 - M_{\text{Bol}}) - 2 \log \frac{T_{\text{eff}}}{5770} =$$

$$= 0.2(4.74 - M_V - 27.58 + 6.8 \log(T_{\text{eff}})) - 2 \log \frac{T_{\text{eff}}}{5770} =$$

$$= 2.954 - 0.2M_V - 0.64 \log(T_{\text{eff}}) \quad [\text{valid only for O-stars with } Z \approx Z_{\odot}]$$



remember relation between M_V and V (distance modulus)

$$M_V = V + 5(1 - \log d) - A_V, \quad d \text{ distance in pc, } A_V \text{ reddening}$$

d from parallaxes (GAIA) or cluster/ association/ galaxy membership (hot stars)
(note: clusters/ assoc. radially extended!)

For Galactic objects, use compilation by
Roberta Humphreys, 1978, ApJS 38, 309 *and/or*
Ian Howarth & Raman Prinja, 1989, ApJS 69, 527

Back to our example

HD 209975 (19 Cep): $M_V = -5.7$
check: belongs to Cep OB2 Assoc., $d \approx 0.83$ kpc
 $V = 5.11, A_V = 1.17 \Rightarrow M_V = -5.65$, OK

From our final model, we calculate $V_{\text{theo}} = -29.08 \Rightarrow R = 17.4 R_{\text{sun}}$
(Alternatively, by using BC, M_V and $T_{\text{eff}} = 31\text{kK}$, we would obtain $R = 16.6 R_{\text{sun}}$)

Finally, from the result of our fine fit, $\log(\dot{M}/R_*^{1.5}) = -7.9$, we find $\dot{M} = 0.91 \cdot 10^{-6} M_{\text{sun}}/\text{yr}$

Finished, determine metal abundances if required,
next star



... but end of lecture!!!